



HAL
open science

Gelatine sizing of paper and its impact on the degradation of cellulose during aging. A study using size-exclusion chromatography

Anne-Laurence Dupont

► **To cite this version:**

Anne-Laurence Dupont. Gelatine sizing of paper and its impact on the degradation of cellulose during aging. A study using size-exclusion chromatography. Chemical Sciences. Université Amsterdam, 2003. English. NNT: . tel-04232436

HAL Id: tel-04232436

<https://hal.science/tel-04232436>

Submitted on 8 Oct 2023

HAL is a multi-disciplinary open access archive for the deposit and dissemination of scientific research documents, whether they are published or not. The documents may come from teaching and research institutions in France or abroad, or from public or private research centers.

L'archive ouverte pluridisciplinaire **HAL**, est destinée au dépôt et à la diffusion de documents scientifiques de niveau recherche, publiés ou non, émanant des établissements d'enseignement et de recherche français ou étrangers, des laboratoires publics ou privés.

Gelatine sizing of paper and its impact on the degradation of cellulose during aging

A study using size-exclusion chromatography

Anne-Laurence Dupont



Gelatine sizing of paper and its impact on the degradation of cellulose during aging

Anne-Laurence Dupont



Gelatine sizing of paper and its impact on the degradation of cellulose during aging

A study using size-exclusion chromatography

ACADEMISCH PROEFSCHRIFT

ter verkrijging van de graad van doctor

aan de Universiteit van Amsterdam

op gezag van de Rector Magnificus

prof. mr. P. F. van der Heijden

ten overstaan van een door het college voor promoties ingestelde
commissie, in het openbaar te verdedigen in de Aula der Universiteit

op maandag 10 maart 2003, te 11:00 uur

door

Anne-Laurence Dupont

geboren te Lille (France)

Promotiecommissie

Promotor: prof. dr. E.R. de la Rie

Overige commissieleden: prof. dr. H. Schenk
prof. dr. J.W. Verhoeven
prof. dr. ir. P.J. Schoenmakers
prof. dr. N.H. Tennent
prof. dr. G. Mortha
dr. H.J. Porck
dr. J.B.G.A. Havermans

Faculteit der Natuurwetenschappen, Wiskunde en Informatica

Cover illustration: Diderot, J.J. *Encyclopédie ou Dictionnaire Raisonné de Sciences, des Arts et des Métiers, par une Société de Gens de Lettres*, volume 11, PL XII, A. Neufchastel, Samuel Faulche et Compagnie (1765).

The research described in this thesis was carried out at the National Gallery of Art, Washington, DC, and was financially supported by the Charles E. Culpeper Foundation.

GELATINE SIZING OF PAPER AND ITS IMPACT ON THE DEGRADATION OF CELLULOSE DURING AGING

A STUDY USING SIZE-EXCLUSION CHROMATOGRAPHY

GENERAL INTRODUCTION	1
CHAPTER 1. ACCESSIBILITY, SOLUBILITY AND REACTIVITY OF CELLULOSE SUBSTRATES	7
<i>Abstract</i>	7
1.1 INTRODUCTION	7
1.2 THE FIBRE STRUCTURE	8
1.2.1 Molecular level	8
1.2.2 Supramolecular level	9
1.2.3 Ultrastructure: the fibre	11
1.3 ACCESSIBILITY BY SWELLING	12
1.4 METHODS OF ACTIVATION OF CELLULOSE SUBSTRATES	13
1.4.1 Activation by solvent exchange	14
1.4.2 Mechanical activation	14
1.5 DISSOLUTION OF CELLULOSE	15
1.6 CHEMICAL REACTIVITY OF CELLULOSE: ACID HYDROLYSIS	16
CHAPTER 2. REVIEW OF MOST COMMONLY USED METHODS FOR THE DISSOLUTION AND THE CHARACTERISATION OF CELLULOSE	23
<i>Abstract</i>	23
2.1 MOLAR MASS AVERAGES	23
2.2 METHODS OF DISSOLUTION AND ANALYSIS OF CELLULOSE	25
2.2.1 Viscometry: solvents and methods	25
2.2.2 Size-exclusion chromatography (SEC) and dissolution methods compatible with SEC	27
2.2.2.1 Principle of SEC	27
2.2.2.2 Cellulose tricarbanilate (CTC) and dissolution in THF	29
2.2.2.3 Direct dissolution of cellulose in lithium chloride / <i>N,N</i> -dimethylacetamide	30
2.2.2.3.1 The dissolution mechanism	30
2.2.2.3.2 The solvent complex specificity	33

CHAPTER 3. DISSOLUTION OF CELLULOSE IN THE SOLVENT SYSTEM LITHIUM CHLORIDE / N,N-DIMETHYLACETAMIDE (LiCl/DMAc)	37
<i>Abstract</i>	37
3.1 LITERATURE REVIEW	37
3.1.1 Dissolution of cellulose in LiCl/DMAc	37
3.1.1.1 <i>Activation procedure</i>	37
3.1.1.2 <i>Proportion of LiCl in DMAc</i>	39
3.1.1.3 <i>Sample source and composition, sample preparation</i>	39
3.1.2 Stability of solutions of cellulose in LiCl/DMAc	41
3.2 DEVELOPMENT OF THE METHOD FOR THE DISSOLUTION OF CELLULOSE IN LiCl/DMAc	42
3.2.1 Experimental	42
3.2.1.1 <i>Solvent and mobile phase preparation</i>	42
3.2.1.2 <i>Sample preparation</i>	43
3.2.1.3 <i>Optimisation of activation and dissolution</i>	43
3.2.1.3.1 High temperature activation and dissolution	44
3.2.1.3.1.1 <i>High temperature activation</i>	44
3.2.1.3.1.2 <i>High temperature dissolution</i>	44
3.2.1.3.2 Polar medium swelling activation followed by warm, ambient or cold dissolution	44
3.2.1.3.2.1 <i>Polar medium swelling and solvent exchange</i>	45
3.2.1.3.2.2 <i>Dissolution</i>	45
3.2.2 Results	45
3.2.2.1 <i>High temperature activation and dissolution</i>	45
3.2.2.2 <i>Polar medium/solvent exchange activation and dissolution in warm, ambient or low temperature</i>	46
3.2.2.2.1 Polar medium/solvent exchange activation	46
3.2.2.2.2 Warm, ambient or low temperature dissolution	48
3.2.3 Conclusion of the activation and dissolution study	48
3.2.4 Final procedure for activation and dissolution	50
3.2.4.1 <i>Final procedure for activation</i>	50
3.2.4.2 <i>Final procedure for dissolution</i>	50
3.3 STABILITY OF CELLULOSE/LiCl/DMAc SOLUTIONS	51
3.3.1 Experimental	51
3.3.2 Results	52
 CHAPTER 4. SIZE-EXCLUSION CHROMATOGRAPHY (SEC) AND MULTIANGLE LIGHT SCATTERING (MALS) DETECTION: PRINCIPLES AND APPLICATION TO THE STUDY OF CELLULOSE	 55
<i>Abstract</i>	56

4.1	MOLAR MASS (M_r) DETERMINATION AND CHOICE OF DETECTION IN SEC	56
4.1.1	Relative M_r determination: conventional calibration	56
4.1.2	Absolute M_r determination	57
	4.1.2.1 <i>Universal calibration</i>	58
	4.1.2.2 <i>Light scattering</i>	58
	4.1.2.2.1 Theory and principles	58
	4.1.2.2.2 MALS and SEC/MALS experiments	60
4.2	APPLICATION OF SEC/MALS TO THE STUDY	64
4.2.1	The instruments	64
4.2.2	Experimental determination of the parameters in the LS equation for calculation of M_w	65
	4.2.2.1 <i>Determination of the calibration constant a of the DRI</i>	66
	4.2.2.1.1 Background	66
	4.2.2.1.2 Experimental determination of α	66
	4.2.2.2 <i>MALS detector</i>	67
	4.2.2.2.1 Calibration of the MALS detector	67
	4.2.2.2.2 Normalisation of the MALS detector	68
	4.2.2.2.2.1 <i>Background</i>	68
	4.2.2.2.2.2 <i>Normalisation</i>	68
	4.2.2.2.3 Alignment	70
	4.2.2.3 <i>Measurement of the refractive index increment (dn/dc) of cellulose in 0.5% LiCl/DMAc</i>	71
	4.2.2.3.1 Background	71
	4.2.2.3.2 Determination of dn/dc	71
	4.2.2.4 <i>Influence of the second virial coefficient A_2</i>	74
4.2.3	SEC method for cellulose in LiCl/DMAc	75
	4.2.3.1 <i>Sample preparation</i>	75
	4.2.3.2 <i>SEC/MALS/DRI instrumental set-up</i>	76
	4.2.3.3 <i>Separation</i>	77
	4.2.3.4 <i>Precision and repeatability of the method</i>	78
4.2.4	Conformation of cellulose in solution and solvent quality	79
 CHAPTER 5. EVALUATION OF DIFFERENT METHODS FOR THE CHARACTERISATION OF CELLULOSE: SIZE-EXCLUSION CHROMATOGRAPHY USING DIRECT DISSOLUTION, SIZE-EXCLUSION CHROMATOGRAPHY USING DERIVATISATION, AND VISCOMETRY		89
	<i>Abstract</i>	89
5.1	INTRODUCTION	90
5.2	AIM OF THE STUDY	91
5.3	EXPERIMENTAL	91

5.3.1	Description of the methods	91
	5.3.1.1 <i>Viscometry in Cadoxen</i>	92
	5.3.1.2 <i>Size-exclusion chromatography (SEC) of cellulose tricarbaniolate in THF</i>	92
	5.3.1.3 <i>SEC of underivatised cellulose in LiCl/DMAc</i>	92
5.3.2	Sample preparation	93
	5.3.2.1 <i>Preparation of the paper samples</i>	93
	5.3.2.2 <i>Sampling for viscometry and SEC</i>	93
5.4	RESULTS AND DISCUSSION	94
5.4.1	Unaged cellulose (UA)	94
	5.4.1.1 <i>SEC of UA</i>	94
	5.4.1.1.1 Precision of the SEC methodologies	96
	5.4.1.1.1.1 <i>Precision of the methodology of SEC_{CTC}</i>	96
	5.4.1.1.1.2 <i>Precision of the methodology of SEC_{DDC}</i>	97
	5.4.1.1.2 Study of the discrepancies due to the dissolution processes	98
	5.4.1.2 <i>Viscometry of UA</i>	103
5.4.2	Aged cellulose (At ₉₄)	104
	5.4.2.1 <i>SEC of At₉₄</i>	104
	5.4.2.2 <i>Viscometry of At₉₄</i>	108
5.4.3	Simplicity and cost effectiveness of the methods	109
5.5	CONCLUSION	109

CHAPTER 6. THE AGING OF PAPER AND THE INFLUENCE OF GELATINE ON THE DEGRADATION PROCESS, A STUDY USING SEC/MALS, pH AND COLOUR MEASUREMENTS

		113
	<i>Abstract</i>	113
6.1	INTRODUCTION	113
6.2	DESCRIPTION OF THE PAPERS STUDIED	114
	6.2.1 Model papers	114
	6.2.1.1 <i>Preparation of the samples</i>	114
	6.2.1.2 <i>Artificial aging</i>	116
	6.2.2 Naturally aged papers	116
6.3	DEGRADATION OF CELLULOSE CHARACTERISED BY SEC/MALS	117
	6.3.1 Experimental: sample preparation and SEC procedure in LiCl/DMAc	117
	6.3.2 Results and discussion	118
	6.3.2.1 <i>SEC/MALS applied to the study of model papers</i>	118
	6.3.2.1.1 The aging of pure cellulose paper	118
	6.3.2.1.2 Kinetics of the degradation of pure cellulose paper	124
	6.3.2.1.3 The aging of gelatine sized pure cellulose paper	126
	6.3.2.1.4 The aging of Arches paper	132
	6.3.2.2 <i>SEC/MALS applied to the study of naturally aged historic papers</i>	135

6.3.2.2.1	Seventeenth and eighteenth century papers	135
6.3.2.2.2	Strathmore papers	139
6.3.3	Conclusions on SEC/MALS	144
6.4	COLOUR MONITORING OF UNSIZED AND SIZED PAPERS DURING AGING	145
6.4.1	Experimental	145
6.4.2	Results and discussion	146
	6.4.2.1 <i>Pure cellulose paper</i>	146
	6.4.2.2 <i>Gelatine sized pure cellulose paper</i>	147
	6.4.2.3 <i>Arches papers</i>	150
	6.4.2.4 <i>Naturally aged Strathmore papers</i>	151
6.4.3	Conclusions on colour measurements	152
6.5	pH OF MODEL PAPERS	152
6.5.1	Experimental	152
6.5.2	Results and discussion	153
6.5	INVESTIGATION INTO CORRELATIONS BETWEEN pH, COLOUR MEASUREMENTS AND M_r ,	154
6.6.1	Background	154
6.6.2	Correlation between M_r , pH and colour measurements	156
6.7	CONCLUSION	158
CHAPTER 7. THE INFLUENCE OF GELATINE AND ALUM IN PAPER STUDIED WITH SEC/MALS, pH AND COLOUR MEASUREMENTS		163
	<i>Abstract</i>	163
7.1	INTRODUCTION	163
7.2	DESCRIPTION OF THE MODEL PAPERS STUDIED	164
	7.2.1 Preparation of the samples	164
	7.2.2 Artificial aging	165
7.3	DEGRADATION OF CELLULOSE CHARACTERISED BY SEC/MALS	165
	7.3.1 Experimental: sample preparation and chromatographic procedure in LiCl/DMAc	165
	7.3.2 Results and discussion	165
	7.3.2.1 <i>The impact of alum in the model papers</i>	165
	7.3.2.2 <i>The impact of gelatine/alum in the model papers</i>	171
	7.3.3 Conclusions on SEC/MALS	171
7.4	COLOUR MONITORING OF THE MODEL PAPERS CONTAINING GELATINE AND/OR ALUM DURING AGING	175
	7.4.1 Experimental	175
	7.4.2 Results and discussion	176
	7.4.2.1 <i>The impact of alum in the papers</i>	176
	7.4.2.2 <i>The impact of gelatine/alum in the papers</i>	178

7.5	pH OF ALUM PAPERS AND GELATINE/ALUM PAPERS	181
7.6	INVESTIGATION INTO CORRELATIONS BETWEEN pH, COLOUR MEASUREMENTS AND M_r	182
	7.6.2 Correlations based on the parameter time	182
	7.6.3 Correlations based on the parameter of the alum concentration	184
7.7	CONCLUSION	186

CHAPTER 8. STUDY OF THE DEGRADATION OF GELATINE IN PAPER UPON AGING USING AQUEOUS SIZE-EXCLUSION CHROMATOGRAPHY 189

Abstract 189

8.1	INTRODUCTION	189
8.2	EXPERIMENTAL	191
	8.2.1 Samples description	191
	8.2.2 Artificial aging	192
	8.2.3 Conditions	192
	8.2.3.1 <i>Method and instrumentation</i>	192
	8.2.3.2 <i>The mobile phase</i>	193
	8.2.3.3 <i>Sample preparation</i>	193
	8.2.4 Calibration	193
	8.2.5 Method validation (220 nm): precision, linearity and limit of detection	195
8.3	RESULTS AND DISCUSSION	196
	8.3.1 The choice of the mobile phase	196
	8.3.2 SEC of gelatine extracted from Whatman No. 1 papers	197
	8.3.2.1 <i>Papers without alum</i>	197
	8.3.2.1.1 Extraction yields of gelatine from unaged and aged papers	197
	8.3.2.1.2 M_r determination and MMD profiles of gelatine from unaged papers	197
	8.3.2.1.3 M_r determination and MMD profiles of gelatine from aged papers	198
	8.3.2.2 <i>Papers with alum</i>	202
	8.3.3 SEC of gelatine extracted from Arches papers	204
	8.3.4 SEC of gelatine extracted from naturally aged papers	205
	8.3.5 Absorption at 254 and 280 nm	206
8.4	CONCLUSIONS	206

GENERAL CONCLUSION 211

APPENDIX 3-1. MAILLARD REACTIONS 213

APPENDIX 5-1. VISCOMETRY METHOD FOR THE ANALYSIS OF DILUTE SOLUTIONS OF CELLULOSE IN CADOXEN 215

A5-1.1 EXPERIMENTAL	215
A5-1.1.1 The dissolution method	215
A5-1.1.1.1 <i>Cadoxen solvent preparation</i>	215
A5-1.1.1.2 <i>Sample pre-treatment</i>	215
A5-1.1.1.3 <i>Dissolution</i>	216
A5-1.1.1.4 <i>Sample solutions</i>	216
A5-1.1.2 Viscosity measurements	216
A5-1.2 CALCULATION OF THE INTRINSIC VISCOSITY AND DP_v	217
APPENDIX 5-2. SIZE-EXCLUSION CHROMATOGRAPHY (SEC) METHOD FOR THE ANALYSIS OF CELLULOSE TRICARBANILATE (CTC) IN TETRAHYDROFURAN	221
A5-2.1 PREPARATION OF THE CELLULOSE TRICARBANILATES	221
A5-2.1.1 Theory: equations	221
A5-2.1.2 Experimental	222
A5-2.1.2.1 <i>Activation</i>	222
A5-2.1.2.2 <i>Derivatisation reaction</i>	222
A5-2.1.2.3 <i>Stop reaction</i>	223
A5-2.1.2.4 <i>Recovery and cleaning</i>	223
A5-2.2 SEC METHOD	223
A5-2.2.1 Dissolution of the CTC	223
A5-2.2.2 SEC method of CTC in THF	224
A5-2.2.2.1 <i>Instrumentation and setup</i>	224
A5-2.2.2.2 <i>KMX-6 characteristics and LALS theory</i>	224
A5-2.2.2.3 <i>Calculation of M_r averages and concentration</i>	226
A5-2.2.2.4 <i>Separation</i>	227
APPENDIX 6-1. SPECIFICATION DATA SHEETS OF THE GELATINES USED IN THIS STUDY	229
APPENDIX 6-2. CALCULATIONS OF THE UPTAKE OF GELATINE IN THE PAPERS	231
A6-2.1 MOISTURE CONTENT OF WHATMAN NO.1 UNSIZED AND SIZED WITH GELATINE	231
A6-2.2 RELATIONSHIP BETWEEN GELATINE CONCENTRATION IN SOLUTION AND GELATINE UPTAKE IN THE PAPER	232
A6-2.3 MOISTURE CONTENT OF GELATINE	233
APPENDIX 6-3. KINETIC MODELS FOR CELLULOSE CHAIN SCISSION	235
A6-3.1 MODEL PROPOSED BY EKAMSTAM	235
A6-3.2 MODEL PROPOSED BY HILL ET <i>al.</i>	237

APPENDIX 6-4. COLOUR MEASUREMENTS	239
A6-4.1 INSTRUMENTATION	239
A6-4.2 CIE L*a*b* TRICHROMATIC SYSTEM	239
A6-4.3 CIE L*C*h SCALE	240
A6-4.4 OTHER COLORIMETRIC PARAMETERS MEASURED	241
A6-4.4.1 ISO brightness R457	241
A6-4.4.2 YI E313-96 and WI E313-96 (ASTM)	241
APPENDIX 8-1. INFLUENCE OF THE PH AND THE IONIC STRENGTH OF THE MOBILE PHASE ON THE MMD PROFILES OF GELATINE AGED AND UNAGED	243
SUMMARY	245
SAMENVATTING	249
LIST OF PUBLICATIONS RELEVANT TO THE THESIS	253
ACKNOWLEDGEMENTS	255

General Introduction

For several decades one of the major concerns in cellulose research has been, and still is, the issue of permanence and durability of paper. A number of past and recent studies investigated in depth the roles played by the paper components in the degradation process of cellulose. As early as the twentieth century, the poor long-term stability of certain types of paper, such as ground wood pulp paper sized with alum and rosin, brought about a general consensus among the conservation professionals and the industry on the need for adapted conservation measures and research into new and less aggressive pulping and sizing processes.

From the conservation research perspective, understanding the long-lasting properties of paper logically starts with directing the investigations towards the characteristics of those papers that have survived for centuries and still remain in good physical condition. This is the case for early European papers from the fourteenth to the eighteenth centuries, which for the most part, are at present in far better conservation conditions than papers of more recent origins. Indeed, certain factors responsible for the longevity of historic papers have been extensively investigated. Some of these include the purity of the source of cellulose, related to the fibre's origin, the presence of mineral salts used as fillers, or the lack of metal inclusions. Many studies also pinpointed early on that low content of both lignins and hemicelluloses was a factor of paper longevity. The studies showed that these wood residues, which are found in large amounts in papers from the nineteenth and the early twentieth centuries, accelerated paper degradation. However, a particular aspect that has received little attention among the diversity of paper components is the sizing material, and especially gelatine, as this protein was used in early European papermaking.

The modern definition of sizing refers to the treatment of paper carried out in order to achieve resistance to the sorption of liquid, either by means of additives incorporated in the papermaking furnish (internal sizing) or by surface application to a formed and dried paper (surface sizing). The historical definition refers to a hybrid form of surface sizing, as it was done after the sheet formation but involved an immersion process, and as such achieved a total penetration of the size in the paper web.

The practices in early European paper mills were inherited from oriental papermaking. They were adapted to the needs and resources of European mills and pioneered in Italy at Fabriano in the second half of the thirteenth century. They underwent various modification stages throughout the thirteenth to the eighteenth centuries as the production pace increased due to the economic expansion. This expansion was feeding an ever-growing demand linked to the commercial, administrative, educational, literary and

artistic activities [1]. The nineteenth century represents a turning point in the history of papermaking, as it witnessed the rise of industrialisation, which led to wood pulp papers.

If in early papermaking the practices are fairly homogeneous compared to those of industrial papermaking, those of the fourteenth century are however hard to compare to those of the eighteenth century on the basis of the literature available. This is mostly due to the scarceness and disparity in the sources of information. But practices also changed with time, as paper passed from being a rare and expensive material, reserved to artistic, intellectual and political use, to becoming a basic commodity. Nevertheless, all along, the imperatives of quantity were common ground with those of quality, and specific skills were needed. In a paper mill, tasks were rigorously divided amongst the “beaterman”, “vatman”, “coucher”, “layer” and the “sizeman”, who were highly qualified workers [2]. Sizing in particular, which required gelatine, and was carried out following the formation of the paper sheet, demanded precise manual skills. These consisted for instance of a rapid yet even manoeuvre, as well as knowledge of the animal by-products to be used, and awareness of the atmospheric conditions that influence the quality of the drying process.

Diderot [2] describes the use of leather, hides, ears, tripe, feet, bones, parchment clippings, and other scraps of any four-footed animal except pig, available from nearby slaughterhouses, tanners or butchers. These were boiled until all the gelatine was extracted. De Lalande [3] observed that sturgeon gelatine that was used to size paper in Holland during the same period yielded what he qualified as the finest quality paper in Europe.

The gelatine solution was then filtered twice by straining it through a cloth, and sometimes was even diluted with water [3], as the proper consistency of the size was subjectively appreciated by the “sizeman”. Diderot [2] and De Lalande [3] describe how a small pile of paper sheets, called “*porce*” (approximately 260 sheets), was dipped into a large copper vat or tub where the gelatine size was kept under moderate heat (around 40°C), as the early papermakers knew that the control of temperature at this stage was crucial. Indeed, at high temperature the proteins become denatured. As the preparation of the gelatine size already involves high temperatures, further denaturation had to be avoided, as it would result in a lower viscosity and hence a poorer quality of the size. The tub-sizing procedure is still in use to date for high quality and artist papers, and is carried out in automated tub-sizers [4].

Papers were then lightly pressed to remove the excess gelatine, which was recycled and reused, and they were allowed to cool in a stack before drying, usually in a loft, by hanging each sheet individually [2,5].

As any protein, gelatine is subject to biodeterioration and fairly quickly degrades at ambient temperature in the presence of moisture. Alum, in the form of aluminium potassium sulphate hydrate ($[AlK(SO_4)_2, yH_2O]$) was added to the size mainly as a preservation agent in order to prevent its rapid putrefaction, but had a number of

additional properties. It acted as a binder between the gelatine and the paper, increased the rattle of the paper, prevented newly sized sheets from adhering to each other, and helped adjusting the consistency of the size. Added in moderation, alum increased the viscosity of the size, yet it decreased it when in larger quantity [6].

Alum was added to the warm gelatine solution after the filtering step, either directly in the form of dry crystals, or as an aqueous solution [6]. Gelatine size and alum could also be applied in two steps, the paper being sized first, and then immersed in an aqueous solution of alum [7]. The sizeman evaluated the alum concentration in the size by tasting its bitterness. According to De Lalande [3], the weight of alum added to the gelatine solution was about one twentieth the weight of the size solution (*i.e.* 5% by weight).

Aluminium potassium sulphate hydrate was extracted from minerals such as alunite, slate, schist and shale [6]. Although its use is already mentioned in sixteenth century recipes, the way it was introduced in papermaking practice remains quite uncertain. It may already have been used in the first European paper mill at Fabriano [6], although no source can confirm this. In the mid-nineteenth century, the double aluminium and potassium salt was replaced in papermaking factories by aluminium sulphate hydrate $[\text{Al}_2(\text{SO}_4)_3, y\text{H}_2\text{O}]$, also called papermakers' alum [6], as the latter became more easily available on an industrial scale. However it was also frequently contaminated with impurities such as iron or the residual sulphuric acid that was used to extract it from the clay and the bauxite ore [6]. The use of alum persisted as alum-rosin was used to size mechanical wood pulp papers from the very early nineteenth well into the twentieth century. Nowadays rosin size is still widely used by the papermaking industry for current quality paper, in the form of dispersed size (free rosin dispersion of resin acids) or soap size (sodium salts of resin acids), and alum remains a necessary additive in the process. Sodium aluminate (NaAlO_2), an alkaline source of aluminium can be used as a partial substitute for alum in rosin soap sizing. However, the need to produce alkaline paper and permanent paper and the use of calcium carbonate filler led to the development of synthetic compounds such as alkyl ketene dimer (AKD) and alkenyl succinic anhydride (ASA) sizes [8,9], which first appeared in 1953 and 1974 respectively [10]. This variety of sizing materials available did never overshadow gelatine/alum sizing which to date continues to be used for fine and artist quality papers.

The best gelatine sizes were those yielding the stiffest gel when cold [11]. The amount of size in the papers depended on their intended use. Historically, for optimal writing properties, the sheets were heavily sized to prevent feathering and blotting effects. Sometimes the paper was passed several times through the size tub until the sizing was considered sufficient. Diderot [2] reports that after sizing, the sheets of paper intended for writing were rubbed with sandarac resin on the writing side. Then on that same side, a solution of alum and brown sugar was applied with a sponge. During the nineteenth century, dry gelatine in the form of powder or sheets became available to papermaking factories. Recipes from that period were therefore more reproducible, although they varied widely among manufacturers.

As mentioned earlier, sizing has been largely neglected to date as a possible factor in the longevity of early European papers. Few studies have been carried out, and some attribute to gelatine a buffering capacity either by reacting with the acids, thus protecting paper from acidic species, such as degradation products and atmospheric or indoor pollutants, or by forming a physical barrier that limits the access of oxygen, acids and other reactive species to the cellulose [12,13]. These studies were the trigger and starting point for the present research. However, their main focus was either on macroscopic examinations, *i.e.* the physical integrity and increased mechanical properties of the paper, or on elemental analysis, by quantifying certain elements in the papers that could explain their durability, such as high levels of calcium, and/or low levels of potassium and aluminium [13,14,15]. Never did they attempt to investigate how the benefits of gelatine sizing translated at the molecular level. It seemed therefore that gelatine sizing and its potentially beneficial effect on paper needed further investigation, and that the new research would have to be directed towards a different aspect, that is the macromolecular level.

Therefore, in the present research the role of gelatine in pure cellulose paper was investigated mainly from the chemical point of view. The changes that occurred upon aging in the molecules of cellulose whether the paper was sized or unsized, and depending on the sizing procedure as well as on the type of gelatine were characterised. The main technique used, size-exclusion chromatography (SEC), was selected from among other commonly used techniques for cellulose analysis for its sensitivity to small chemical changes, thus providing a precise determination of the molar mass and molar mass distribution of polymers. SEC was used for the characterisation of both the cellulose and the gelatine, and two different methods were developed for this purpose. In the method for the analysis of cellulose, the coupling of SEC with the detection technique of multiangle light scattering (MALS) allowed the determination of the absolute values of the molar mass and size of the polymer (radius), from which other characteristics, such as the polymer conformation in solution could be derived. The method developed using this technique was compared with other chromatographic and viscometric methods commonly used for cellulose characterisation.

The methodology that was developed for dissolving the paper in order to perform SEC was evaluated compared to other methods, with the aim of studying the efficiency and the inertness of the solvent. Light scattering detection provided important information in that respect. Nevertheless, as the analytical and polymer chemistry techniques used to characterise such chemical changes are not easily available to the paper conservation practitioner, other methods more commonly used for macroscopic examination were included in order to search for possible macroscopic changes that would assist in the molecular characterisation and reflect the actual degradation state.

With regard to the materials and methods and their implementation for the present study, the short review of historic sizing reported earlier showed that, if gelatine, and later alum, were always present, no one single recipe prevailed, as the raw materials and the practices varied both with geography and time. Historic recipes are fairly imprecise and therefore

difficult to reproduce. However, for the purpose of the present research, in order to model early practices, it was important to study and understand them. The study by Barrett and Mosier [16] on fifteenth to eighteenth century papers was used as a guide for the range of amounts of gelatine needed to size the model papers. However, historic seventeenth and eighteenth century recipes [2,3] and early industrial twentieth century gelatine sizing and gelatine/alum sizing procedures for artists' papers were also taken into account to finalise the range of concentrations required [4,11,17,18,19]. The model papers prepared were artificially aged, as no closer tool to an exact natural aging process is available to date in conservation research to mimic and understand the degradation processes of materials. Naturally aged historic papers were also included in the study, in order to relate the findings obtained with the model papers as much as possible to real case situations.

However, it has to be noted that, as is generally the case in conservation science, one of the biggest challenges of research project such as in the present study resides in being able to correctly extrapolate the results obtained from models to real artefacts. One important role of scientific research in the conservation field is to assess the overall state of deterioration of materials to help predict the life expectancy of objects of the cultural heritage. Finding ways of increasing the longevity of these artefacts and understanding the degradation pathways of the materials upon aging are important in the evaluation of the conservation needs of collections, and the design of proper long-term preservation strategies.

This study is therefore not intended as an exhaustive investigation on the effects of gelatine sizing and gelatine/alum sizing on the longevity of paper, but as a contribution to the knowledge of the materials used historically in papermaking and their behaviour in time.

References

1. Reynard, P.C. *Looking at Paper: Evidence and Interpretation Symp. Proc.*, Slavin, J.; Sutherland, L.; O'Neill, J.; Haupt, M. and Cowan, J. Eds, Toronto (1999) 112-121.
2. Diderot, J.J. *Encyclopédie ou Dictionnaire Raisonné de Sciences, des Arts et des Métiers, par une Société de Gens de Lettres*, 11, A. Neufchastel, Samuel Faulche et Compagnie (1765).
3. De Lalande, J.J.J.F. *Art de faire le papier*, Académie Royale des Sciences (1761).
4. *Paper Making, A General Account of Its History, Processes, And Applications*, The Technical Section of the Paper Makers' Association, 1912 (Inc) (1949) 168-169.
5. Green, S.B. *Conference Papers Manchester 1992*, Institute of Paper Conservation, Fairbrass, S. Ed., Leigh Lodge (1992) 197-200.
6. Brückle, I. *Conference Papers Manchester 1992*, The Institute of Paper Conservation, Fairbrass, S. Ed., Leigh Lodge (1992) 201-206.
7. Brückle, I. *Abbey Newsl.*, 17, 4 (1993) 53-57.
8. Scott, W.E. *Principles of Wet End Chemistry*, Ch. 12 to 14, TAPPI Press, Atlanta, GA, (1996), 85-110.

-
-
9. Au, C.O. *Paper Chemistry*, Ch. 13, Roberts, J.C. Ed., 2nd Ed., Blackie, Glasgow (1996) 250-263.
 10. Roberts, J.C. *Paper Chemistry*, Ch. 9, Roberts, J.C. Ed., 2nd Ed., Blackie, Glasgow (1996) 140-160.
 11. Norris, F.H. *Paper and Paper Making*, Ch. 16, Oxford University Press (1952) 228.
 12. Wilson, W.K. and Parks, E.J. *Restaurator*, Int. J. for the Preservation of Library and Archival Material 5 (1983) 191-241.
 13. Barrett, T. *Conference Papers Manchester 1992*, The Institute of Paper Conservation, Fairbrass, S. Ed., Leigh Lodge (1992) 228-233.
 14. Barrow, W.J., *Manuscripts and Documents: Their Deterioration and Restoration*, University Press of Virginia (1972) 35-37
 15. Barrett, T. *Paper Conservator*, 13 (1989) 1-108.
 16. Barrett, T. and Mosier, C. *J. Am. Inst. Conserv.*, 34 (1995) 173-186.
 17. Balston, T. *The Mill Ledger, James Whatman, Father and Son*, Balston, T. Ed, James Whatman, Father and Son, Methusen, London (1957) 59.
 18. Norris, F.H. *Paper and Paper Making*, Ch.16, Norris, F.H. Ed., Oxford University Press, Oxford (1952) 228.
 19. Sanburn, W.H. *personal folder notebook*, Waroronoro Paper, MA (1909).

Chapter 1. Accessibility, solubility and reactivity of cellulose substrates

Abstract

In order to better comprehend the solvation mechanism, the structure of cellulose and the characteristics of the molecule that condition its accessibility to reactants are presented. The types of activation necessary prior to the dissolution of cellulose are reviewed, together with the most current solvents used, and their properties. Finally, the mechanism of acid-catalysed hydrolysis of cellulose, which is the most relevant degradation pathway of cellulose for the present study, is briefly presented.

1.1 Introduction

Research into new solvent systems for non-water-soluble polysaccharides, such as cellulose, is an area of constant development mostly because of the significant economical impact these polymers have in the pharmaceutical, food, paper and textile industries. In that respect, it is important to study solution properties of polysaccharides, because this knowledge is essential in order to determine their structure and molar mass distribution and predict their behaviour in processes and products. This knowledge is essential for the optimisation of the end-use functions of polysaccharides. Nevertheless, the characterisation of polysaccharides of natural origin is often a difficult task.

In the area of preservation of cultural objects, the stakes are different, but the knowledge and development of methods for polysaccharide analysis are no less important. Research applied to paper and its degradation and to polymers used in the field of conservation of cultural heritage, whether they are constituents of objects or materials used in the preservation and conservation of the objects, directly benefits from the advances in research in the academic and applied industrial fields.

The choice of appropriate methods for analysis and characterisation of polymers strongly depends on their nature and the type of information sought. Except in the case of techniques such as solid-state Nuclear Magnetic Resonance (NMR) or Matrix-Assisted Laser Desorption/Ionisation–Time Of Flight Mass Spectrometry (MALDI-TOF MS), the methods most often used for the determination of the molar mass are usually based on a solubilisation of the polymer in a suitable solvent.

The present chapter reviews the characteristics of cellulose that are relevant in the frame of this study to understand the behaviour of the polymer in solution and when submitted to chemical degradation. The properties of cellulose that govern the accessibility to solvent molecules and the type of solvents that can be used are presented. Finally, the mechanism of degradation of cellulose by acid-catalysed hydrolysis is given.

1.2 The fibre structure

In order to understand the accessibility to solvents and how the molecule chemically reacts it is important to consider the structure of the cellulose fibre and the forces linking the molecules together. The reader can be referred to several good reviews [1,2,3,4,5] for further details on cellulose structure.

As most natural polymers, cellulose has several organisational levels:

- The molecular level, determined by molecular composition, molar mass distribution and intramolecular bonding (hydrogen-bonding),
- The supramolecular level, determined by the intermolecular hydrogen-bonding and the aggregation of macromolecules into elementary crystals and fibrils,
- The morphological level, determined by the superior level of organisation from elementary fibrils to fibres and to cell wall layers.

1.2.1 Molecular level

Cellulose is a linear homopolysaccharide made of repeating units of β -(1,4)-D-glucopyranose. The carbon atoms in the pyranose ring are numbered 1 to 5, and the carbon in the attached methanolic group is numbered 6 (Figure 1-1).

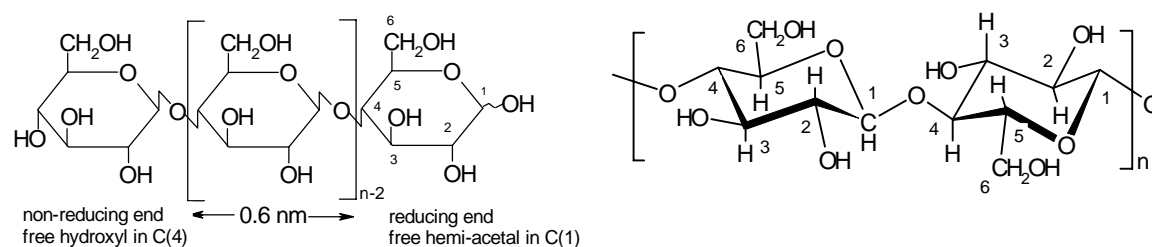


Figure 1-1. Cellulose molecule, planar (left) and 3-D (right) representations.

Depending on the plant source, native cellulose, *i.e.* cellulose that did not undergo any alteration after biosynthesis, can reach average degrees of polymerisation (DP) higher than 10,000, in other words average molar masses above $1.5 \times 10^6 \text{ g mol}^{-1}$.

After processing into pulp and paper substrates, cellulose becomes composed of a mixture of polymers differing in chain length. This is a characteristic of most polymers, and is called polydispersity (PD). Whether cellulose in its native state is or not polydisperse is still debated, but although this has not been studied, there is no obvious reason to believe it would not be. Typically, undegraded cellulose from cotton in paper is composed of molecules with DP ranging from 1,000 to 12,000, *i.e.* molar masses spanning from 2×10^5 to $2 \times 10^6 \text{ g mol}^{-1}$, with the average molar mass usually within 4×10^5 to $8 \times 10^5 \text{ g mol}^{-1}$. Polydispersity greatly depends on the source of cellulose; cotton and linen cellulose is less polydisperse than wood cellulose. On the other hand it depends also on the degradation state and on the degradation mechanism.

Secondary valence intramolecular hydrogen bonding is a key feature in cellulose and occurs between two oxygen atoms of two hydroxyl groups or between one oxygen atom of a hydroxyl group and the ring oxygen. Although still currently debated, the intramolecular H-bonds are thought to occur between O(6)H and O(2)H and between O(3)H and cyclic (O) (Figure 1-2).

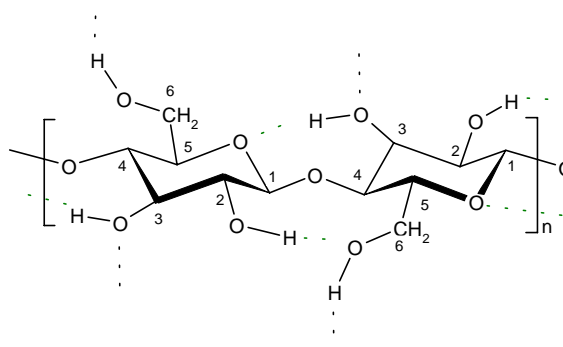


Figure 1-2. Representation of intramolecular hydrogen bonding in cellulose between O(6)H and O(2)H, and between O(3)H and cyclic (O).

1.2.2 Supramolecular level

Hydrogen bonding occurring between the oxygen atoms of hydroxyl groups of different molecules is the basis of the supramolecular structure of cellulose fibres. Intermolecular hydrogen bonds are thought to occur between O(3)H and O(6)H in the *ac* plan (Figure 1-3), but this is not ascertained. Assisted by dipole and van der Waals interactions occurring in the *b* plan (Figure 1-4), H-bonding favours the alignment in parallel strands resulting in a highly regular sequence and rigid molecular chains. The average distance between cellulose chains is 0.54 nm.

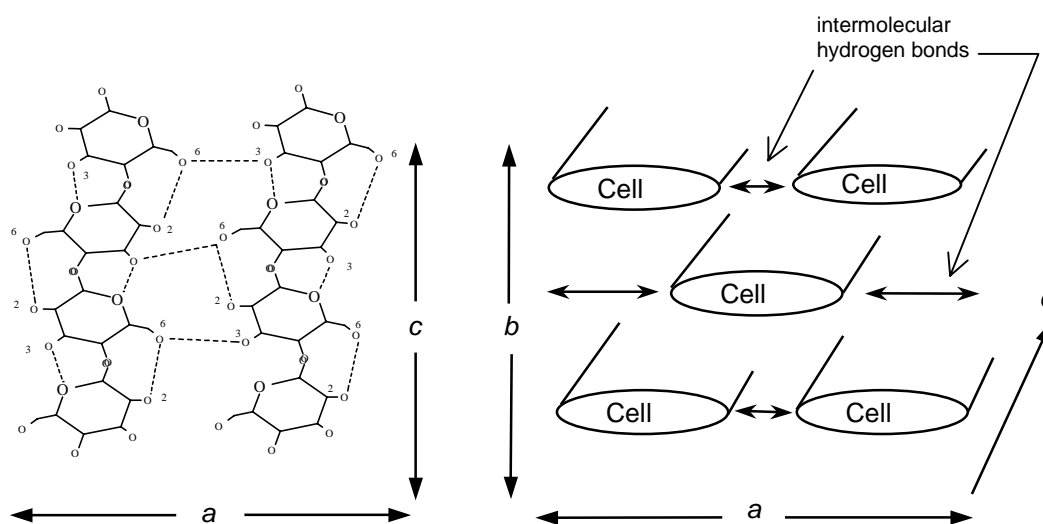


Figure 1-3. Intermolecular hydrogen bonds in cellulose between O(3)H and O(6)H.

Figure 1-4. Alignment of cellulose molecules in parallel strands

The basic fibrillar element is the elementary fibril with dimensions of 2-4 nm in cross-section and 100 nm in length. Elementary fibrils are composed of successions of elementary crystallites. The internal cohesion between the crystallites is achieved through polymer molecules extending from less ordered interlinking and non-crystalline regions (Figure 1-5). This is the “fringe-fibrillar” model of fibre structure proposed by Hearle in 1958 [6] that was experimentally confirmed in more recent studies by Pionteck *et al.* [7]. Despite some current controversy it is nonetheless a widely accepted model.

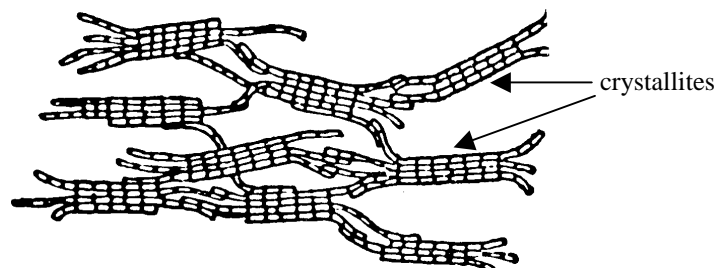


Figure 1-5. Structure model of cellulose (from Gardner and Blackwell [8])

The first studies in the 1920s on crystal arrangement of the cellulose molecules in the crystallites classified both native and modified cellulose based on their X-ray diffraction patterns. Native cellulose from any source was defined as presenting “cellulose-I” crystal lattice structure. The hydroxyl groups in the interior of the crystals, involved in intermolecular hydrogen bonds, are responsible for the very dense and packed structure of the crystal lattice. Slight differences in the description of the cell unit arrangements are reported in the literature and the debate on the exact crystal structure of native cellulose remained active until the mid-1980s. These slight differences seemed to be most likely due to the fact that during biosynthesis, cellulose having different chain arrangements are produced, resulting in basic unit cells that vary slightly from each other [2]. In 1984, the discovery of a crystalline dimorphism of native cellulose by Vanderhaart and Atalla [9]

shed some light on the debate. Using solid state ^{13}C NMR, the authors established that native cellulose was composed by two distinct crystalline phases, which they called $\text{I}\alpha$ and $\text{I}\beta$, and that these were present in variable proportions depending on the cellulose source. Cellulose in phase $\text{I}\alpha$ is dominantly produced by lower organisms such as bacteria and algae whereas cellulose from higher plants is mainly in phase $\text{I}\beta$.

The molecule arrangement within the crystal units in parallel or antiparallel strands remains unresolved. The most currently accepted model for native cellulose (cellulose-I) and regenerated cellulose (cellulose-II) is the antiparallel arrangement model as first proposed by Meyer *et al.* [10].

1.2.3 Ultrastructure: the fibre

Native cellulose fibres are single plant cells. They have different morphologies depending on their origin. Cotton fibres are isolated long lint and linter fibres. Therefore the cellulose in paper from cotton fibres is always relatively pure. Wood pulp on the other hand, even when highly processed, contains certain amounts of other constituents, as in wood the fibres are bound together by a cement-like polymeric complex composed of lignins highly linked to hemicelluloses. This cement is present in the cell wall and the middle lamella.

The ultrastructure of native celluloses is the more or less random aggregation of elementary fibrils into microfibrils of 10-30 nm width, themselves grouped into macrofibrils 100-400 nm wide, which are structured in different cell wall layers. In wood fibres, hemicelluloses and traces of lignin are involved in the microfibrillar assembly at the periphery of the cellulose well-ordered chains. Hemicelluloses play the role of an adhesive that impregnates the microfibrils. The cell wall layered structure of cotton fibres and wood fibres is shown in Figure 1-6 (A) and (B).

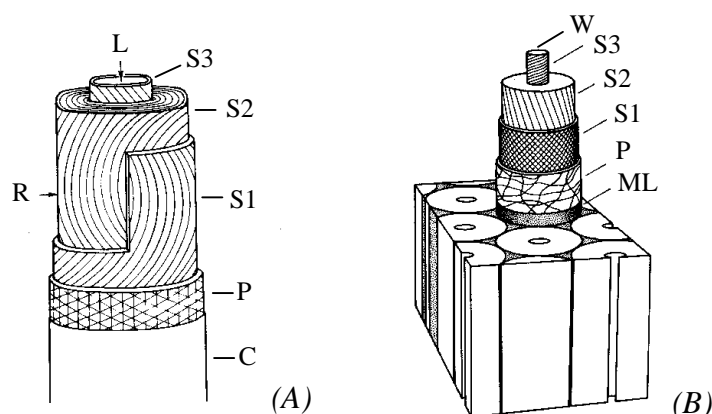


Figure 1-6 . Morphological structure of a cotton fibre (A), and a wood fibre (B). L= lumen, S1 = secondary wall outer layer, S2 = secondary wall middle (main) layer, S3 = secondary wall inner layer, R = reversal of the fibril spiral, P = primary wall, C = cuticle (pectins, waxes, fats), W = wart layer (lining the fibre lumen, present in conifers and in some hardwoods), ML = middle lamella (mainly lignin and hemicelluloses complexes). Figures are reproduced from Young R.A. & Rowell R.M. [4].

This distinctly layered structure implies the presence of spaces and void volumes. Practically these are interfaces, pores and channels ranging from 1 nm to 5 nm width. For instance, voids about 1 nm wide are present between crystallites inside the elementary fibrils and also in interfibrillar longitudinal crevices [2]. This void system determines the internal active surface and plays an important role in the accessibility and swelling properties of the fibres.

1.3 Accessibility by swelling

The internal cohesion of the fibrillar elements building the cellulose fibres, governed by the inter- and intramolecular hydrogen bonding as described above, considerably limits swelling properties and accessibility of reactive agents to cellulose substrates. This physical hindrance governs the rate of any chemical reaction of cellulose. In this respect, hemicelluloses in the fibres play an important role for the paper strength. As a hydrophilic bulk glue, they are mostly responsible for the inter-fibre bonding in paper, water penetration in the microfibrillar structure, and its opening during pulp refining stages by mechanical friction.

Crystalline swelling can be both inter- or intracrystalline. Only intercrystalline swelling is described below since intracrystalline swelling leads to crystal lattice disturbance (as in cellulose-II), which is not relevant in the frame of the present study.

For a long time, the areas of the fibres that were predominantly amorphous were thought to be the only accessible zones. It was later proven that the molecules located at the surface of crystalline areas and in the interlinking regions between the crystallites were also accessible.

During intercrystalline swelling, the liquid enters through pores and capillaries into the interstices between the fibrillar structure units and swells the less ordered surface areas and the less ordered interlinking areas between the elementary crystallites, the basic fibrils, and their aggregates. In water-swollen state, natural fibres show an increase in cross-sectional surface of 20 to 35%.

At equal crystallinity, accessibility of cellulose substrates to vapour and liquid sorbents will therefore strongly depend on the crystallite size variations and crystal size distribution, as well as on the size and distribution of the interfibrillar interstices. Research on intercrystalline swelling with water yielded useful information such as maximum pore size, average size, pore size distribution and internal surface area. Concepts such as “free water” and “bound water” were postulated [3 (Zeronian, S.H., Ch.5)] in order to differentiate water with varying states of binding as observed with NMR spectroscopy. As opposed to cotton fibres, in wood fibres the presence of hemicelluloses plays an important role in allowing better water and water vapour penetration.

Swelling in organic liquids has been extensively studied by Philipp *et al.* [11]. The time dependence and the extent of swelling in various liquids are determined by the supramolecular and morphological structure of cellulose, as well as by parameters of the swelling liquid such as solubility parameter (δ). The theory of swelling is based on the “pore and void” model described above, with an initial stage depending mainly on the size, distribution and interconnection of voids, as well as on the molar volume of the swelling agent. This can be accompanied by more or less significant splitting of hydrogen bonds, which in turn induces a change in the size and the distribution of the voids.

1.4 Methods of activation of cellulose substrates

In order to achieve uniform chemical reactions or solubilisation of cellulosic substrates, it is important to allow optimal accessibility. Activation is a paramount stage before dissolution and consists in opening the internal pores and cavities and interfibrillar interstices and making them accessible to further action of reactants.

Varying degrees of chemical activation achieved by different liquids can be distinguished, and these are:

- Opening and expanding existing capillaries, interfibrillar voids and interstices as achieved by water, solvents, dilute acids and bases.
- Disruption of fibrillar aggregation, and increase in accessible surface with fluids with a higher swelling power, such as dilute caustic soda (6-10%), dilute quaternary bases or aqueous zinc chloride.
- Disruption of the crystalline structure, such as with liquid ammonia or 20% caustic soda (“mercerising strength”), which induces cellulose-I to cellulose-II (also called viscose) crystal modification.

Treatments by acid hydrolysis and oxidation, thermal and mechanical treatments by grinding, ultrasonic treatment and freeze-drying are also activation methods but they can degrade the molecules to a certain extent.

In the frame of this research the purpose of using activation is to ease solvent access to the cellulose substrate for further efficient dissolution. Therefore, in the following sections the focus will be only on the first type of chemical activation described above, and on mechanical activation, these two methods being used in the present study.

1.4.1 Activation by solvent exchange

With organic solvents, swelling depends on the ability to form hydrogen bonds with cellulose. Especially high swelling is obtained with liquids that are unassociated proton acceptors.

Prior swelling with a liquid of high swelling power (Figure 1-7 (A)) and replacement by a solvent of lower swelling power can substantially enhance the extent of swelling achieved with the solvent. Dehydration by solvent exchange and drying with hydrophilic organic solvents helps maintain and even widen the active internal surface (C) and avoid collapse of the interfibrillar interstices (B).

The accessibility and reactivity of cellulose by exchange with polar liquids is achieved as follows. The polar liquid opens interfibrillar spaces and make them more accessible to the organic reaction medium layer introduced by solvent exchange. The reaction is topochemical but occurs down to the fibrillar level, and on the surfaces that are most available, such as the surfaces of fibrillar assemblies and of elementary fibrils. Additionally, interlinking regions between crystallites situated at the reactive surface level will be reached, and from there, the progression of the reaction medium to the interior of the fibrils and into the crystallites is facilitated.

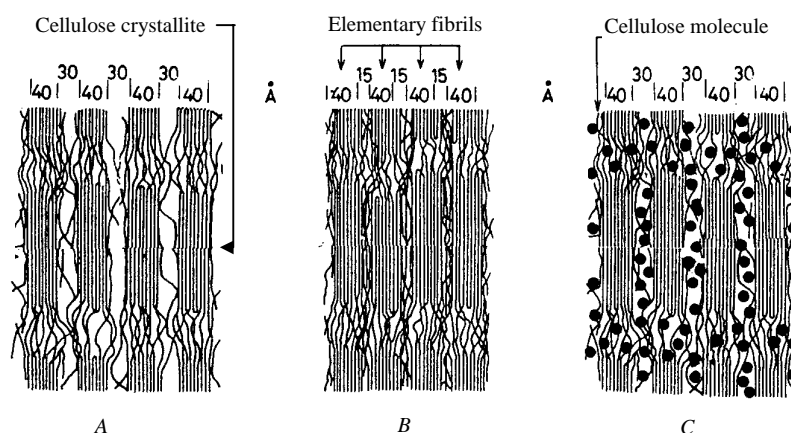


Figure 1-7. Schematic illustration of the action of water and inclusion compounds (●) (less polar non aqueous reactants) (reproduced from Krässig [5, p.235]). (A) Water swelling opens the interfibrillar interstices. (B) In drying from the water-wet state the interfibrillar interstices collapse and elementary fibrils as well as their aggregations are fused together by interfibrillar hydrogen-bonding from surface to surface. (C) Inclusion compounds introduced into the interfibrillar interstices opened by the water swelling prevent their collapse and keep them open for the penetration of reactants.

1.4.2 Mechanical activation

Mechanical activation, such as dry-milling or wet-milling, increases the accessible and reactive surface. Under certain conditions, these treatments can be quite degrading for high molar mass cellulose and result in molar mass reduction and crystal lattice disturbance.

In dry-milling, the effect depends on the type of mill. With mills exerting cutting action, the fibres are cut and shortened thereby increasing the reactive surface but no degradation occurs. When the action of the mill is shearing and grinding, the local overheating favours an internal structure collapse called hornification, leading to a decrease in reactivity for

instance in the production of cellulose ethers. Dry milling in a vibratory ball has yet a different effect: the cellulose fibres are not only defibrillated and shortened, but also their morphology and crystalline order are greatly disrupted. The fibres show higher amorphous cellulose content and an increase in carbonyl and carboxyl content.

It can be noted that for the purpose of this study dry-milling was necessary in order to prepare the paper samples. Cutting-action (two-blade blender) and hammering action mills were chosen in order to avoid conditions that would lead to degradation.

1.5 Dissolution of cellulose

As seen in the previous sections, dissolution of cellulose is particularly difficult, as it requires the disruption of intermolecular hydrogen bonds by interaction of solvent molecules with cellulosic hydroxyl groups.

Many suitable solvent systems for cellulose are currently used in the paper and textile industry as well as in the field of research in conservation of cellulosic artefacts. These systems are classified according to the type of reaction between solvent molecules and hydroxyl groups. Several authors have proposed a classification of cellulose solvents based upon four types of chemical reaction systems [3(Johnson, D.C., Ch.7),12,13,14]:

- **cellulose acting as a base** can be protonated and donate an unshared pair of electrons to a Lewis acid. Aqueous solutions of metal salts such as calcium thiocyanate or zinc chloride, in which the cation plays the role of a Lewis acid are cellulose solvents. Protic acids like phosphoric, sulphuric, hydrochloric, nitric and trifluoroacetic are cellulose solvents (within a narrow concentration range).
- **cellulose acts as an acid** when the hydroxyl groups interact with strong inorganic bases (e.g. sodium hydroxide) or with quaternary ammonium hydroxides, amine oxides (e.g. *N*-methylmorpholine-*N*-oxide monohydrate) or dimethylsulfoxide/methylamine to produce salts. Quaternary amines such as tetraalkylammonium bases with a molar mass under 150 g mol^{-1} are only swelling agents while those with higher molar mass are cellulose solvents.
- **cellulose forms complexes** with transition metals. Organometallic compounds such as metal-amine complexes are particularly interesting because at limited concentration of metal ion in the aqueous amine solution they are good swelling agents, while at higher metal concentration, they are good cellulose solvents. These are:
 - copper ethylene diamine hydroxide (CED or Cuen),
 - copper ammonium hydroxide (Cuam),

- cadmium ethylene diamine hydroxide (Cadoxen), nickel ethylene diamine hydroxide (Nioxen)
- iron sodium tartrate (EWNN or FeTNa)
- **cellulose is modified to form derivatives**, such as with:
 - formic acid, to form cellulose formate
 - carbon disulfide/sodium hydroxide to form cellulose xanthate (also called viscose),
 - nitrogen oxides such as dinitrogen tetraoxide/dimethylformamide, and dinitrogen tetraoxide/dimethylsulfoxide, to form cellulose nitrite,
 - paraformaldehyde/dimethylsulfoxide, to form methylol cellulose,
 - phenyl isocyanate/dimethylsulfoxide or phenyl isocyanate/pyridine, to form cellulose tricarbonyl.

It must be noted at this point that lithium chloride with *N,N*-dimethylacetamide (LiCl/DMAc), the solvent for cellulose chosen in the present study, is not classified in any of the above-mentioned categories. It is indeed rather difficult to classify this solvent system, and the problem arises as well with lithium chloride / *N*-methyl-pyrrolidone (LiCl/NMP), since NMP is the cyclic analogue of DMAc.

Although the solvation mechanism of cellulose in LiCl/DMAc is quite complex and not fully understood to date, the category of complexing solvents seems nevertheless the most approaching. This solvation mechanism is detailed in Chapter 2, together with the reasons leading to LiCl/DMAc as the solvent of choice for cellulose in the present research. Reviews of recent evaluations of the solvent system LiCl/DMAc as well as comparative effects and efficiency of this one and other solvents are included in Chapter 2.

1.6 Chemical reactivity of cellulose: acid hydrolysis

Chemical reactivity of cellulose is of paramount importance in all fields dealing with cellulose transformation, end-products, and characterisation. Changes in organic groups on the molecule can arise from secondary reactions like hydrolysis and oxidation, which occur during the processing of cellulose into paper or into other cellulosic substrates. They also occur upon natural or accelerated aging leading to a wide array of degradation compounds such as small organic acids and saccharidic residues [15,16]. Acetic acid has been characterised as a major degradation product of newsprint paper among other low molecular weight carboxylic acids such as formic, lactic, malonic, malic, succinic and α -ketoglutaric acid [17,18,19]. C3 and C4-alkyl substituted cyclohexanols and C4 to C12 aliphatic alcohols have also been identified as main degradation products in cotton and

chemical wood pulp books among numerous volatile organic compounds (VOCs) represented by aldehydes, ketones, and furan derivatives [20,21,22]. The latter have been proposed as indicators of chain scission of cellulose [23]. The reactions producing such compounds mainly occur in the most accessible areas: the fibril surface and interlinking regions between crystallites.

Chemical reactivity of cellulose is governed by the sensitivity of the β -1,4-glycosidic bond and the presence of three hydroxyl groups on each repeating unit. The glycosidic bond is particularly sensitive to acid hydrolysis and its cleavage induces depolymerisation. The extent of the depolymerisation depends on the acid strength, concentration, as well as on the temperature and duration of the reaction.

Oxidation reactions are based on the transformation of the cellulose hydroxyls in carbonyl and carboxyl groups. They are complex and lead to a wide array of possible degradation products depending on the oxidant [3(Nevell, T.P., Ch.10),5,24]. These reactions are sometimes qualified as “potentially” degrading because they favour subsequent hydrolytic degradation [24,25]. In this section, acid hydrolysis is further detailed, being the main degradation mechanism relevant in the frame of this study.

As the end-use properties of cellulose products, such as tensile strength of fibres, depend largely on the length of the molecules, the degradation by acid hydrolysis of cellulose has been extensively studied in the past, and thorough studies and reviews have been published [1,2,3(Nevell, T.P., Ch.9)]. These reactions are described as proceeding in three stages, (1) starting by a rapid protonation of the glycosidic oxygen atom, (2) continuing by a slow transfer of the positive charge to C(1), which leads to the formation of a carbonium ion with a simultaneous split of the β -glycosidic link, and (3) ending with the fast addition of water to the carbonium ion in order to yield a free saccharidic residue, accompanied by reformation of a hydroxonium ion [3(Nevell, T.P., Ch.9)] (Figure 1-8). Protonation of the ring oxygen can happen resulting in a ring opening leading to the formation of a non-cyclic carbonium ion.

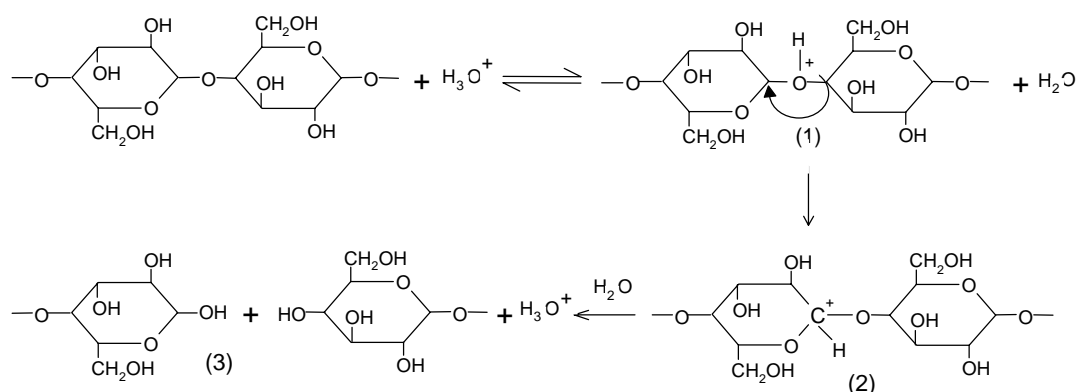


Figure 1-8 Scheme for acid-catalysed hydrolysis of cellulose.

The rate of the hydrolytic degradation of cellulose is governed by the macromolecular properties of the polymer. It obeys to a law of first order kinetics, which is expressed in the following equation as proposed by Ekamstam for polymer degradation [26]:

$$\frac{1}{DP_n(t)} - \frac{1}{DP_n(t_0)} = k t$$

Where $DP_n(t)$ and $DP_n(t_0)$ are the number average degree of polymerisation at time t and initial time t_0 respectively, and k is the reaction rate constant. The Ekamstam model is given in Appendix 6-3.

The temperature dependence of the reaction rate constant in chemical reactions is described by the Arrhenius equation:

$$k = A e^{(-E_A/RT)}$$

Where A is a constant called the frequency factor or pre-exponential factor, E_A the activation energy (J mol^{-1}), T the temperature in degrees Kelvin (K), and R the universal gas constant equal to $8.314 \times 10^{-3} \text{ J mol}^{-1} \text{ K}^{-1}$.

If the degradation of cellulose occurs statistically, the plot of $1/DP_n(t)$ as a function of t should lead a straight line with $1/DP_n(t_0)$ as intercept. This relationship has been experimentally verified in a number of cases. However, in the high molar mass range, a deviation from linearity was observed by some workers [27,28] with the first degradation stages characterised by a rapid decrease of the reaction rate before constancy was reached. This behaviour was explained by the simultaneous action of two kinds of splitting reactions: in addition to the expected β -1,4-glycosidic bond cleavage, the cleavage of “weak links” occurred, which were numbered as four per native molecule. The rate constant of the second cleavage reaction was found to be 10^5 times higher than the rate constant of the first. The “weak link theory” was held responsible for the rapid drop in the degree of polymerisation when it initially exceeded 4000 during acid attack, even at moderate temperature. As the weak links are hydrolysed, the reaction rate decreases to a constant until the medium range molar mass is reached, and thus the second kinetic phase takes place.

The theory of ‘weak links’ in the cellulose molecule, particularly sensitive to acid hydrolysis has received considerable interest. Emsley *et al.* [29] showed that the degradation of cellulose upon acid hydrolysis was not purely random and appeared to occur preferentially at chain centres. The authors obtained size-exclusion chromatograms showing initial monomodal MMD of high molar masses that became multimodal during aging, before returning to monomodal at lower molar masses.

In a computer model of polymer degradation, Guaita *et al.* [30] predicted that polydispersity would approach a value of 2 and remain fairly constant during the degradation process of cellulose when scissions in molecules were purely random. The authors predicted that polydispersity would fall below 2 if the scissions were primarily at

the centre of the chains. Elmsley *et al.* [29] based the interpretation of the slight increase in polydispersity on this model.

Various interpretations exist to explain this weak links theory. The presence of an electron attracting aldehyde or carboxyl group in the neighbouring area of the glycosidic oxygen was proven to be the cause for the higher rate of acid hydrolysis in wood pulp as compared with cotton [31]. The presence of occasional monosaccharides other than glucose, such as xylose, along the cellulose chain at regular intervals of 500 anhydroglucose units was suggested as a possible cause for the weak links [32,33]. A third cause was proposed in [5], based on physical and steric considerations with an easier accessibility of the acid to the molecules on the surface of the elementary fibrils - and their aggregations - and in the interlinking crystallite regions. The latter theory only applies when the substrate is in fibrous state, *i.e.* in heterogeneous hydrolysis, and not in a homogeneous medium such as a true solution. A suggested origin of the weak links by Pascu [32] is related to the biosynthesis of the molecules likely proceeding in a semi-continuous way with the formation of primary strands of monomers that can subsequently yield longer chains via condensation reactions.

Contrary to the above considerations, Zou *et al.* [34] obtained no weak link effect in cellulose degradation during heat/humid aging, the degradation rate being constant over time at any given temperature tested, for a wide range of aging temperatures. The experiments supported the applicability of the Arrhenius equation to the case of degradation of paper by heat/humid aging, which was described as being governed by acid-catalysed hydrolysis.

At the supramolecular level, chain scission occurs in the more easily accessible regions resulting in a decrease of the molar mass of cellulose. From the point of view of the fibre strength, when the reaction is homogeneous and the scissions occur randomly in the molecule, the result is minor loss of fibre strength. However when the reaction is heterogeneous, and with localised attack, a small molar mass decrease results in drastic fibre strength loss [35]. At the macroscopic level, this translates as decay in mechanical properties of the paper such as tensile strength [36].

In homogeneous reactions, when reaching the state where the molecular length of the cellulose is approaching that of the elementary crystallite (or fibrillar aggregation), hydrolysis proceeds mainly by splitting-off terminal saccharidic fragments from the accessible ends. At this stage the decrease in molar mass becomes less pronounced. Therefore, after the sharp initial and mid-reaction downfall, the molar mass of cellulose decreases asymptotically upon prolonged reaction time. This is called the levelling-off degree of polymerisation (LODP). LODP is the third kinetic phase in acid-catalysed degradation of cellulose. The three phases are characterised by a continuous drop in reaction rate.

The LODP value is only dependent on the nature of the fibre, and not on the hydrolysis conditions. The latter only influences the speed at which the plateau is reached. Most

authors report LODP between 200 and 400, closer to 200-300 for wood pulp and to 300-400 for cotton (Figure 1-9).

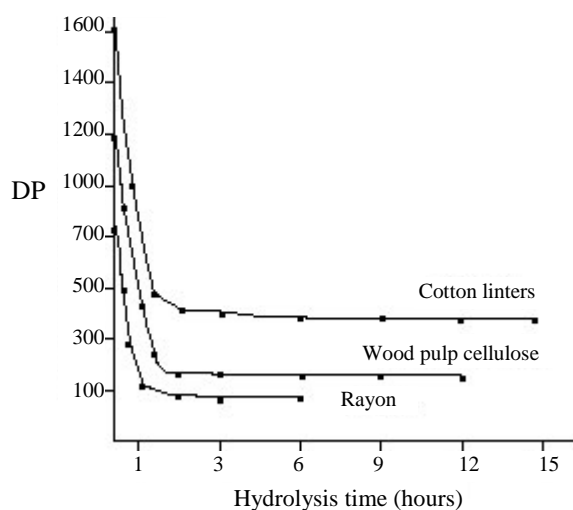


Figure 1-9. Graphical representation of the LODP for different cellulose fibres (reproduced from <http://www.chem.vt.edu/chem-dept/helm/3434WOOD/notes1/polyrxn.html>)

References

1. Ott, E.; Spurlin, H.M. and Grafflin, M.W. *Cellulose and Cellulose Derivatives*, 2nd Ed., Wiley, New York (1971).
2. Fengel, D. and Wegener, G. *Wood: Chemistry Ultrastructure, Reactions*, Walter de Gruyter, Berlin (1984).
3. Nevell, T.P. and Zeronian, S.H. *Cellulose Chemistry and its Applications*, Wiley, New York (1985).
4. Young, R. A. and Rowell, R.M. *Cellulose. Structure, Modification and Hydrolysis*, Wiley-Interscience, New York (1986).
5. Krässig, H.A., *Cellulose. Structure, Accessibility and Reactivity*, Gordon and Breach Sci. Pub., Singapore (1993).
6. Hearle, J.W.S. *J. Polym. Sci.*, 28 (1958) 432-435.
7. Pionteck, H.; Berger, W., Morgenstern, B. and Fengel D. *Cellulose*, 3 (1996) 127-139.
8. Gardner, K.H. and Blackwell, J. *Biopolym.*, 13 (1974) 1975-2001.
9. VanderHart, D.L. and Atalla, R.H. *Macromolecules*, 17 (1984) 1465-1472.
10. Meyer, K.H. and Misch, L. *Ber.*, 70B (1937) 266.
11. Philipp, B.; Schleicher, H. and Wagenknecht, W. *J Polym. Sci.*, 42 (1973) 1531-1543.
12. Brandup, J; Immergut, E.H. and Grulke E.A. *Polymer Handbook*, 4th Ed., Wiley, New York (1999).
13. Turbak, A.F.; Hammer, R.B.; Davies, R.E. and Hergert, H.L. *Chemtech.* (1980) 51.

14. Debzi, El M. *Celluloses issues du traitement à la vapeur: évolution des masses moléculaires moyennes, transformations morphologiques et cristallines*, Thèse de Doctorat, Université Joseph Fournier – Grenoble I (1992) 43.
15. Erhardt, D. and Mecklenburg, M.F. *Materials Issues in Art and Archeology IV Symp.*, Cancun, Mexico (1994), 247-270.
16. Dupont, A-L. *Restaurator*, 17 (1996) 145-164.
17. Parks, E.J.; Guttman, C.M.; Jewett, K.L. and Brinckman, F.E. *National Institute of Standards and Technology Report 4456*, National Institute of Standards and Technology, Institute for Materials Science and Engineering, Polymers Division (1990).
18. Shahani, C.J.; Harrison, G.; Hengemihle, F.H.; Lee, S.B.; Sierra, M.L.; Song, P. and Weberg, N. *ISR Annual report 1998*, Preservation Research and Testing Division, Library of Congress, Washington, DC (1998).
19. Dupont, A-L. and Vasseur, F., unpublished results.
20. Buchbauer, G.; Jirovetz, L.; Wasicky, M. and Nikifirov, A. *J. Pulp and Paper Sci.*, 21, 11 (1995) J398-J400.
21. Molton, P.M.; Miller, R.K; Donovan, J.M. and Demmitt, T.F. *Carbohydr. Res.*, 75 (1979) 199-206.
22. Hill, D.J.T.; Le, T.T.; Darveniza, M. and Saha, T. *Polym. Degrad. Stab.*, 51 (1996) 211-218.
23. Scheirs, J.; Camino, G.; Avidano, M. and Tumiatti, W. *J. Appl. Polym. Sci.*, 69 (1998) 2541-2547.
24. Meller, A. *APPITA Proc.* 9, Australian Pulp and Paper Industry Technical Association, Melbourne (1955) 192-208.
25. Shahani, C.J. and Harrison, G. *IIC Congress: Works of Art on Paper, Books, Documents and Photographs. Techniques and Conservation*, Daniels, V.; Donithorne, A. and Smith, P. (Eds), Int. Inst. for Conservation, London (2002) 189-192.
26. Ekamstam, A. *Ber. Dtsch. Chem. Ges. A.*, 69 (1936) 553-559.
27. Marx-Figini, M. *J. of Applied Polym. Sci.*, 33 (1987) 2097-2105.
28. Emsley, A.M; Ali, M and Eley, C.M. *Cellulose*, 4 (1997) 1-5.
29. Emsley, A.M; Ali, M and Heywood, R.J. *Polymer*, 41 (2000) 8513-8521.
30. Guaita, M.; Chiantore O. and Luda M.P. *Macromolecules*, 23 (1990) 2087-2092.
31. Immergut, E.H.; Ranby, B.G. and Mark, H. *Ricerca Sci.*, 25 (1955) 308.
32. Schulz, G.V. and Husemann, E. G.V. *Z. Phys. Chem. B*, 52 (1942) 23-49.
33. Pascu, E. *Text. Res. J.*, 17 (1947) 405.
34. Zou, X.; Uesaka, T. and Gurnagul, N. *Cellulose*, 3 (1996) 243-267.
35. Gurnagul, N.; Page, D.H. and Paice, M.G. *Nordic Pulp and Paper Res. J.*, 3 (1992) 152-154.
36. Yang, C.Q; Weishu, W. and Lickfield, G.C. *Text. Res. J.*, 70, 10 (2000) 910-915.

Chapter 2. Review of most commonly used methods for the dissolution and the characterisation of cellulose

Abstract

The techniques available to date for the analysis and the characterisation of cellulose, such as viscometry and size-exclusion chromatography (SEC), are evaluated in terms of the quality of the information obtained, as well as their overall advantages and drawbacks. The solvents most currently associated with these methods and their potential effects on the degradation of cellulose are reviewed. In order to understand the choices made in this study, the advantages of the solvent lithium chloride/N,N-dimethylacetamide (LiCl/DMAc) and its action on cellulose are detailed.

2.1 Molar mass averages

The polymerisation process is inherently random; therefore most natural and synthetic polymers are composed of a mixture of molecules of different size. Proteins can be considered as a special type of polymer in that their biosynthesis is a complex biochemical process, which results in identical molecules at all structural levels, from the amino acid assembly to the three-dimensional arrangement. This spatial conformation of a native protein is a key factor to its bioactivity.

Most of the analytical techniques commonly used to evaluate polymerisation, such as batch light scattering, fractionation, sedimentation, osmometry and viscometry, each provide average values for only one of the molar mass averages of a polymer.

The different molar mass averages are the number-average molar mass \overline{M}_n , the weight-average molar mass \overline{M}_w and the z-average molar mass \overline{M}_z . For ease throughout the text we will hereafter and in the following chapters omit the bar (\overline{M}), and refer to the molar mass averages as M_n , M_w and M_z .

The molar mass averages are expressed as follows:

$$M_n = \frac{\sum n_i M_i}{\sum n_i} \quad M_w = \frac{\sum n_i M_i^2}{\sum n_i M_i} \quad M_z = \frac{\sum n_i M_i^3}{\sum n_i M_i^2}$$

Where n_i is the number of molecules with molar mass M_i .

An additional molar mass average that is sometimes used when working with very high- M_r polymers is M_{z+1} .

$$M_{z+1} = \frac{\sum n_i M_i^4}{\sum n_i M_i^3}$$

From these expressions, it can be derived that the impact of high molar mass (M_r) molecules on these molar mass averages is in decreasing order: $M_{z+1} > M_z > M_w > M_n$.

Specifically, if upon degradation cleavage occurs preferentially in the high- M_r molecules, the relative decrease in the values of M_z and M_{z+1} will be larger than the relative decrease in M_n . Conversely, if the low- M_r molecules are preferentially degraded, the relative decrease in M_n will be larger than the relative decrease in M_w and M_z . This concept of course has its limitations since high- M_r molecules are statistically more likely to undergo random cleavage than low- M_r molecules.

The polydispersity index (PD) is expressed by the ratio $\frac{M_w}{M_n}$

M_n is usually determined by end-group analysis or by osmometry, M_w by light scattering - which also provides the root mean square radius (rms or r_g), and M_z by ultracentrifugation (z stands for the German word “zentrifuge”).

In terms of physical properties, there is a direct relationship between M_r averages and processing characteristics of polymers. M_z relates to elongation and flexibility. M_n relates to brittleness, flow properties and compression set. M_w relates to strength properties such as tensile strength and impact resistance.

Molar mass can also be expressed relative to intrinsic viscosity. The viscosity-average molar mass M_v is usually determined in batch or capillary viscometry and relates to extrudability and molding properties.

$$M_v = \left[\frac{\sum n_i M_i^{1+a}}{\sum n_i M_i} \right]^{1/a}$$

Where a is the exponent in the Mark-Houwink-Sakurada (MHS) equation:

$$[\eta] = K' M_v^a$$

$[\eta]$ is the intrinsic viscosity, determined by viscometry. K' and a are constants for a given polymer-solvent system, temperature and molar mass range. These constants are tabulated for a wide range of polymer-solvent systems [1]. M_v depends on a number of factors, including the solvent and the molar mass distribution (MMD), *i.e.* chain size distribution, of the polymer in solution. Viscosity measurements are generally more affected by the high- M_r components of the polymer reflected in M_w , and practically, M_v is usually closer to M_w than to M_n [2]. In the specific case where a is equal to unity, M_v is equal to M_w .

2.2 Methods of dissolution and analysis of cellulose

2.2.1 Viscometry: solvents and methods

Viscometry measurements allow the calculation of the polymer's intrinsic viscosity $[\eta]$. The intrinsic viscosity is determined by extrapolation towards concentration zero of the viscosity of solutions of the polymer in the solvent at different concentrations:

$$[\eta] = \lim_{c \rightarrow 0} \left[\frac{(\eta - \eta_{\text{solv}})}{\eta_{\text{solv}} \times c} \right]$$

Where η is the viscosity of the polymer solution at concentration c in the solvent, and η_{solv} is the solvent viscosity.

The relationship between intrinsic viscosity and M_r in dilute solutions is given by the MHS equation described in section 2.1.

There are different viscometry methods used for cellulose analysis. The method with copper di-ethylene diamine dihydroxide (called CED or CuEn) $[\text{Cu}(\text{En})_2(\text{OH})_2]$ (with $\text{En} = \text{H}_2\text{N}(\text{CH}_2)_2\text{NH}_2$) gained considerable acceptance because of the wide range of papers that this solvent system is capable of dissolving.

Most standard viscometry methods for cellulose are based on dissolution in CED: ASTM D539-51 [3], ISO 5351/1 [4], TAPPI T 230 om-89 [5], AFNOR NF T12-005 [6], and SCAN-CM 15:88 [7]. The advantage of these standard methods is that no sophisticated equipment is required; the measurements are done with a capillary glass viscometer. There are nonetheless major drawbacks, as these methods provide information on only one M_r average (M_v), and not on the molar mass distribution (MMD) of the cellulose, which is critical in relation to the mechanical strength and expected longevity of a cellulosic material. Furthermore, when the MMD of a polymer changes upon aging, it is difficult to relate M_v with the real bond scission rate since M_v varies with a number of factors, among which is MMD. In this case it is necessary to know M_n . Viscometry methods also have limitations as to the type of paper they can be applied to. In addition, the presence of mineral fillers and sizes can modify the solution viscosity and hence lead to erroneous values of M_v .

An additional drawback of these methods resides in the fact that the solvents used in viscometry are fairly alkaline. The pH of CED is 11, and the pH of Cadoxen (see next paragraph) is 13. This inevitably leads to degradation of the cellulose by atmospheric oxygen [8]. Jerosch [9] showed that the temperature and age of cellulose solutions in CED played an important role in the extent of the degradation. The author reported that the DP_v of a softwood pulp of high- M_r ($5.8 \times 10^5 \text{ g mol}^{-1}$) decreased by 13% after 8 days in solution when kept at room temperature, and by 8% when kept at 4°C. Strlič *et al.* [10] showed that degradation of oxidised cellulose in CED was pronounced; leading to a

systematic error of up to 56% in M_r . Santucci and Plossi Zappalà [11] also reported the sensitivity of oxidised cellulose to CED. This is probably due to the fact that oxycelluloses are easily hydrolysed in alkaline medium through a process called β -alkoxy elimination. It has been shown that cellulose that was reduced with sodium borohydride prior to dissolution underwent less solvent-induced degradation [10,12,13].

Cadoxen is sometimes used as an alternative to CED because it is colourless and was shown to be less degrading than CED [14,15] in addition to being stable at room temperature [8]. Cadoxen, an aqueous solution of cadmium tri-ethylene diamine dihydroxide $[\text{Cd}(\text{En})_3](\text{OH})_2$ ($\text{En} = \text{H}_2\text{N}(\text{CH}_2)_2\text{NH}_2$), was first described by Jayme [16,17], and shortly after the first viscometric studies were carried out [18,19]. Cadoxen makes more stable solutions with cellulose, and is less prone to oxidation than CED solutions [20]. However, the use of Cadoxen is limited because no standard method of viscometry in this solvent exists, and because it is not commercially available. The solvent has to be prepared in the laboratory, which often results in poor repeatability in batch-to-batch quality.

In Cadoxen and similar solvents, hydrogen bonding occurs between the amino groups of the ethylenediamine and the two equatorial hydroxyl groups of cellulose on C3 and C6 [21]. ^{13}C and ^{113}Cd Nuclear Magnetic Resonance (NMR) showed that enhanced hydrogen bonding takes place arising from a combination of steric and electronic factors due to the presence of the metal ions.

In the MHS equation, typical values for the coefficient a of cellulose are in the range of 0.8 to 1.0 for most solvent systems [22]. Donetzhuber [23] and Henley [24] were the first researchers to study the system cellulose/Cadoxen using cotton linters. The first found $K' = 3.85 \times 10^{-4} \text{ dL g}^{-1}$ and $a = 0.76$ at 30°C ; and the second, $K' = 5.4 \times 10^{-4} \text{ dL g}^{-1}$ and $a = 0.735$. Other values reported in the literature for cellulose in Cadoxen are $K' = 3.15 \times 10^{-5} \text{ dL g}^{-1}$ and $a = 0.93$ at 25°C [25].

Experiments of viscometry in lithium chloride/*N,N*-dimethylacetamide (LiCl/DMAc) have also been reported. McCormick *et al.* [26] determined $K' = 1.278 \times 10^{-4} \text{ dL g}^{-1}$ and $a = 1.19$ for cellulose in 9%LiCl/DMAc at 30°C . Such a high value of a indicated rod-like rigid conformation of cellulose in LiCl/DMAc. This was later confirmed by light scattering measurements by Dawsey and McCormick [27]. It can be noted at this point that the experiments carried out in the present work (see section 4.2.4 of Chapter 4) allowed to determine the coefficient a for cellulose in 0.5%LiCl/DMAc as 0.81, using size-exclusion chromatography with multiangle light scattering detection (SEC/MALS).

For cellulose tricarbonylates - the structure of which can be found in Appendix 5-2- in THF at 25°C , K' was found equal to $5.3 \times 10^{-5} \text{ dL g}^{-1}$ [25] and $4.3 \times 10^{-5} \text{ dL g}^{-1}$ [28], and a to 0.84 [25,28]; at 20°C , the value of K' found was $2.01 \times 10^{-5} \text{ dL g}^{-1}$, and the value of a was 0.92 [29].

Paraformaldehyde with dimethylsulfoxide (PF/DMSO) was acknowledged as a good solvent for cellulose by Johnson [8] and by Minor [30], who reported it as a fast and simple dissolution process, non-degrading for cellulose. More recently, He and Wang [31] studied solutions of cellulose in PF/DMSO using viscometry and confirmed the solvent was non-degrading, showing negligible drop in DP after 2 years in solution. However, it must be noted that the authors used low- M_r cellulose, with which a depolymerisation effect is less noticeable. The authors found that PF/DMSO was a better solvent than Cadoxen and FeTNa (iron sodium tartrate), but that LiCl/DMAc had better solvation capacity.

It has to be noted that intrinsic viscosity $[\eta]$ as well as a and K' parameters in the MHS equation can also be obtained with a capillary viscosity detector that has a flow cell allowing its use on-line in size-exclusion chromatography. In this case, as explained in the next section, information such as the various M_r averages defined earlier can be obtained.

2.2.2 Size-exclusion chromatography (SEC) and dissolution methods compatible with SEC

2.2.2.1 Principle of SEC

Knowing only one M_r average of a polymer is sometimes sufficient. However, in order to assess polymer properties and characterise degradation it is important to obtain the MMD.

Size-exclusion chromatography (SEC) is the technique of choice to evaluate composition and MMD of polymers. The separation mechanism in SEC is based on differences in size, *i.e.* differences in the hydrodynamic volume of solutes. Polymer molecules travel with the mobile phase through porous particles, which constitute the packing material of the column (the solid phase). The small molecules can penetrate smaller pores than the large molecules. As a result the smaller molecules travel longer through the packing material and elute from the column in higher volumes than the larger molecules (Figure 2-1). SEC hence results in a separation of the polymers according to their molar mass, and more precisely to their hydrodynamic volume in solution. The number n_i of molecules of molar mass M_i in each slice of a chromatogram can be calculated and yields M_n , M_w , M_z and M_{z+1} . Although M_v values can be determined by SEC if the MHS coefficient a is (accurately) known, M_v is usually only determined when on-line viscosity detectors are used.

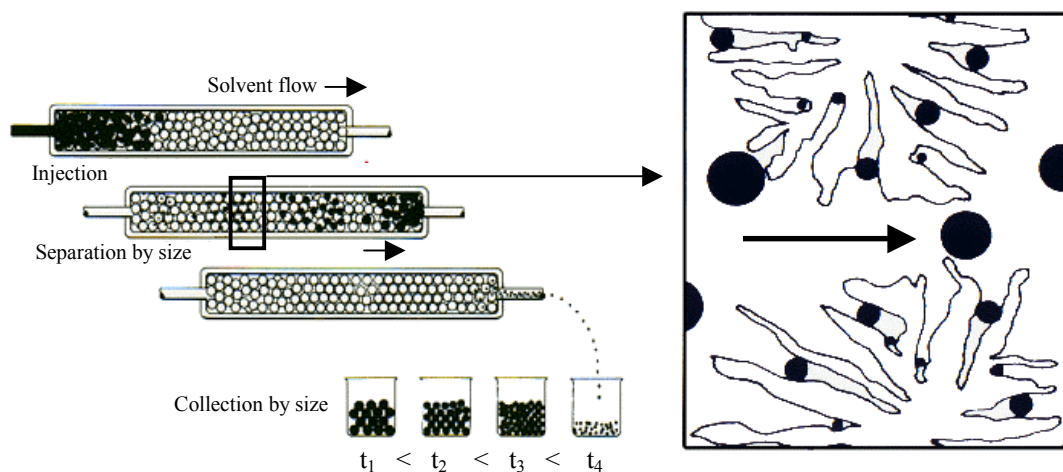


Figure 2-1. Schematic representation of a separation of a polydisperse polymer solution in a SEC column containing porous particles with different pore size (mixed bed).

SEC has been widely used to determine cellulose MMD and to monitor degradation arising from the pulping, bleaching and viscose processes. Valuable information can be found in publications originating from the pulp and paper industry, and from the electrical engineering sector since paper is, still to date, used as the main insulation material in electrical transformers. Developments in new column packings technology and in detection systems for molecular size and MMD have increased the range of information on molecular characteristics that can be obtained from SEC measurements [32,33,34,35].

Solvents used for SEC must allow polymer chains to open up into their most relaxed conformation: from solid state (crystalline or semi-crystalline) to liquid state, and they must be compatible with the column packing material.

For the study of a protein such as gelatine, which is soluble in water under moderate heat, aqueous SEC with mobile phases such as buffers and salt solutions can be applied. For a biopolymer such as cellulose, which has a limited solubility in most common solvents used in chromatography, the use of SEC is conditional to overcoming the solubility/system compatibility difficulty. For example solvents used for viscosity are incompatible with most SEC columns packings. Emsley *et al.* [36] reported Cadoxen was too aggressive and rapidly dissolved the poly (styrene-divinyl benzene) (PSDVB) column packing. Nevertheless, Schwald *et al.* [37] and Geresh *et al.* [38] used Cadoxen as SEC eluent and reported no column problem. The first used columns packed with Fractogel TSK (Merck), and the second, with a hydrophilic gel material, PSS Suprema (Jasco). Minor [30] successfully did SEC of methylol cellulose with DMSO as mobile phase on PSDVB columns, and Agg and Yorke [39] used iron sodium tartrate as cellulose solvent and mobile phase on Sepharose columns.

The following section presents the two methods that were tested in the frame of this study for characterisation of cellulose.

2.2.2.2 Cellulose tricarbanilate (CTC) and dissolution in THF

The first processes that were used to analyse cellulose by SEC involved “derivatising” the polymer in order to be able to dissolve it in organic solvents that are compatible with SEC column packings.

The very first methods were based on the modification of cellulose into nitrate [40,41] and acetate derivatives [42,43,44]. Cellulose nitrate has a relatively small refractive index difference with tetrahydrofuran (THF), the preferred solvent, which limited the sensitivity of the method and the precision (mostly baseline instability) [44]. More importantly, the poor stability of the cellulose nitrate, the significant chain scission of the polymer induced during the derivatisation, and the difficulty in obtaining uniform and consistent degrees of substitution (DS) - which introduced additional uncertainty in the results - were major drawbacks and the methods employing nitrate and acetate derivatives were rapidly abandoned.

Research into less degrading derivatisation methods led to other cellulose derivatives such as methylol cellulose [45] and cellulose tricarbanilate (CTC). The latter appeared as the most viable solution.

The suitability of CTC derivatives for SEC was first advocated in the mid-1970s [25,29]. The methods were widely used and further improved through the 1980s [28,46,47,48]. CTC proved to be a good alternative to cellulose acetate, showing fairly reproducible DS, and inducing no apparent degradation of the cellulose [25,49]. Hemicelluloses could also be carbanilated, which extended the applicability of the method to holocelluloses (*i.e.* cellulose and hemicelluloses) that are present in wood pulps. The CTC was shown to more readily dissolve in organic solvents than trinitrate, and THF was found to be the best solvent and SEC mobile phase [25]. The development of the first low-angle light scattering detectors in the early 1980s set ideal conditions for the development of methods of characterisation of cellulose using tricarbanilation.

CTC are prepared in DMSO or in pyridine, and are re-dissolved in THF for the SEC run. With cotton linters, faster reaction rates were reached in DMSO than in pyridine, but partial degradation of high- M_r cellulose fractions during derivatisation was observed [50]. For softwood Kraft pulps, DMSO was a better solvent for carbanilation than pyridine. With the latter solvent aggregation occurred in THF [51]. Hill *et al.* [52] showed that under specific reaction conditions, substitution was complete (DS = 3). Shroeder and Haigh [53] showed that no degradation occurred when the reaction was performed at 80°C but that higher temperatures induced depolymerisation within the first hours.

The effectiveness of the procedure for analysing CTC in THF was found to vary depending on the source of cellulose. Complete delignification is necessary prior to derivatisation. Therefore, certain lignin-containing pulps and papers cannot be derivatised [53]. Additionally, low- M_r cellulose may be lost during the precipitation step with methanol or ethanol [50,54], which makes hemicelluloses very vulnerable.

2.2.2.3 Direct dissolution of cellulose in lithium chloride/*N,N*-dimethylacetamide

Due to the problems associated with the derivatising methods, research into new direct solvent systems continued in parallel, and led to the development of the solvent system lithium chloride / *N,N*-dimethylacetamide (LiCl/DMAc).

LiCl/DMAc was first discovered to dissolve polyamides and chitin in 1972 [55,56,57,58,59]. The use of LiCl/DMAc quickly spread and it was applied for the first time for cellulose dissolution almost concomitantly by McCormick [60] and Turbak [61], who both patented a similar dissolution process. Other non-derivatising solvent systems for cellulose, such as amine oxide and liquid ammonia/ammonium salt systems, were developed around the same time under the economic pressure of the textile industry [62]. However, the use of LiCl/DMAc grew more rapidly and the methods initially proposed were quickly adapted to suit the cellulose source and the sample characteristics. For instance, it appeared that bimodal or multimodal SEC MMD profiles obtained for certain types of wood pulps yielded information on the hemicelluloses content [63,64].

The popularity of LiCl/DMAc is linked to the clear advantage that a direct dissolution method has over derivatisation by being faster, easier and more reproducible. Additionally, none of the common solvents for cellulose allows as wide a range of organic reactions with polysaccharides as does LiCl/DMAc, yielding a number of cellulose derivatives of industrial interest such as esters, ethers, carbamates and sulfonates [27]. LiCl/DMAc is also currently used for a number of other non-water-soluble polysaccharides of commercial interest, such as chitin, amylose, amylopectin, arabinogalactan, dextrans and pullulans, which differ from cellulose only in the extent of branching, type of linkages and anomeric configuration [65].

The major advantage of LiCl/DMAc is that it can be used as mobile phase in SEC with column packings such as PSDVB. The solvent and mobile phase being identical simplifies the procedure. The SEC of cellulose in LiCl/DMAc was applied for the first time by Ekmanis [66,67].

2.2.2.3.1 *The dissolution mechanism*

The first studies by McCormick [60], Turbak [61] and McCormick and Dawsey [27] showed the unique characteristics of LiCl/DMAc as solvent system.

However, after two decades of use, a generally accepted mechanism still remains to be revealed in order to fully explain the solvation of cellulose in LiCl/DMAc, in particular the solvent-lithium interaction, and the crucial role of the chloride ion. Slightly different interpretations on the structure of LiCl/DMAc were found in the literature, but all emphasise as basic principle that the polar aprotic nature of DMAc allows ionic compounds to readily dissolve. LiCl forms ion pairs, held together by electrostatic rather

than covalent bonds. Unable to form hydrogen bonds, DMAc does not solvate anions to any appreciable extent while cations are strongly solvated. The lithium ions are more tightly linked with the carbonyl group of DMAc, while the chloride ions are left unencumbered and thereby highly active as nucleophilic bases.

Many models have been proposed, all are based on this special structure of the ion pair $[\text{Li} \cdot n(\text{DMAc})]^+ \text{Cl}^-$ (Figure 2-2). The concept of the formation of $[\text{Li} \cdot (\text{DMAc})]^+$ as a macrocation where Li^+ is located adjacent to the carbonyl of DMAc in a mesomeric equilibrium (Figure 2-2 (a)) emerged as the most likely to occur after infrared spectroscopy studies [68]. The latter showed the appearance of a different absorbance spectrum upon adding LiCl to DMAc. In addition it was demonstrated that an increase in viscosity of DMAc occurred when LiCl was added. According to McCormick *et al.* [26], the complexation involves one Li^+ with the carbonyl oxygen atom of up to four DMAc molecules. The cation $[\text{Li} \cdot n(\text{DMAc})]^+$ ($n \approx 4$) formed is only loosely associated with Cl^- . This likely forms a tetrahedral-like structure [69]. The stability of this complex is paramount for the dissolution of cellulose. If too stable or too weak, the solvent power is affected. Figure 2-2 (b) represents a model proposed by Turbak of a cation complex where the Li^+ interacts simultaneously with both electronegative atoms O and N of the DMAc [70]. In Figure 2-2 (c) the lithium moiety of LiCl interacts with the amide oxygen and the complex stability is due to electron transfer from the amide on the LiCl ion pair. Figure 2-2 (d) represents a possible nucleophilic addition of a lithium halogenide to DMAc eventually resulting in a covalent complex. [27].

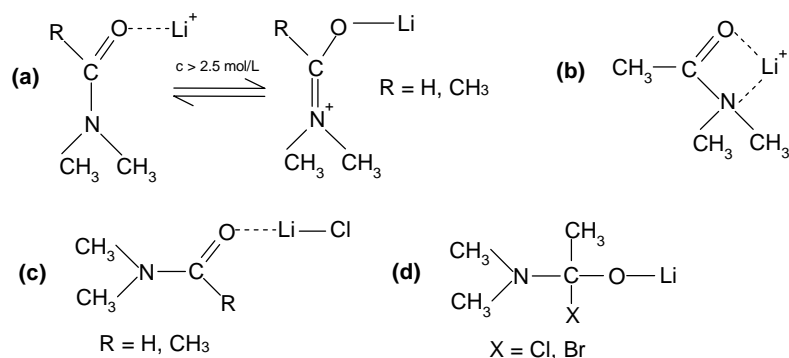


Figure 2-2. Proposed structures of the LiCl/DMAc complexes [69].

^1H , ^7Li and ^{13}C -NMR [58,71,72,73,74] yielded important information for the understanding of the dissolution process of cellulose in LiCl/DMAc. The solvent was shown to be a true non-derivatising solvent, *i.e.* one that does not form chemical bonds with the cellulose molecule [22].

A number of structural models for solvation and complexes formed have been proposed, which place the emphasis on the chloride anion being highly active as a nucleophile towards cellulose. Cl^- enters in competitive hydrogen bond formation with hydroxyl

protons of cellulose, thereby disrupting the existing intermolecular hydrogen-bonded structure, ultimately leading to dissolution [26,69,70,72] (Figure 2-3 (a) to (c)).

The lithium cation was shown to play an important role in the dissolution process. Using ^7Li -NMR, Morgenstern and Kammer showed that the solvated lithium strongly interacted with the hydroxyl groups of cellulose (Figure 2-3 (d)) [69]. Using ^{13}C -NMR, Davé *et al.* [75] also observed that strong ionic interactions existed between the carbonyl oxygens of DMAc and cellulose acetate butyrate with Li^+ , and postulated the formation of electrostatic bonds between the cation and the molecule backbone. Interactions between Li^+ and cellulose were recently studied by Brendler *et al.* [76] with cellobiose as model molecule, using ^7Li -NMR and ^7Li - ^1H HOESY NMR (Heteronuclear Overhauser Effect Spectroscopy). The authors showed that cellobiose was part of the coordination sphere of Li^+ , and therefore expected cellulose also taking part in the solvation of lithium ions, this being one of the driving forces for the dissolution of the polymer.

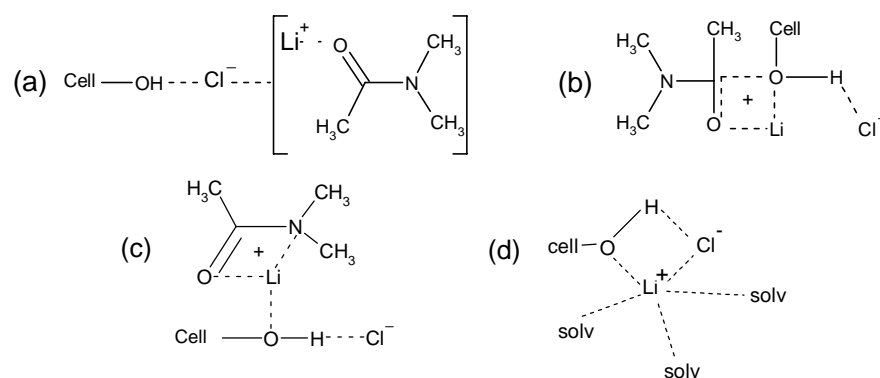


Figure 2-3. Models of the cellulose –LiCl-DMAc complexes. (a): proposed by Mc Cormick *et al* [26], (b): proposed by El-Kafrawy [72], (c): proposed by Turbak [70], (d): proposed by Morgenstern *et al* [69].

Since the addition of cellulose in LiCl/DMAc displaces a DMAc molecule by a cellulosic hydroxyl group, as expressed by the equilibrium shown in Figure 2-4, steric considerations are paramount in the dissolution process of cellulose in LiCl/DMAc. The latter can be visualised as an exchange of ligands that can occur if the solvent complex has an adequate spatial configuration, so that steric hindrance cannot prevent solvation.

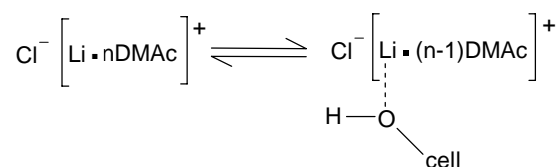


Figure 2-4. Ligand exchange reaction in the cellulose-LiCl-DMAc solutions.

Considering the cellulose chain in its entire length, accumulated associations of Cl^- along the chain produce a negatively charged polymer with the macrocation $[\text{Li-DMAc}]^+$ as counter-ion. It is assumed that each hydroxyl of the anhydroglucose may be approached by a single LiCl/DMAc complex [26]. The molecules of cellulose are therefore also forced apart by charge repulsion [27].

Studies with Scanning and Transmission Electron Microscopy (SEM and TEM) on the morphological changes of cellulose during the dissolution in LiCl/DMAc showed that there was no degradation occurring at the supramolecular level [77]. Firstly, the solvent penetrates into the fibre wall and then into the fibres and fibrils structure, starting preferentially in the less ordered regions. Displaced fragments appear gradually, and progressively, fibrils are separated to a greater extent and isolated to finally result in dissolution of the fibrils structure.

2.2.2.3.2 The solvent complex specificity

Investigation into the suitability of other polar aprotic solvents showed among a wide array of solvents tested (dimethyl sulfoxide, dimethyl formamide, formamide, ethanolamine) that very few could achieve dissolution of cellulose, and those that did induced degradation. Apart from DMAc, only *N*-methylpyrrolidinone (NMP), the cyclic analogue of DMAc was found effective (albeit less than the former). This was attributed to the greater polarisability of DMAc and NMP as compared with the other solvents [72].

Lithium halides other than LiCl were inefficient [22]. The order of nucleophilicity of non-solvated halide ions is the same as that of the electronegativity of the halogen atoms, with $\text{Cl}^- > \text{Br}^- > \text{I}^-$. Bromide (Br^-) and iodide (I^-) are larger ions than Cl^- . They are more tightly bound to DMAc and less available to break inter- and intramolecular cellulose hydrogen bonds [22,27,78]. Under such consideration it could be hypothesised that LiF would provide even more efficient ion pairing than LiCl . However, there is no practical organic solvent for LiF [78]. Furuhata *et al.* [79] achieved dissolution of microcrystalline cellulose in LiBr/DMAc , but found that the concentration of LiBr needed to be larger than LiCl in order to achieve comparable dissolution.

Nitrate and sulfate lithium salts were also inefficient along with other alkali and alkali-earth chlorides such as sodium, potassium, barium, calcium, magnesium and zinc chlorides [22]. With alkali chlorides, in the range of alkali cations Li , Na , K and Cs , the solvation by DMAc decreased as the ionic radii increased, because they provided a smaller charge to radius ratio and weaker ion dipole interactions [22].

References

1. Brandup, J.; Immergut, E.H. and McDowell W. *Polymer Handbook*, 4th Ed., Wiley, New York (1999).
2. Ross-Murphy, S.B. *Cellulose Chemistry and its Applications*, Ch.8, Wiley, New York (1985).
3. ASTM Standard D539-51 (1955).
4. ISO Standard 5351-1:1981, *ISO Standards Handbook: Paper, board and Pulps*, 2nd Ed., (1998).
5. TAPPI Standard T 230 om-89, *TAPPI test methods*, Technical Association of the Pulp and Paper Industry, TAPPI press, Atlanta, US (1994).
6. AFNOR NF T12-005, Association Française de Normalisation (1981).
7. SCAN-CM 15:88, Scandinavian Pulp, Paper and Board Testing Committee, Stockholm, Sweden (1988).
8. Johnson, D.C. *Cellulose Chemistry and its Applications*, Ch.7, Wiley, New York (1985).
9. Jerosch, H. *Evaluation de l'état de dégradation de la cellulose/holocellulose dans différents types de papiers par chromatographie d'exclusion stérique*, Thèse de Doctorat, Université Versailles-St. Quentin-En-Yvelines (2002) 71.
10. Strlič, M.; Kolar, J.; Žigon, M. and Pihlar, B. *J. Chromatogr. A*, 805 (1998) 93-99.
11. Santuci, L. and Plossi Zappalà, M. *Restaurator*, 22 (2001) 51-65.
12. Burgess, H.D. *Int. Council of Museums, Committee for Conservation (ICOM-CC), 9th Trien. Meet. Dresden*, ICOM, Paris, France (1990) 447-452.
13. Lee, S.B.; Feller, R.L. and Bogaard, J. *J. Imaging Sci.*, 29 (1985) 61.
14. Brown, W. *Svensk Papperstidning* 70 (1967) 458-461.
15. Segal, L. and Timpa, J.D. *Svensk Papperstid. Årg*, 72, 20 (1969) 656-661.
16. Jayme, G. and Newschaffer, K. *Makromol. Chem.*, 23 (1957) 71.
17. Jayme, G. *Cellulose and Cellulose Derivatives*, Part IV, Bikales, N. M. and Segal, L. Eds, John Wiley and Sons, New York (1971) 381-410.
18. Henley, D. *Svensk Papperstidn.*, 63 (1960) 143.
19. Jayme, G. and Kleppe, P. *Das Papier*, 15 (1961) 6.
20. Browning, B.L. *Methods of Wood Chemistry II*, Interscience, New York (1967) 541-542.
21. Bain, A.D.; Eaton, D.R.; Hux, R.A. and Tong, J.T.K. *Carbohydr. Res.*, 84, 1 (1980) 1-12.
22. Striegel, A. *Carbohydr. Polym.*, 34 (1997) 267-274.
23. Donetzhuber, A. *Svensk Papperstidning årg*, 63, 14 (1960) 447-448.
24. Henley, D. *Arkiv för Kemi.*, 18 (1961) 327.
25. Daňhelka, J. and Kössler, I. *J Polym. Sci.*, 14 (1976) 287-298.
26. McCormick, C.L.; Callais, P.A. and Hutchinson Jr, B.H. *Macromolecules*, 18 (1985) 2394-2401.
27. Dawsey, T.R and McCormick, C.L. *J. Macromol. Sci - Rev. Macromol. Chem. Phys.*, C30, 384 (1990) 405-440.
28. Cael, J.J.; Cietek, D.J. and Kolpak, F.J. *J. Appl. Polym. Sci.*, 37 (1983) 509-529.
29. Valtasaari, L. and Saarela, K. *Paperi ja Puu*, 1 (1975) 5-10.
30. Minor, J.L. *J Liq. Chromatogr.*, 2,3 (1979) 309-318.
31. He, C. and Wang, Q. *J. Macromol. Sci., Pure Appl. Chem.*, A36 (1999) 105-114.
32. Churms, S.C. *J. Chromatogr. A*, 720 (1996) 151-166.
33. Berek, D. *Prog. Polym. Sci.*, 25 (2000) 873-908.

34. Schult, T.; Moe, S.T.; Hjerde, T. and Christensen, B.E. *J. Liq. Chromatogr. & Rel. Technol.*, 23 (2000) 2277-2288.
35. Melander, M. and Vuorinen, T. *Carbohydr. Polym.*, 46 (2001) 227-233.
36. Elmsley, A.M.; Ali, M and Heywood, R.J. *Polymer*, 41 (2000) 8513-8521.
37. Schwald, W. and Bobleter, O. *J Appl. Polym. Sci.*, 35 (1988) 1937-1944.
38. Geresh, S.; Adin, I.; Yarmolinsky, I. And Karpasas, M. *Carbohydr. Polym.*, 50, 2 (2002) 183-189.
39. Agg, G. and Yorke, R.W. *5th Int. Dissolving Pulps Conf.*, TAPPI (1980) 224-229.
40. Segal, L. *J. Polym. Sci.*, B4 (1966) 1011.
41. Meyerhoff, G. and Hovanovics, S. *J. Polym. Sci.*, B5 (1966) 459.
42. Alexander, W.J. and Muller, T.E. *J. Polym. Sci., C*, 12 (1968) 283.
43. Alexander, W.J. and Muller, T.E. *Separation Sci.*, 6, 1 (1971) 47.
44. Alexander, W.J. and Muller, T.E. *J. Polym. Sci., C*, 36 (1971) 87-101.
45. Minor, J.L. *J Liq. Chromatogr.*, 2,3 (1979), 309-318.
46. Lauriol, J-M.; Froment, P.; Pla, F. and Robert, A. *Holzforschung*, 41, 2 (1987) 109-113.
47. Lauriol, J-M.; Froment, P.; Pla, F. and Robert, A. *Holzforschung*, 41, 3 (1987) 165-169.
48. Lauriol, J-M.; Froment, P.; Pla, F. and Robert, A. *Holzforschung*, 41, 4 (1987) 215-224.
49. Cael, J.J.; Cannon, R.E. and Diggs, A.O. *ACS Symp. Series 150*, ACS, Washington DC (1981) 43-59.
50. Evans, R.; Wearne, R.H. and Wallis, A.F.A. *J. Appl. Polym. Sci.*, 37 (1989) 3291-3303.
51. Lapierre, L. and Bouchard, J. *9th Int. Symp. on Wood and Pulping Chem. Proc.*, Montreal, Canada (1997) 1-6.
52. Hill, D.J.T.; Le, T.T.; Darveniza, M. and Saha, T. *Polym. Degrad. Stab.*, 48 (1995) 79-87.
53. Schroeder, L.R. and Haigh, F.C. *Tappi J.*, 62, 10 (1979) 103-105.
54. Wood, B.F.; Connor, A.H. and Hill Jr, C.G. *J. Appl. Polym. Sci.*, 32 (1986) 3703-3712.
55. Huglin, M. *Light Scattering from Polymer Solutions*, Academic Press, New York (1972).
56. Kwolek, S.L.; Morgan, P.W.; Schaeffgen, J.R. and Gulrich, L.W. *Macromolecules*, 10 (1977) 1390.
57. Austin, P.R. *Chitin Solutions*, US Patent No. 4,059,457 (1977).
58. Gagnaire, D.; Saint-Germain, J. and Vincendon, M. *J. Appl. Polym. Sci., Appl. Polym. Symp.*, 37 (1983) 261-275.
59. McCormick, C.L. and Lichatowich, J. *Polym. Sci., Polym. lett. Ed.*, 17 (1979) 479-484.
60. McCormick, C.L. US patent No. 4,278,790 (1981).
61. Turbak, A.F. US patent No. 4,302,252 (1981).
62. Turbak, A.F. *Int. Dissolving and Specialty Pulps* (1983) 105-115.
63. Sjöholm, E; Gustafsson, K.; Berthold, F. and Colmsjö, A. *Carbohydr. Polym.*, 41 (2000) 1-7.
64. Kennedy, J.F.; Rivera, Z.S.; White, C.A.; Lloyd, L.L. and Warner, F.P. *Cellulose Chem. Technol.*, 24, 3 (1990) 319-325.
65. Striegel, A.M. and Timpa, J.D. *Proc. Int. GPC Symp.*, Lake Buena Vista, Florida, Waters Corp., Milford (1995) 567-591.
66. Ekmanis, J.L. and Turbak, A.F. *Lab Highlights* 251, Waters Chromatography Division, Millipore, Milford (1986).
67. Ekmanis, J.L. *Am. Lab. News* Jan-Feb (1987) 10-11.
68. Panar, M. and Betse, L.F. *Macromolecules*, 10 (1977) 1401-1406.

69. Morgenstern, B. and Kammer H-W. *Trends Polym. Sci.*, 4, 3 (1996) 87-92.
70. Turback, A.F. *Tappi J.*, 67,1 (1984) 94-96.
71. Rao, C.P.; Balaram, P. and Rao, C.N.R. *J. Chem. Soc. Faraday I*, 76 (1980) 1008-1013.
72. El-Kafrawy, A. *J Appl. Polym. Sci.*, 27 (1982) 2435-2443.
73. McCormick, C.L. and Shen, T.C. *Macromolecular Solutions*, Pergamon Press, New York (1982) 101-107.
74. Nehls, I.; Wagenknecht, W. and Philipp, B. *Cellulose Chem. Technol.*, 29 (1995) 243-251.
75. Davé, V.; Wang, J.Z.; Glasser, W.G. and Dillard, D.A. *J. Polym. Sci. : Part B: Polym Phys.*, 32, 6 (1994) 1105-1114.
76. Brendler, E.; Fischer, S and Leipner, H. *Cellulose*, 8 (2001) 283-288.
77. Pionteck, H. and Berger, W. *Cellulose*, 3 (1996) 127-139.
78. Striegel, A.M. and Timpa, J.D. *Strategies in Size Exclusion Chromatography*, ACS Symposium Series 635, American Chemical Society, Washington, DC (1996) 366-378.
79. Fuhurata K.-I.; Koganei, K.; Chang, H.-S.; Aoki, N. and Sakamoto, M. *Carbohydr. Res.*, 230 (1992) 165-177.

Chapter 3. Dissolution of cellulose in the solvent system lithium chloride / *N,N*-dimethylacetamide (LiCl/DMAc)

Abstract

*Activation and dissolution methods of cellulose in lithium chloride/*N,N*-dimethylacetamide (LiCl/DMAc) are studied. A literature review shows the importance of the multiple parameters involved such as salt concentration, sample source and preparation. The experiments carried out in order to perfect the activation and dissolution method to be used throughout the present study are presented and the suitability and efficiency obtained in the different trials is evaluated. The final procedure involves as a first step the activation by solvent exchange, with a water/methanol/DMAc sequence, followed in a second step by dissolution in 8% LiCl/DMAc at 4°C. A study of the stability of the cellulose solutions in the actual experimental conditions showed that no degradation occurred during the solvation process and confirmed the non-aggressiveness of LiCl/DMAc.*

3.1 Literature review

3.1.1 Dissolution of cellulose in LiCl/DMAc

3.1.1.1 Activation procedure

As explained in chapter 1, the activation step is crucial for opening up the polymer chains into the most relaxed conformation in order to enhance the diffusion kinetics of the solvent to the tightly packed crystalline regions that are less accessible. For most polymers, this means mainly allowing sufficient time for chains to unfold. The larger the molar mass (M_r) and crystallinity are, the longer is the time needed to obtain a true solution.

The most effective activation methods prior to dissolution in LiCl/DMAc as described in the two US patents No. 4,302,252 [1] and No. 4,278,790 [2] and by Dawsey and McCormick [3] are:

- **Polar medium swelling and DMAc exchange**

This can be achieved by either of the following:

- Water activation followed by DMAc exchange. Water swells and opens the structure; inter- and intramolecular hydrogen bonds are replaced by hydrogen bonds with H₂O. DMAc introduced subsequently impedes the inter- and intra-hydrogen bonds to re-form (shown in Figure 1-7 (A) and (C) of Chapter 1)¹.
- Steam activation followed by DMAc exchange, which works with a similar mechanism as water activation but at a higher vapour pressure, where the efficiency of penetration of water is enhanced.
- Water activation in LiCl/DMAc/H₂O by fractional distillation to less than 4% water.
- Liquid ammonia activation followed by DMAc exchange.

- **Heat activation with DMAc**

This method first proposed by Ekmanis [4,5] is based upon the fact that at or near its boiling point, the amide has sufficiently high vapour pressure to penetrate in the fibre and swell it. In heat activation, DMAc is therefore allowed to reflux with the cellulose at a temperature close to the solvent boiling point [6,7]. This procedure was reported as more advantageous over polar medium activation because it requires less LiCl in the subsequent dissolution phase but foremost because it is a one-step procedure thereby allowing easier handling of a large number of samples [8].

Recovered cellulose from heat activated solutions were found to have lost 10% in intrinsic viscosity, which indicated a slight but non significant polymer degradation [1]. Dawsey and McCormick [3], and Terbojevich *et al.* [9] observed that solutions prepared via heat activation were slightly coloured, which they attributed to oxidative degradation of the polymer at high temperature. They found that flushing nitrogen in the solutions minimised this oxidation and resulted in clear solutions. More recently Potthast *et al.* [10] showed that heat activation indeed resulted in the depolymerisation of cellulose, which was more or less pronounced depending on the pulp type and the time of activation. The authors demonstrated that this degradation occurred via endwise peeling reactions and random cleavage. The first reactions take place through the formation of *N,N*-dimethylacetoacetamide, a condensation product of DMAc. The second reactions occur through the formation of *N,N*-dimethylketeniminium ions at temperatures above 80°C, which are extremely reactive electrophilic ions able to cleave glycosidic bonds.

¹ In the papermaking industry, the fabrication of handsheets designated for the physical testing involves an aqueous impregnation of the pulp which is carried out before the disintegration. One hour in hot water or 24 hours in cold water are usually considered necessary in order to obtain a good hydration state of the fibres and even swelling that will allow optimal intra-fibre cohesion and reproducible inter-fibre linking in the subsequent drying phase of the handsheets. This step ensures stable and reproducible physical characteristics of the testing material.

3.1.1.2 Proportion of LiCl in DMAc

After the activation phase, the cellulose substrate is ready to dissolve in LiCl/DMAc. The thorough literature review by Dawsey and McCormick [3] of the experimental conditions tested by different authors showed that the relative proportions of LiCl and cellulose were critical for optimal dissolution. “Ideal” concentrations of LiCl by weight of cellulose were reported ranging between 2 and 12 % [1,2]. For cotton fibres [7,8] and for a wide variety of wood fibres such as softwood and hardwood in Kraft pulps [7], 8% LiCl was found the least amount necessary to achieve complete dissolution. Using heat activation, even high- M_r cotton celluloses appeared to completely dissolve at lower LiCl concentrations [8,11]. Nevertheless this could be an experimental error due to the degradation occurring at high temperature. According to McCormick *et al.* [12] a critical number of complexed sites seem to be required and concentrations greater than 6% are necessary for a complete dissolution of low- M_r celluloses. Reportedly, at LiCl concentration above 12% [7] to above 15% [1], the DMAc becomes supersaturated with the salt and the cellulose tends to precipitate out of solution.

Aggregate free solutions of polymers are in general difficult to prepare [13]. Sjöholm *et al.* [14] found the concentration of LiCl to be critical in the formation of aggregates upon dissolution of wood pulp and cotton linter, independently of the sample concentration. For hardwood Kraft pulp, the proportion of aggregates increased when the concentration of LiCl increased from 6% to 8% and from 8% to 10%.

Strlič *et al.* [15] recently reported the important role of the LiCl concentration. They showed that after dissolution of cellulose in 8% LiCl/DMAc, and further dilution for size-exclusion chromatography (SEC) analysis, 3% LiCl in the sample resulted in lower M_r than 1%. The authors attributed this to a decrease in the intermolecular interactions and extent of aggregation during sample preparation thereby pointing sample preparation prior to injection as a decisive process.

3.1.1.3 Sample source and composition, sample preparation

Other parameters in the dissolution process such as the cellulose concentration as well as the supramolecular structure of the polymer (which depends on the cellulose source), and the sample preparation for the activation step greatly influence the dissolution process.

In paper substrates, the access of the activation liquids to the cellulose molecules has to be facilitated. Grinding until a good defibrillation is achieved is necessary in order to reduce surface heterogeneity (see section 1.4.2 of Chapter 1). Native and chopped or cut fibres have been reported to result in incomplete and inconsistent dissolution [8,16]. This could be confirmed experimentally in the present chapter (section 3.2.1.2).

McCormick [2] reported that complete solutions of 1 to 5% cellulose powder could be achieved in less than one hour, while it took 24 to 48 hours for solutions of 6 to 15% cellulose. Turbak [17] reported that upon activation by water swelling and solvent exchange, up to 12-15% cellulose of relatively low- M_r (9×10^4 g mol⁻¹) could be solubilised in 10% LiCl/DMAc in 4-6 hours. However with higher M_r (3×10^5 g mol⁻¹), solutions up to about only 4% cellulose could be prepared. According to Silva and Laver [7], among solutions ranging from 0.8% to 1.6% cellulose, the concentration resulting in ideal dissolution was 1.2%. Similarly, Timpa [8] found the ideal cellulose concentration also being 1.2%.

Molar mass and presence of lignin [18] are also described as important parameters in the dissolution process. Ekmanis [4] noted that the higher the M_r , the more difficult the dissolution. But while most of the early studies focussed on concentrated solutions of low- M_r cellulose, Striegel and Timpa chose to study the dissolution and characterisation of high- M_r cellulose [11]. Kennedy *et al.* [19] reported that in 10% LiCl/DMAc the maximum concentration of cotton cellulose for complete dissolution was 0.075% as compared with 0.15% for softwood and hardwood cellulose. The author suggested this was due to the higher crystallinity of the cotton cellulose, and to the difference in composition and processing of the pulps. This referred especially to the treatment used to remove lignins in wood pulps, which creates voids and a wide distribution of pores. Such a microporous structure eases the penetration by activation liquids and solvent.

After water activation, sulphite pulp was reported to dissolve faster than cotton linters, which in turn dissolved faster than partially hydrolysed cotton linters [20]. Again, this was attributed to the high crystallinity of cotton cellulose.

According to Silva and Laver [7], depending on the cellulose source (pulp from softwood, hardwood, Kraft, sulphite, bleached or unbleached), the necessary time required for the different steps (activation, dissolution) in order to achieve clear solutions varied widely. Here also, the author suggested that, for higher M_r , crystallinity, α -cellulose and lignins contents, longer times were required in each step leading to dissolution. According to Sjöholm *et al.* [18], the high lignins content in softwood pulps was responsible for a decrease in the ability to swell the fibres, and therefore a decrease in solubility.

Despite these observations, inconsistencies were noted about the role of crystallinity in the solubilisation process. Hardwood Kraft pulp (low crystallinity) was reported to dissolve much more slowly than cotton (high crystallinity) [7]. Recent publications also confirmed that the degree of crystallinity is not responsible for the difference in solubility between cellulose substrates [21].

In wood pulps, differences were reported between softwood and hardwood, the former showing slower dissolution [19] or lower solubility [22]. Softwood Kraft pulp dissolved in LiCl/DMAc was shown to lead to the formation of gel-like structures consisting of mannans and lignins, which could not be related to the crystallinity [18]. In that case two hypotheses were submitted, the first being that lignins content was more probably

involved in the long solubilisation times required, and the second being the formation of a gel constituted of glucomannans hemicelluloses, which quickly covered the fibres and hindered the progress of further dissolution.

Other studies confirmed the presence of aggregates under specific conditions [9]. Aggregates and associates that were shown to form in solutions of cellulose from diverse sources (micro-crystalline cellulose and cellulose from softwood Kraft pulp and hardwood sulphite pulp) in 6% and 9% LiCl/DMAc could be disintegrated by a dilution to 2.6% LiCl (*i.e.* SEC concentration). But this was only possible within certain limits of cellulose versus salt concentration [23]. A maximum concentration of 1% cellulose in 9% LiCl/DMAc was required to form a true (disaggregated) solution upon dilution to 0.9% LiCl. Cellulose often forms so-called fringe-micelles in solution. These large associates or aggregates were proven to be highly swollen parts of the former crystalline regions of the cellulose. In a solution with too low LiCl concentration and/or too high cellulose concentration, the solvent is unable to completely rupture the strong hydrogen bonds in the cellulose [24].

Recently, Schult *et al.* [25] published a modified polar medium activation process that reportedly allowed them to obtain the complete dissolution of high- M_r cellulose from sulphite pulp in 8% LiCl/DMAc. The procedure involves first a swelling, in 0.1 M LiCl instead of water, and subsequent steps of washing with chelating agents such as EDTA (ethylene diamine tetraacetic acid), DTPA (diethylene triamine pentaacetic acid) and citric acid. These washings allow to remove any remaining ion in the pulp, as these are thought to interfere in the association of the cellulose with the solvent complex, thereby hindering the dissolution process. Following, a second swelling in LiCl ensures that all the ions associated with the cellulose are Li^+ . Then a Soxhlet extraction in acetone removes any possible extractive left in the pulp and acts as first stage in the solvent exchange, which proceeds with methanol and DMAc.

However, probably the most difficult situation remains that of mechanical wood pulp because of the strong interactions between cellulose, hemicelluloses and lignins. Heat activation was reported to be more efficient than polar medium activation in allowing dissolution of a higher proportion of groundwood pulp. However, total dissolution of mechanical pulp in LiCl/DMAc has never been reported.

It is noteworthy that very few authors have included sized papers in their studies. Concerning residual presence of non-fibrous components, only one small mention could be found in the literature, reportedly that small amounts (<2%) of pectins and waxes should not interfere in the dissolution process [8].

3.1.2 Stability of solutions of cellulose in LiCl/DMAc

The solutions of cellulose in LiCl/DMAc are reported to be extremely stable [26]. Some researchers found no degradation of the cellulose after several months in solution [9] and

even years at room temperature [1,27]. High LiCl concentrations (above 10%) were reported to have no degradation effect on cellulose over time [19]. McCormick *et al.* [12] noted a slight decrease of 2% in relative viscosity of cellulose solutions in 9% LiCl/DMAc over 30 days, which they attributed to changes in inter and intra-molecular hydrogen bonding.

Strlič *et al.* [28] showed that cellulose from linters powder that were submitted to an oxidation treatment, in order to increase the sensitivity to solvent-induced degradation, did not undergo further degradation in 8% LiCl/DMAc. In a more recent study, the authors found for cellulose in 1% LiCl/DMAc at room temperature a constant k of random glycosidic bond cleavage (derived from the Ekamstam equation described in Appendix 6-3) of $6.9 \times 10^{-8} \text{ mol mol}^{-1}_{\text{monomer}} \text{ day}^{-1}$, *i.e.* a decrease in M_r of 47 g mol^{-1} per day [15].

In contrast, a recent study by Jerosch [29] found LiCl/DMAc had some degrading action on cellulose in specific cases. When cellulose was kept in 8% LiCl/DMAc at 40°C over 5 days, M_r was stable for 2 weeks only, and fell with a decrease of 23% after 22 days. The initial degradation state of cellulose and the temperature-time history was found paramount in the stability of cellulose solutions. However, with softwood bleached Kraft pulp paper and cotton linters paper, no decrease in M_r was found when dissolution was carried out at 4°C . With papers that had been subjected to accelerated aging, including either heat/humidity or pollution, the stability of the solutions was lower as the M_r started dropping slightly after one week.

3.2 Development of the method for the dissolution of cellulose in LiCl/DMAc

3.2.1 Experimental

3.2.1.1 Solvent and mobile phase preparation

As outlined in Chapter 1, water has to be excluded from the solvent system since its presence hinders the complexation with cellulose [1]. The amount of water has to be kept to less than 5% in the final solution. As both LiCl and DMAc are hygroscopic, special care has to be taken in the preparation of the solvent.

LiCl was oven-dried and stored in a desiccator over drierite (CaSO_4). Aliquots of LiCl were weighted swiftly when needed and placed back in the desiccator until dry before use.

For drying DMAc two methods were tested: the first was heating at $100\text{--}110^\circ\text{C}$ for 10 minutes in order to drive off the residual moisture, and the second was adding aluminium sodium silicate molecular sieve (0.4 nm effective pore size) to the solvent bottle. Both

methods worked equally well; therefore the method of drying with molecular sieve was chosen because it was feared that the heating method could lead to some oxidation of the DMAc.

When dry, DMAc was filtered through 0.5 μm pore, 25 mm diameter Millex LCR filters (Millipore) with a hydrophilised polytetrafluoroethylene (PTFE) membrane. If not used immediately, the solvent was stored under nitrogen at 4°C until use within the same week.

In the trials of high temperature activation/dissolution, the appropriate amount of LiCl was added directly in the reacti-vials (Pierce) containing the activating cellulose in the appropriate volume of DMAc (see section 3.2.1.3.1).

In the procedure of dissolution following solvent exchange activation, LiCl/DMAc was prepared in stock solution by adding the required amount of dry LiCl (8%) to warm DMAc (40°C) under magnetic stirring. LiCl dissolved within about one hour. Warm DMAc allowed for the best dissolution of the salt over room temperature DMAc and DMAc heated to 100°C (Table 3-2).

Samples of 200 mL of this stock solution were prepared at a time. Only 50 mL was used as dissolution solvent and the rest made the size-exclusion chromatography (SEC) mobile phase (0.5% LiCl/DMAc) by diluting with anhydrous DMAc, in order to have the same batch of solvent for the dissolution and the SEC run. When not used immediately, the LiCl/DMAc solutions were flushed with nitrogen and stored at 4°C to limit any possible degradation.

3.2.1.2 Sample preparation

The necessity of defibrillating the paper in order to ease the solvent access was verified by a trial of heat activation/dissolution of paper cut in small pieces (2 mm \times 2 mm) which did result in very incomplete dissolution. Under the same experimental conditions paper defibrillated as described hereafter, resulted in complete dissolution.

Two to 2.5 g of paper were taken out of four different samples of Whatman No.1 paper in different part of the sheets (150 mm \times 190 mm), left, middle and right portions. The paper was ground during five minutes in a small two-blade blender (50 mL volume capacity). The samples were then placed in a controlled environment chamber at 50% relative humidity (rH) and 23°C, conditions corresponding to TAPPI standard T 412 om-94 [30], in order to equilibrate for at least 2 days. The reason for equilibrating the samples was mainly because it ensured the reproducibility of the weighting. About 5×10^{-2} g ($\pm 0.02\%$) was weighted for activation/dissolution.

3.2.1.3 Optimisation of activation and dissolution

Two methods were tested to obtain an appropriate and efficient dissolution.

The first method was heat activation/dissolution as proposed by Timpa [8,31], adapted from the 'one-pot' procedure developed by Ekmanis [5]. This procedure was tried in the first place since the activation phase was reported to be faster and less work intensive than the solvent exchange activation method. The latter procedure was tried afterwards and was derived from the original method as proposed by Turbak [1] and McCormick [2].

In all cases, the activation was done in conical bottom 10 mL reacti-vials (Pierce) capped with Teflon lined screw caps, under constant stirring in a heating/stirring unit (Pierce), using V-shaped Teflon-coated magnetic stirrers.

3.2.1.3.1 High temperature activation and dissolution

3.2.1.3.1.1 High temperature activation

Several conditions were tested by varying the activation time and the concentration of LiCl, which are listed in Table 3-1. In all the trials, 5 mL of anhydrous DMAc was heated to 150°C, just below boiling temperature (boiling point =164-166°C) in the reacti-vial left uncapped for 10 minutes in order to drive residual moisture out. Fifty milligrams ($\pm 1 \times 10^{-5}$ g) of defibrillated paper was added, and the reacti-vial was then tightly capped. The activation proceeded at 150°C with refluxing DMAc.

3.2.1.3.1.2 High temperature dissolution

After activation, the temperature was lowered from 150°C to 100°C and allowed to stabilise for 20 minutes. Then LiCl was added directly in the reacti-vial. The temperature was either kept at 100°C or lowered to 50°C.

In the different trials, the amounts of dry LiCl added in the DMAc activation mixture were: 5%, 8%, 10%, 12% and 13% (0.25 g, 0.4 g, 0.5 g, 0.6 g and 0.7 g in 5 mL DMAc). The sample was left heating/stirring until maximum dissolution stage was reached, which took from 3 to 4 days. Assuming dissolution was complete, the cellulose solution was then 10 mg mL⁻¹, *i.e.* 1% (wt/v). Table 3-1 reports the experimental conditions in the different trials.

3.2.1.3.2 Polar medium swelling activation followed by warm, ambient or cold dissolution

Table 3-2 lists the trials of solvent preparation, polar medium activation, dissolution time, cellulose concentration and LiCl concentration in order to optimise the dissolution conditions.

3.2.1.3.2.1 Polar medium swelling and solvent exchange

Polar medium swelling and solvent exchange activation consisted in a thorough swelling in water followed by exchange first with methanol and second with DMAc. Activation volumes were 8 to 10 mL. The time and the number of exchanges varied in the different trials.

The extra step of methanol exchange was added compared to the methods described in the literature in order to help expel the residual water, thus avoiding a collapse of the fibres and pores structure, and thereby enhancing further penetration of DMAc.

Two methods were tested for the elimination of the swelling liquid after each of the exchanges: centrifugation and filtration. Centrifugation at 2500 rpm during 20 minutes was unsatisfactory as the liquid was not eliminated and a non-negligible amount of fibres was lost after several centrifugation steps. Filtration under vacuum was found more appropriate, with almost no fibre loss and a satisfactory elimination of the liquids. Filtration was therefore adopted and was carried out with a 25 mm glass microanalysis vacuum filter holder and fritted glass 15 mL funnel capacity (Millipore), using 0.5 μm pore Millex LCR filters.

3.2.1.3.2.2 Dissolution

Dissolution took place after filtering out the last DMAc exchange volume, by adding 5 mL of the stock solution 8% LiCl/DMAc to the paper fibres in the reacti-vial. Solutions with lower salt concentrations were achieved by diluting this stock solution with dry DMAc. The reacti-vial was tightly capped and left stirring. Different dissolution temperatures (warm, ambient and cold) were tested. The different conditions are reported in Table 3-2.

3.2.2 Results

3.2.2.1 High temperature activation and dissolution

Table 3-1 reports the results of the different trials carried out. The hot DMAc procedure often resulted in yellow cellulose solutions. This discolouration was present regardless of the state of degradation (unaged, artificially aged) and composition of the samples (plain Whatman No.1, with/without alum, and with/without gelatine). This is consistent with the results from Terbojevitch *et al.* [9]. Complete dissolution was not achieved in any case.

It was found that long activation time (22 hours) was detrimental, resulting in significant yellowing and lack of improved dissolution, and that one-hour activation was found

sufficient. Maximum dissolution was usually reached within 3 to 4 days and did not proceed further even upon prolonged periods of up to 11 days.

The concentration of LiCl appeared to be critical. The best - yet incomplete - dissolution of plain Whatman No.1 paper (unsized unaged) was achieved in 3 days with exactly 8% LiCl. No yellowing of the solution occurred. This corresponded to a ratio of cellulose to LiCl of 1/8. Less or more LiCl resulted in a poorer dissolution and/or yellowing.

After activation and upon adding LiCl it was found that if temperature was lowered from 100°C to 50°C, the yellowing of the solution could be avoided. The yellowing was believed to arise from degradation of the cellulose in the solvent at high temperature. Indeed, it was expected that prolonged activation times at 150°C, as well as a dissolution at 100°C in the presence of lithium salts, would most likely partially degrade the paper constituents. This effect would increase in the case of partially oxidised (oxicelluloses) or hydrolysed cellulose. Additionally, at such temperatures, any residual oxygen present in the reacti-vial would contribute to the oxidative degradation of the polysaccharides.

Residual moisture present in the paper that would not have been totally eliminated during the activation in the anhydrous DMAc could also play a role in the low efficiency of the dissolution.

According to the results, a gelatine content of 0.5% (wt/wt) did not seem to hinder the dissolution (sample No. 5c) but with higher gelatine content in the paper, such as 12.5% (wt/wt), a precipitation of the gelatine out of solution occurred (sample No. 4). However, the visual examination did not allow to determine whether the precipitate was gelatine alone or a co-precipitate of gelatine and cellulose.

3.2.2.2 Polar medium/solvent exchange activation and dissolution in warm, ambient or low temperature

3.2.2.2.1 *Polar medium/solvent exchange activation*

Given the unsatisfying results obtained with the high temperature activation/dissolution method reported in the previous section, namely of irreproducible efficiency yet incomplete dissolution, and yellowing associated with potential degradation at high temperature, it was decided to test activation and dissolution at lower temperature. The extra step of the exchange from water to methanol prior to the exchange with anhydrous DMAc was done in order to ensure the total elimination of water from the paper substrate and eliminate the suspected negative effect of residual moisture.

Table 3-1. High temperature activation and dissolution experiments.

No.	sample	activation	LiCl concentration	dissolution time and efficiency	yellowing
1a	W ¹ unsized unaged RC ³	1h DMAc 150°C	1) 5% - 100°C - 3 days 2) after 3 days, added to 10% -100°C	1) 3 days, no dissolution 2) 5 days, mostly dissolved	- ² -
1b	W / A5 aged 4 days ⁴ RC	1h DMAc 150°C	1) 5% - 100°C - 3 days 2) after 3 days, added to 10% -100°C	1) 3 days, no dissolution 2) 11 days, mostly diss., crystalline deposit	+ ²
1c	W / A5 aged 13 days ⁴ RC	1h DMAc 150°C	1) 5% - 100°C - 3 days 2. after 3 days, added to 10% -100°C	1) 3 days, no dissolution 2) 11 days, mostly diss., crystalline deposit	+
2	W unsized unaged RC	22 h DMAc 150°C	1) 8% - 100°C - 6 days 2) after 6 days, added to 12% - 100°C	1) 6 days, no dissolution 2.) 9 days, little dissolved	+ +
3	W unsized unaged, RC	1h DMAc 150°C	10% - 100°C	5 days, mostly dissolved	+ / -
4	W / 12.5% K ⁵ , RC	1h DMAc 150°C	13% - 100°C	8 days, mostly diss., gelatine precipitated	++
5a	W unsized unaged, C ⁶	1h DMAc 150°C	1) 8% - 100°C 2) T° immediately lowered to 50°C	3 days, mostly dissolved	-
5b	W unsized aged 91 days, C	1h DMAc 150°C	1) 8% - 100°C - 2) T ↓ 50°C	3 days, mostly dissolved	-
5c	W / K0.5 aged 91 days ⁷ , C	1h DMAc 150°C	1) 8% - 100°C - 2) T ↓ 50°C	3 days, mostly dissolved	-
6a	W unsized unaged, C	1h DMAc 150°C	1) 12% - 100°C - 2) T ↓ 50°C	1) 3 days, partly dissolved 2) no further dissolution with ↑ time	-
6b	W unsized unaged, RC	1h DMAc 150°C	1) 12% - 100°C - 2) T ↓ 50°C	1) 3 days, partly dissolved 2) no further dissolution with ↑ time	-
7a	W unsized unaged, C	1h DMAc 150°C	1) 5% - 100°C - 2) T ↓ 50°C	11 days, partly dissolved	-
7a'	W unsized unaged C	1h DMAc 150°C	1) 8% - 100°C - 2) T ↓ 50°C	11 days, partly dissolved	-
7b	W unsized unaged, dry ⁸	1h DMAc 150°C	1) 5% - 100°C - 2) T ↓ 50°C	11 days, partly dissolved	-
7b'	W unsized unaged, dry	1h DMAc 150°C	1) 8% - 100°C - 2) T ↓ 50°C	11 days, partly dissolved	-
8a	W / N0.5 aged 91 days ⁹ , C	1h DMAc 150°C	1) 10% - 100°C - 2) T ↓ 50°C	4 days, little dissolved, no further dissol.	-
8b	W / N2 aged 91 days ⁹ , C	1h DMAc 150°C	1) 10% - 100°C - 2) T ↓ 50°C	4 days, little dissolved, no further dissol.	-
8c	W / K0.5 aged 91 days ⁹ , C	1h DMAc 150°C	1) 10% - 100°C - 2) T ↓ 50°C	4 days, little dissolved, no further dissol.	-
8d	W / K2 aged 91 days ⁹ , C	1h DMAc 150°C	1) 10% - 100°C - 2) T ↓ 50°C	4 days, little dissolved, no further dissol.	-

¹ Whatman No.1 paper.² “-“ = no yellowing; “+” = yellowing.³ room environment conditions.⁴ A5 = sample immersed in 5% aqueous alum solution (wt/v), accelerated aging conditions of 80°C and 50% rH.⁵ K12.5 = sample sized with Kind and Knox gelatine 12.5% uptake (wt/wt).⁶ C = conditioned to TAPPI standard conditions [30] (23°C and 50% rH).⁷ K0.5 = sample sized with Kind and Knox gelatine, 0.5% uptake (wt/wt); accelerated aging conditions of 80°C and 50% rH.⁸ sample dried in a desiccator over drierite for 7 days.⁹ N0.5, N2, K0.5 and N2 = samples sized with Norland and Kind and Knox gelatines, 0.5% and 2% uptake (wt/wt), accelerated aging conditions of 80°C and 50% rH.

The trials reported in Table 3-2, carried out in order to optimise time and efficiency of dissolution allowed to conclude that:

- Thorough swelling in water was crucial and was more efficient when done at 40°C than at room temperature.
- One water exchange at 40°C was sufficient for unsized papers, but for sized papers the operation was more efficient if repeated twice. The water helped wash out part of the gelatine, which eased dissolution in the next step.
- One hour for the water exchange was enough; prolonging swelling beyond that was not necessary.
- Thorough “drying” by two consecutive exchanges in methanol and in DMAc resulted in faster and more efficient subsequent dissolution.
- Two DMAc exchanges of 45 minutes proved sufficient but for convenience of a one-day work, the second exchange was prolonged overnight.

3.2.2.2 Warm, ambient or low temperature dissolution

Water and solvent exchange activation allowed for better subsequent dissolution and turned out much less aggressive for the cellulose than high temperature activation/dissolution. The different trials reported in Table 3-2 allowed to conclude that:

- Complete dissolution could be achieved, as opposed to high temperature activation/dissolution.
- Complete dissolution was fast, as in most cases it took 48 hours and in some cases even less (samples No. 4a, 4b, 5a, 5b).
- No yellowing of the solutions occurred.
- Concentrations of LiCl in DMAc below 8% were not sufficient for complete dissolution.
- A concentration of 1% cellulose was suitable.
- After initial dissolution at room temperature for 15 to 16 hours, completion of the dissolution could be achieved at 4°C.

3.2.3 Conclusion of the activation and dissolution study

Polar medium swelling and solvent exchange activation although more labour intensive than the one-pot method at high temperature, allowed to achieve better, faster and more reproducible subsequent dissolution. Therefore this activation method was preferred for the following experiments over heat activation. Additionally, degradation of cellulose when submitted to high temperatures was a major concern. Also, the possibility of Maillard reactions (see Appendix 3-1) leading to browning of the samples where residual gelatine was present could not be ruled out when performing heat activation.

Activation with warm water (40°C) and exchange with solvents at ambient conditions was therefore less aggressive and allowed to carry out subsequent dissolution at ambient temperature for 15 hours (first) and completion at 4°C in about 30 additional hours. Ideal dissolution conditions were obtained with 8% LiCl/DMAc and 1% cellulose.

Table 3-2. Polar medium/solvent exchange activation and warm, ambient or cold temperature dissolution experiments.

No.	sample type	activation phase	solvent preparation	dissolution phase	cellulose conc	dissolution time and efficiency
1	W unsized unaged	1) 60 min H ₂ O room T° 2) 30 min MeOH room T° 3) 1h DMAc room T° 4) 65 h DMAc room T°	LiCl added to DMAc room T°	8 % LiCl/DMAc room T°	1 %	dissolution in 48 h
2	W unsized unaged	1) 30 min H ₂ O room T° 2) 15 min MeOH room T°, 2x 3) 15 min DMAc room T°, 2x	LiCl added to hot DMAc ¹	6.7 % LiCl/DMAc room T° ²	0.83 %	dissolution in 9 days
3	W unsized unaged	same as sample "2"	LiCl added to hot DMAc	6.7 % LiCl/DMAc at 40°C	0.83 %	diss. incomplete after 9 days
4a	W unsized unaged	1) 60 min H ₂ O 40°C	LiCl added to cooled DMAc	8 % LiCl/DMAc room T°	1 %	diss. in less than 48 h both
4b	W unsized aged ³	2) 45 min MeOH room T°, 2x 3) 45 min DMAc room T°, 2x				
5a	W / K2 ⁴ unaged	1) 30 min H ₂ O 40°C, 2x	LiCl added to cooled DMAc	8 % LiCl/DMAc room T°	1 %	diss. in less than 48 h both
5b	W / K0.5 ⁵ aged ³	2) 45 min MeOH room T°, 2x 3) 45 min DMAc room T°, 2x				
6	W unsized unaged	1) 3 h H ₂ O 40°C 2) 15 min MeOH room T°, 2x 3) 15 min DMAc room T°, 2x	LiCl added to cooled DMAc	8 % LiCl/DMAc room T°	1 %	dissolution in 48 h
7	W unsized unaged	1) 16 h H ₂ O 40°C 2) 15 min MeOH room T°, 2x 3) 15 min DMAc room T°, 2x	LiCl added to cooled DMAc	8 % LiCl/DMAc room T°	1 %	dissolution in 48 h
8	W unsized unaged	1) 60 min H ₂ O 40°C 2) 45 min MeOH room T°, 2x 3) 45 min DMAc room T° 4) 16 h DMAc room T°	LiCl added to dry DMAc ⁶	1) 8 % LiCl/DMAc room T° 2) placed at 4°C after 16 h	1 %	dissolution in 48 h

¹ DMAc is heated to 100-110°C for 10 minutes to drive off the moisture.

² 6.7% LiCl/DMAc was achieved by adding 5 mL 8%LiCl/DMAc and 1 mL of DMAc to the cellulose sample.

³ Accelerated aging conditions: 94 days at 80°C and 50% rH.

⁴ K2 = sample sized with Kind & Knox gelatine, 2% uptake (wt/wt).

⁵ K0.5 = sample sized with Kind & Knox gelatine, 0.5% uptake (wt/wt).

⁶ DMAc was dried with molecular sieve.

3.2.4 Final procedure for activation and dissolution

3.2.4.1 Final procedure for activation

This section summarises the final conditions chosen for activation and dissolution of cellulose in LiCl/DMAc according to the different trials carried out. Figure 3-1 shows a schematic representation of the process.

Defibrillated paper samples were swelled during one hour in 10 mL deionised water at 40°C (milli-Q, Millipore) twice consecutively.

Two consecutive exchanges of 45 minutes each with 8 mL methanol were carried out subsequently, followed by two consecutive exchanges with 8 mL anhydrous DMAc (prepared as described in section 3.2.1.1). The first DMAc exchange lasted for 45 minutes and the second was prolonged overnight.

After each exchange, the activation liquids were filtered under vacuum through 0.5 µm pore Millex LCR filters (Millipore) and the paper fibres were carefully removed with tweezers from the filter and placed back in the reacti-vial for the next liquid exchange. For each sample, the same filter was kept through the whole activation procedure in order to minimise fibre loss, to the exception of the heavily sized papers, which tended to clog the filters.

3.2.4.2 Final procedure for dissolution

The dissolution solvent was a solution of 8% LiCl/DMAc, and was prepared by adding the required amount of dry LiCl to dry warm DMAc (40°C) (see section 3.2.1.1) previously filtered through 0.5 µm pore, 25 mm diameter Millex LCR filters with a hydrophilised PTFE membrane. The solvent was freshly made every week, and if not used immediately, was stored under nitrogen at 4°C until use.

Dissolution took place under magnetic stirring after filtering out the second DMAc exchange, by adding 5 mL of the stock 8% LiCl/DMAc to the fibres.

The sample was stirred at room temperature for 24 hours and the reacti-vial, still capped, was placed at 4°C to complete dissolution. In all cases, the solutions were clear in a reasonable period of time with no visible residue or cloudiness, no gel formation, and no yellowing. The Whatman No.1 samples dissolved totally within 2 to 6 days, depending on the presence or absence of sizing (and on the gelatine content of the samples), and on the state of degradation (aging). Other paper types tested such as softwood chemical pulp paper dissolved totally in 30 minutes. It was noted that if the sample was not totally dissolved within 7 days, the dissolution did not progress further. In the stock sample solution, the concentration of cellulose was about 10 mg mL⁻¹, *i.e.* 1% (wt/v), assuming no fibre loss during the procedure.

Right after dissolution was achieved, the samples were diluted for size-exclusion chromatography with multiangle light scattering detection (SEC/MALS) experiments to 0.5% LiCl/DMAc with anhydrous DMAc, *i.e.* to a sample concentration of about 0.625 mg mL^{-1} (0.0625% wt/v). They were filtered through $0.5 \mu\text{m}$ Millex LCR filters before injection on the SEC columns. The remaining cellulose solutions were stored at 4°C under nitrogen.

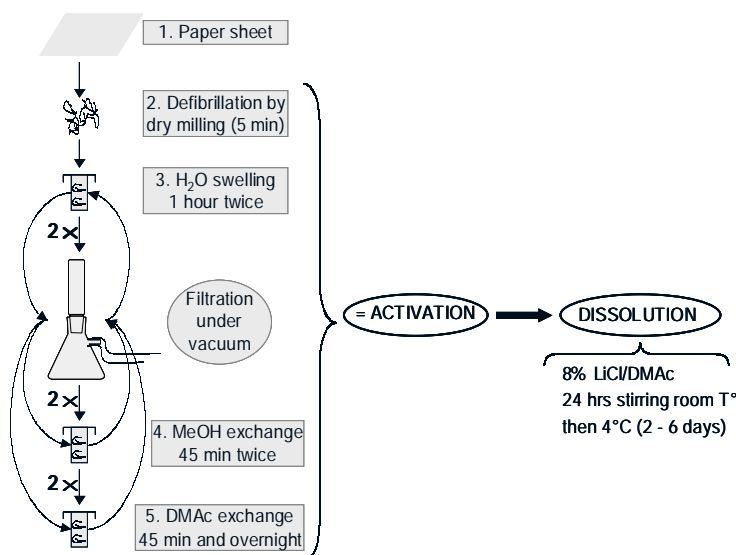


Figure 3-1. Diagram of the activation and dissolution procedure chosen for cellulose in LiCl/DMAc

3.3 Stability of cellulose/LiCl/DMAc solutions

Good stability of cellulose solutions in LiCl/DMAc over time is generally, but not unanimously, reported in the literature (see section 3.1.2). However, fewer mentions could be found of the stability of cellulose/LiCl/DMAc at low temperature [29]. In the present study it was important to investigate this stability under the experimental conditions chosen.

3.3.1 Experimental

Two samples of Whatman paper No.1 unaged were dissolved in LiCl/DMAc according to the final procedure (section 3.2.4). After completing dissolution, one sample was left in 8% LiCl/DMAc (sample denoted C_{t_0} 8%LiCl 10m) and the second sample was diluted $\frac{1}{4}$ to 2% LiCl/DMAc (sample denoted C_{t_0} 2%LiCl 10m). Both were left standing at 4°C for a period of 10 months (10m), after which they were diluted to 0.5% LiCl/DMAc for analysis by SEC/MALS. Each sample was run twice. The values of molar mass (M_r) obtained were averaged.

Three other samples of Whatman paper No.1 unaged were dissolved in the same manner and immediately diluted to 0.5% LiCl/DMAc to be analysed right after completion of the dissolution (C_{t_0} ref). Each sample was run in two to three replicates for a total of seven runs, and the values of M_r obtained were again averaged.

At this stage, the method of SEC with MALS detection used has not been described but in order to alleviate the text of redundant descriptions, the reader is referred to Chapter 4. The theory of light scattering measurements is described in section 4.1.2.2 and the analytical method applied for cellulose characterisation is in section 4.2.3.

3.3.2 Results

Table 3-3 reports the average values of M_n , M_w and M_z of each sample. The molar mass distribution (MMD) profiles of C_{t_0} ref, C_{t_0} 2%LiCl 10m and C_{t_0} 8%LiCl 10m are represented in Figure 3-2 which shows overlaid differential molar mass graphs.

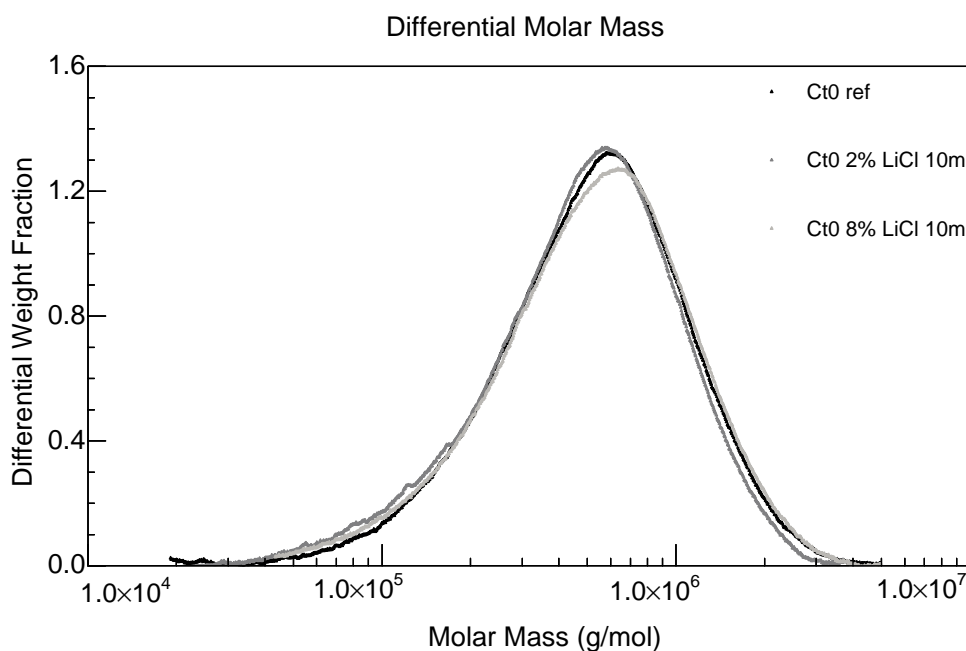


Figure 3-2. Overlaid differential molar mass graphs of C_{t_0} ref, C_{t_0} 2%LiCl 10m and C_{t_0} 8%LiCl 10m.

Table 3-3. Average M_r values and polydispersity (PD) of the cellulose samples in fresh and long-standing solutions.

	AVG $M_n \times 10^{-5}$ (g mol ⁻¹)	AVG $M_w \times 10^{-5}$ (g mol ⁻¹)	AVG $M_z \times 10^{-5}$ (g mol ⁻¹)	AVG PD
C_{t_0} ref (\pm RSD %)	3.96 (\pm 7.8%)	6.68 (\pm 2.0%)	10.09 (\pm 4.6%)	1.70 (\pm 7.1%)
C_{t_0} 2%LiCl 10m	3.66	6.50	10.29	1.78
C_{t_0} 8%LiCl 10m	3.51	6.68	10.80	1.91

The MMD profiles look almost identical, and only a 2.7% difference in the average M_w was found between the three samples, which falls within the calculated relative standard deviation (RSD). Therefore we can conclude that no degradation of the cellulose seems to have occurred in 10 months at 4°C.

A slight difference between the samples was observed in the value of the polydispersity PD (M_w/M_n). PD was a little larger for the two 10-months old solutions, but while this slight increase falls within the RSD for Ct₀ 2%LiCl 10m compared to Ct₀ ref, it falls just outside the RSD for Ct₀ 8%LiCl 10m. The broader MMD was due to a slightly lower M_n and slightly higher M_z .

The somewhat higher proportion of low- M_r and high- M_r fractions in Ct₀ 8%LiCl 10m may be due to variations in the hydrogen bonding, and for the high- M_r specifically, to association of the cellulose molecules upon standing at high concentration.

In conclusion, despite minute changes occurring over a period of 10 months, the solutions of cellulose/LiCl/DMAc exhibited remarkable stability at 4°C.

Chemicals and materials

Lithium chloride (LiCl), methanol and *N,N*-Dimethylacetamide (DMAc) were purchased from Acros Organics (Springfield, NJ, USA). Aluminium sodium silicate molecular sieve (0.4 nm effective pore size), Drierite and Whatman No.1 filter paper were obtained from Fisher Scientific (Springfield, NJ, USA). Millex LCR filters (0.5 µm, 25 mm diameter) and the vacuum filter holder, adapted fritted glass and 15 mL funnel were from Millipore (Bedford, MA, USA) and purchased through Fisher Scientific.

Instruments

Multiangle light scattering detector Dawn EOS and interferometric differential refractometer Optilab DSP were from Wyatt Technologies Corp. (Santa Barbara, CA, USA). The four-channel HPLC solvent degasser Degassit™ was obtained from Metachem Technologies Int. (Torrance, CA, USA) and HP 1100 isocratic pump G1310A was from Hewlett Packard, now Agilent Technologies (Palo Alto, CA, USA). Injector model 7725i was from Rheodyne L.P. (Cotati, CA, USA). The heating/stirring unit was from Pierce (Rockford, IL, USA).

References

-
1. Turbak, A.F. *US patent No. 4,302,252 (1981)*.
 2. McCormick, C.L. *US patent No. 4,278,790 (1981)*.
 3. Dawsey, T.R and McCormick, C.L. *J. Macromol. Sci - Rev. Macromol. Chem. Phys.*, C30, 384 (1990) 405-440.

4. Ekmanis, J.L. and Turbak, A.F. *Lab Highlights* (Internal communication) 251, Waters Chromatography Division, Millipore, Milford (1986) LAH 0305 2/86.
5. Ekmanis, J.L. *Am. Lab. News* Jan-Feb (1987) 10-11.
6. Striegel, A.M. and Timpa, J.D. *Strategies in Size Exclusion Chromatography*, ACS Symposium Series 635, American Chemical Society, Washington, DC (1996) 366-378.
7. Silva, A.A. and Laver, M.L. *Tappi J.*, 80, 6 (1997) 173-180.
8. Timpa, J.D. *J. Agric. Food Chem.*, 39 (1991) 270-275.
9. Terbojevich, M.; Cosani, A.; Conio, G.; Ciferri, A. and Bianchi, E. *Macromolecules*, 18 (1985) 640-646.
10. Potthast, A.; Rosenau, T.; Sartori, J.; Sixta, H. and Kosma, P. *Polymer*, 44 (2003) 7-17.
11. Striegel, A.M. and Timpa, J.D. *Carbohydr. Res.*, 267 (1995) 271-290.
12. McCormick, C.L.; Callais, P.A. and Hutchinson Jr, B.H. *Macromolecules*, 18 (1985) 2394-2401.
13. Rinaudo, M. *J. Appl. Polym. Sci.: Polym. Symp.*, 52 (1993) 11-17.
14. Sjöholm, E; Gustafsson, K.; Eriksson, B.; Brown, W. and Colmsjö, A. *Carbohydr. Polym.* 41 (2000) 153-161.
15. Strlič, M.; Kolenc, J.; Kolar, J. and Pihlar, B. *J. Chromatogr. A*, 964 (2002) 47-54.
16. Debzi, El M. *Celluloses issues du traitement à la vapeur: évolution des masses moléculaires moyennes, transformations morphologiques et cristallines*, Thèse de Doctorat, Université Joseph Fournier – Grenoble I (1992) 43.
17. Turback, A.F. *Tappi J.* 67,1 (1984) 94-96.
18. Sjöholm, E; Gustafsson, K.; Pettersson, B. and Colmsjö, A. *Carbohydr. Polym.*, 32 (1997) 57-63.
19. Kennedy, J.F.; Rivera, Z.S.; White, C.A.; Lloyd, L.L. and Warner, F.P. *Cellulose Chem. Technol.*, 24, 3 (1990) 319-325.
20. Pionteck, H. and Berger, W. *Cellulose*, 3 (1996) 127-139.
21. Matsumoto, T.; Tatsumi, D.; Tamai, N. and Takaki, T. *Cellulose*, 8 (2001) 275-282.
22. Karlsson, O. and Westermark, U. *Proc. Tappi Pulping Conf.*, 1 (1994) 1-4.
23. Röder, T.; Morgenstern, B.; Schelosky, N. and Glatter, O. *Polymer*, 42 (2001) 6765-6773.
24. Röder, T.; Morgenstern, B. and Glatter, O. *Macromol. Symp.*, 162, Wiley (2000) 87-93.
25. Schult, T.; Hjerde, T., Optun, O.I.; Kleppe, P.J. and Moe, S. *Cellulose*, 9 (2002) 149-158.
26. Johnson, D.C. *Cellulose Chemistry and its Applications*, Ch. 7, Wiley, New York (1985).
27. Turbak, A.F. *Wood and Agricultural Residues*, Academic Press, New York (1983) 87-99.
28. Strlič, M.; Kolar, J.; Žigon, M. and Pihlar, B. *J. Chromatogr. A*, 805 (1998) 93-99.
29. Jerosch, H. *Evaluation de l'état de dégradation de la cellulose/holocellulose dans différents types de papiers par chromatographie d'exclusion stérique*, Thèse de Doctorat, Université Versailles-St. Quentin-En-Yvelines (2002).
30. T 412 om-94, *TAPPI test methods*, Technical Association of the Pulp and paper Industry, TAPPI press, Atlanta, US (1994).
31. Timpa, J.D. and Ramey Jr, H.H. *Text. Res. J.*, 59, 11 (1989) 661-664.

Chapter 4. Size-Exclusion Chromatography (SEC) and Multiangle Light Scattering (MALS) detection: principles and application to the study of cellulose

Abstract

As detection is a crucial aspect of size-exclusion chromatography (SEC), the detection modes that are available and the type of information each one provides are reviewed. The principles and the advantages of multiangle laser light scattering (MALS) coupled with differential refractive index (DRI) detection are outlined. A section is especially dedicated to the detectors set-up, and to the determination of the parameters required for the characterisation of the molar mass distribution (MMD) of the polymer, the calculation of the molar mass (M_r) averages, and the root mean square (rms) radii averages. Among these parameters is the refractive index increment (dn/dc) of cellulose in 0.5% LiCl/DMAc. The precision and reproducibility of SEC/MALS/DRI for the analysis of cellulose are evaluated in order to validate the method. MALS also allowed for the characterisation of the polymer in solution. The conformation of cellulose in LiCl/DMAc was determined to be random coil, and a study of the solvent efficiency showed that LiCl/DMAc was a good solvent for the conditions chosen.

4.1 Molar mass (M_r) determination and choice of detection in SEC

Detection of eluted solutes in size-exclusion chromatography (SEC) can be done either relative to known standards or in absolute mode. The detectors most used in SEC as classified according to their functioning mode (some detectors pertain to several categories) are:

- universal detectors with a response proportional to the concentration, such as refractive index (RI) and ultraviolet (UV) detectors;
- detectors with a response function of molar mass (M_r): either directly proportional to M_r such as light scattering detectors (LS), inversely proportional to M_r such as

mass spectrometers (MS) or proportional to M_r to a certain power, such as viscometry detectors (V);

- detectors with a response to particular chemical functions of the polymer, such as UV and photodiode array (PDA) detectors and Fourier-Transform Infra Red (FTIR) detectors.

4.1.1 Relative M_r determination: conventional calibration

Conventional calibration is the simplest method used in SEC for M_r determination, it relies on a single detector. The calibration curve is established with narrowly distributed standards (low polydispersity standards), relative to which the M_r of the polymer can be calculated. For accurate M_r determination, the method is based upon the assumption that the standards used have the same hydrodynamic volume and same elution behaviour as the solute with the method used. This method has limitations since standards for every polymer are not available.

Calibration standards used for SEC of cellulose include polystyrene [1,2,3], dextrans [4,5] and pullulans [6,7,8,9,10,11,12]; the latter have been the preferred choice. Pullulans are linear polysaccharides made of repeated units of maltotriose. Polymaltotriose differs from cellulose in that at regular intervals, one out of three glycosidic bonds is α -D-(1,6) instead of β -D-(1,4). Because of their linearity pullulans are considered as having a similar relationship between M_r and hydrodynamic volume as cellulose. However, one drawback is that the M_r range of commercially available pullulans does not cover the entire elution range of most cellulose, which makes extrapolation of the calibration curve necessary at the high- M_r end. Recently, Bikova and Treimanis [13] showed that at same M_r , cellulose had a higher hydrodynamic volume than pullulan (under equal conditions of solvent and temperature) due to higher backbone rigidity. Consequent to this difference in hydrodynamic properties, the M_r of cellulose relative to pullulans as determined with SEC is overestimated. The authors warn about the widespread acceptance that considers pullulans and cellulose as having similar hydrodynamic volume and point out a need for further investigation on the hydrodynamic properties of pullulans.

Strlič *et al.* recently showed that the salt concentration in the solvent and run temperature in SEC were important parameters leading to a difference in the determined M_r , and even if these effects were of the same order of magnitude for pullulans and cellulose, they led to systematic errors in M_r of tens of percents [14].

The calibration using pullulans is therefore not a clear issue and needs further investigation.

A similar problem arises with gelatine, a protein characterised in the frame of this work, for which no commercial standard provides a good structural match. This is due to the spatial conformation of the collagen from which gelatine is produced. Unlike most

proteins, collagen has a fibrous quaternary structure and protein standards commercially available are only from globular proteins (see Chapter 8).

Conventional calibration is nevertheless a useful tool in many situations as it allows for relative comparisons, which within a same group of polymers are useful for monitoring, for instance, degradation. This is often the case in conservation research when studying the behaviour of a polymer upon accelerated aging or upon a specific treatment.

4.1.2 Absolute M_r determination

Absolute M_r determination refers to measurements that permit the determination of polymers weight-average molar mass (M_w) without reference to any molar mass standards. Several detection systems achieve absolute molar mass determination. In this section will be considered only those that have been applied to cellulose analysis, namely universal calibration and laser light scattering detection.

4.1.2.1 Universal calibration

Universal calibration is carried out with refractive index and viscosity detectors (RI/V). The universal calibration theory [15] is based upon the observation that for a given mobile phase, column set and temperature, macromolecules that have the same hydrodynamic volume elute with the same retention time. The viscosity detector response is proportional to both the concentration and the hydrodynamic volume of the solute, the latter being the product of intrinsic viscosity $[\eta]$ and molar mass, as given by the Mark-Houwink-Sakurada (MHS) equation (Appendix 5-1). However, the viscometer does not allow to determine the concentration, which explains the necessity of coupling a refractometer. Universal calibration gives plots of $\log([\eta] \times M_r)$ as a function of retention time, which are linear on most of the working elution volume. The determination of the M_r of the polymer is therefore deduced from these measurements.

The advantage of universal calibration is that it is independent of the chemical nature and structure of the polymer standards, and can be done with any narrowly distributed standards regardless of the polymer studied. However, it is worth noting that refractometers give a more sensitive response to low- M_r fractions while viscometers are more sensitive to high- M_r fractions. This results in slight distortions in the M_r determination for polymers of either very high or very low- M_r .

The first application of universal calibration with a viscometry detector to cotton cellulose samples was carried out by Timpa and Ramey [1], and latter by Striegel and Timpa [16,17]. The method is still currently used [18,19].

4.1.2.2 Light scattering

4.1.2.2.1 Theory and principles

Laser light scattering can be performed in batch mode or in chromatography mode. Detailed information can be found in Flory [20], and in the review article by Wyatt [21]. The light scattering theory is summarised below.

The phenomenon of light scattering occurs when electromagnetic radiation hitting a molecule is partly scattered. When charge separation, induced by the interaction of the electrons of the molecule with the oscillating electric field component of light, creates an oscillating dipole, the molecules emit scattered light. Almost all of the scattered light has the same wavelength as the incident radiation and comes from elastic scattering, also called Rayleigh scattering. This is the classical theory; it does not consider other phenomena resulting from the interaction of light with matter such as absorption, fluorescence, depolarisation and magnetic scattering. In static light scattering the time-averaged, *i.e.* the total intensity of the scattered light is measured.

For large molecules like polymers, with dimensions exceeding 1/20 of the incident wavelength, intramolecular interference leads to a decrease in the scattering intensity as the scattering angle increases. Only when light radiation enters the molecule at a zero degree angle does phase interference not occur. Since detection at 0° is impractical because the detector would be overloaded by the non-scattered light, a single detector placed close to 0° can be used to determine the molar mass of a polymer. This is the principle of low-angle light scattering (LALS). In right-angle light scattering (RALS), the LS response is based on a single angle measure at 90°. In multiangle light scattering (MALS) the scattering intensity is measured at several different angles and the molar mass is computed by extrapolation to 0°.

The two principles in light scattering are:

Principle 1

The intensity of light scattered (*LS*) is proportional to the product of the polymer weight-average molar mass M_w and the polymer concentration c .

$$LS \propto M_w c \left(\frac{dn}{dc} \right)^2$$

Where $\frac{dn}{dc}$ is the refractive index increment, which expresses the variation of the refractive index of a solution with solute concentration.

Principle 2

The angular variation of the scattering is directly related to the radius of the polymer.

MALS experimentally determines the root mean square radius (rms) also abbreviated r_g because sometimes called radius of gyration. The mean square radius $\langle r_g^2 \rangle$ is an expression of the distribution of mass within the molecule (Figure 4.1-1) and thus informs about the structure of the polymer in solution. We have:

$$\langle r_g^2 \rangle = \frac{\sum r_i^2 m_i}{\sum m_i}$$

The number-average ($\langle r^2 \rangle_n$), weight-average ($\langle r^2 \rangle_w$), and z-average ($\langle r^2 \rangle_z$) mean square radii of the molecules can be calculated as follows:

$$\langle r^2 \rangle_n = \frac{\sum \left(\frac{c_i}{M_i} \langle r^2 \rangle_i \right)}{\sum \frac{c_i}{M_i}} \quad \langle r^2 \rangle_w = \frac{\sum (c_i \langle r^2 \rangle_i)}{\sum c_i} \quad \langle r^2 \rangle_z = \frac{\sum (c_i M_i \langle r^2 \rangle_i)}{\sum (c_i M_i)}$$

Where c_i is the mass concentration, M_i , the molar mass, and $\langle r^2 \rangle_i$ the mean square radius of the i^{th} slice of the chromatogram.

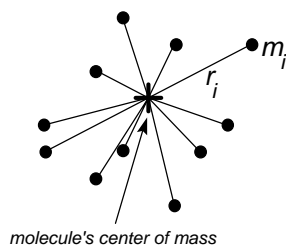


Figure 4.1-1. Schematic representation of the mean square radius $\langle r_g^2 \rangle$.

The light scattering equation (Equation 4-1) is based on Zimm's formalism of the Rayleigh-Debye-Gans model for dilute polymers. It reflects the two principles and includes both intermolecular and intramolecular effects.

$$\frac{K^* c}{R_\theta} = \frac{1}{M_w P_\theta} + \frac{2A_2 c}{P_\theta} + \frac{3A_3 c^2}{P_\theta} + \dots \text{(Equation 4-1)}$$

Where

- K^* is an optical parameter related to the polymer in its solvent defined as:

$$K^* = 4\pi^2 \left(\frac{dn}{dc} \right)^2 n_0^2 N^{-1} \lambda_0^{-4} \text{(Equation 4-2)}$$

Where,

$\frac{dn}{dc}$ is the refractive index increment ($\text{cm}^3 \text{g}^{-1}$)

n_0 is the refractive index of the solvent

N is Avogadro's number (mol^{-1})

λ_0 is the vacuum wavelength of the incident light (cm)

- c is the concentration of the solute molecules (g cm^{-3}).
- R_θ is the Rayleigh ratio (cm^{-1}). It is the excess intensity of the scattered light at angle θ . The Rayleigh ratio includes also the terms of the square of the distance between the scattering centre and the detector, the incident intensity, and the deviation due to crossing of the cell by the laser beam.
- M_w is the weight-average molar mass (g mol^{-1})
- A_2 is the second virial coefficient ($\text{mol cm}^3 \text{g}^{-2}$), a thermodynamic term which characterises solvent-solute interaction:

$A_2 > 0$ is indicative of a good solvent: the surrounding system gains energy when solvent molecules surround solute molecules.

$A_2 = 0$ means the solvent is an "ideal" solvent also called a "theta" (θ) solvent. The polymer is said to be in theta conditions.

$A_2 < 0$ means the solvent is a poor solvent. The polymer may precipitate out of solution if A_2 is a large negative number.

- P_θ is a form factor, also called particle scattering factor. It is the expression of the variation of the scattered light due to phase interference with the measuring angle. It is a function of the mass distribution inside the molecule and hence varies with the size and shape of the polymer in solution. The variation is determined by the mean square radius $\langle r_g^2 \rangle$. The larger $\langle r_g^2 \rangle$, the greater the angular variation.

$$\frac{1}{P_\theta} = 1 + \frac{16\pi^2}{3\lambda^2} \cdot \langle r_g^2 \rangle \cdot \sin^2\left(\frac{\theta}{2}\right) + \dots \text{(Equation 4-3)}$$

From Equation 4-3, $\langle r_g^2 \rangle$ can be determined by the plot $\frac{1}{P_\theta} = f\left(\sin^2\left(\frac{\theta}{2}\right)\right)$

4.1.2.2.2 MALS and SEC/MALS experiments

In batch experiments with MALS or in SEC/MALS, the unknown parameters are the molar mass M_w , the mean square radius $\langle r_g^2 \rangle$ of the polymer and the second virial coefficient A_2 . The known parameters are the Rayleigh ratio R_θ , the concentration c (given by the concentration detector), the constant K^* , the vacuum wavelength of the incident light λ_0 and the measuring angle θ . The $\frac{dn}{dc}$ needs to be accurately measured or otherwise obtained from the literature. There are three limits of interest:

- Low concentration limit ($c \rightarrow 0$): infinite dilution of the solute eliminates intermolecular scattering effects. In this case, the term $A_2 c = 0$
- Low angle limit ($\theta \rightarrow 0$), where $P_0 = 1$. This is used in LALS measurements. In this case, there is no phase interference in the scattered light, intramolecular effects are eliminated and Equation 4-1 becomes:

$$\frac{K^*c}{R_0} = \frac{1}{M_w} + 2A_2 c$$

- Low concentration and low angle ($c \rightarrow 0, \theta \rightarrow 0$); Equation 4-1 becomes:

$$\frac{K^*c}{R_0} = \frac{1}{M_w}$$

In MALS, the scattering intensity is measured at several different angles. The extrapolation to zero angle allows to determine the values of M_w and A_2 . The extrapolation to zero concentration allows to determine the value of $\langle r_g^2 \rangle$.

A Zimm plot expresses both the angular and the concentration dependence of the scattering. A Zimm plot (Figure 4.1-2) can be constructed with several relatively high concentrations and yields M_w , rms radius and A_2 in one single plot (Equation 4-4).

$$\frac{K^*c}{R_\theta} = f\left(\sin^2\left(\frac{\theta}{2}\right) + kc\right) \quad (\text{Equation 4-4})$$

Where k is a “stretch” factor selected to place (kc) and $\sin^2(\theta/2)$ in the same order of magnitude.

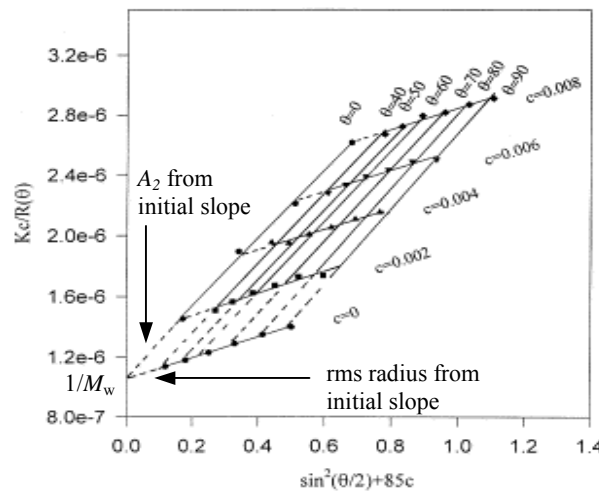


Figure 4.1-2. Typical Zimm plot (example of polymethyl-methacrylate in acetone at 24°C). Reproduced from Ghazy *et al.* [22].

A Zimm plot can be constructed only in batch (or microbatch) mode. In chromatography mode (SEC/MALS), the working concentrations are too low. More fundamentally, at any one time there is one concentration, but as time changes the concentration changes and so

does M_w . Thus a Zimm plot cannot be created as a matter of principle. The approach is therefore to use the Debye plot, which has the same coordinates as the Zimm plot but at one single low concentration. At low concentrations the term $A_2 c$ in the Rayleigh-Debye-Gans equation approaches zero. Combination of Equation 4-1 and Equation 4-3 yields:

$$\frac{K^*c}{R_\theta} \approx \frac{1}{M_w} \left[1 + \frac{16\pi^2}{3\lambda^2} \langle r_g^2 \rangle \sin^2\left(\frac{\theta}{2}\right) \right] \quad (\text{Equation 4-5})$$

Working with polydisperse polymers in SEC, each slice of a peak can be considered as representing a monodisperse fraction so a Debye plot can be built for each data slice. Debye plots can be built using Zimm, Debye, or Berry formalisms. The Zimm formalism is given by K^*c/R_θ as a function of $\sin^2(\theta/2)$, and is generally used for mid-sized polymers (rms radius between 10 and 100 nm). Debye formalism is used with smaller polymers (rms < 50 nm), and Berry formalism with very large polymers (rms of 100-200 nm).

Figure 4.1-3 shows a Debye plot (Zimm formalism) for a slice of the distribution near peak molar mass (M_p). The sample is Whatman No.1 dissolved in 8% LiCl/DMAc, as described in section 3.2.4 of Chapter 3, and analysed in SEC/MALS using 0.5% LiCl/DMAc as mobile phase as described in section 4.2.3 of the present chapter.

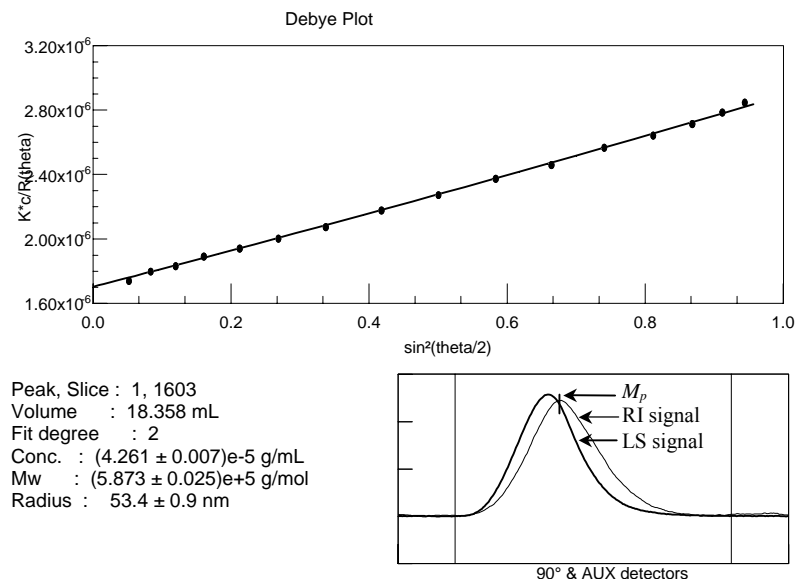


Figure 4.1-3. Debye plot display of K^*c/R_θ as a function of $\sin^2(\theta/2)$ (Zimm formalism) for cellulose in LiCl/DMAc obtained by SEC/MALS/RI with a Dawn EOS (Wyatt Technologies) and interferometric differential refractometre Optilab DSP (Wyatt Technologies), and computed by the ASTRA software version 4.73.04 (Wyatt Technologies), from the slice of the chromatogram at $V_e = 18.358$ mL. The error bars, which as can be seen, are extremely small, represent the baseline noise for each detector's photodiode. The data reported in the lower left part corresponds to the results calculated from the slice selected by moving the vertical ticker over the LS chromatogram. Thus values of M_r can be obtained for each V_e . On the figure, the ticker is placed on the LS signal at the point corresponding to the apex of the DRI signal, which yields the peak molar mass M_p .

SEC/MALS allows the determination of weight, number and z-average molar mass averages (M_n , M_w , M_z), root mean square (rms) radii (number-average r_n , weight-average r_w , and z-average r_z), as well as size distribution and conformation. The parameters directly measured by the MALS detector are M_w , yielded from (Equation 4-1) and z-average rms radius (r_z). A concentration detector online with the light scattering detector measures the concentration of the solute in each slice of the chromatogram, for which the polymer is considered monodisperse. Generally a differential refractive index (DRI) detector is used. DRI detectors need the value of the dn/dc to calculate the concentration of the polymer from the RI signal. The calculation is made according to:

$$c = \frac{V \alpha}{\left(\frac{dn}{dc}\right)}$$

Where,

- c is the concentration of the polymer in solution.
- V is the output voltage.
- α is the calibration constant of the DRI detector, *i.e.* a proportionality constant between the difference in refractive index between the pure solvent and the polymer solution (Δn), and the change in the output voltage (ΔV), with:

$$\alpha = \frac{d(\Delta n)}{d(\Delta V)}$$

The value of dn/dc required to determine the molar mass by online light scattering is the dn/dc of the studied polymer in the working solvent at the working temperature and working wavelength. For many molecular species, dn/dc remains constant over a broad range of M_r . For others, especially copolymers, the value changes significantly with M_r . This can happen even for homopolymers, below 10,000 g mol⁻¹. In the cases when dn/dc varies with M_r , the DRI detector is not sufficient for precise measurements, and both DRI and UV detectors can be used online with a MALS detector.

A UV detector is sometimes also used as the concentration detector instead of the DRI, especially when working with proteins. This requires knowing the extinction coefficient of the polymer at the working wavelength (ϵ), the response factor for the UV detector (AU V⁻¹), and the cell path length of the UV detector, as well as the dn/dc for the accompanying LS detector.

There are a few drawbacks to LS measurements. One of them is that the maximum resolution in molecular size is 1/20 of the incident light, thus for M_w below a few thousands, relatively high concentrations may be required in order to have a detectable signal. Therefore, in the very low- M_r DRI detectors are less accurate, but they are also less sensitive in the very high- M_r , thus less precise. However recent research showed that

accurate values of M_r could be obtained for low- M_r monodisperse polymers in the range of 2.5×10^3 to 10^4 g mol⁻¹ [23].

4.2 Application of SEC/MALS to the study

4.2.1 The instruments

The multiangle light scattering detector (MALS) used throughout the present study was a Dawn EOS (Wyatt Technologies). The laser has a nominal power of 25 mW (23.5 mW effective) and operates at 690 nm. The flow cell has a volume of 70 μ L, and the scattering volume is in the order of 0.5 μ L. The detection is done by 18 photodiodes placed in array around the flow cell as schematised in Figure 4.2-1.

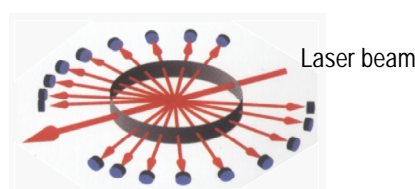


Figure 4.2-1. Schematised flow cell and photodiodes of the MALS detection cell.

The DRI detector is an interferometric differential refractometer Optilab DSP (Wyatt Technologies), it is schematised in Figure 4.2-2. The light source emits at the same wavelength as the laser of the MALS (690 nm). The light is plane-polarised at 45° by a polariser. The beam is then split by the first Wollaston prism, resulting in two orthogonal plane-polarised beams that are in phase. One is vertically rotated and passes through the reference cell and the other is horizontally rotated and passes through the sample cell. The phase shift between the beams at the exit of the cells is directly proportional to the refractive index difference between the solutions in the reference and sample cells. The beams are recombined in the second Wollaston prism to yield a plane-polarised beam rotated with respect to the initial beam according to the phase shift. Based on the rotation, the quarter wave plate and analyser detect the rotation of the plane of polarisation, at the wavelength selected by the interference filter. The cell temperature is controlled between 35°C and 80°C by internal heaters.

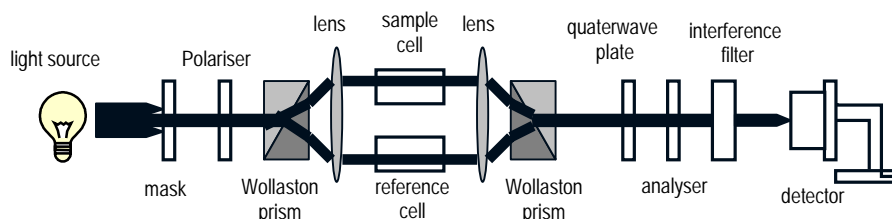


Figure 4.2-2. Scheme of the interferometric differential refractive index detector Optilab DSP.

4.2.2 Experimental determination of the parameters in the LS equation for calculation of M_w

In order to compute the polymer concentration c and hence M_w , it is necessary to determine a number of constants.

This section is dedicated to the instrumental tuning that was necessary after installation of the SEC/MALS, and to the determination of the constants and parameters required for the calculation of molar mass, root mean square radius and polymer conformation. It includes the determination of the calibration constant of the MALS detector Dawn EOS and that of the interferometric differential refractometer Optilab DSP (α), the normalisation of the MALS detector and the alignment of the detectors with the determination of the delay interdetector volume. As it is also necessary to know the dn/dc of the polymer in the chosen solvent (Equation 4-2), a section is dedicated to the determination of the dn/dc of cellulose in LiCl/DMAc. Data acquisition and molecular parameters calculations were performed using ASTRA software version 4.73.04 for Windows (Wyatt Technologies).

4.2.2.1 Determination of the calibration constant α of the DRI

4.2.2.1.1 Background

The calibration constant α of a DRI detector is the proportionality constant between the difference in refractive index between the pure solvent and the polymer solution (Δn) and the change in the output voltage (ΔV) (see section 4.1.2.2.2), with:

$$\alpha = \frac{d(\Delta n)}{d(\Delta V)}$$

It is a geometrical constant related to the structure of the detection cell.

The refractive index n_i of a solution of concentration c_i depends on the refractive index of the solvent n_0 according to:

$$n_i = n_0 + \left(\frac{dn}{dc} \right) c_i$$

If $\Delta n_i = n_i - n_0$, thus:

$$\Delta n_i = \left(\frac{dn}{dc} \right) c_i$$

The output signal h_i of the DRI is proportional to Δn_i with:

$$h_i = \alpha^{-1} \Delta n_i = \alpha^{-1} \left(\frac{dn}{dc} \right) c_i$$

The constant α can thus be measured with solutions of known c and known dn/dc .

4.2.2.1.2 Experimental determination of α

The constant α was measured offline (without the columns) with aqueous solutions of NaCl (anhydrous) of known concentration (Table 4.2-1). A large enough sample volume must be injected in order to obtain a flat apex region of the signal for each solution (Figure 4.2-3). A syringe pump was used. The dn/dc of anhydrous NaCl in water at the working wavelength (690 nm) is 0.172 ml g^{-1} .

In order to ensure exact concentration of the solutions, NaCl was oven-dried. Five dilutions were made from a stock solution $1.0117 \times 10^{-3} \text{ g mL}^{-1}$. The dilutions were made by weight, solution mass being more easily accurately determined than volume.

The voltage output ΔV , which is the solvent baseline corrected voltage of the signal h_i of the DRI for each of the six solutions was measured with DNDC software (Wyatt Technologies). Δn was computed for each solution and plotted against ΔV (Figure 4.2-4). The slope of the plot is the DRI calibration constant α . The experiment was repeated twice. Table 4.2-1 reports the values obtained for the signal (raw and adjusted output) for the six NaCl solutions for one of the two experiments.

The two values obtained for α were $2.2517 \times 10^{-4} (\pm 5.4 \times 10^{-6}) \text{ V}^{-1}$ and $2.2614 \times 10^{-4} (\pm 5.2 \times 10^{-6}) \text{ V}^{-1}$. The average of these 2 values, $2.25655 \times 10^{-4} \text{ V}^{-1}$, was used as the α constant throughout the SEC/MALS experiments. This value is in good agreement with the value provided by the manufacturer of $2.2314 \times 10^{-4} (\pm 1.6 \times 10^{-7}) \text{ V}^{-1}$.

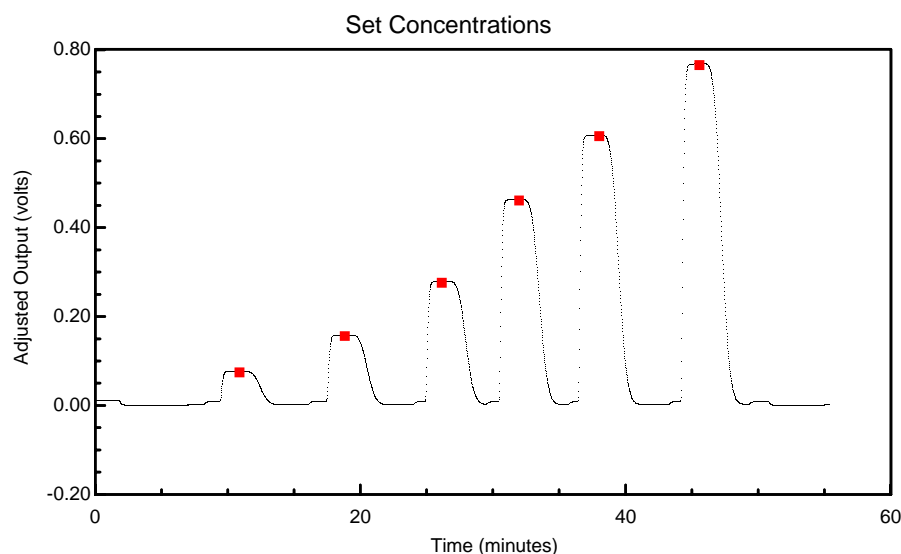


Figure 4.2-3. Saturated response of the DRI for the six NaCl solutions.

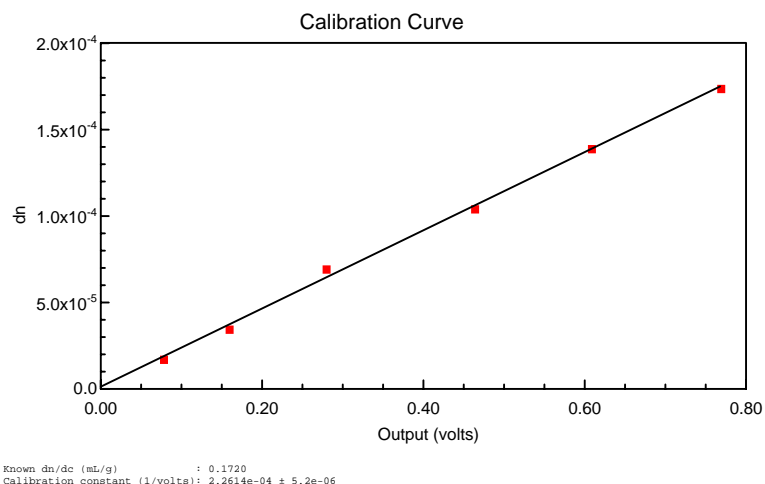


Figure 4.2-4. Plot of the DRI response as a function of the variation in refractive index.

Table 4.2-1. Response of the DRI to each solution of NaCl

Raw Output (V)	Adj. Output (V)	Concentrations (g mL ⁻¹)
0.0656	0.0770	1.0117×10^{-4}
0.1471	0.1585	2.0234×10^{-4}
0.2670	0.2785	4.0468×10^{-4}
0.4514	0.4629	6.0702×10^{-4}
0.5963	0.6078	8.0936×10^{-4}
0.7562	0.7678	1.0117×10^{-3}

It has to be noted that according to the adjusted gain of the DRI detector, the α constant to be input in the ASTRA software when reducing the data is the constant corrected to the gain. For our experiments the auxiliary gain was set to 10, the constant input in ASTRA was therefore $2.25655 \times 10^{-5} \text{ V}^{-1}$.

4.2.2.2 MALS detector

4.2.2.2.1 Calibration of the MALS detector

The voltages of the photodiode detectors in the Dawn EOS are proportional to the light scattered intensities. The calibration of the detector is the determination of this proportionality constant. It is done for the 90° detector only, with ASTRA software, which measures the voltages from the 90° and the laser monitor photodiodes with the laser on and the laser off (dark currents), and then correlates to the Rayleigh ratio (scattered light intensity). The collection trace is the calibration graph.

Calibration was done with HPLC-grade toluene filtered with 0.02 μm filter Anotop 25. Toluene is recommended for calibration because it has a high and accurately determined Rayleigh ratio (9.78×10^{-6} at 690 nm), it is generally a dust-free solvent, available in high

purity grade, its refractive index is very similar to that of the flow cell windows, and it is easy to purge from the flow cell

Calibration of the MALS detector considers not only the 90° detector sensitivity but also incorporates the geometrical scattering volume, solid angle corrections and the reflective losses at the glass surfaces (Fresnel factors).

The injections were done with a syringe pump at a flow rate of 0.2 ml min⁻¹. The trace on the calibration graph showed no long-term drift and peak-to-peak fluctuated within 2 mV (according to the manufacturer the fluctuation should be within 5 mV).

The calibration was repeated three times. The constant obtained by averaging the three measures was 6.071×10^{-6} ($\pm 0.06\%$). The value of the constant provided by the manufacturer was 6.356×10^{-6} . The difference between the experimentally determined value and the manufacturer's value is 4.5%, which falls within the maximum difference recommended of 5%.

4.2.2.2.2 Normalisation of the MALS detector

4.2.2.2.2.1 Background

In the MALS, the array of detectors (18 photodiodes) is positioned at fixed angles θ . Each photocell detector may subtend a different solid angle at the central scattering volume, and have slightly different gains. As only the 90° photodiode is calibrated, the responses from the other photodiodes have to be normalised to the 90° photodiode response. The normalisation consists in multiplying the excess Rayleigh ratio factors at each detector by a suitable constant to yield the same value as that measured at the 90° angle, which has been set equal to one. ASTRA software computes normalisation coefficients for each detector and uses them for data processing.

The actual scattering angle and the scattering volume seen by each of the photodiodes depends on the refractive index of the solvent and the refractive index of the flow cell glass. The normalisation has therefore to be performed in the actual solvent used in the SEC/MALS experiment. The polymer used for normalisation has to be an isotropic scatterer, *i.e.* a polymer small enough to scatter in same intensity in all directions. Usually polymers with rms radius below 10 nm are isotropic scatterers.

4.2.2.2.2.2 Normalisation

Normalisation was carried out on-line (with the columns) with a polystyrene 30,000 g mol⁻¹ at 0.5016 g.mL⁻¹ in 0.5% LiCl/DMAc. The sample was filtered through 0.02 µm filter Anotop 25. The runs were done at 55°C. The refractive index of 0.5% LiCl/DMAc was considered to be the same as that of DMAc ($n = 1.436$).

The quality of the normalisation was evaluated by comparing the relative peak heights of the light scattering detectors. This allows as well to verify that the flow cell is clean and check for stray light.

Figure 4.2-5 shows a three dimensional plot with rotation and elevation angles set to 0° . The peak heights were the same and the detector signals overlaid almost perfectly except for one detector, which seemed slightly off-set. Figure 4.2-6 of a three dimensional plot with 30° elevation and rotation angles shows a regular decrease in the peak heights which indicates a good normalisation, and shows also that the detector slightly off-set is the 2° angle photodiode. The very low-angle detectors are often slightly off because they are the most sensitive to dust and particles. The 2° angle photodiode was therefore not used for the calculations of M_w in the SEC/MALS experiments.

The normalisation was considered acceptable and the normalisation coefficients were entered in ASTRA software and used for all the SEC/MALS experiments.

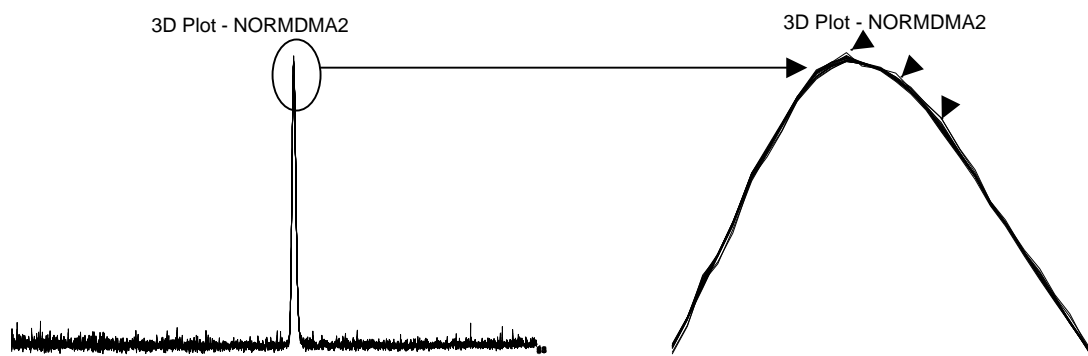


Figure 4.2-5. 3-D plot in ASTRA software at 0° angle rotation and elevation, showing the response of the 18 photodiodes after normalisation. The small triangles on the right point to the signal corresponding to the off-set photodiode.

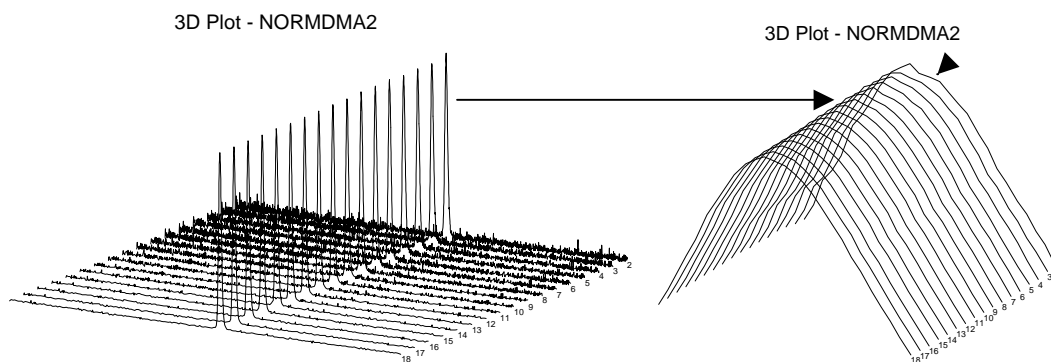


Figure 4.2-6. 3-D plot in ASTRA software at 30° rotation and elevation, showing the response of the 18 photodiodes after normalisation. The small triangle on the right shows the off set signal of the 2° angle photodiode.

4.2.2.2.3 Alignment

The alignment allows the determination of the interdetector (or delay) volume between the MALS and the DRI detector in order to correlate their measurements. The delay volume is obtained by injecting a monodisperse polymer standard and by aligning the LS peak with the DRI peak. Only monodisperse samples result in perfect overlapping of the two signals but very narrow polymer standards can also be used. The delay volume has to be as small as possible in order to minimize band broadening. Normally, it should fall between 0.08 and 0.25 mL.

With the present chromatographic set-up, an interdetector delay volume of 0.15 mL was determined by injecting a polystyrene 30,000 g mol⁻¹ narrow standard dissolved in 0.5% LiCl/DMAc (Figure 4.2-7). The correctness of this value was confirmed by a good overlay of the LS (90°) and DRI signals. The line crossing the peak in the plot of M_r as a function of elution volume (V_e) (Figure 4.2-8) represents the variation in M_r across the elution, and is expectedly flat as the PS standard is monodisperse.

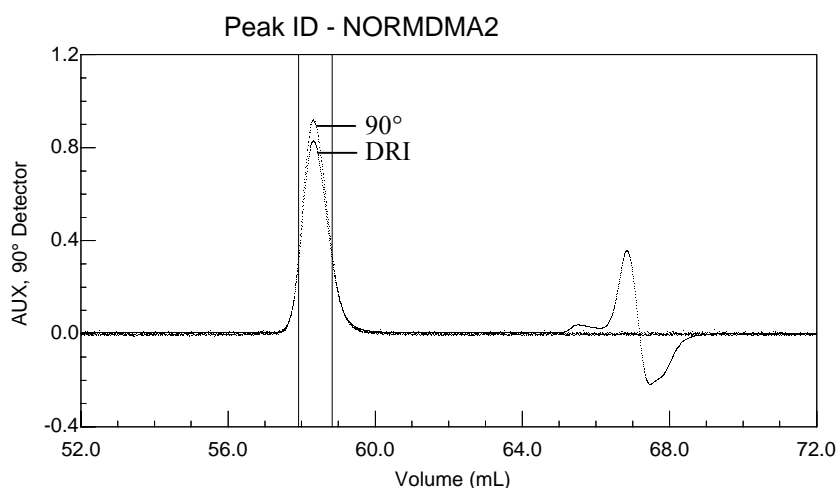


Figure 4.2-7. Aligned DRI and LS signals after the injection of PS 30,000.

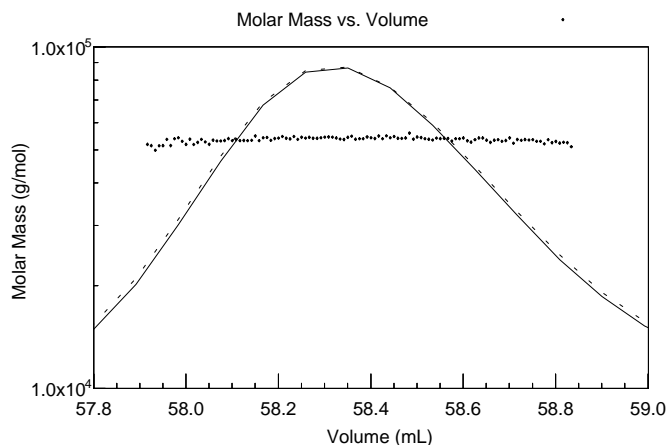


Figure 4.2-8. Zoom in the apex area of Figure 4.2-7. The flat line across the peaks indicates that there is no variation of mass across V_e .

4.2.2.3 Measurement of the refractive index increment (dn/dc) of cellulose in 0.5% LiCl/DMAc

4.2.2.3.1 Background

An accurate value of the refractive index increment is required because the DRI signal is inversely proportional to dn/dc which, as shown in (Equation 4-2) appears in a quadratic form.

The difficulty in determining the dn/dc of cellulose in LiCl/DMAc was observed by several authors [24,25]. Values as varied as 0.057 [24], 0.091 [11], 0.104 [26], 0.136 [27] and 0.163 mL g⁻¹ [16] have been reported. This variability in the dn/dc values and the poor repeatability and reproducibility are sometimes attributed to the solvent hygroscopicity [28].

Additional parameters that could influence the measures of dn/dc include instrumental as well as sample related parameters. The instrumental variable that certainly plays a major role is the measuring wavelength since dn/dc is a function of the wavelength. For an accurate determination of the dn/dc and optimal results in the subsequent M_w determination, the wavelength at which dn/dc is determined should be the same as that of the laser of the LS detector. Sample related variability includes the degree of dissolution of cellulose in LiCl/DMAc and the possible molecular associations or aggregation [12,25].

4.2.2.3.2 Determination of dn/dc

Knowing the DRI detector constant α and the concentrations c_i , the dn/dc of solutions of cellulose in 0.5% LiCl/DMAc is obtained by measuring the voltage output of the signal h_i . (see section 4.2.2.1.1).

The dn/dc of cellulose solutions in 0.5% LiCl/DMAc was measured off-line with the Optilab DSP, which as described earlier works at the same wavelength as the monochromatic laser beam of the Dawn EOS (690 nm).

The cellulose source was Whatman No.1 filter paper, the model paper used throughout this research. The paper was defibrillated for 5 minutes in a small two-blade blender and dried in a desiccator over drierite for several days. The sample was weighed in dry state in order to avoid errors on the mass due to the moisture content of the paper.

The dissolution in 8% LiCl/DMAc and dilution to 0.5% LiCl/DMAc was carried out according to the final procedure described in section 3.2.4 of Chapter 3. Eight dilutions (wt/wt) were made from a stock cellulose solution 9.86×10^{-4} g L⁻¹. Dilutions were made

using the same solvent batch 0.5% LiCl/DMAc as used in the preparation of the stock cellulose solution. The concentrations of the nine solutions are reported in Table 4.2-2.

The experiments proceeded at constant temperature (37°C), at a flow rate of 0.2 mL min⁻¹ with an injection loop of 500 µL, and manual injector (Rheodyne model 7725i, low pressure Teflon rotary valve) connected directly to the Optilab DSP.

The experiment started by passing pure solvent (0.5% LiCl/DMAc) through the detector cell. It was noticed that in order to obtain a stable baseline, the experiment had to be carried out without degassing the solvent. Indeed, a degassed solvent resulted in baseline dips due to the difference in refractive index with the solvent in the cellulose solution, which is not degassed.

Once the readings were stable, each cellulose solution was passed through the DRI detector starting with the lowest concentration, and the change in the voltage (ΔV) was recorded. Time was allowed between each injection for the signal to return to baseline. Solvent was injected at the end of each measurement in order to set the baseline. The dn/dc experiment was repeated three times. Table 4.2-2 reports the values of the voltages obtained in the three experiments.

From the change in the DRI detector voltage (ΔV) and the calibration constant α ($\alpha = d(\Delta n)/d(\Delta V)$), the Δn for each different concentration can be calculated with:

$$\Delta n = \Delta V \frac{d(\Delta n)}{d(\Delta V)}$$

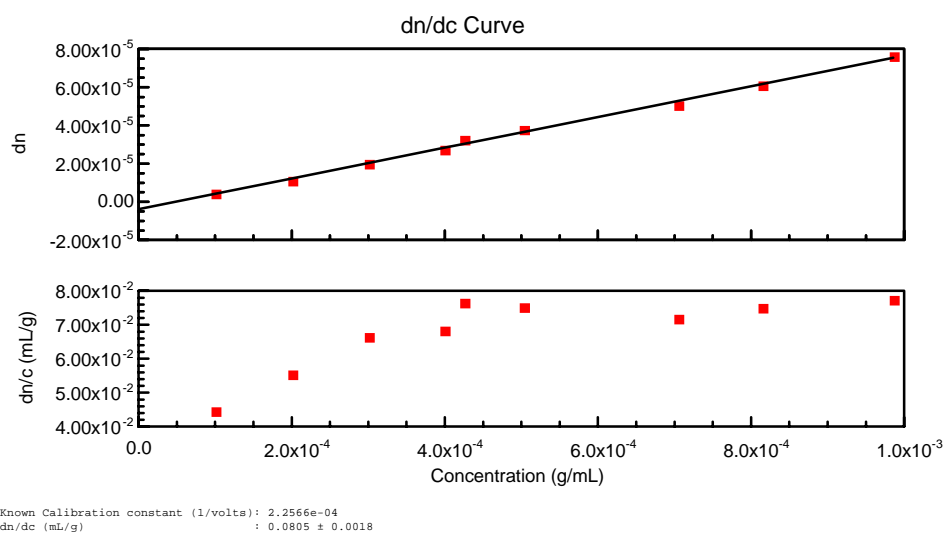
The slope in the plot of Δn as a function of c equals $d(\Delta n)/dc$ or dn/dc . Figure 4.2-9 (top), Figure 4.2-10 (top) and Figure 4.2-11 (top) show the plots for experiments 1 to 3 respectively. The values of dn/dc obtained are reported below each figure. The data was reduced with DNDC software version 5.20 for Windows (Wyatt Technologies).

The plot of $\Delta n/c$ as a function of c yielding a flat line indicates invariable dn/dc at all concentrations. Such plots, presented in the bottom part of Figure 4.2-9, Figure 4.2-10 and Figure 4.2-11 show slopes equal to zero over the larger part of the concentration spectrum. The first one or two data points are, however, off the flat line, which was attributed to a possible experimental error on these lowest dilutions.

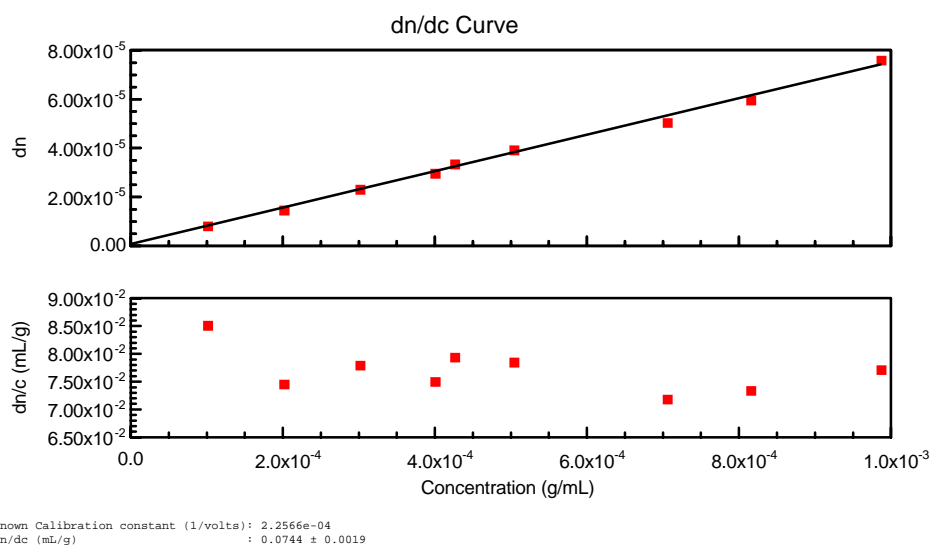
The average of the three values of dn/dc obtained was 0.077 ± 0.008 mL g⁻¹. The precision on the three values being satisfactory, 0.077 mL.g⁻¹ was used as dn/dc of cellulose in 0.5% LiCl/DMAc throughout the study.

Table 4.2-2. Response of the DRI detector to cellulose in 0.5% LiCl/DMAc at different concentrations.

c (g mL ⁻¹) (× 10 ⁴)	Output (V)		
	exp.1	exp.2	exp.3
1.0001	0.2151	0.2083	0.2151
2.0042	0.2405	0.2374	0.2408
3.0029	0.2756	0.2756	0.2832
3.9920	0.3040	0.3052	0.3116
4.2505	0.3238	0.3229	0.3281
5.0290	0.3430	0.3488	0.3592
7.0460	0.3958	0.3989	0.4078
8.1460	0.4390	0.4401	0.4514
8.1460	0.5035	0.5127	0.5206



**Figure 4.2-9. dn/dc graph for experiment 1 using $\alpha = 2.2566 \times 10^{-4} \text{ V}^{-1}$
 $dn/dc = 0.0805 (\pm 1.8 \times 10^{-3}) \text{ mL g}^{-1}$**



**Figure 4.2-10. dn/dc graph for experiment 2 using $\alpha = 2.2566 \times 10^{-4} \text{ V}^{-1}$
 $dn/dc = 0.0744 (\pm 1.9 \times 10^{-3}) \text{ mL g}^{-1}$**

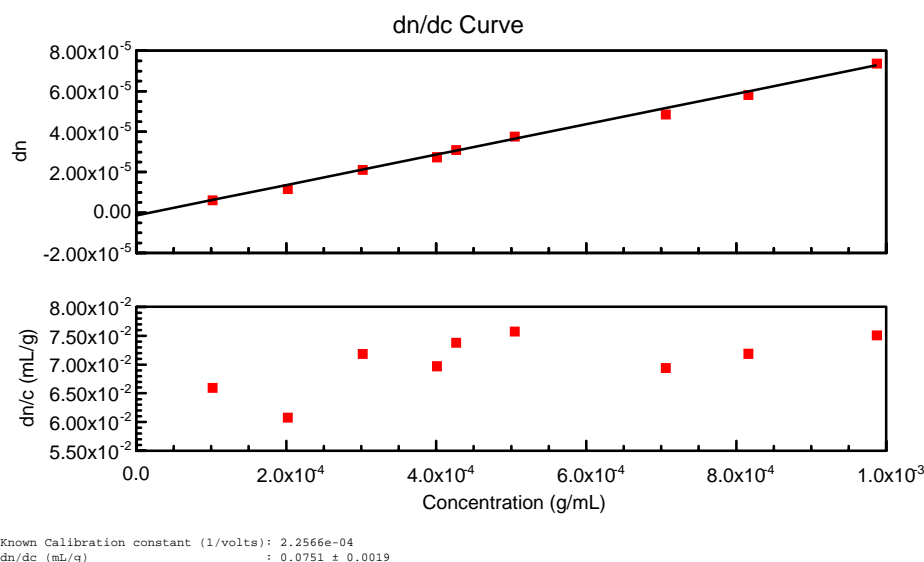


Figure 4.2-11. dn/dc graph for Experiment 3 using $\alpha = 2.2566 \times 10^{-4} \text{ V}^{-1}$
 $dn/dc = 0.0751 (\pm 1.9 \times 10^{-3}) \text{ mL g}^{-1}$

4.2.2.4 Influence of the second virial coefficient A_2

The second virial coefficient A_2 is a thermodynamic parameter indicative of solvent-solute interactions. In other words, it is a measure of the amount of energy gained by the system upon surrounding polymer molecules by solvent molecules.

A_2 is a parameter in the LS equation (Equation 4-1) for the calculation of M_w . This equation shows that $2A_2$ is the slope of a linear plot of K^*c/R_θ as a function of c . A_2 is thus determined by measuring R_θ at several concentrations with the LS detector. It is obtained in batch mode, since different concentrations are required, from a Zimm plot (see section 4.1.2.2.2). In SEC mode, the concentrations being very low, A_2 can safely be omitted if the following relationship is verified:

$$2A_2 c M_w \ll 1$$

Values of A_2 for cellulose in LiCl/DMAc in the literature vary widely due to solubilisation difficulties since at high cellulose concentration, molecules associations and aggregation can be a problem.

Röder *et al.* [29] reported values of A_2 of $3 \times 10^{-4} \text{ mol mL g}^{-2}$ for microcrystalline cellulose (1.3% in 2.6% LiCl/DMAc), and $1.5 \times 10^{-3} \text{ mol mL g}^{-2}$ for softwood Kraft pulp (0.3% in 2.6% LiCl/DMAc). McCormick *et al.* [24] reported values of A_2 ranging from 3.5×10^{-3} to $5.3 \times 10^{-3} \text{ mol mL g}^{-2}$, depending on the cellulose source, with solutions of 1% to 3% cellulose in 9% LiCl/DMAc. The value they found for cotton cellulose was $3.5 \times 10^{-3} \text{ mol mL g}^{-2}$. Matsumoto *et al.* [30] reported a value of $1.33 \times 10^{-3} \text{ mol mL g}^{-2}$ for cotton linters in 8% LiCl/DMAc.

The experimental conditions that most closely resemble the conditions of the present study are those of Röder *et al.*, since the authors reported A_2 values at SEC

concentrations. Simulations were made by entering the value 3×10^{-4} mol mL g^{-2} instead of 0 as A_2 coefficient in the ASTRA software, for a recalculation of M_w of a cellulose sample from Whatman No.1 paper. The sample chosen had one of the highest M_w , of 6.65×10^5 g mol $^{-1}$, when calculated with A_2 set to 0. The resulting M_w was only 1.45% higher. Inputting the highest literature value reported for A_2 , of 1.5×10^{-3} mol mL g^{-2} , the increase in M_w was 7.24%.

The simulation was also carried out with a degraded paper: Whatman No.1 immersed in a solution of alum at 0.83 g mL $^{-1}$, aged 35 days at 80°C, 50% relative humidity (A10t₃₅) that had one of the lowest M_w , of 1.709×10^5 g mol $^{-1}$, when calculated with A_2 set to 0. In this case, the value 3×10^{-4} mol mL g^{-2} as A_2 coefficient resulted in only a 0.41% increase in M_w , while a value of A_2 of 1.5×10^{-3} mol mL g^{-2} resulted in a marginal increase of 2.06% in M_w .

These simulations showed that indeed the second virial coefficient A_2 could be omitted in the series of SEC/MALS experiments to be carried out in the present research, as the resulting error in M_w would not likely ever exceed 2 %.

4.2.3 SEC method for cellulose in LiCl/DMAc

4.2.3.1 Sample preparation

Solutions of about 1% cellulose in 8% LiCl/DMAc are prepared according to the final procedure described in section 3.2.4 of Chapter 3. The stock cellulose solutions are diluted to 0.5% LiCl/DMAc with anhydrous DMAc to a sample concentration of about 0.625 mg mL $^{-1}$, *i.e.* 0.0625% (wt/v) and filtered through 0.5 μ m pores Millex LCR filters (Millipore) before injection on the SEC columns. The remaining cellulose solutions are stored at 4°C under nitrogen to avoid possible degradation in the solvent.

It has to be noted that both the salt concentration in the mobile phase and the polymer concentration in the injected sample have to fall within a certain range in order to avoid excessive viscosities (leading to high back-pressure), low efficiency and erroneous elution volumes. A concentration of LiCl of 0.5% in the mobile phase was a good compromise between the need of a certain amount of LiCl to keep cellulose molecules in solution in a non-aggregated state, and the need to avoid corrosion of the chromatographic system, as LiCl is corrosive to metal, as well as too high a solvent viscosity. As for cellulose solutions, the usual recommendation for polymers of M_r ranging from 10^5 to 10^6 g mol $^{-1}$ is to work with concentrations between 0.02% and 0.1% in the sample injected. The initial cellulose concentration of 1% in 8% LiCl/DMAc was chosen considering the balance required between cellulose and solvent given the solvation capacity of LiCl/DMAc, but also the required final solution concentration in the injected sample after the dilution to 0.5% LiCl.

It has to be noted that the sample concentration of 1% is indicative; the exact concentration has to be corrected by withdrawing the moisture content and the eventual gelatine or gelatine/alum contents of the differently prepared paper samples (see section 6.2.1.1 of Chapter 6 and section 7.2.1 of Chapter 7). However, seeking to know the exact concentration to start with is superfluous as in SEC/MALS, once the α constant of the DRI and the dn/dc of the sample in the working solvent are known, the exact mass injected is subsequently computed by the software. Prior knowledge of the exact concentration of the solutions injected can nonetheless be useful in certain cases to determine a “computed” dn/dc when it is not possible to obtain this value experimentally. It can also help to check for column retention or other non-exclusion behaviour of the solutes or for solvent complexation with the polymer (see Chapter 5) by comparing the computed and the theoretical injected concentrations.

4.2.3.2 SEC/MALS/DRI instrumental set-up

The experimental SEC set-up is represented in Figure 4.2-12. It consisted of a four channels HPLC solvent degasser (Degassit™, Metachem Technologies Int.), HP 1100 isocratic pump G1310A (Hewlett Packard), injector (model 7725i, Rheodyne) with a 100 μL loop, multiangle light scattering detector (MALS) Dawn EOS (Wyatt Technologies) and interferometric differential refractometer (DRI) Optilab DSP (Wyatt Technologies).

Since light scattering measurements are very sensitive to short-term flow fluctuations, the pumping system has to fulfil certain requirements for the flow delivery. The pump worked on a hydraulic system with dual pistons. The amplitude of the pressure pulsation was less than 2% (typically less than 1%) at 1 mL min^{-1} isopropanol at all pressures above 10 bars. The flow precision was repeatable within less than 0.3% relative standard deviation (RSD) (typically 0.15% based on retention time at 1 mL min^{-1}). An on-line membrane filter 0.22 μm pore size (Millipore) was placed between the pump and the injector to filter any remaining particulates in the mobile phase.

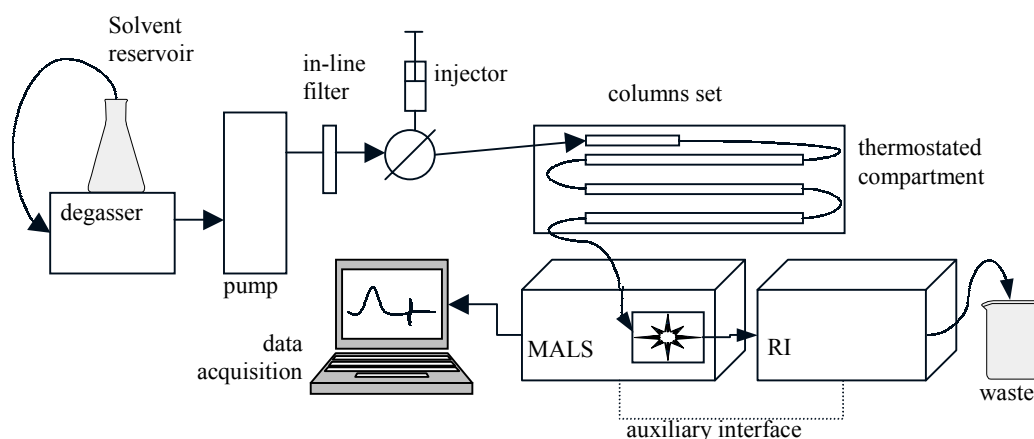


Figure 4.2-12. Schematic representation of the SEC/MALS/DRI.

Both the Dawn EOS and Optilab DSP are described in section 4.2.1. The MALS was placed between the columns and the DRI detector. This was to avoid exposing the DRI detector to a high backpressure, which could damage the cells, and also to provide some backpressure to the MALS in order to improve baseline stability. In addition, with this configuration the dead-volume between the DRI and the MALS was minimal, given the location of the inlet and outlet valves.

The interdetector delay volume was 0.15 mL, the constants of the instruments are 6.071×10^{-6} for the Dawn EOS and $2.256 \times 10^{-4} \text{ V}^{-1}$ for the Optilab DSP (as determined in section 4.2.2). The gain of the Optilab DSP was set to 10, the actual working α constant was therefore $2.256 \times 10^{-5} \text{ V}^{-1}$. The data acquisition interval was 0.5 seconds.

4.2.3.3 Separation

The separation was carried out on a set of 3 poly (styrene-divinyl benzene) columns packed with 10 μm diameter particles MIXED-B pores, 300 mm \times 7.5 mm (Polymer Laboratories) preceded by a guard column 10 μm particles 50 mm \times 7.5 mm (Polymer Laboratories). The columns have a linear separation from 500 g mol^{-1} to 10^7 g mol^{-1} (specification from the supplier). They were placed in a thermostatted heating compartment (Figure 4.2-12) at 60°C and the system was operated at 60°C with a flow rate of 1 mL min^{-1} . The mobile phase bottle was kept at 55-56°C under low stirring in a heating/stirring unit (Pierce). The injection volume was 100 μL and the run time was 40 minutes.

It has been shown that the run temperature had a clear influence on the elution behaviour of cellulose on PSDVB columns, lower temperatures resulting in longer retention times [14]. However, if this has consequences when M_r is determined relative to standards, in MALS, such phenomenon has no impact on the calculated M_w . In the present method, it was therefore preferred to run the samples at lower temperatures than usually reported for SEC of cellulose in LiCl/DMAc (80°C), in order to avoid degradation of the polymer during the analysis as much as possible. A run temperature of 60°C was chosen as it also provided for a reasonable backpressure between 65 and 69 bars.

The mobile phase, 0.5% LiCl/DMAc, was filtered through 0.5 μm pore Millex LCR filters (Millipore). The mobile phase and the stock 8% LiCl/DMAc (prepared as reported in section 3.2.1.1 of Chapter 3) were stored under nitrogen at 4°C if not used immediately.

The data acquisition was carried out by the ASTRA software version 4.73.04 (Wyatt Technologies). The RSD for the mass of cellulose injected calculated by the ASTRA software for all the reference Whatman No.1 papers was 4.2%, which corresponds to the uncertainty on the computed values only, excluding other systematic errors in the sample preparation and SEC runs.

4.2.3.4 Precision and repeatability of the method

The precision of the method related to the instrumentation (SEC/MALS set-up) and to sample preparation was determined by injecting two different samples of Whatman No.1 paper (samples 1 and 2) dissolved on different days, in three (A, B and C) and two (A and B) replicates respectively (total of five runs), as described in section 3.2.4 of Chapter 3. All injections were done on different days.

With ASTRA software, both differential and cumulative distribution graphs of molar masses and mean square radii $\langle r_g^2 \rangle$ can be calculated. Figure 4.2-13 (left) and (right) show the overlaid differential molar mass and cumulative molar mass graphs of the five runs. Figure 4.2-14 (left) and (right) shows the overlaid differential root mean square radii and cumulative root mean square radii graphs of the five runs.

Table 4.2-3 reports the values of M_n , M_w and M_z obtained for the two samples with the averages and RSD. The RSD on M_w and M_z was about 2.5%, which shows a very good repeatability of the method. M_n had slightly higher RSD (7%) but that was still within the acceptable error. The error was slightly larger on the low- M_r molecules than on the high- M_r molecules. This could be due to the precision of the MALS detector, which is lower in the low- M_r range.

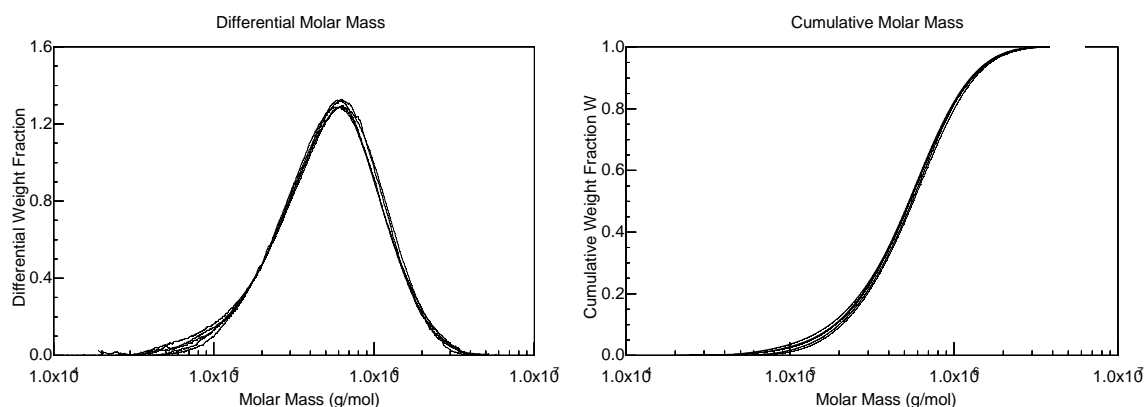


Figure 4.2-13. Overlaid differential molar mass graphs (left), and cumulative molar mass graphs (right) for five runs of Whatman No.1 paper, cellulose concentration 0.625% in 0.5% LiCl/DMAc.

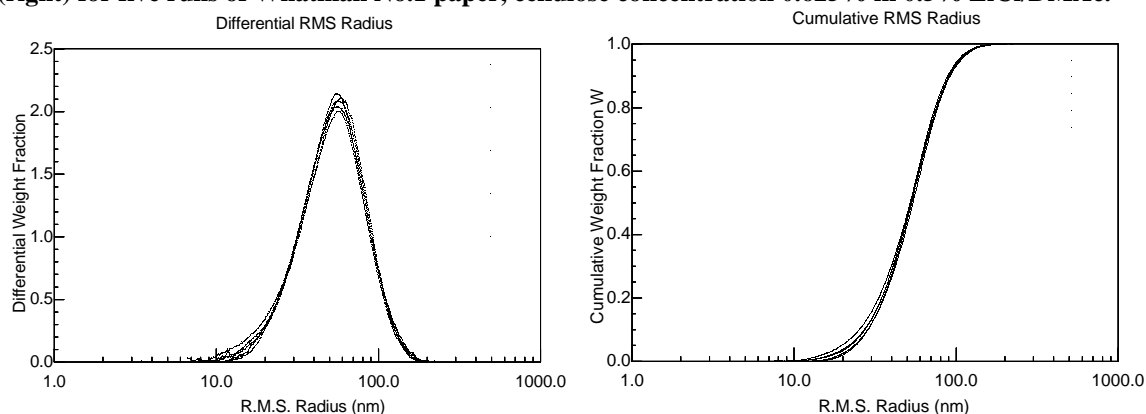


Figure 4.2-14 Overlaid differential root mean square radii (left), and cumulative root mean square radii (right) for five runs of Whatman No.1 paper, cellulose concentration 0.625% in 0.5% LiCl/DMAc.

Table 4.2-3. M_r averages and RSD% obtained in the five runs of Whatman No.1 paper.

sample	$M_n \times 10^{-5}$ g mol ⁻¹	$M_w \times 10^{-5}$ g mol ⁻¹	$M_z \times 10^{-5}$ g mol ⁻¹
1A	4.177	6.959	10.62
1B	3.686	6.65	10.39
1C	3.679	6.515	9.988
2A	4.006	6.731	10.24
2B	3.523	6.628	10.39
average	3.814	6.697	10.33
RSD	0.268	0.166	0.233
RSD%	7.0%	2.5%	2.3%

4.2.4 Conformation of cellulose in solution and solvent quality

As seen in previous sections, SEC with MALS and DRI detection allows the determination of absolute molar masses and the direct measurements of the polymer size, expressed as the mean square radius ($\langle r_g^2 \rangle$ or r_{ms}^2), from which information on the polymer conformation in solution can be derived.

At the very low concentrations used in SEC, the values of the z-average rms radius (r_z) are independent of both dn/dc and M_r . Therefore r_z is a good parameter to study the size of the polymer, as long as its value remains larger than $\lambda/20$ in order to measure the angular dependence of the scattered intensity.

Figure 4.2-16 and Figure 4.2-16 show respectively the molar mass and the root mean square radius (rms) versus the elution volume (V_e) for the cellulose of Whatman No.1 paper dissolved in 8% LiCl/DMAc, and diluted to 0.5% LiCl. The DRI trace chromatogram is superimposed onto the distribution line. At the edges of the distribution curve, the signal-to-noise ratio is low and there is a large uncertainty in the values, which is visible from the dispersion of the data points. The cellulose showed a linear relationship of both molar mass and rms radius with V_e across most of the elution range. This indicated a normal elution with no column retention.

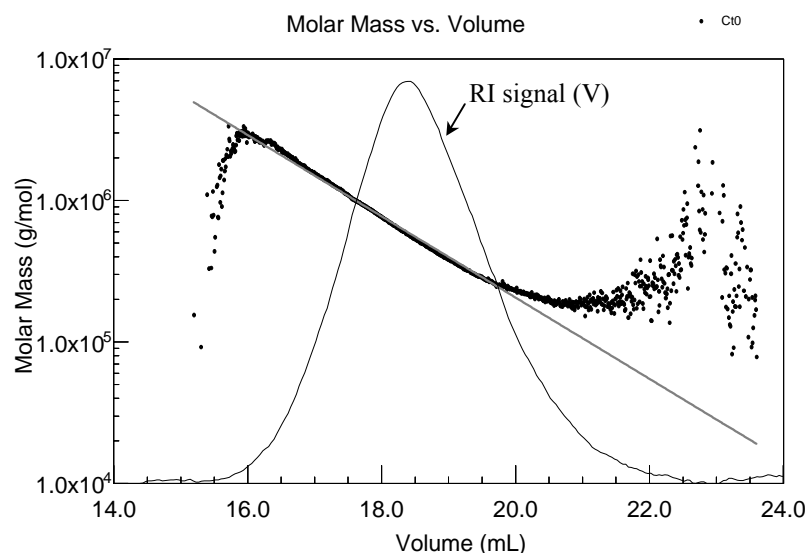


Figure 4.2-15. Molar mass distributions across elution volume for cellulose of Whatman No.1 0.625% in 0.5% LiCl/DMAc.

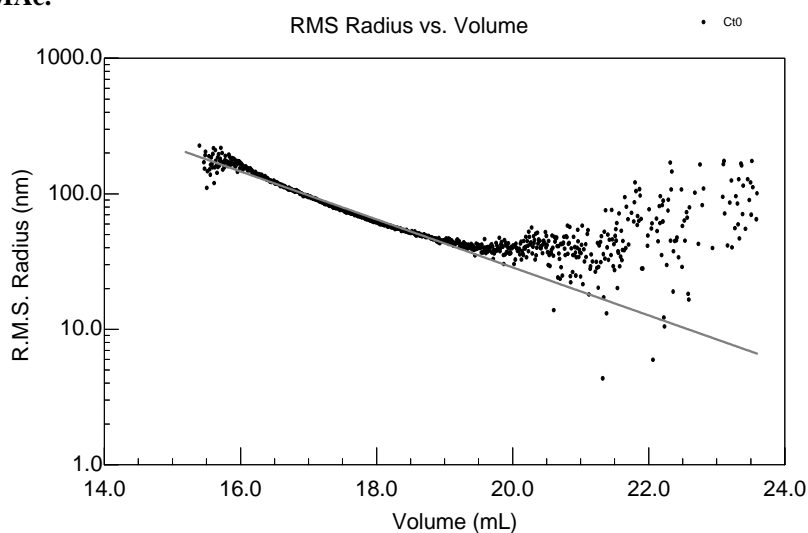


Figure 4.2-16. rms radius distributions across elution volume for cellulose of Whatman No.1 0.625% in 0.5% LiCl/DMAc.

The technique of SEC/MALS also provides the possibility of obtaining a direct relationship between M_r and polymer size. This relationship between polymer size and molar mass is usually represented as a scaling law of the form [31,32,33]:

$$\sqrt{\langle r_g^2 \rangle} = Q M_r^q \quad \text{(Equation 4-6)}$$

As the polymer dimensions depend on polymer-solvent interactions, this law yields information on the properties of the polymer in solution. The power order q (scaling factor) is related to the shape of the chains, *i.e.* to polymer-solvent interactions and macromolecular conformation of the polymer. Values of q comprised between 0.5 and 0.6 are expected for random coil polymer chains; q is closer to 0.5 for a polymer in a theta solvent ($A_2 = 0$) and is closer to 0.6 for a polymer in a good solvent ($A_2 > 0$). Rigid rod polymers have q values of 1 - or very close to 1, and spherical polymers have values of q around 0.33. Most real random coils have $q \approx 0.55$ -0.60. Branched molecules may have

slopes much smaller than the typical random coil value, making the slope a possible indicator of branching.

The slope in the log-log plot of rms radius as a function of M_r yields q . The value of q can be related to the Mark-Houwink-Sakurada (MHS) parameter a by the equation [20]:

$$q = \frac{(a+1)}{3}$$

Thus, $a = 3q - 1$

Hence, for true random coil polymers in a theta solvent, $q = a = 0.5$

Figure 4.2-17 shows a plot of rms radius versus M_r on a log-log scale for cellulose in 0.5% LiCl/DMAc with its best-fit match. The linear relationship obtained and the value q of 0.59 indicated that cellulose chains were in random coil conformation and that LiCl/DMAc was a very suitable solvent. This is true not only for the dissolution solvent 8% LiCl/DMAc, but also for the SEC mobile phase 0.5% LiCl/DMAc, where upon dilution the cellulose molecules stayed in solution in very good thermodynamic conditions.

In the literature, cellulose in 9% LiCl/DMAc was first reported to have a rigid rod conformation [24,34], with a MHS coefficient a of 1.19, reflecting the enhanced stiffness of the cellulose backbone. The suggested explanation was that due to the complexing nature of the solvent LiCl/DMAc, the repulsive interaction of the chloride ions associated with the chain favoured a fully extended molecule. These results were obtained with viscosity measurements. SEC studies later reported a values of 0.7 and 1 for cellulose in LiCl/DMAc showing both a linear polymer conformation and the good solvating power of this solvent [16,35]. More recent studies reported a values of 0.957 [13] and 0.65 [36].

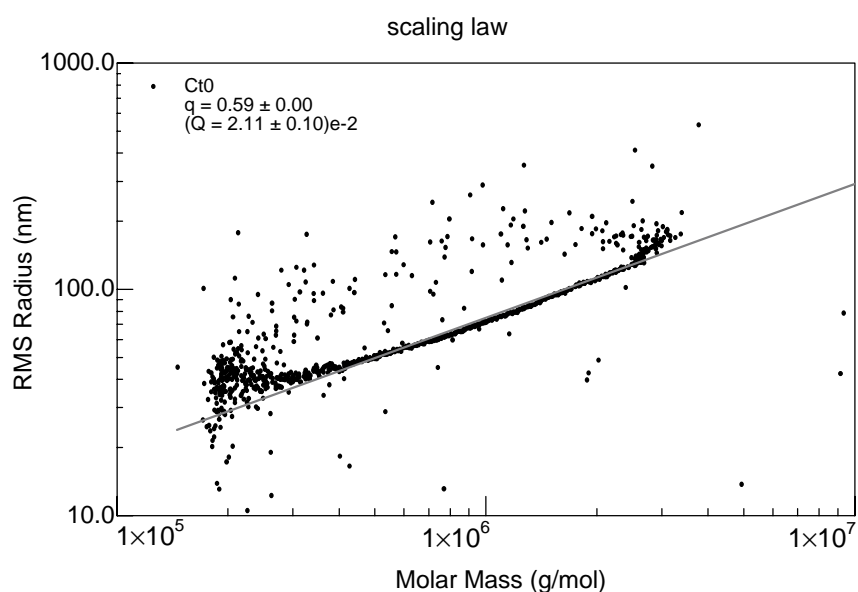


Figure 4.2-17. rms radius Vs M_r for cellulose of Whatman No.1, 0.625% in 0.5% LiCl/DMAc.

Table 4.2-4 reports the values of q and Q obtained running three samples of unaged Whatman No.1 in 0.5% LiCl/DMAc prepared as described in section 4.2.3.1 and dissolved as reported in section 3.2.4 of Chapter 3. One of them was run in three replicates (1A, 1B and 1C) and the remaining two in duplicate (2A, 2B and 3A, 3B) for a total of seven runs.

The value of q was higher for samples 1 and 3, with $0.59 \leq q \leq 0.62$, and average value of 0.6 (RSD of 2%), indicating optimal solvation conditions. It was slightly lower for sample 2, with $q \approx 0.56-0.57$, indicating that in this case cellulose was somewhat closer to theta conditions. Nevertheless, all values of q indicated a random coil polymer conformation in solution.

The average value of Q found using samples 1 and 3, *i.e.* five runs, as these were the samples showing optimal solvation, yielded 2.0×10^{-2} with a RSD of 19.6%.

It can therefore be statistically concluded that cellulose in 0.5% LiCl/DMAc is in random coil conformation, and Equation 4-6 thus becomes:

$$\sqrt{\langle r_g^2 \rangle} = 2.0 \times 10^{-2} M_r^{0.6}$$

From the values of q and considering only samples 1 and 3 (for the same reason as earlier), the MHS coefficient a for the cellulose in 0.5% LiCl/DMAc was found to be between 0.77 and 0.86, with an average value of 0.81 (Table 4.2-4). This finding corroborates the data reported by Schult *et al.* [26] who found a scaling factor q of 0.55 for cellulose in 0.5% LiCl/DMAc, the corresponding value for a being 0.65. The authors justify this surprisingly low coefficient compared to the earlier published values by a weakening of the intramolecular hydrogen bonding leading to an increased freedom of rotation of the cellulose molecule around the glycosidic bond, and consequently lower chain stiffness. The hypothesis that intermolecular associations play a role in lowering the hydrodynamic volume of the cellulose in solution thus yielding this low a value was also proposed by the authors.

The values of q reported above were obtained from plotting and integrating across the entire peak area. However, the slope in the log-log plot may not be constant over the whole M_r range. This is most often reported in the case of linear polymers that have branched components at high- M_r . In such a case, as branched molecules are more compact, the slope becomes shallower at large M_r .

Table 4.2-5 reports the values of q for log-log plots of rms radius versus M_r for the seven runs of Whatman No.1 paper across three different regions of the peak, covering the entire V_e range (*i.e.* from 15.5 mL to 23 mL). The latter spans from the baseline to the apex, across the peak's half height, and from the apex back to the baseline. Table 4.2-6 reports the corresponding values of M_w averages over these three peak regions.

Table 4.2-7 reports the values of q for the same seven runs across the area of the peaks for which the log-log plots of rms radius versus M_r were found strictly linear. This corresponded to a common V_e among the seven runs between 17 and 19 mL. In this case, the calculations of q were performed over the specific peak region (17-19 mL) in four fractions of 0.5 mL each. Table 4.2-8 reports the corresponding values of M_w averages over these four volume fractions. Figure 4.2-18 illustrates the location of the V_e fraction 17 to 19 mL on the chromatogram of one of the samples.

In both cases, whether calculated over the entire V_e split into three fractions or over a partial V_e split into four, the value of q was found to decrease from the beginning to the end of the elution. Hence, q decreased with M_r , and this is represented in Figure 4.2-19. In this figure, the average q of the seven values from Table 4.2-5 and Table 4.2-7 is plotted versus the logarithm of corresponding average M_w .

As cellulose is not a branched polymer, this change in the slope q as a function of M_r can be interpreted as due to a variation in the quality of the solvent depending on the length of the chains. Very-high- M_r chains ($M_w > 10^6$ g mol⁻¹) seem to have a slightly stiffer conformation ($q > 0.6$) than high and mid- M_r chains ($10^6 > M_w > 5 \times 10^5$ g mol⁻¹). The latter have a perfect random-coil conformation with q between 0.5 and 0.6. Low- and very-low- M_r chains ($M_w < 3.5 \times 10^5$ g mol⁻¹) have lower q values (average $q = 0.43$). This either means that they are less well solvated than mid- and high- M_r chains, or they tend to adopt a more compact conformation in solution.

This finding can also partly explain the variations in the values of dn/dc reported in the literature for cellulose in LiCl/DMAc reported in section 4.2.2.3.1.

Table 4.2-4. Values of Q , q and a for seven runs of the three samples of cellulose in LiCl/DMAc.

	Q ($\times 10^2$)	q	a
1A	2.38 ± 0.14^1	0.61	0.83
1B	2.11 ± 0.10	0.59	0.77
1C	1.97 ± 0.06	0.60	0.80
2A	3.62 ± 0.10	0.57	0.71
2B	1.11 ± 0.07	0.56	0.68
3A	2.27 ± 0.08	0.59	0.77
3B	1.37 ± 0.05	0.62	0.86

¹ The uncertainty range on the values of Q is calculated by the ASTRA software. The software estimates the uncertainties in all calculated quantities by determining the statistical fluctuation in each detector's signal, including all photodiodes and the RI signals. These uncertainties are statistical only, and do not include any of the many possible systematic errors that may be present from sample preparation to injection and separation. The reported errors are merely a measure of the statistical consistency of the data, not an absolute limit on the error in the results.

Table 4.2-5. Values of q for seven runs of the three samples of cellulose in LiCl/DMAc, across three overlaying peak regions.

	q from V_e peak start to V_e peak apex	q in V_e peak 1/2 heights	q from V_e peak apex to V_e peak end
1A	0.62	0.58	0.48
1B	0.65	0.50	0.34
1C	0.63	0.57	0.41
2A	0.56	0.58	0.47
2B	0.58	0.55	0.48
3A	0.64	0.54	0.45
3B	0.68	0.58	0.37
Average	0.62	0.56	0.43
RSD	0.041	0.030	0.056

Table 4.2-6. Values of M_w and $\log M_w$ for the seven runs of the three samples of cellulose on three fractions of V_e from beginning to end.

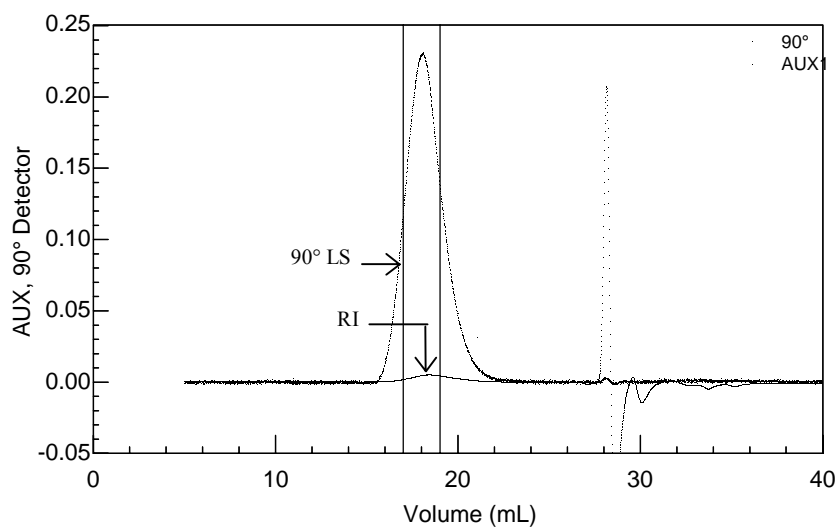
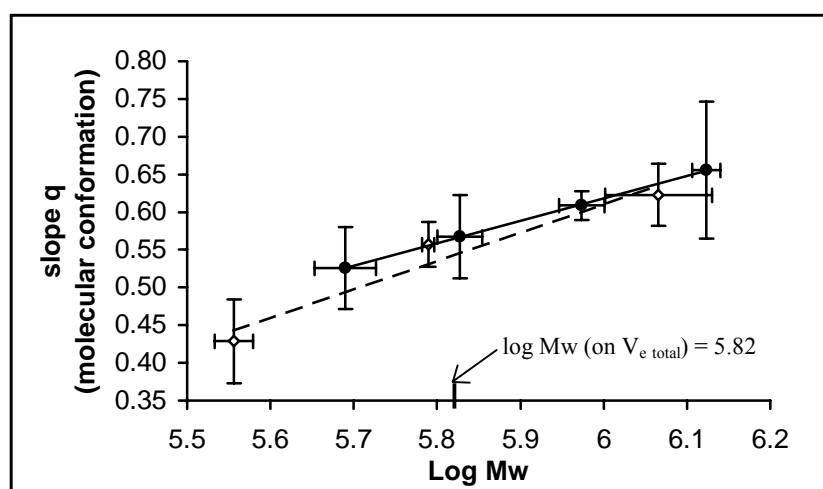
sample	V_e peak start to V_e peak apex		V_e peak 1/2 heights		V_e peak apex to V_e peak end	
	M_w (g/mol)	$\log M_w$	M_w (g/mol)	$\log M_w$	M_w (g/mol)	$\log M_w$
1A	1.620×10^6	6.210	6.133×10^5	5.788	3.553×10^5	5.551
1B	1.109×10^6	6.045	6.023×10^5	5.780	3.873×10^5	5.588
1C	1.074×10^6	6.031	6.072×10^5	5.783	3.344×10^5	5.524
2A	1.069×10^6	6.029	6.141×10^5	5.788	3.655×10^5	5.563
2B	1.087×10^6	6.036	6.268×10^5	5.797	3.775×10^5	5.577
3A	1.131×10^6	6.053	6.270×10^5	5.797	3.621×10^5	5.559
3B	1.138×10^6	6.056	6.195×10^5	5.792	3.393×10^5	5.531
average	1.175×10^6	6.066	6.157×10^5	5.789	3.602×10^5	5.556
RSD	1.98×10^5	0.064	9.4×10^4	0.007	1.9×10^4	0.023

Table 4.2-7. Values of q for the seven runs of the three samples of cellulose in LiCl/DMAc, across the V_e range where the relationship between rms radii Vs M_r (log-log) is strictly linear.

sample	q over V_e 17-17.5mL	q over V_e 17.5-18mL	q over V_e 18-18.5mL	q over V_e 18.5-19mL
	1A	0.84	0.58	0.59
1B	0.69	0.59	0.46	0.49
1C	0.64	0.64	0.6	0.53
2A	0.6	0.61	0.6	0.57
2B	0.58	0.61	0.57	0.52
3A	0.58	0.61	0.53	0.47
3B	0.66	0.62	0.62	0.48
Average	0.66	0.61	0.57	0.53
RSD	0.091	0.020	0.055	0.054

Table 4.2-8. Values of M_w and $\log M_w$ for the seven runs of the three samples of cellulose over four fractions of V_e between 17 and 19 mL.

sample	V_e 17-17.5 mL		V_e 17.5-18 mL		V_e 18-18.5 mL		V_e 18.5-19 mL	
	M_w (g/mol)	$\log M_w$						
1A	1.412×10^6	6.150	1.056×10^6	6.024	7.430×10^5	5.871	5.571×10^5	5.746
1B	1.294×10^6	6.112	9.089×10^5	5.959	6.403×10^5	5.806	4.569×10^5	5.660
1C	1.362×10^6	6.134	9.593×10^5	5.982	6.900×10^5	5.839	4.964×10^5	5.696
2A	1.301×10^6	6.114	9.097×10^5	5.959	6.574×10^5	5.818	4.850×10^5	5.686
2B	1.339×10^6	6.127	9.333×10^5	5.970	6.807×10^5	5.833	5.128×10^5	5.710
3A	1.348×10^6	6.130	9.579×10^5	5.981	6.881×10^5	5.838	5.028×10^5	5.701
3B	1.249×10^6	6.097	8.732×10^5	5.941	6.113×10^5	5.786	4.278×10^5	5.631
Average	1.329×10^6	6.123	9.426×10^5	5.974	6.730×10^5	5.827	4.913×10^5	5.690
RSD	4.9×10^4	0.016	5.4×10^4	0.024	3.9×10^4	0.025	3.8×10^4	0.034

**Figure 4.2-18. 90° photodiode LS signal and DRI signal as a function of V_e for sample 3A. Vertical bars enclose the fraction of V_e used in the calculations of q and shown in Tables 4.2-6 and 4.2-7.****Figure 4.2-19. (●): q as a function of $\log M_w$ over four V_e fractions of 0.5 mL between 17 and 19 mL; (◇): q as a function of $\log M_w$ over three V_e fractions covering the whole peak region.**

Chemicals and materials

Whatman No.1 filter paper was obtained from Fisher Scientific (Springfield, NJ, USA). Sodium chloride (NaCl) was purchased from Sigma-Aldrich Corp. (St. Louis, MO, USA) and HPLC grade toluene was from Acros Organics (Springfield, NJ, USA). Anotop filters (0.02 μm pore size, 25 mm diameter) were from Whatman Inc. (Clifton, NJ, USA). Millex LCR filters (0.5 μm pore size) from Millipore (Bedford, MA, USA) purchased through Fisher Scientific. Drierite was from Fisher Scientific. Polystyrene (PS) standard 30,000, poly (styrene-divinyl benzene) (PSDVB) columns 10 μm diameter particles MIXED-B pores, 300 mm \times 7.5 mm and guard column 10 μm particles 50 mm \times 7.5 mm were from Polymer Laboratories Inc. (Amherst, MA 01002, USA).

Instruments

Multiangle light scattering detector Dawn EOS and interferometric differential refractometer Optilab DSP were from Wyatt Technologies Corp. (Santa Barbara, CA, USA). The four-channel HPLC solvent degasser DegassitTM was obtained from Metachem Technologies Int. (Torrance, CA, USA) and HP 1100 isocratic pump G1310A was from Hewlett Packard, now Agilent Technologies (Palo Alto, CA, USA). Injector model 7725i was from Rheodyne L.P. (Cotati, CA, USA). The heating/stirring unit was from Pierce (Rockford, IL, USA).

References

1. Timpa, J.D. and Ramey Jr, H.H. *Text. Res. J.*, 59, 11 (1989) 661-664.
2. Timpa, J.D. *J. Agric. Food Chem.*, 39 (1991) 270-275.
3. Silva, A.A. and Laver, M.L. *Tappi J.*, 80, 6 (1997) 173-180.
4. Schwald, W. and Bobleter, O. *J Appl. Polym. Sci.*, 35 (1988) 1937-1944.
5. Striegel, A.M. and Timpa, J.D. *Proc. Int. GPC Symp.*, Lake Buena Vista, Florida, Waters Corp., Milford (1995) 567-591.
6. Kennedy, J.F.; Rivera, Z.S.; White, C.A.; Lloyd, L.L. and Warner, F.P. *Cellulose Chem. Technol.*, 24, 3 (1990) 319-325.
7. Westermark, U. and Gustafsson, K. *Holzforschung*, 48 (Suppl.) (1994) 146-150.
8. Karlsson, O. and Westermark, U. *J. Pulp Pap. Sci.*, 22, 10 (1996) J397-J401.
9. Strlič, M.; Kolar, J.; Žigon, M. and Pihlar, B. *J. Chromatogr. A*, 805 (1998) 93-99.
10. Sjöholm, E; Gustafsson, K.; Berthold, F. and Colmsjö, A. *Carbohydr. Polym.*, 41 (2000) 1-7.
11. Sjöholm, E; Gustafsson, K.; Eriksson, B.; Brown, W. and Colmsjö, A. *Carbohydr. Polym.*, 41 (2000) 153-161.
12. Jerosch, H.; Lavédrine, B. and Cherton, J-C. *J. Chromatogr. A*, 927 (2001) 31-38.
13. Bikova, T. and Treimanis, A. *Carbohydr. Polym.*, 48 (2002) 23-28.
14. Strlič, M.; Kolenc, J.; Kolar, J. and Pihlar, B. *J. Chromatogr. A*, 964 (2002) 47-54.
15. Grubisic, Z.; Rempp, P. and Benoit, H. *J. Polym. Sci. Polym. Lett.*, 5 (1967) 753-759.
16. Striegel, A.M. and Timpa, J.D. *Carbohydr. Res.*, 267 (1995) 271-290.

17. Striegel, A.M. and Timpa, J.D. *Strategies in Size Exclusion Chromatography*, ACS Symposium Series 635, American Chemical Society, Washington, DC (1996) 366-378.
18. Elmsley, A.M.; Ali, M. and Heywood, R.J. *Polymer*, 41 (2000) 8513-8521.
19. Stol, R.; Pedersoli Jr, J.L.; Poppe, H and Kok, W.Th. *Anal.Chem.*, 74, 10 (2002) 2314-2320.
20. Flory, P.J. *Principles of Polymer Chemistry*, Cornell University Press, Ithaca (1953).
21. Wyatt, P.J. *Analytica Chimica Acta*, 272 (1993) 1-40.
22. Ghazy, R.; El-Baradie, B.; El-Shaer, A. and El-Mekawey F. *Optics & Laser Technology*, 31 (1999) 447-453.
23. Xie, T.; Penelle, J. and Verraver, M. *Polymer*, 43 (2002) 3973-3977.
24. McCormick, C.L.; Callais, P.A. and Hutchinson Jr, B.H. *Macromolecules*, 18 (1985) 2394-2401.
25. Terbojevich, M.; Cosani, A.; Conio, G.; Ciferri, A. and Bianchi, E. *Macromolecules*, 18 (1985) 640-646.
26. Schult, T.; Moe, S.T.; Hjerde, T. and Christensen, B.E. *J. Liq. Chromatogr. & Rel. Technol.*, 23 (2000) 2277-2288.
27. Shelosky, N.; Röder, T and Badinger, T. *Das Papier*, 12 (1999) 728-738.
28. Debzi, El M. Celluloses issues du traitement à la vapeur: évolution des masses moléculaires moyennes, transformations morphologiques et cristallines, Thèse de Doctorat, Université Joseph Fournier – Grenoble I (1992) 55.
29. Röder, T.; Morgenstern, B.; Schelosky, N. and Glatter, O. *Polymer*, 42 (2001) 6765-6773.
30. Matsumoto, T.; Tatsumi, D.; Tamai, N. and Takaki, T. *Cellulose*, 8 (2001) 275-282.
31. Pincus, P. *Macromolecules*, 9 (1976) 386-388.
32. De Gennes, P.G. *Scaling Concepts in Polymer Physics*, Cornell University Press, Ithaca, NY (1979).
33. Laguna, M.T. R.; Medrano, R.; Plana, M.P. and Tarazona, M.P. *J Chromatogr. A*, 919 (2001) 1-19.
34. Dawsey, T.R and McCormick, C.L. *J. Macromol. Sci. - Rev. Macromol. Chem. Phys.*, C30, 384 (1990) 405-440.
35. Striegel, A. *Carbohydr. Polym.*, 34 (1997) 267-274.
36. Schult, T.; Hjerde, T., Optun, O.I.; Kleppe, P.J. and Moe, S. *Cellulose*, 9 (2002) 149-158.

Chapter 5. Evaluation of different methods for the characterisation of cellulose: size-exclusion chromatography using direct dissolution, size-exclusion chromatography using derivatisation, and viscometry

Abstract

The method developed in the present study, i.e. size-exclusion chromatography (SEC) using multiangle light scattering (MALS) and differential refractive index (DRI) detection applied to what is referred as 'directly dissolved cellulose' or DDC in lithium chloride/N,N-dimethylacetamide (LiCl/DMAc), is evaluated compared to two other methods currently used for cellulose analysis. These are SEC using low-angle light scattering (LALS) and ultra-violet detection of cellulose derivatised to tricarbonyl or CTC, and viscometry (V) in cadmium tri-ethylene diamine dihydroxide or Cadoxen. The values of the molar mass (M_r) averages of cellulose obtained with the different methods, and the discrepancies between these values are discussed on the basis of the precision of each methodology and the action of the solvents on the polymer. As SEC of the DDC yielded the highest M_r averages values and viscometry the lowest, several hypotheses are presented in order to account for these differences. Each method is also discussed on the basis of its suitability to characterise the aging-induced degradation of the paper. The complexity of carrying out such comparisons between different methods is outlined.

5.1 Introduction

When analysing cellulose a key parameter for the accuracy of the data obtained is the integrity of the polymer. A non-degradative dissolution process is paramount if the M_r of dissolved cellulose is to reflect the molar mass (M_r) of the cellulose source. The type and quality of the data and the precision in the M_r determination also greatly depend on the methods used and their sensitivity.

Viscometry (V) is fast and convenient, which often makes it the preferred method to estimate the average degree of polymerisation (DP_v) of cellulose and its derivatives. However, the method has obvious limitations since only one single M_r average value, the

viscosity-average molar mass (M_v) is determined, and no information on the molar mass distribution (MMD) of the polymer can be obtained. Additionally viscometry methods are based on the dissolving action of complexing organometallic solvents (copper ammonium hydroxide, copper ethylene diamine, cadmium ethylene diamine), which often result in degradation of the polymer [1,2,3] especially when analysing oxidised cellulose [4]. Viscometry is still widely used in cellulose analysis despite the multiple applications of size-exclusion chromatography (SEC) in polymer chemistry. The main reason is that among the solvents that are able to swell cellulose, penetrate the fibres and break the intermolecular hydrogen bonds, few are compatible with SEC column packings. But the advantages of SEC over viscometry are manifold, and these are chiefly providing information on MMD and allowing the determination of all the molar mass averages (M_n , M_w , M_z , M_{z+1} and M_v). SEC provides also information on the degraded fractions thus leading to insight in the degradation mechanisms.

In SEC, the type and quality of the data and the precision in the M_r determination depend on the detection method. The refractive index (RI) detectors require a calibration using narrowly distributed polymer standards of known M_r , leading to the relative MMD and M_r . The lack of structurally identical standard fractions for cellulose is responsible for the well-known problem of structural mismatch between the chosen calibration standard and the analyte, as well as the resulting uncertainty on the real M_r (section 4.1.1 of Chapter 4).

One alternative in order to avoid a calibration of the type $\text{Log } M_r$ as a function of elution volume (V_e) relative to narrowly distributed standards is the universal calibration method [5], which is based on the hydrodynamic volume of the polymers in solution. This method requires coupling SEC with RI and viscometry (V) detectors or the knowledge of accurate MHS values for both the sample polymer and the reference standards (section 4.1.2.1. of Chapter 4). It has been applied to cellulose M_r determination by Timpa *et al.* [6,7,8].

UV detectors can be used when cellulose has been modified to derivatives that absorb in UV like cellulose esters such as tricarbonyl (underivatised cellulose has no absorption in ultraviolet radiation) or when studying UV absorbing species such as lignins.

However, the best solution is to avoid calibration of any kind by using light scattering (LS) detectors, which online with a concentration detector - UV or RI - allow for absolute M_r determination. Low-angle LS, multiangle LS or V coupled to LS detectors can be used. Further details on detection methods are in section 4.1 of Chapter 4.

5.2 Aim of the study

Chapter 3 and Chapter 4 outlined the reasons based on the literature search that led us to opt for analysing cellulose in lithium chloride/*N,N*-dimethylacetamide (LiCl/DMAc) using SEC for the current research, and reported the development of an appropriate method to carry out the study. The present chapter is aimed at searching for experimental

evidence of the reported superiority of this method by comparing it to other commonly used methods in cellulose analysis.

The experiment was based on evaluating SEC in LiCl/DMAc of cellulose versus SEC in tetrahydrofuran (THF) of cellulose tricarbanilate (CTC), and versus viscometry of cellulose in cadmium tri-ethylene diamine dihydroxyde (Cadoxen). The latter methods were chosen because they are prominently used in paper and cellulose research and are both reported to be the least degrading in their category.

So far, few studies have been dedicated to the comparative evaluation of different methods for cellulose characterisation. SEC in LiCl/DMAc and viscometry for M_r determination of oxidised cellulose [4], cellulose from different sources [9], and cellulose which originated from specific pulp processes [10] have been compared in the past. In these studies, viscosity measurements were performed in copper di-ethylene diamine dihydroxide (CED). Lawther *et al.* [11] studied SEC of derivatised cellulose (CTC) and underivatised cellulose (dissolved in LiCl/DMAc), and compared it with viscometry of the CTC in pyridine.

To our knowledge no study including both SEC methods of derivatised and underivatised cellulose, and viscometry of underivatised cellulose in Cadoxen has been published. Moreover, the present study bases the comparisons not only on the characterisation of unaged cellulose but also on cellulose artificially aged by a combination of heat and humidity.

The task of making global experimental comparisons between different methods that involve a number of parameters ranging from sample preparation to instrumentation is far from simple. The comparison was rationalised by studying several aspects of the three methods. Precision, information obtained and its quality were assessed. The methods were also investigated in terms of their suitability for the analysis of non-degraded as well as degraded cellulose. Lastly, their relative simplicity, as for instance the ease of sample preparation was evaluated.

5.3 Experimental

5.3.1 Description of the methods

5.3.1.1 Viscometry in Cadoxen

The majority of standardised methods for viscometry measurements use CED as the solvent [12,13,14,15,16]; one method uses iron (III) sodium tartrate complex (FeTNa or EWNN) [17]. However, Cadoxen, a cadmium tri-ethylene diamine dihydroxide complex $[\text{Cd}(\text{En})_3](\text{OH})_2$ ($\text{En} = \text{H}_2\text{N}(\text{CH}_2)_2\text{NH}_2$) is sometimes preferred over CED because the solvent induced degradation of cellulose is significantly lower [18,19,20,21]. Additionally, as opposed to CED, Cadoxen is a colourless solvent, which makes the

experiment easier to follow. In the present study, instead of the one-point viscosity measurement recommended by the standard methods, three-point measurements were carried out with solutions of different concentrations, from which the value of the intrinsic viscosity $[\eta]$ was obtained by extrapolation to zero concentration. This provided greater accuracy in the results with a relative standard deviation (RSD) of 1.5% for repeatability of the values of DP_v [22].

In the present experiment, dissolution was preceded by a reduction of the paper in sodium borohydride (NaBH_4) [4,22]. The measurements were done with a capillary glass viscometer Routine 100 (Cannon-Fenske). The method and the calculation of the DP_v are described in Appendix 5-1. From this point onward, cellulose analysed by viscometry in Cadoxen will be abbreviated V.

5.3.1.2 Size-exclusion chromatography (SEC) of cellulose tricarbaniolate in THF

Both SEC methods used allow for absolute M_r determination by using LS detectors. The cellulose tricarbaniolate was produced by reaction of cellulose with phenylisocyanate (PIC) in dimethylsulfoxide (DMSO). Cellulose was activated in DMSO prior to the derivatisation. After the reaction, CTC was precipitated out of the derivatising mixture and re-dissolved in THF in order to allow SEC in THF mobile phase. The concentration detector was a UV detector UV 2000 (Spectra Physics) working at 270 nm, and was connected online with the M_r detector, a low-angle laser-light scattering detector (LALS) KMX-6 (Chromatix). Sample preparation, activation and dissolution, instrumentation and chromatographic conditions for SEC of CTC (further abbreviated SEC_{CTC}) are described in Appendix 5-2. The data reduction and M_r calculations were performed using SEC software CARB made by Lauriol [23] at EFPG¹ especially for the analysis of CTC.

5.3.1.3 SEC of underivatised cellulose in LiCl/DMAc

As seen in previous chapters, LiCl/DMAc is a direct solvent of cellulose, the solvation mechanism was described in Chapter 3. One of the advantages is that LiCl/DMAc can be used as mobile phase in SEC. Detection was done with an interferometric differential refractometer (DRI) Optilab DSP (Wyatt Technologies) as concentration detector and online multiangle light scattering detector (MALS) Dawn EOS (Wyatt Technologies) as M_r detector. In this method, dissolution was preceded by activation of the cellulose substrate followed by water/solvent exchange (water/methanol/DMAc). The activation and dissolution methods are described in section 3.2.4 of Chapter 3, and the SEC procedure is described in section 4.2.3 of Chapter 4. The data reduction and M_r calculations were performed with ASTRA software v. 4.73.04 (Wyatt Technologies).

¹ Ecole Française de Papèterie et des Industries Graphiques (St-Martin d'Hères).

Cellulose dissolved in LiCl/DMAc is further referred to as DDC (Directly Dissolved Cellulose) and the SEC method as SEC_{DDC}.

5.3.2 Sample preparation

5.3.2.1 Preparation of the paper samples

Whatman No.1 pure cellulose filter paper was used as cellulose source. A pool of papers were left unaged (abbreviated UA) and a pool was subjected to artificial aging at 80°C and 50% relative humidity (rH) for 94 days (abbreviated At₉₄) by hanging the sheets individually in a climate chamber Versatenn (Tenney Environmental). As shown in section 6.3.2.1 of Chapter 6, and supported by literature evidence [24,25,26] these aging conditions favoured the degradation of the cellulose by acid-catalysed hydrolysis.

For the viscosity measurements, the paper was cut in small pieces of 2 mm × 2 mm. For SEC, the paper was defibrillated by dry milling. This was done in a hammer mill (Poitemill/Forplex) for SEC_{CTC}, and in a two-blade cutting mill for SEC_{DDC}. This type of preparation allows to further facilitate the access of the swelling liquids to the fibres during the activation phase. Activation is necessary in order to make cellulose more readily accessible to solvent molecules, as the solvents compatible with SEC have a lower swelling power than the complexing solvents used for viscometry (see section 1.3 of Chapter 1).

5.3.2.2 Sampling for viscometry and SEC

In order to fall within the viscosity range of the capillary glass viscometer, the required concentration of cellulose was about 1.5 g L⁻¹ for the unaged paper, and 2.1 g L⁻¹ for the aged paper, which corresponded to sample weights of 6.2×10⁻² g and 8.8×10⁻² g respectively. Three different solutions of each paper were prepared and three measurement repeats per solution were carried out.

CTC of aged and unaged paper were prepared. Injected weights were 1.461×10⁻⁴ g and 1.548×10⁻⁴ g respectively. The two samples were analysed in duplicate runs. The values reported are the average. The value of dn/dc of CTC in THF 0.169±0.002 mL g⁻¹ was used [23,28]. As in SEC the working concentrations are very low, the second virial coefficient A_2 can safely be omitted (see section A-5.2.2.2.2 of Appendix 5-2).

For DDC, three unaged and two aged paper samples were dissolved, each one was run two to three times. The runs were non-consecutive. The values reported are the average of the multiple runs. The sample preparation was performed according to the method described in section 3.2.4 of Chapter 3. In the case of DDC, the knowledge of the exact injected weights was not required in order to calculate M_w with SEC/MALS. The injected

mass is calculated by ASTRA software by inputting the values of the calibration constant of the DRI (α) and the refractive index increment (dn/dc) of cellulose in LiCl/DMAc. These two parameters were determined experimentally as $\alpha = 2.25655 \times 10^{-4} \text{ V}^{-1}$ and $dn/dc = 0.077 \text{ mL g}^{-1}$ (section 4.2.2 of Chapter 4). Here also, the second virial coefficient A_2 can be neglected (see section 4.2.2.4 of Chapter 4).

The RSD% on the mass of cellulose injected calculated by the ASTRA software for all the DDC unaged papers was 4.2%. RSD% refers here to the uncertainty related to the statistical fluctuation in each detector's signal (including all photodiodes and the DRI) and does not include any of the many possible systematic errors that may be present. The precision and repeatability of the SEC/MALS method was studied in section 4.2.3.4 of Chapter 4.

5.4 Results and discussion

5.4.1 Unaged cellulose (UA)

5.4.1.1 SEC of UA

The overlaid UV and LS signals obtained in one of the SEC_{CTC} runs of unaged paper (UA) are represented in Figure 5.4-1 and the DRI and LS (90° angle photodiode) signals obtained in one of the SEC_{DDC} runs are in Figure 5.4-2. The small peak present on the UV signal at high elution volume (V_e) for the CTC was due to residual diphenylurea that was still present despite the thorough washing in ethanol. The compound was trapped in the CTC network during the precipitation phase.

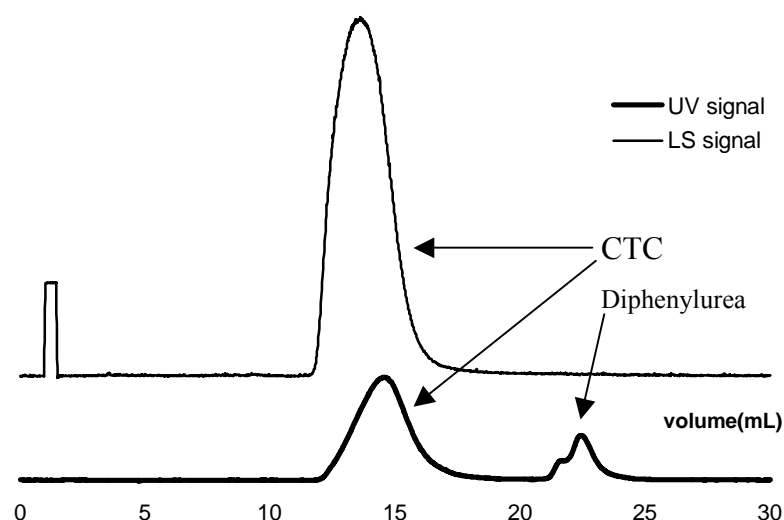


Figure 5.4-1. UV (270 nm) and LS (LALS) signals of CTC UA (unaged).

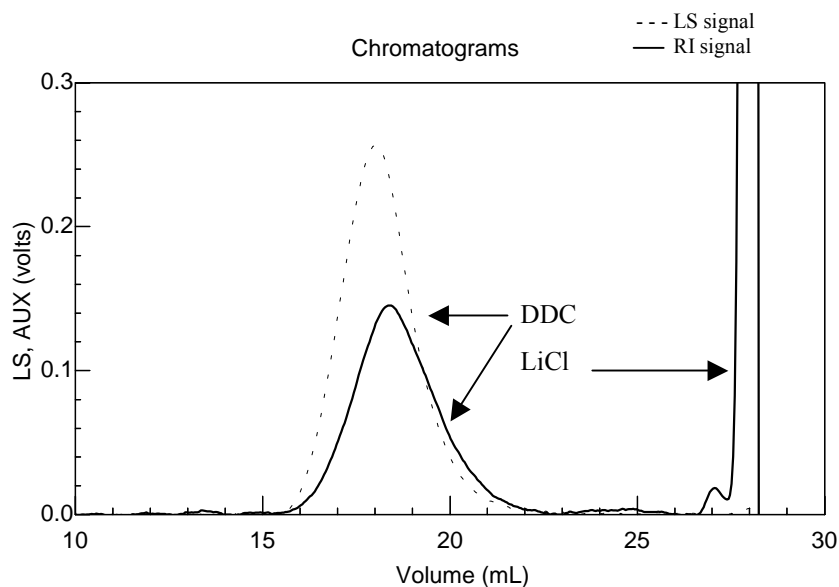


Figure 5.4-2. DRI and LS (MALS) signals of DDC UA (unaged).

SEC_{CTC} and SEC_{DDC} differential molar mass graphs are overlaid in Figure 5.4-3. The MMD profile of CTC was considerably smaller than that of DDC. In order to better compare the shape and position of the peaks, the MMD of CTC normalised to that of DDC is added. The correction factor was 7.24, which is the ratio of the weight fraction (wt frt) at peak molar mass (M_p) of DDC (wt frt = 1.325%, $M_p=6\times 10^5$ g mol⁻¹) to the weight fraction at M_p of CTC (wt frt = 0.183%, $M_p=2.9\times 10^5$ g mol⁻¹). Figure 5.4-4 shows the cumulative molar mass graphs of SEC_{CTC} and SEC_{DDC}. Table 5.4-1 reports the values of the M_r averages obtained with the three methods for UA.

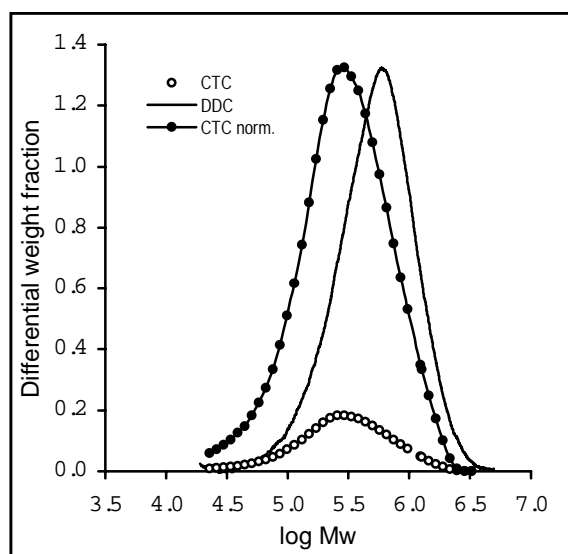


Figure 5.4-3. Overlaid differential molar mass graphs of DDC UA, CTC UA and CTC UA normalised to DDC UA.

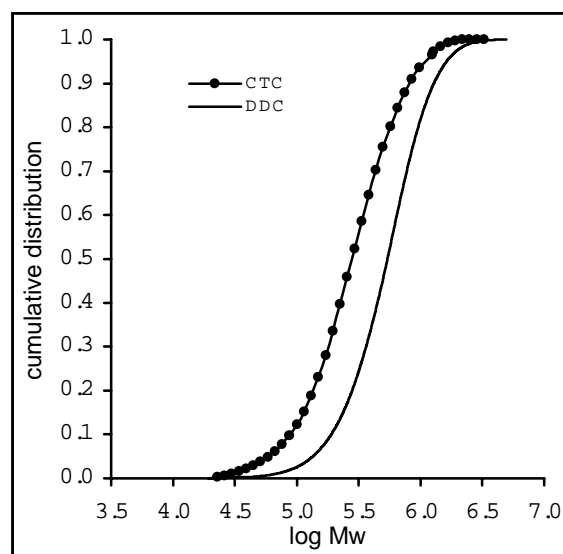


Figure 5.4-4. Overlaid cumulative molar mass graphs of DDC UA and CTC UA.

Both the MMD and the cumulative molar mass graphs of CTC were shifted towards lower M_r compared to DDC. The values of M_n , M_w , M_z and M_p obtained with SEC_{CTC} were all lower than with SEC_{DDC}, respectively by 57%, 40%, 28% and 53% (Table 5.4-1). Among the literature cited earlier, Lawther *et al.* [11] also found significant differences, of about 43% between CTC and DDC in the M_w of cotton cellulose. However, Kennedy *et al.* [27] reported only a small difference between M_v of CTC determined by viscometry and M_w of DDC (in 10% LiCl/DMAc) for cotton linters determined by SEC, which they attributed to incomplete substitution of the CTC.

In the present study, in order to explain this significant difference, possible reasons can be ventured, including on the one hand the accuracy and limits of the two SEC methods and on the other, the dissolution procedures that can have a more or less degrading or modifying effect towards cellulose. The comparison between the two SEC methods in the following section is based on M_w , as it is the average M_r directly calculated by the LS measurements.

Table 5.4-1. M_r averages, corresponding DP and polydispersity (PD) obtained for CTC, DDC and V for unaged cellulose (UA).

	M_n ($\times 10^5$ g mol ⁻¹)	DP_n	M_w ($\times 10^5$ g mol ⁻¹)	DP_w	M_z ($\times 10^5$ g mol ⁻¹)	DP_z	M_p ($\times 10^5$ g mol ⁻¹)	M_r ($\times 10^5$ g mol ⁻¹)	DP_v	PD
SEC _{CTC} UA*	1.72	1062	4.03	2485	7.23	4462	2.92	3.80	2344	2.38
SEC _{DDC} UA	3.96 +/- 0.31	2444	6.68 +/- 0.14	4122	10.09 +/- 0.46	6226	6.24 +/- 0.35	6.44	3973	1.70 +/- 0.12
V UA								2.88 +/- 0.18	1778	

(*) : The values of the M_r averages for CTC are adjusted to the molar mass of an anhydroglucose monomer, *i.e.* 162 g mol⁻¹.

5.4.1.1.1 Precision of the SEC methodologies

In this section, the precision and possible sources of uncertainties in both methods were investigated in order to explain the difference in M_w between CTC and DDC.

5.4.1.1.1.1 Precision of the methodology of SEC_{CTC}

In the SEC_{CTC}, the precision was inherent to both the chemistry parameters (related to the derivatisation reaction) and the instrumental parameters.

The factor related to the instrumental parameters that most probably bore the greatest uncertainty in LALS was the attenuation factor (D) of the incident beam (Appendix 5-2). The attenuation factor was assumed to be correct from previous calibration measurements. Experimental records showed that the attenuation factor varied within $\pm 10\%$. Errors associated with the value of the dn/dc could not be evaluated as this parameter was a literature value, but underestimating slightly dn/dc would result in overestimating slightly M_w (in the same proportion), and vice-versa.

The injected mass and the degree of substitution (DS) of the cellulose tricarbonyl were the two chemistry factors that in all likelihood had the highest uncertainty. The error on the injected mass can arise from the presence of residual diphenylurea. This error was estimated to $\pm 3\%$ by Lauriol [23]. Incomplete substitution reaction can lead to errors on the M_r of the CTC monomer. As the lowest DS expected using the present derivatisation procedure was 2.8 [23], and the highest DS being 3, the uncertainty on the M_r of the CTC monomer was estimated at 5%.

An experimental variability plan was designed where the three above mentioned parameters were cross-varied within their maximal and minimal values. The variability equation obtained with one of the SEC_{CTC} runs was:

$$DP_w = 2525 + 253 x_1 - 75 x_2 - 60 x_3 - 7 x_1 x_2 - 6 x_1 x_3 + 2 x_2 x_3 \quad \text{Equation 5-1}$$

Where,

x_1 = attenuation factor (D) (variation limits: 1.277×10^{-8} to 1.561×10^{-8})

x_2 = injected mass (variation limits: 1.502×10^{-4} to 1.594×10^{-4} g)

x_3 = molar mass of the CTC monomer (variation limits: 495 to 519 g mol⁻¹)

The parameter that most influenced the value of M_w was found to be the attenuation factor, highest coefficient in Equation 5-1.

Across the variability plan, M_w varied within 3.49×10^5 g mol⁻¹ to 4.74×10^5 g mol⁻¹, which corresponds to $\pm 13\%$.

5.4.1.1.1.2 Precision of the methodology of SEC_{DDC}

In the SEC_{DDC} methodology, the uncertainty can only arise from instrumental parameters. In MALS, M_w is calculated by the software. Therefore the uncertainty on the value of dn/dc and on the values of the MALS and DRI calibration constants can lead to errors.

The uncertainty on the dn/dc taken within the repeatability of the three values obtained experimentally (section 4.2.2.3.2 of Chapter 4) was $\pm 2\%$. The errors on the instruments calibration constants taking into account the experimental measures and the value provided by the manufacturer were $\pm 2\%$ for the LS constant, and $\pm 0.6\%$ for the α constant (DRI) (sections 4.2.2.2.1 and 4.2.2.1.2 of Chapter 4).

An experimental variability plan was designed where the three parameters were cross-varied within their maximal and minimal values. The variability equation obtained was:

$$DP_w = 4199 + 97 x_1 - 28 x_2 - 165 x_3 - x_1 x_2 - 4 x_1 x_3 + x_2 x_3 \quad \text{Equation 5-2}$$

Where,

x_1 = LS constant (variation limits: 6.069×10^{-6} to 6.356×10^{-6})

$x_2 = \text{DRI constant } \alpha \text{ (variation limits: } 2.231 \times 10^{-5} \text{ to } 2.261 \times 10^{-5} \text{ V}^{-1}\text{)}$

$x_3 = dn/dc \text{ cellulose/0.5\% LiCl/DMAc (variation limits: } 0.0744 \text{ to } 0.0805 \text{ mL g}^{-1}\text{)}$

The dn/dc showed the highest coefficient in Equation 5-2, followed by that of the LS constant. These were therefore the two parameters that most influenced the value of M_w in the present experimental conditions.

Across the variability experiment M_w varied from $6.34 \times 10^5 \text{ g mol}^{-1}$ to $7.28 \times 10^5 \text{ g mol}^{-1}$, *i.e.* $\pm 6.5\%$. It has to be noted that this is a very small error, at half that of the estimated error for SEC_{CTC} . This shows further that the SEC_{DDC} method developed in the present study is quite precise.

The sum of the possible cumulated errors of SEC_{CTC} and SEC_{DDC} brought a maximal possible difference ΔM_w of about 40% ($\pm 19.5\%$). However, it is quite unlikely that all these statistical errors be cumulated as to yield such difference in the experimental M_w and other possible error sources had to be investigated.

5.4.1.1.2 Study of the discrepancies due to the dissolution processes

Factors, in particular related to the dissolution processes have to be investigated in order to account for a difference in M_w as large as 40% between CTC and DDC. Several propositions are made hereafter.

The first hypothesis is that the procedure leading to CTC degraded the cellulose molecules to a certain extent. The second hypothesis is related to the complex chemistry involved during the dissolution of cellulose in LiCl/DMAc, that could lead to a possible overestimation of M_w . The third hypothesis is related to non-steric elution phenomena of DDC and pseudo-exclusion behaviour of cellulose dissolved in LiCl/DMAc.

Hypothesis 1. Degradation of cellulose during derivatisation to CTC

The differences in the values of M_n , M_w and M_z of DDC and CTC for the unaged papers ($M_r \text{ DDC UA} - M_r \text{ CTC UA}$) followed the sequence $\Delta M_n\% > \Delta M_p\% > \Delta M_w\% > \Delta M_z\%$. Such sequence indicated that the number of low- M_r fractions in the MMD of CTC is comparatively smaller than in the MMD of the DDC (knowing that the low- and high- M_r fractions in DDC and CTC are relative to each respective MMD). Another explanation would be that these low- M_r fractions are underestimated in the CTC- hence the latter appear as if containing proportionally more of the high- M_r fractions than the DDC. Concerning the polydispersity PD ($\text{PD} = M_w/M_n$), that of CTC was 1.4 times higher than that of DDC.

It has to be noted at this point that the software program CARB used to calculate the values of M_w of the CTC applies a smoothing equation based on a polynomial regression

in the higher elution volume portion in order to recalculate values of M_n [23,28]. This is aimed at correcting the value of M_n for axial diffusion because M_n is most affected by the lower signal to noise ratio of the LALS at the end of the elution (low- M_r and low concentration). Since this phenomenon does not affect the signal of the UV detector, the elution curve of the LS is smoothed according to the curve of the UV. After smoothing the data, M_w remains unchanged while M_n is significantly decreased.

Using the raw (not smoothed) data, the PD of CTC was 1.69, which was equal to the PD of DDC, and M_n was $2.38 \times 10^5 \text{ g mol}^{-1}$, which was 28% higher than M_n using smoothing (but still about 40% lower than M_n of the DDC). Smoothed CTC data is further referred to as CTC_{smo} and raw CTC data as CTC_{raw} .

Based on hypothesis 1, and according to the results, cellulose appeared as if undergoing significant degradation during the derivatisation process to tricarbonylates, resulting in an overall decrease in the M_r averages. The degradation seemed more directed towards the elimination of the lower- M_r molecules of the CTC. This could result from the washing in ethanol after the precipitation phase of the CTC (see Appendix 5-2), as ethanol can dissolve the low- M_r CTC [23]. The precipitation phase was unavoidable since the preparation of the CTC and the SEC runs were carried out in two different solvents.

The literature is unanimous on the fact that degradation occurs upon derivatisation of cellulose to CTC depending on reaction time and temperature as well as on the co-reactant, but no real agreement could be found among the different authors as to the best procedure in order to minimize this degradation. According to Evans *et al.* [29], in the preparation of CTC of high- M_r cellulose from bleached cotton linters with phenylisocyanate (PIC) in DMSO at 70°C, reaction times above 32 hours resulted in a depolymerisation. The M_w decreased by 9% when the reaction time increased from 32 to 56 hours, and by 24% when it increased from 32 to 96 hours. According to the authors, the lower temperature had to be compensated by a longer reaction time thereby also resulting in increased degradation. The least degrading conditions achieved in this case were using PIC in pyridine at 80°C, which resulted in a slight decrease in M_w of only 5.4% and 6.4% when the reaction time increased from 32 to 56 hours, and from 32 to 96 hours respectively. Additionally, under these conditions, the initial M_r after 32 hours of reaction was higher by 7.2% than when the reaction was carried out with PIC in DMSO. The authors concluded that the drawback of DMSO was that it led to partial degradation of high- M_r cellulose during derivatisation but the advantage lied in faster reaction rates than with pyridine.

Contrary to the findings of the previous authors, Daňhelka *et al.* [30] found no degradation during the carbanilation of cellulose with PIC in pyridine at 110°C for 12 hours when SEC data was compared to viscosity data (using Cadoxen). But Shroeder and Haigh [31] showed that, although no degradation occurred when carbanilation was carried out at 80°C for up to 48 hours, higher temperatures induced depolymerisation already within the first hours of the reaction.

For Lauriol *et al.* [23,28], and Lapierre and Bouchard [32], using PIC in DMSO led to the most appropriate carbanilation procedure. The latter found that PIC in pyridine resulted in an overestimated M_r in the case of softwood Kraft pulps, and attributed the fact to aggregation possibly caused by incomplete carbanilation.

Hill *et al.* [33] showed that complete substitution (DS=3) was achieved by derivatising cellulose with PIC in four times the reaction stoichiometry, for 48 hours at 80°C in pyridine. Lauriol *et al.* advocated using 10 times the reaction stoichiometry in order to obtain complete substitution [23,28].

In the present experiment the procedure of Lauriol was followed, which used a derivatisation temperature of 70°C, that is even lower than most of the above-mentioned studies. Therefore, according to the authors cited above, such conditions should lead to no or little degradation in the worst case.

Hypothesis 2. Overestimation of M_r averages of cellulose when dissolved in LiCl/DMAc

According to the considerations described earlier, another cause for the molar mass discrepancy between the two SEC methods would help in the interpretation. This could arise from an overestimation of M_w by the SEC_{DDC} method. This hypothesis is examined below.

Such an overestimation can happen through the formation of aggregates and/or the association of molecules in LiCl/DMAc. According to Terbojevitch *et al.* [34] values of M_w seven-fold those of M_v for cellulose can be found. The authors showed the formation of stable aggregates and inter-aggregate associations of cellulose molecules (especially in the case of acid hydrolysed cellulose) when dissolution took place at low LiCl concentration (5% LiCl/DMAc). They demonstrated that the aggregates were formed by seven molecules in fully extended conformation, and proposed they arose from the native structure of the fibrils. Sjöholm *et al.* [9] later reported the formation of high- M_r aggregates of cellulose molecules in LiCl/DMAc solutions for softwood pulp, but these did not form with cotton linter.

A study by Röder *et al.* [35] showed that the solution state of cellulose molecules in LiCl/DMAc was influenced by both the cellulose and LiCl concentrations. Dissolution at high LiCl concentration (9%) and high cellulose concentration (1% wt/wt) resulted in a bimodal SEC molar mass distribution profile, indicating a high level of aggregation. The distribution became monomodal after 10 times dilution (to 0.9% LiCl and 0.1% cellulose (wt/wt)), indicating that the large aggregates had dissociated. The same initial cellulose concentration but with a lower salt concentration (6%) resulted in large particles not totally dissolved that did not dissociate upon 10 times dilution.

Aggregates are easily detectable in MALS in the high- M_r end (small V_e) of the photodiodes signals, especially in the high degree angles. The chromatograms obtained in this study showed monomodal LS signals at all measuring angles, same as displayed in

Figure 5.4-2. Thus no evidence of aggregation was found. Additionally, our experimental conditions were the most favourable for a total dissolution with no aggregation or association as advocated by Röder *et al.* [35]. The detailed study of the conformation of cellulose in LiCl/DMAc reported in section 4.2.4 of Chapter 4 showed a polymer in random coil conformation and proved LiCl/DMAc to be a good solvent, and a theta solvent in the worst case.

Excluding the formation of aggregates, a second explanation for an overestimate of the M_r of cellulose using the method SEC_{DDC} can be one related to the chemistry of the dissolution of cellulose in LiCl/DMAc. The dissolution involves the formation of complexes between cellulose and LiCl/DMAc with a major role played by the chloride anion breaking up the inter- and intra-molecular hydrogen bonds (section 2.2.2.3.1 of Chapter 2). Previous studies showed that Cl⁻ formed complexes with the three hydroxyl groups of an anhydroglucose unit (AGU) by hydrogen bonding and that the counterpart of the solvent complex, *i.e.* the macrocation [Li DMAc]⁺, was more loosely bound [36]. If Cl⁻ ions were linked by hydrogen bonds to the hydroxyl groups, as represented in Figure 5.4-5, the resulting apparent M_r of the AGU could be considerably increased. If a bare AGU has a M_r of 162 g mol⁻¹, adding three chloride atoms would increase the M_r by 39%, to 266 g mol⁻¹. This could explain the difference in M_w between the two SEC methods. If this hypothesis were to be verified, it would also show that the procedure leading to CTC is not as degrading as suggested earlier.

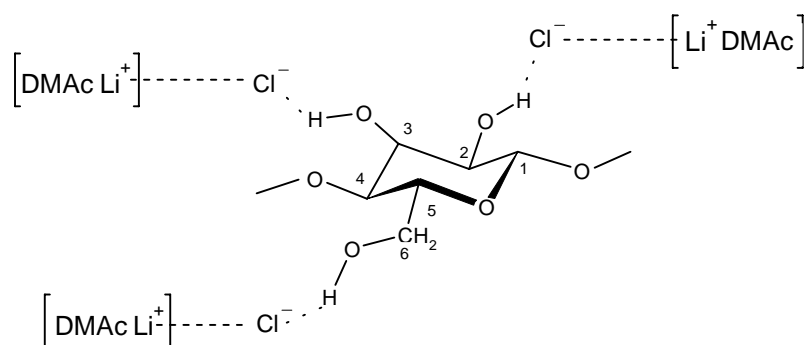


Figure 5.4-5. Cellulose in LiCl/DMAc, Cl⁻ linked to the hydroxyl groups of the AGU through hydrogen bonds as proposed in Hypothesis 2.

It has to be noted that this hypothesis holds only if there is indeed formation of a hydrogen bond between the cellulose and the chloride ions, since the MALS detector does not see a simple solvation layer, which has a refractive index very close to that of the solvent.

The values of the masses injected for the seven samples of DDC UA were re-calculated using 266 g mol⁻¹ as M_r for the AGU. This was achieved by decreasing the mass

calculated by the ASTRA software by 39%. M_w was then re-calculated by entering the α constant and the new (decreased) mass as known variables (instead of α and dn/dc as in the typical M_w software calculation throughout this study). The resulting average molar masses were: $M_n = (2.42 \pm 0.15) \times 10^5 \text{ g mol}^{-1}$, $M_w = (4.10 \pm 0.15) \times 10^5 \text{ g mol}^{-1}$, and $M_z = (6.19 \pm 0.40) \times 10^5 \text{ g mol}^{-1}$, with the same polydispersity of 1.69 (± 0.12) as before. The value of dn/dc calculated by ASTRA was then 0.126 mL g^{-1} .

These re-calculated values of the M_r averages for DDC UA resulted in a difference between DDC UA and CTC UA of: $\Delta M_n = 1.7\%$ with CTC_{raw} ($\Delta M_n = 29\%$ with CTC_{smo}), $\Delta M_w = 1.7\%$, and $\Delta M_z = -14\%$. DDC with the re-calculated M_r are later referred as DDC_{rec} , and DDC with the uncorrected M_r as DDC.

Hypothesis 3. Non-steric exclusion phenomena in SEC

The third hypothesis proposed for the difference in M_w between CTC and DDC is related to the column packing. Poly (styrene-divinyl benzene) (PSDVB) is the preferred packing material used in SEC analysis of cellulose [4,6,7,8,9,10,23,27,28,29,32,33,37,38,39,40,41,42,43,44,45]. However, little is known about the elution behaviour of solutions of cellulose in LiCl/DMAc on this column packing. A recent study by Bikova & Treimanis [46] pointed to a possible contribution of pseudo-exclusion effects in SEC of cellulose with 0.5% LiCl/DMAc as mobile phase, at 60°C to 80°C using PSDVB columns. The authors mentioned several possible causes for non-steric exclusion effects. One was the presence of electronegative groups on the cellulose. Despite the fact that cellulose is always considered as a neutral polymer, some ionisable carboxyl groups can be present from other polysaccharidic components such as hemicelluloses or from pulping and bleaching. It is noted at this point that in the present study, the accelerated aging some of the samples were subjected to could cause carbonyl and carboxyl groups to form along the cellulose chain. The second cause the authors pointed to was pH and salt concentration of the mobile phase, usually 0.5 to 1% LiCl in DMAc, *i.e.* 0.11 to 0.22 M , as being quite high and potentially able to lead to a modification of the viscosity of the polymer in solution due to a change in the hydrodynamic volume.

In the present case, the peaks profiles of Figure 5.4-1 and Figure 5.4-2 indicated suitable columns sets in both SEC_{CTC} and SEC_{DDC} . Figure 5.4-6 shows the elution curves and the plot of $\log M_r$ as a function of V_e for DDC UA. The MMD is quasi-Gaussian and the distribution of mass across the elution is constant, which corroborates a good separation, with no retention phenomena under the current conditions. This confirmed the suitability of PSDVB as packing material for SEC columns as acknowledged in the literature [45]. Therefore, the hypothesis of a non-adequate separation range of the columns was excluded and was not investigated further in the framework of the present study.

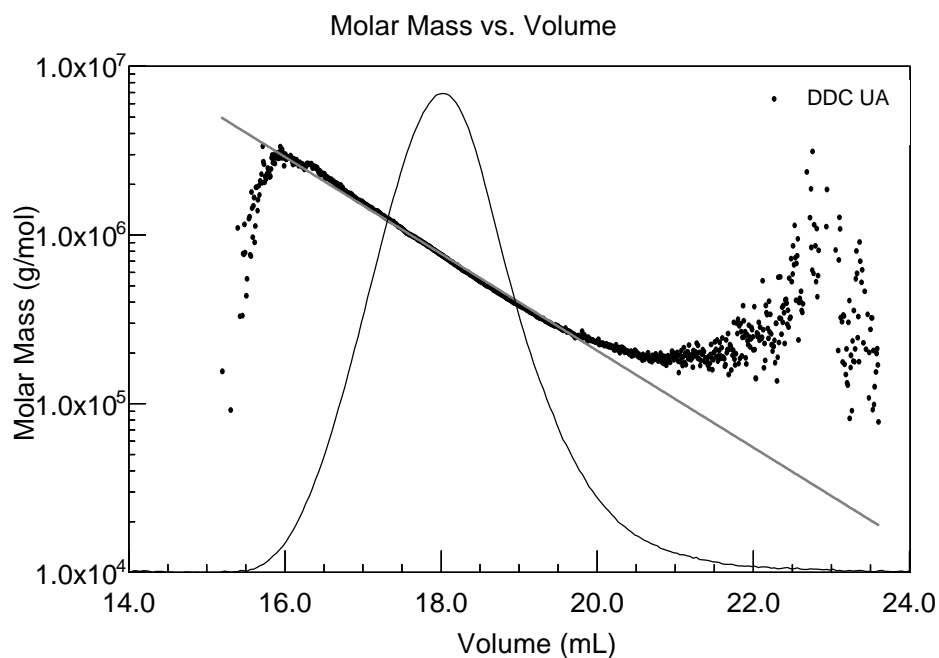


Figure 5.4-6. DRI signal and M_r obtained from light scattering of DDC UA.

5.4.1.2 Viscometry of UA

M_v always falls between M_n and M_w (section 2.1 of Chapter 2). In the specific case where the coefficient a in the Mark-Houwink-Sakurada (MHS) equation (described in Appendix 5-1) is equal to unity, M_v is equal to M_w . For pure cellulose paper, the MHS coefficient a is often found close to unity, and M_v is usually reported in the literature to be closer to M_w than to M_n . In the present study with SEC/MALS (section 4.2.4 of Chapter 4), the experimental average value of a for Whatman No.1 paper in 0.5% LiCl/DMAc was found of 0.81.

Table 5.4-1 reports the average value obtained for M_v of unaged cellulose in Cadoxen. This value was considerably smaller than the values obtained for M_w for both SEC_{DDC} and SEC_{CTC}: 57% lower than the M_w of DDC (30% lower than that of DDC_{rec}), and 28% lower than that of CTC.

A difference in M_r is often reported in the literature when comparing viscometry in CED with LS for SEC_{CTC} [23] and for SEC_{DDC} [34]. It has to be noted that CED is more aggressive to cellulose and especially to oxidised cellulose than Cadoxen [3,22]. This difference in M_r was also reported when great care was taken to minimize the degradation of the cellulose during dissolution in CED by working in a N₂ atmosphere and in the absence of light [10].

With the data collected by the UV and the LALS detectors for SEC_{CTC}, and with the DRI and MALS detectors for SEC_{DDC} it was possible to calculate M_v for CTC and DDC (see formulae in section A5-2.2.2.3 of Appendix 5-2). This was done in order to more

accurately evaluate viscometry and SEC by comparing the same M_r average (M_v). The MHS coefficient a used in the calculation of M_v for DDC UA was the experimentally determined value of 0.81, and for CTC UA, the value 0.84 found in the literature was used [30,47], as the current SEC_{CTC} method did not allow for the calculation of a .

The values thus obtained for M_v were of 6.44×10^5 g mol⁻¹ for DDC UA and 3.80×10^5 g mol⁻¹ for CTC UA (Table 5.4-1). These values are indeed quite close to M_w . However, for V UA M_v was still lower respectively by 55% and 24% than M_v calculated for DDC UA and for CTC UA. Using the re-calculated average M_w of DDC (DDC_{rec} UA) obtained with the seven samples unaged, the average value obtained for the calculated M_v for DDC_{rec} UA was then 3.95×10^5 g mol⁻¹, which is still 27% higher than the value obtained for M_v V UA. However, this difference approaches the 24% difference reported above obtained subtracting the M_v of V UA to the calculated M_v of CTC UA.

This difference can be attributed to either solvent-induced degradation or the precision in the value of the calculated M_v . Indeed, errors on the MHS constants K' and a can lead to considerable errors in the M_v . This is especially true for the value of a , as it is a power exponent in the MHS equation, and contrary to K' , a is used in the calculation of M_v based on the MMD in SEC. However, the present study (section 4.2.4 of Chapter 4) showed that the RSD on the average a value of 0.81 determined for DDC UA was 4.9%, with a ranging from 0.77 to 0.86. The subsequent error on the calculated M_v for DDC UA was therefore $\pm 6.8 \times 10^3$ g mol⁻¹, which yields a value of M_v within 6.37×10^5 to 6.5×10^5 g mol⁻¹. Such a very small error cannot account for the discrepancy in the values of the different M_v . Thus, it can be concluded that the latter is most probably due to a considerable underestimation of M_v due to the method of viscometry in Cadoxen, which is then attributed mainly to solvent-induced degradation.

5.4.2 Aged cellulose (At_{94})

5.4.2.1 SEC of At_{94}

The overlaid SEC_{CTC} and SEC_{DDC} differential and cumulative molar mass graphs of cellulose from aged papers are represented in Figure 5.4-7 and Figure 5.4-8 respectively.

As already observed for unaged cellulose, the MMD profile of CTC At_{94} was lower than that of DDC At_{94} (Figure 5.4-7). Here also, in order to better compare the MMD profiles, the differential molar mass graph for CTC normalised to that of DDC was added. The correction factor was 6.78, which corresponds to the ratio 1.166/0.172 (ratio of the wt fit at M_p of DDC (3.5×10^5 g mol⁻¹) divided by the wt fit at M_p of CTC (2.3×10^5 g mol⁻¹)).

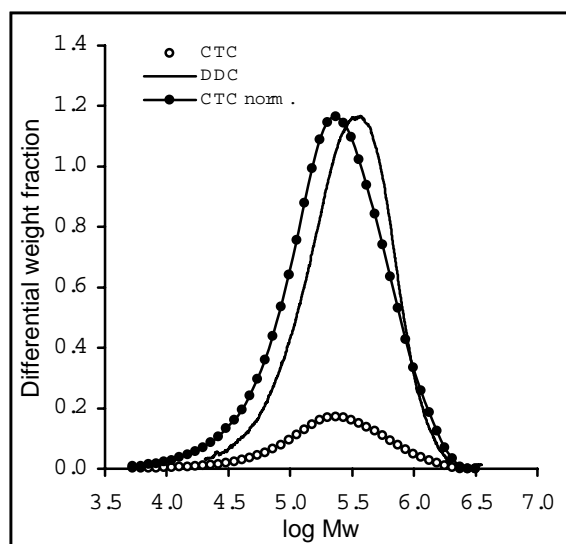


Figure 5.4-7. Overlaid differential molar mass graphs of DDC At₉₄, CTC At₉₄, and CTC At₉₄ normalised to DDC At₉₄.

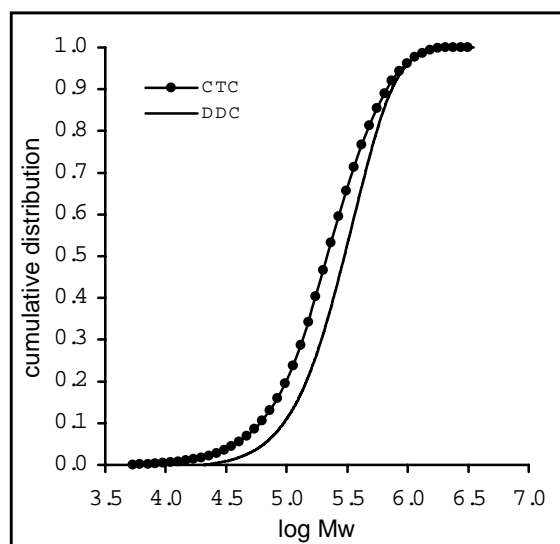


Figure 5.4-8. Overlaid cumulative molar mass graphs of DDC At₉₄ and CTC At₉₄.

The values of M_r averages obtained with SEC_{CTC} (CTC_{smo} and CTC_{raw}) and SEC_{DDC} for the papers aged 94 days are reported in Table 5.4-2. M_n and M_w resulted in lower values for CTC than for DDC, by 9% for CTC_{raw} (40% for CTC_{smo}), and by 15% respectively, while the two M_z were similar. The PD of CTC_{smo} was 1.4 times higher than that of DDC, while the PD of CTC_{raw} and that of DDC were similar. Here also, it seemed more appropriate to use CTC_{raw} rather than CTC_{smo} for the comparison with DDC.

According to the calculations of uncertainties reported in section 5.4.1.1.1, a 15% change in M_w falls within the experimental error in the precision of the methods. It has to be noted at this point that the RSD of 2.1% on M_w of DDC UA, *i.e.* $(6.68 \pm 0.14) \times 10^5 \text{ g mol}^{-1}$, and 3.4% on M_w of DDC At₉₄, *i.e.* $(3.81 \pm 0.13) \times 10^5 \text{ g mol}^{-1}$ reported in Table 5.4-1 and Table 5.4-2 were calculated based only on the different values of M_w obtained in the multiple runs repeats and do not consider the experimental uncertainties that were estimated in section 5.4.1.1.1.

The values of the M_r averages for DDC_{rec} At₉₄ were $M_n = (1.26 \pm 0.09) \times 10^5 \text{ g mol}^{-1}$, $M_w = (2.33 \pm 0.08) \times 10^5 \text{ g mol}^{-1}$, and $M_z = (3.70 \pm 0.2) \times 10^5 \text{ g mol}^{-1}$. These values for DDC_{rec} At₉₄ of M_n , M_w and M_z were smaller than for CTC_{raw} At₉₄ by 33%, 28% and 39% respectively. However, the reader is reminded that these M_r averages of DDC_{rec} At₉₄ were calculated on the basis of a hypothetical 39% increment in M_r , as in the case of DDC_{rec} UA. This increment was based on the assumption of the availability of three hydroxyl groups on each AGU to form hydrogen bonds with the chloride anions of the solvent complex. The number of hydroxyl groups on a chain of aged cellulose is however most probably less than three, due to oxidation as consequence of the aging process. Therefore, the average number of Cl⁻ along the chain would in all likelihood be less than three per AGU. In addition, charge repulsion with the Cl⁻ can occur if negatively charged oxidised groups are present on the chain. The average M_r of the AGU of aged cellulose in LiCl/DMAc

would be less than 266 g mol^{-1} , *i.e.* between 162 and 266 g mol^{-1} . With such a large molar mass spread, results are rather difficult to interpret. The conformational characteristic of aged cellulose in solution studied in section 6.3.2.1.1 of Chapter 6, showed it was less well solvated than unaged cellulose, which tends to confirm the hypothesis of a lower complexation degree with the solvent.

However, it has to be noted that if aged cellulose bears fewer hydroxyl groups on its chains, this should affect the CTC prepared from aged samples as well, as PIC reacts with available hydroxyl groups to form the carbanilate. Therefore, with a DS lower than three, the average M_r of the CTC monomer would be below 519 g mol^{-1} , which in turn would result in the underestimation of M_w of CTC. But this could not be investigated further here.

This shows that for aged cellulose the discrepancies in the M_r averages between the two SEC methods cannot be interpreted with certainty. It is thus extremely difficult to draw conclusions about the respective performance of the two SEC procedures for the aged samples.

Figure 5.4-9 shows on the same graph the overlaid differential molar mass graphs of aged and unaged CTC and DDC. This allows for a better visualisation of the smaller shift towards the low- M_r that exists between DDC At₉₄ and CTC At₉₄ compared to that between DDC UA and CTC UA (using the MMD of CTC normalised to that of DDC). Table 5.4-3 reports the percent difference in M_r averages between aged and unaged paper according to the relevant method.

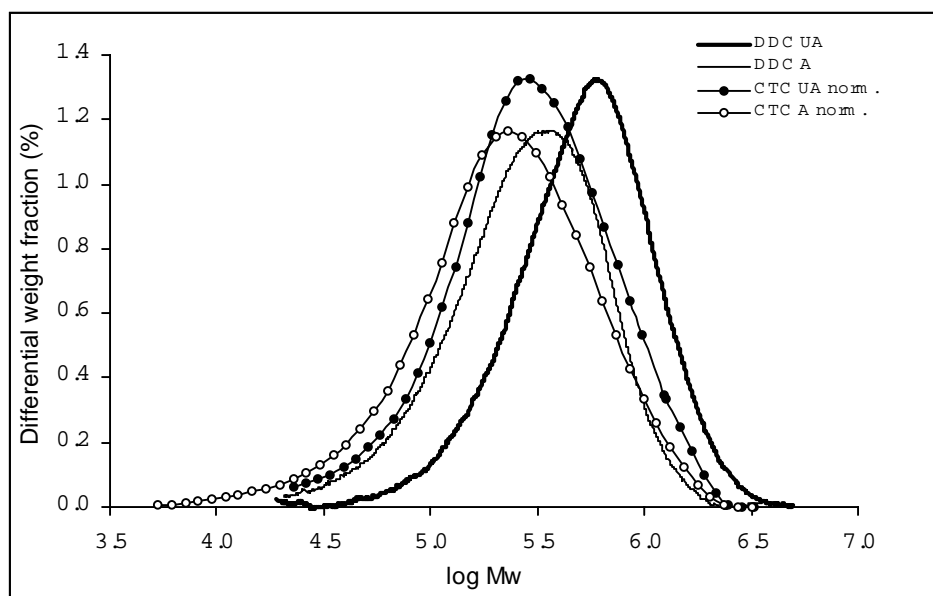


Figure 5.4-9. Overlaid differential molar mass graphs of aged and unaged DDC and CTC (CTC are normalised to DDC using same factors as in Figure 5.4-7).

Table 5.4-2. M_r averages, corresponding DP and PD obtained for CTC, DDC and V of aged cellulose (At₉₄).

	M_n ($\times 10^{-5}$ g mol ⁻¹)	DP_n	M_w ($\times 10^{-5}$ g mol ⁻¹)	DP_w	M_z ($\times 10^{-5}$ g mol ⁻¹)	DP_z	M_p ($\times 10^{-5}$ g mol ⁻¹)	M_v ($\times 10^{-5}$ g mol ⁻¹)	DP_v	PD
SEC _{CTCsmo} At ₉₄ [*]	1.25	770	3.24	1997	6.07	3749	2.34	3.04	1876	2.59
SEC _{CTCraw} At ₉₄ [*]	1.88	1158	3.24	1997	-	-	-	-	-	1.72
SEC _{DDC} At ₉₄	2.07 +/- 0.16	1275	3.81 +/- 0.13	2353	6.06 +/- 0.34	3741	3.48 +/- 0.22	3.66	2260	1.85 +/- 0.13
V At ₉₄	-	-	-	-	-	-	-	1.77 +/- 0.19	1092	-

(^{*}): The values of the M_r averages for CTC are adjusted to the molar mass of an anhydroglucose monomer, *i.e.* 162 g mol⁻¹.

Although direct comparisons between SEC_{CTC} and SEC_{DDC} are extremely difficult, comparisons within each method between aged and unaged cellulose can be drawn. Whether using DDC or DDC_{rec}, the difference in M_r averages between unaged and aged cellulose as characterised by SEC_{DDC} resulted in the same sequence $\Delta M_n\% > \Delta M_w\% > \Delta M_z\%$. This indicated a cleavage process mostly governed by acid hydrolysis but with a slight preferential attack in the low- M_r fractions (kinetics of degradation are detailed in section 6.3.2.1.2 of Chapter 6). This was consistent with the very slight increase of 8% in the PD of DDC At₉₄ versus DDC UA.

For CTC, the decrease in M_r averages between UA and At₉₄ followed the same sequence as above, with $\Delta M_n\%$ (CTC_{sm}) $>$ $\Delta M_w\%$ $>$ $\Delta M_z\%$ or $\Delta M_n\%$ (CTC_{raw}) \approx $\Delta M_w\%$ $>$ $\Delta M_z\%$, albeit in about halved proportions than for DDC (Table 5.4-3). Due to the step of precipitation in ethanol in the case of the CTC, which can lead to an underestimate of the low- M_r molecules, it is also possible to speculate that the difference $\Delta M_n\%$ between CTC aged and unaged is attenuated compared to $\Delta M_n\%$ between DDC aged and unaged, as indeed low- M_r molecules are present in higher amount in the aged cellulose.

Table 5.4-3. Percentage difference in M_r averages and in PD between aged and unaged samples.

	ΔM_n	ΔM_w	ΔM_z	ΔM_p	ΔM_v	ΔPD
CTC _{raw} UA – CTC _{raw} At ₉₄	27%	20%	16%	20%	20%	-8%
CTC _{smo} UA – CTC _{smo} At ₉₄	21%	20%	16%	20%	20%	-2%
DDC UA - DDC At ₉₄	48%	43%	40%	44%	43%	-8%
V UA- V At ₉₄					38.5%	

So far in the present comparison, no mention was made of the impact of the mechanical activation of the paper, as the defibrillation was carried out by different means in the case of the CTC and the DDC.

The hammering action of the hammer mill (Poitemill/Forplex) used to defibrillate the paper for the preparation of CTC leads to a slightly different shortening of the fibres than the cutting action of the two-blades mill used to prepare the paper for DDC.

As aged and unaged samples in each respective case were prepared in the same manner, the sample preparation could not account for the ΔM_r between aged and unaged cellulose within each method. However, regardless of the defibrillation method, a detrimental mechanical effect on the aged papers compared to the unaged papers, as these are less degraded to start with, cannot be ruled out. It has also to be noted that both millings induce a rise in temperature during the defibrillation. The Forplex hammering was shown to lead to the formation of carbonyl groups on the cellulose, especially ketons [48], but no information could be found in the literature concerning a similar effect by the cutting mill used for the preparation of the DDC.

The two SEC methods for cellulose characterisation lead to different estimates of the extent of the degradation upon aging as illustrated by the changes in M_n , M_w and M_z . As mentioned earlier, the value that can more reliably be compared between the methods is M_w . This value decreased between unaged and aged papers by 20% for CTC, and by 43% for DDC. This inevitably led to the conclusion that regardless of the method used, the estimation of the extent of the degradation is significantly different. Whether this difference was due to an increased degradation of the unaged paper during derivatisation of the CTC, or to a lower complexation degree of the solvent chloride anion with the AGU along the cellulose chain of the aged paper in the case of DDC could not be elucidated here. The literature would tend to corroborate the former with the findings that the CTC method degraded preferentially the high- M_r cellulose [29], *i.e.* that tricarbanilation would indeed be more aggressive towards unaged cellulose than towards aged cellulose.

5.4.2.2 Viscometry of At₉₄

The M_v of aged cellulose in Cadoxen was 42% lower than that of CTC, and 52% lower than that of DDC (Table 5.4-2), as calculated using $a = 0.81$ for DDC, and $a = 0.84$ for CTC (see section 5.4.1.2). As was observed for the unaged cellulose, viscometry in Cadoxen of degraded (aged) cellulose resulted in underestimated values of M_v . The decrease in M_v observed between UA and At₉₄ in Cadoxen was of 38.5%. This value was intermediate between that calculated between UA and At₉₄ for the M_v of DDC (43%) and for the M_v of CTC (20%) (Table 5.4-3). The value of DDC_{rec} At₉₄ was not used here in the comparisons for the reason cited above, namely of unknown M_r for the AGU of aged cellulose in LiCl/DMAc, which could be anywhere between the real value of 162 g mol⁻¹ and the hypothesised value of 266 g mol⁻¹.

It is noteworthy that the M_r average closer to M_v for aged paper was M_n rather than M_w . The same sequence as with UA was obtained with At₉₄, *i.e.* M_n (CTC_{smo} At₉₄) < M_v (VAt₉₄) < M_n (DDC At₉₄); M_v for V At₉₄ was 29% higher than CTC_{smo} At₉₄ (but only 6% lower than M_n of CTC_{raw} At₉₄), and 14.5% lower than M_n of DDC At₉₄.

Compared to SEC, viscometry in Cadoxen underestimated the values of M_r . Moreover; the comparison between aged and unaged papers did not yield the same degradation rate as either of the two SEC methods. Although Cadoxen is reported to be relatively stable and not significantly aggressive for cellulose [18], this is contrary to the present results, as even with the reduction pre-treatment in NaBH_4 that was introduced in order to limit solvent-induced degradation, it was shown that Cadoxen was quite aggressive for cellulose.

5.4.3 Simplicity and cost effectiveness of the methods

From the point of view of time and cost effectiveness, the time required from activation to dissolution for the CTC method was slightly lower (88 hours) than for DDC (96 hours). Both methods were found equally work-intensive and cost effective, and the solvents are both rather toxic. The sample preparation for the viscometry method in Cadoxen was faster than for both SEC methods, the dissolution taking place in 16 hours. However, the viscosity measurements themselves turned out far more time-consuming and labour-intensive than the SEC methods. A day of analysis with SEC_{CTC} or SEC_{DDC} allows about 10 to 12 samples to be run, while only about half as many can reasonably be analysed using the viscometry method. Additionally, it must be noted that pure cellulose paper is an ideal case for dissolution, and that for high lignin content papers a delignification process prior to dissolution in Cadoxen is necessary, which considerably lengthens the procedure when analysing such papers. On the other hand, delignification is necessary prior to both SEC methods too. In the case of DDC, the complete dissolution of ligneous papers in LiCl/DMAc could not be achieved even after partial delignification [49].

5.5 Conclusion

The present study showed the complexity of comparing methods involving a number of different parameters that cannot fully be cross-evaluated at the same level. According to our results, and considering the discrepancies in the M_r averages that were obtained, it was unclear whether the derivatisation method of cellulose to tricarbonylates led to a significant degradation of the polymer, or the method of dissolution in LiCl/DMAc led to an overestimation of the M_r . Both those phenomena could to a certain extent be involved in order to account for the 40% difference found in the M_w of unaged cellulose between the two SEC methods. This study shows also that despite the widespread use of LiCl/DMAc as a solvent for cellulose, and the numerous studies and reviews that have focus on the solvation mechanism over the past twenty years, the molecular structure of the complex formed between cellulose and LiCl/DMAc solvent is not totally understood, and more research is needed.

From the present results it appeared that the M_r averages obtained with both SEC methods were more consistent for aged cellulose than for the unaged cellulose. This would support the hypothesis that if any degradation occurred, the tricarbonylation method was more aggressive towards unaged cellulose than towards aged cellulose, *i.e.* that, in agreement with the literature [29], the CTC method degraded preferentially high- M_r rather than the low- M_r cellulose.

Viscometry in Cadoxen was found to be the method that most underestimated the M_r of aged as well as unaged cellulose. This was attributed to solvent-induced degradation. This method was therefore not considered the most appropriate method for M_r determination. Additionally, the relative difference in M_v between unaged and aged paper could not be correlated to the decrease in the M_r averages between unaged and aged as observed by SEC_{CTC} and SEC_{DDC}. Viscometry was therefore also found inappropriate to estimate relative M_r changes, as those occurring for instance between a sample after a certain treatment and its untreated counterpart (here: between aged and unaged samples). As such comparisons are frequent in conservation research when following the course of action of accelerated aging or other treatments on various materials, it is advised to carefully choose the analytical technique in order not to misinterpret the results.

Chemicals and materials

Whatman No.1 filter paper was obtained from Fisher Scientific (Springfield, NJ, USA). Sodium borohydride (NaBH_4) was obtained from Sigma-Aldrich Corp (St. Louis, MO, USA). Lithium chloride (LiCl), methanol and *N,N*-Dimethylacetamide (DMAc) were purchased from Acros Organics (Springfield, NJ, USA). Phenylisocyanate (PIC) and dimethylsulfoxide (DMSO) were from Fluka (Saint-Quentin Fallavier, France).

Instruments

The climate chamber Versatenn was from Tenney Environmental (Parsippany, NJ, USA).

The UV detector 2000 was from Spectra Physics (Darmstadt, Germany) and the low angle light scattering (LALS) detector KMX-6 was from Chromatix (Neckargemünd, Germany).

Multangle light scattering detector Dawn EOS and interferometric differential refractometre Optilab DSP were from Wyatt Technologies Corp. (Santa Barbara, CA, USA).

Additional instrumentation related to the viscometry measurements and to the separation and analysis of CTC and DDC, not cited in the present chapter are reported in the sections Instruments of Appendix 5-1, Appendix 5-2 and Chapter 4 respectively.

References

1. Santuci, L. and Plossi Zappalà, M. *Restaurator, Int. J. for the Preservation of Library and Archival Material*, 22 (2001) 51-65.
2. Jerosch, H. *Evaluation de l'état de dégradation de la cellulose/holocellulose dans différents types de papiers par chromatographie d'exclusion stérique*, Thèse de Doctorat, Université Versailles-St. Quentin-En-Yvelines (2002).
3. Johnson, D.C. *Cellulose Chemistry and its Applications*, CH.7, Wiley, New York (1985).
4. Strlič, M.; Kolar, J.; Žigon, M. and Pihlar, B. *J. Chromatogr. A*, 805 (1998) 93-99.
5. Grubisic, Z.; Rempp, P. and Benoit, H. *J. Polym. Sci. Polym. Letters*, 5 (1967) 753-759.
6. Timpa, J.D. and Ramey Jr, H.H. *Text. Res. J.*, 59, 11 (1989) 661-664.
7. Timpa, J.D. *J. Agric. Food Chem.*, 39 (1991) 270-275.
8. Striegel, A.M. and Timpa, J.D. *Carbohydr. Res.*, 267 (1995) 271-290.
9. Sjöholm, E; Gustafsson, K.; Eriksson, B.; Brown, W. and Colmsjö, A. *Carbohydr. Polym.*, 41 (2000) 153-161.
10. Debzi, El M. *Celluloses issues du traitement à la vapeur: évolution des masses moléculaires moyennes, transformations morphologiques et cristallines*, Thèse de Doctorat, Université Joseph Fournier-Grenoble I (1992).
11. Lawther, J.M.; Rivera, Z.S.; Jumer, K. and White, C.A. *Cellulose Sources and Exploitation*, Ellis Horwood Ed. (1990) 41-47.
12. ASTM Standard D539-51 (1955).
13. ISO Standard 5351-1: 1981, *ISO Standards Handbook: Paper, board and Pulps*, Ed. 2, (1998).
14. TAPPI Standard T 230 om-89, *TAPPI test methods*, Technical Association of the Pulp and paper Industry, TAPPI press, Atlanta, US (1994).
15. AFNOR NF T12-005, Association Française de Normalisation (1981).
16. SCAN-CM 15:88, Scandinavian Pulp, Paper and Board Testing Committee, Stockholm, Sweden (1988).
17. ISO Standard 5351-2: 1981, *ISO Standards Handbook: Paper, board and Pulps*, Ed. 2, (1998).
18. Blair, H.S. and Chromie, R. *J. Appl. Polym. Sci.*, 16 (1972) 3063-3071.
19. Browning, B.L. *Methods of Wood Chemistry, II*, Interscience, New York (1967) 530-545.
20. Brown, W. *Svensk Papperstidning årg.*, 70, 15 (1967) 458-461.
21. Segal, L. and Timpa, J.D. *Svensk Papperstidning årg.*, 72, 20 (1969) 656-661.
22. Kaminska, E. *Mat. Res. Soc. Symp. Proc.*, 462 (1997) 45-51.
23. Lauriol, J-M. *Contribution à l'étude de Celluloses Dégradées par la Détermination de leurs Distributions de Masses Moléculaires*, Thèse de Docteur-Ingénieur, Institut National Polytechnique de Grenoble (1983).
24. Whitmore, P.M. and Bogaard, J. *Restaurator*, 15 (1994) 26-45.
25. Zou, X., Gurnagul, N., Uesaka, T. and Bouchard, J., *Polym. Deg. and Stab.*, 43 (1994) 393-402.
26. Zou, X.; Uesaka, T. and Gurnagul, N. *Cellulose* 3 (1996) 243-267.
27. Kennedy, J.F.; Rivera, Z.S.; White, C.A.; Lloyd, L.L. and Warner, F.P. *Cellulose Chem. Technol.*, 24, 3 (1990) 319-325.
28. Lauriol, J-M.; Froment, P.; Pla, F. and Robert, A. *Holzforschung*, 41, 2 (1987) 109-113.
29. Evans, R.; Wearne, R.H. and Wallis, A.F.A. *J. Appl. Polym. Sci.*, 37 (1989) 3291-3303.
30. Daňhelka, J. and Kössler, I. *J Polym. Sci.*, 14 (1976) 287-298.
31. Schroeder, L.R. and Haigh, F.C. *Tappi J.*, 62, 10 (1979) 103-105.

32. Lapierre, L. and Bouchard, J. 9th *Int. Symp. on Wood and Pulping Chem. Proc.*, Montreal, Canada (1997) 1-6.
33. Hill, D.J.T.; Le, T.T.; Darveniza, M. and Saha, T. *Polym. Degrad. Stab.*, 48 (1995) 79-87.
34. Terbojevich, M.; Cosani, A.; Conio, G.; Ciferri, A. and Bianchi, E. *Macromolecules*, 18 (1985) 640-646.
35. Röder, T.; Morgenstern, B.; Schelosky, N. and Glatter, O. *Polymer*, 42 (2001) 6765-6773.
36. McCormick, C.L.; Callais, P.A. and Hutchinson Jr, B.H. *Macromolecules*, 18 (1985) 2394-2401.
37. Elmsley, A.M.; Ali, M. and Heywood, R.J. *Polymer*, 41 (2000) 8513-8521.
38. Striegel, A. *Carbohydr. Polym.*, 34 (1997) 267-274.
39. Striegel, A.M. and Timpa, J.D. *Proc. Int. GPC Symp.*, Lake Buena Vista, Florida, Waters Corp., Milford (1995) 567-591.
40. Striegel, A.M. and Timpa, J.D. *Strategies in Size Exclusion Chromatography*, ACS Symposium Series 635, American Chemical Society, Washington, DC (1996) 366-378.
41. Striegel, A.M. and Timpa, J.D. *Carbohydr. Res.*, 267 (1995) 271-290.
42. Sjöholm, E; Gustafsson, K.; Berthold, F. and Colmsjö, A. *Carbohydr. Polym.*, 41 (2000) 1-7.
43. Silva, A.A. and Laver M.L. *Tappi J.*, 80, 6 (1997) 173-180.
44. Strlič, M.; Kolenc, J.; Kolar, J. and Pihlar, B. *J. Chromatogr. A*, 964 (2002) 47-54.
45. Schult, T.; Moe, S.T.; Hjerde, T. and Christensen, B.E. *J. Liq. Chrom. & Rel. Technol.*, 23, 15 (2000) 2277-2288.
46. Bikova, T. and Treimanis, A. *Carbohydr. Polym.*, 48 (2002) 23-28.
47. Cael, J.J.; Cietek, D.J. and Kolpak, F.J. *J. Appl. Polym. Sci.*, 37 (1983) 509-529.
48. De la Chapelle, V. *Etude du jaunissement à la chaleur des pâtes papetières chimiques blanchies par des séquences sans chlore*, Thèse de Doctorat, Université de Grenoble, Ch. 5 (1999) 177-182.
49. Harrison, G. *personal communication*.

Chapter 6. The aging of paper and the influence of gelatine on the degradation process, a study using SEC/MALS, pH and colour measurements

Abstract

The analysis method of cellulose dissolved in lithium chloride/N,N-dimethylacetamide (LiCl/DMAc) by size-exclusion chromatography (SEC) using multiangle light scattering (MALS) and differential refractive index (DRI) detection is applied to the study of the cellulose of model papers and naturally aged papers. Firstly, the degradation of pure cellulose papers upon heat and humidity aging is characterised. Hydrolytic scissions seem to occur more or less randomly on the cellulose chains. The role of the gelatine sizing in the aging-induced degradation of the papers is evaluated, whether these are laboratory sized, commercially sized or historic samples. Although not always in a significant manner, the presence of gelatine in the paper is shown to be beneficial to the papers, as evidenced by the lower rate of aging-induced depolymerisation of the cellulose, especially in the case of the high molar mass molecules. However upon aging, the gelatine induced some discolouration of the papers as well as a decrease in their pH, which varied with the type of gelatine, its purity and its concentration in the papers. It was found that the purest grade gelatine, i.e. the photographic gelatine type B made from cattle bones, induced less yellowing and less acidification of the paper than the food/pharmaceutical grade gelatine type A made from fish, and of lowest quality.

6.1 Introduction

Washing paper documents is a common conservation practice but can result in the dissolution of the size in the water, especially in warm water. A survey conducted in 1982 among American paper and book conservators on issues like sizing and resizing following aqueous treatments showed that resizing practices were quite varied and evidenced the little consensus there was about the function and benefit of such procedures. The outcome was an enormous interest in the subject and a need for research on the implications of washing and resizing [1]. However, twenty years later, very few studies have been dedicated to the size in paper and thus far the contribution of sizing to the durability of paper has been largely ignored. In particular the role of a traditional sizing agent like gelatine in the longevity of historical papers is unknown.

The aim of this study was to investigate the role of gelatine sizing in the aging behaviour of paper. Cellulose was characterised in order to investigate possible correlations between the changes in molar mass (M_r) induced by the aging process and by the presence of gelatine in the paper as M_r is reported as a good indicator of polymer integrity.

The paper was dissolved in lithium chloride/*N,N*-dimethylacetamide (LiCl/DMAc), and was analysed by size-exclusion chromatography (SEC) with on-line multi-angle light scattering (MALS) and differential refractive index (DRI) detection. SEC is an extremely sensitive technique for the detection of early changes and hence, is widely used to characterise polymers and follow their degradation. SEC chromatograms provide information on the molar mass distribution (MMD) of a polymer, a clear advantage over viscometry, a method widely used in paper research that yields only the viscosity-average molar mass (M_v). With MALS, absolute values of M_r averages (M_n , M_w , M_z) are determined without the need for calibration with polymer standards. Polydispersity, size distribution and additional parameters such as the root mean square (rms) radius, which informs on the conformation of the polymer in solution, are also computed during online MALS experiments (see Chapter 4). As chemical structure relates to physical properties, these parameters correlate with all key physical characteristics of polymers such as tensile strength, elongation, flexibility, and brittleness.

Other physical and chemical properties of the papers such as the trichromatic values CIE $L^*a^*b^*$ [2] and cold extraction pH [3] were measured in order to investigate possible correlations with the M_r of cellulose, as these characteristics are easily measured, and are often available to non-specialised laboratories and conservation workshops in museums, archives and libraries.

6.2 Description of the papers studied

6.2.1 Model papers

6.2.1.1 Preparation of the samples

The model papers selected for this study were gelatine sized modern papers. These included Whatman No.1 filter paper, which contains nothing else than pure cellulose, that were sized manually in the laboratory, and Arches paper (Canson) cold pressed, which is 100% cotton.

Arches paper does not contain any optical brighteners and is sized to saturation by the manufacturer after the sheet formation (surface sizing) with a type B gelatine¹. A microscopic fibre analysis confirmed the composition of Arches to be pure cotton rag paper. Arches papers are henceforth abbreviated as “Ar”.

¹ Information provided by Canson (now Arjo-Wiggins).

The other model paper chosen, Whatman No.1, was sized with two types of gelatine. One was a photographic grade type B gelatine (Gelita Type 8039, Lot 1, Kind and Knox, Inc.) produced from alkali treated cattle bones - later referred as 'K' - and the second, a pharmaceutical/food grade type A gelatine (High Molecular Weight Gelatin batch No. 7345, Norland products, Inc.) produced from acid treated fish skin – which shall be called 'N'. The technical data sheets of the gelatines provided by the suppliers can be found in Appendix 6-1.

Type B gelatine is closer in composition to the gelatine used historically. Recipes from the eighteenth century refer to the use of leather, hides, ears, tripes, feet, parchment clippings, and other little bits from four-footed animals available from tanners or butchers, except pig [4]. Dutch paper of the same period, reported to be the best quality paper in Europe, was sized with sturgeon gelatine [5]. Because fish gelatine has a lower amount of proline and hydroxyproline amino acids, its gel point is lower (10°C) than that of mammals (40°C). At room temperature fish gelatine forms solutions while mammal's gelatine forms gels and needs to be heated for sizing purposes.

The sizing was carried out by immersing paper sheets (150 mm x 190 mm) one by one in aqueous solutions of gelatine, kept at 40°C in a temperature-controlled water bath. The water used throughout the experiment was milli-Q 18.2 MΩ cm (RiOs ElIX, Millipore). After sizing, the papers were air-dried at ambient conditions by hanging. Tub-sizing and individual sheet drying were chosen as they were current practices in 18th century paper mills as described by Diderot [4] and De Lalande [5]. Figure 6.2-1 shows the sizing thermostated bath and the drying of the papers in the scientific research laboratory at the National Gallery of Art (Washington, DC).

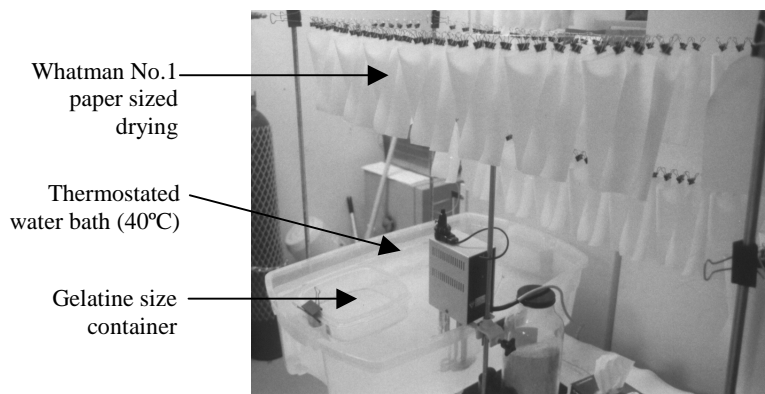


Figure 6.2-1. Sizing and drying process of model papers.

For the purpose of the present study, the varying amounts of gelatine that were absorbed in the model papers needed to be controlled and known while closely reflecting historic and modern sizing practices. However, one of the problems of early recipes is the lack of information sources and the very little data available concerning gelatine content of early European papers. The study by Barrett and Mosier [6] of over 40 historic papers dating from 15th to 18th centuries reports gelatine contents ranging from 0.013% to 7.6% (wt/wt).

Schaeffer [7] reports that Whatman commercial artist's paper made in 1956 has a gelatine content of 6.1%.

The dry weight uptakes of gelatine in the model papers, of 0.5%, 2% and 8% (dry gelatine weight / dry paper weight) were therefore chosen as they were representative of light, mid and heavy sizing as indicated in the above mentioned studies [6,7] as well as in historic 17th-18th century recipes, and early industrial 20th century gelatine sizing procedures [4,5,8,9,10,11,12]. The required concentrations of the aqueous size solutions were 2.3, 8.3 and 32.3 g L⁻¹ of K, and 2.1, 8.9 and 36.1 g L⁻¹ of N. The gelatine used to prepare these solutions was equilibrated according to TAPPI standard T 412 om-94 at 50% relative humidity (rH) and 23°C [13]. The samples were called K0.5, K2, K8 and N0.5, N2, N8 respectively. The experiments and calculations that allowed to establish the relationship between gelatine solution concentration and actual gelatine uptake in the paper are reported in Appendix 6-2.

6.2.1.2 Artificial aging

Sized model papers and unsized control papers (C) were artificially aged at 80°C and 50% rH for thirty-five and ninety-four days (t_{35} , t_{94}) by hanging the sheets individually in a climate chamber SE-600-3 (Thermotron Industries). The aging conditions were chosen in order to remain below the glass transition temperature of gelatine, T_g [14,15]. At T_g , gelatine undergoes physical and chemical changes inducing a denaturation of the protein, which needed to be avoided in order to prevent reactions from occurring during accelerated aging that do not take place under natural aging conditions. T_g strongly depends on the moisture content (MC). According to McCormick-Goodhart [14], at 80°C and 50% rH, the MC of gelatine is about 11% and at such conditions, T_g is not reached. In the present experiment, MC was found of 12.1% for both K and N gelatines at 23°C, 50% rH (see Appendix 6-2). This means that at 80°C and 50% rH, MC was well below 12% and confirms that the aging conditions chosen for the present study were not denaturing conditions for the protein.

Because of the significant number of samples produced for the present study, two different climate chambers were needed to artificially age them simultaneously (including the samples containing alum described and studied in Chapter 7). Therefore a second set of control samples (unsized) was aged in the same manner under the same conditions in a Versatenn heat/humidity chamber (Tenney Engineering, Inc). In each category, a set of papers was kept in the dark at 23°C, 50% rH [13] as the unaged reference.

6.2.2 Naturally aged papers

In order to evaluate the applicability of the SEC/MALS method to historic documents, different naturally aged papers were analysed. Historic papers from the seventeenth and

eighteenth centuries and early twentieth century papers from Strathmore Paper C^{ie} (West Springfield, Mass., USA) were chosen to represent naturally aged papers. The 17th–18th century papers were rag papers of apparent varying quality, composition, and conservation condition. They are referred as NAT1, NAT2, NAT3 and NAT4¹.

Strathmore papers, which are chemical wood pulp papers, were chosen for the following reasons: their fabrication date was known (1932), and they were precisely referenced in composition and fabrication batch. They represented a unique pool of naturally aged papers (70 years) that had been kept together and therefore, were homogeneous with respect to their conservation history. The Strathmore papers are hereafter abbreviated S140, S160, S220 and S320 (the numbers correspond to the grammage: 140 to 320 g m⁻²). Each group was composed of two types of papers with identical fabrication batch number, one labelled “Aqua-set (unsized)” (referred as S140U to S320U), and one sized with photographic gelatine (unknown origin), labelled “Photo-Gelatin (Sized)” (referred as S140S to S320S)². These naturally aged papers were not subjected to artificial aging.

6.3 Degradation of cellulose characterised by SEC/MALS

6.3.1 Experimental: sample preparation and SEC procedure in LiCl/DMAc

The samples for SEC/MALS were prepared by defibrillating the paper in a two-blade cutting mill as described in section 3.2.1.2 of Chapter 3.

The preparation of the solvent, mobile phase, and sample, as well as the methods for cellulose activation and dissolution in LiCl/DMAc are reported in section 3.2.4 of Chapter 3. The instrumentation, the SEC/MALS set-up, and the method in LiCl/DMAc are reported in section 4.2.3 of Chapter 4.

Each sample type was dissolved once or twice and each cellulose solution was analysed at least in duplicate runs. Only the average values are reported here. For aged and unaged control papers two to three sets of dissolutions were carried out, and each dissolved sample was analysed in duplicate or triplicate runs. The relative standard deviation (RSD) on number-average, weight-average and z-average molar mass (M_n , M_w and M_z) of the reference papers, are reported in Table 6.3-1. The RSD% on the mass of cellulose injected as calculated by the ASTRA software (Wyatt Technologies) for all the control papers was 4.2%. This RSD refers to the statistical fluctuations in the MALS and RI detectors, *i.e.* to consistency in the data, and not to possible systematic errors due to sample preparation and separation method. The latter are the subject of a separate study in Chapter 5. Only four of the Strathmore papers were analysed by SEC/MALS, and these are: S160U, S160S, S320U and S320S.

¹ Naturally aged 17th–18th c. papers provided by the museum Boijmans Van Beuningen, Rotterdam, The Netherlands.

² Strathmore papers are part of the twentieth century paper collection of the National Gallery of Art, Washington, DC.

6.3.2 Results and discussion

6.3.2.1 SEC/MALS applied to the study of model papers

6.3.2.1.1 The aging of pure cellulose paper

Table 6.3-1 reports the average M_r obtained for Ct₀ - Whatman No.1 unsized control (C) at time zero (t_0). M_n was $3.96 \times 10^5 \text{ g mol}^{-1}$, M_w was $6.68 \times 10^5 \text{ g mol}^{-1}$, and M_z was $10.09 \times 10^5 \text{ g mol}^{-1}$. The peak molar mass (M_p) was $6.24 \times 10^5 \text{ g mol}^{-1}$ and the polydispersity PD ($PD = M_w/M_n$) was 1.70, which indicated a polydisperse sample where about half the molecules are distributed fairly close around M_p , and a smaller proportion of molecules have very low or very high molar mass. This low polydispersity is typical of pure cellulose. For wood cellulose the molar mass distribution (MMD) is usually broader, mainly due to the presence of lignins and hemicelluloses, and PD of 7 and higher is not uncommon [16].

The control papers aged in the two climate chambers showed no difference in M_r (Table 6.3-2). Therefore for the rest of the study, the data obtained for the aged control samples (C) was averaged regardless of the aging chamber used.

After artificial aging, M_w for Ct₃₅ and Ct₉₄ was $5.55 \times 10^5 \text{ g mol}^{-1}$ and $3.87 \times 10^5 \text{ g mol}^{-1}$ respectively. The decrease as compared with Ct₀ was 17% for Ct₃₅ and 42% for Ct₉₄. M_p decreased by 15% and 45% for Ct₃₅ and Ct₉₄, to $5.28 \times 10^5 \text{ g mol}^{-1}$ and $3.45 \times 10^5 \text{ g mol}^{-1}$. Table 6.3-3 reports these percent differences in the M_r averages before and after aging.

Between t_0 and t_{35} the decrease in all the M_r averages M_n , M_w and M_z of C was identical (Table 6.3-3). This indicated that cleavage of the polymer chains during the first 35 days of aging occurred randomly and equally in the low- M_r and in the high- M_r molecules. Between t_0 and t_{94} the decrease in M_r averages for C followed the sequence $\Delta M_n\% > \Delta M_p\% > \Delta M_w\% > \Delta M_z\%$. This indicated enhanced production of low- M_r molecules from t_{35} to t_{94} . Upon prolonged aging low- M_r fractions outnumbered high- M_r fractions. It has to be noted that the mass of the degradation products formed during aging such as small organic acids, and other small molecules have a negligible effect on the mass of the bulk cellulose. These molecules are too small to be visible on the MALS signal, and they were excluded from the selected integration limits on the DRI signal. Hence the value of M_n , which is the molar mass average that better represents low- M_r molecules, was not affected by these degradation products and reflected exclusively the polymer itself.

The decrease in M_n , M_w and M_z is illustrated in Figure 6.3-1 and in the shift towards low- M_r which is visible in the overlaid differential molar mass graphs of Ct₀, Ct₃₅ and Ct₉₄ in Figure 6.3-2. Differential molar mass graphs (or MMD graphs) indicate how much material (differential weight fraction) is contained in any molar mass interval. The polydispersity increased by 8% between Ct₀ and Ct₉₄ but this is insignificant considering the RSD% on these PD values.

The shape of the peaks in the MMD profiles for Ct₀, Ct₃₅ and Ct₉₄ are almost Gaussian (Figure 6.3-2). This is quite remarkable since Gaussian peaks are not a usual feature in SEC. The sharpness of the apex of the peaks eroded from Ct₀ to Ct₉₄ indicating that the fraction of mid-size molecules in the MMD decreased with aging.

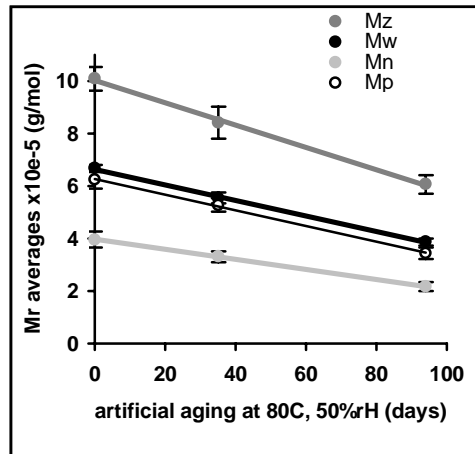


Figure 6.3-1. Change in M_r averages of Ct₀, Ct₃₅ and Ct₉₄ with aging time.

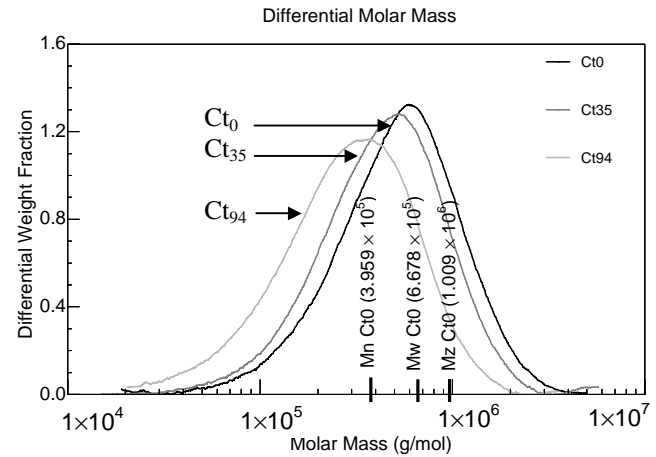


Figure 6.3-2. Overlaid differential molar mass graphs of Ct₀, Ct₃₅ and Ct₉₄.

Table 6.3-1. M_r averages and polydispersity indices of the model papers aged and unaged: control (C) and sized samples (K2, K8, N2, N8 and Ar).

	AVG $M_n \times 10^{-5}$ g mol ⁻¹	RSD % M_n	AVG $M_w \times 10^{-5}$ g mol ⁻¹	RSD % M_w	AVG $M_z \times 10^{-5}$ g mol ⁻¹	RSD % M_z	AVG $M_p \times 10^{-5}$ g mol ⁻¹	RSD % M_p	AVG PD (M_w/M_n)	RSD % PD	AVG M_z/M_w	RSD % M_z/M_w
Ct ₀	3.96	7.8	6.68	2.0	10.09	4.5	6.24	5.5	1.70	7.1	1.51	4
Ct ₃₅	3.33	6.2	5.55	3.5	8.42	7.2	5.28	5.0	1.68	4.5	1.52	6.0
Ct ₉₄	2.17	8.1	3.87	3.7	6.06	5.9	3.45	6.2	1.79	7.0	1.57	4.2
K2t ₀	4.04	6.9	6.86	3.3	10.53	0.9	6.08	9.7	1.70	3.7	1.54	2.5
K2t ₃₅	3.19	2.4	5.80	2.0	9.50	7.7	5.33	3.3	1.82	1.3	1.64	5.8
K2t ₉₄	2.16	10.4	3.97	3.8	6.36	4.2	3.47	5.2	1.85	6.3	1.60	5.4
K8t ₀	-	-	-	-	-	-	-	-	-	-	-	-
K8t ₃₅	3.94	8.8	6.29	2.4	9.08	1.4	6.17	4.7	1.60	7.0	1.44	3.8
K8t ₉₄	2.70	N/A ¹	4.64	N/A	7.02	N/A	4.26	N/A	1.73	N/A	1.52	N/A
N2t ₀	-	-	-	-	-	-	-	-	-	-	-	-
N2t ₃₅	3.46	N/A	6.10	N/A	9.75	N/A	5.56	N/A	1.77	N/A	1.60	N/A
N2t ₉₄	2.04	N/A	3.99	N/A	6.50	N/A	3.41	N/A	1.96	N/A	1.63	N/A
N8t ₀	-	-	-	-	-	-	-	-	-	-	-	-
N8t ₃₅	3.30	10.8	6.63	3.4	10.63	4.2	6.39	7.3	1.95	8.2	1.61	5.5
N8t ₉₄	2.26	N/A	5.18	N/A	9.33	N/A	4.39	N/A	2.30	N/A	1.80	N/A
Art ₀	2.84	3.7	5.59	2.6	9.91	5.1	4.90	2.0	1.97	6.4	1.77	2.6
Art ₃₅	2.12	N/A	4.61	N/A	8.52	N/A	3.29	N/A	2.18	N/A	1.85	N/A
Art ₉₄	1.55	5.8	3.68	7.5	7.60	18.2	2.60	0.4	2.38	10.5	2.06	12.6

¹ N/A is reported when only two analyses were done

Table 6.3-2. M_r averages of the control papers aged in the SE-600-3 and in the Versatenn climate chambers.

	AVG $M_n \times 10^{-5}$ g mol ⁻¹	RSD % M_n	AVG $M_w \times 10^{-5}$ g mol ⁻¹	RSD % M_w	AVG $M_z \times 10^{-5}$ g mol ⁻¹	RSD % M_z	AVG $M_p \times 10^{-5}$ g mol ⁻¹	RSD % M_p	AVG PD (M_w/M_n)	RSD % PD
C1t₃₅¹	3.39	7.3	5.65	3.7	8.42	2.5	5.32	4.8	1.67	4.2
C1t₉₄	2.28	4.9	3.97	3.5	6.20	5.5	3.41	6.8	1.74	3.7
C2t₃₅²	3.24	4.6	5.45	2.7	8.42	10.7	5.23	5.7	1.68	5.3
C2t₉₄	2.07	7.6	3.81	3.5	6.06	5.6	3.48	6.2	1.85	7.0

Table 6.3-3. Percent difference in M_r averages between aged and unaged, unsized (C) and sized (K2, K8, N2, N8 and Ar) samples.

Row	samples	ΔM_n %	ΔM_w %	ΔM_z %	ΔM_p %
1	Ct₀ – Ct₃₅	16.3	16.9	16.6	15.4
2	Ct₀ – Ct₉₄	45.2	42.1	39.9	44.7
3	–Ct₃₅ + K2t₃₅	-3.8	4.3	11.4	1.1
4	–Ct₉₄ + K2t₉₄	-0.5	2.6	4.6	0.8
5	–Ct₃₅ + K8t₃₅	15.8	11.8	7.3	14.5
6	–Ct₉₄ + K8t₉₄	19.7	16.6	13.7	19
7	–Ct₃₅ + N2t₃₅	4.1	9.0	13.6	5.1
8	–Ct₉₄ + N2t₉₄	-5.9	3.0	6.8	-1.1
9	–Ct₃₅ + N8t₃₅	-0.4	16.3	20.8	17.5
10	–Ct₉₄ + N8t₉₄	3.9	25.3	35.0	21.5
11	Ct₀ – K2t₃₅	19.5	13.2	5.8	14.5
12	Ct₀ – K2t₉₄	45.5	40.5	37.0	44.3
13	Ct₀ – K8t₃₅	0.5	5.8	10.0	1.1
14	Ct₀ – K8t₉₄	31.8	30.6	30.8	31.8
15	Ct₀ – N2t₃₅	12.7	8.7	3.4	10.8
16	Ct₀ – N2t₉₄	48.4	40.3	35.5	45.3
17	Ct₀ – N8t₃₅	16.6	0.7	-5.1	-2.4
18	Ct₀ – N8t₉₄	43.0	22.4	7.5	29.6
19	Art₀ – Art₃₅	25.1	17.5	14.0	33.0
20	Art₀ – Art₉₄	45.4	34.1	23.3	47.0

Figure 6.3-3 and Figure 6.3-4 are the signals of the LS (90° angle photodiode) and the DRI detectors as a function of elution volume (V_e) respectively. On both graphs a slight tailing in the low- M_r portion (large V_e) is visible. As adsorption on the columns does not occur (see section 5.4.1.1.2 in Chapter 5), this tailing is more likely due to the presence of very-low- M_r components.

¹ C1 corresponds to the control papers series aged in the chamber SE-600-3 (Thermotron)

² C2 corresponds to the control paper series aged in the Versatenn chamber (Tenney).

The signals do not show particularly steep slopes in the high- M_r fractions, which indicated that even the higher- M_r molecules were within the separation range and confirmed the suitability of the column set. The trend lines across the chromatograms represent the distribution of molar mass across V_e . The actual molar masses are represented by the dots and show dispersion from the trend lines at the extreme values of V_e , especially at the low- M_r end. This represents the limit of the detection in the low concentrations (low DRI signal) for the very-high- and very-low- M_r molecules, and reflects also the M_r limits of the separation.

From the signals, it can be concluded that no aggregation occurred in the solvent system. Aggregation would result in the formation of very high- M_r molecules, which would translate at the detectors level in a signal with a very steep slope at low V_e , especially significant in the LS signals of the higher angles photodiodes.

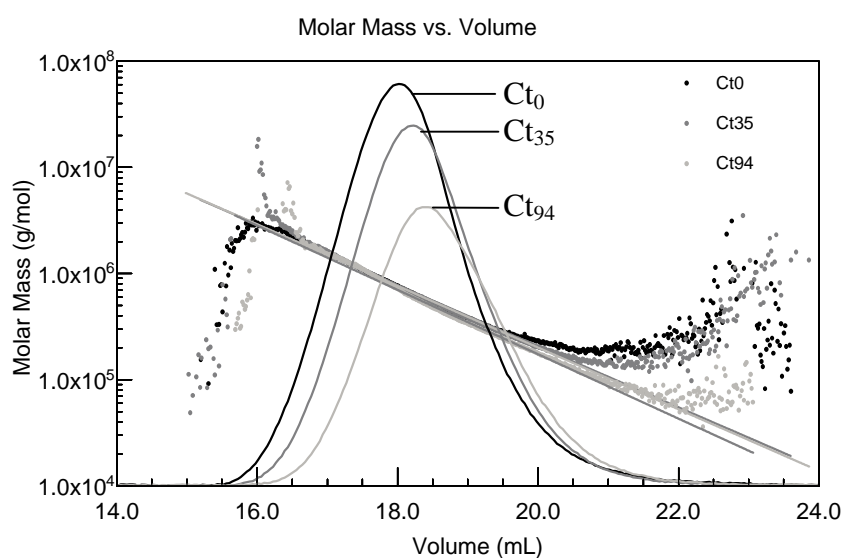


Figure 6.3-3. Overlaid 90° angle photodiode LS signals of Ct₀, Ct₃₅ and Ct₉₄.

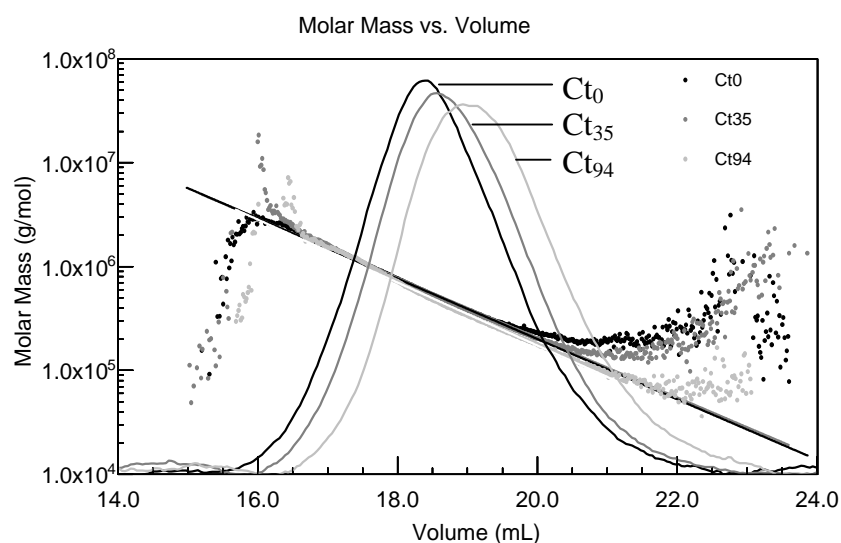


Figure 6.3-4. Overlaid DRI signals of Ct₀, Ct₃₅ and Ct₉₄.

Information on the properties of the polymer in solution is contained in the relationship between polymer dimensions and M_r that can be established by a scaling law of the type [17,18,19,20]:

$$\sqrt{\langle r_g^2 \rangle} = QM_r^q$$

The exponent q is related to the shape of the chains, *i.e.* to polymer-solvent interactions and macromolecular conformation of the polymer (section 4.2.4. of Chapter 4). The value q is given by the slope in a log-log plot of rms radius as a function of M_r , as shown in Figure 6.3-5 for the control papers aged and unaged. Table 6.3-4 reports the values of q for these model papers. For Ct₀, $q = 0.59 (\pm 5\%)$, for Ct₃₅, $q = 0.57 (\pm 5\%)$, and for Ct₉₄, $q = 0.54 (\pm 7\%)$. All these values are comprised between 0.5 and 0.6, which is characteristic of a polymer in random coil conformation in the solvent. The slight decrease in q with aging seems to indicate that when aged, cellulose in the solvent comes closer to theta conditions. This could be due to a higher solvation power of LiCl/DMAc for high- M_r than for low- M_r molecules. However, the reason lies more likely in the fact that with aging, the number of hydroxyl groups on the cellulose chains decreases due to oxidation and formation of carboxyl and carbonyl groups, inducing a lower complexation level between solvent molecules and cellulose molecules, hence slightly lower solvation capacity of LiCl/DMAc. The solvation mechanism is detailed in section 2.2.2.3.1 of Chapter 2.

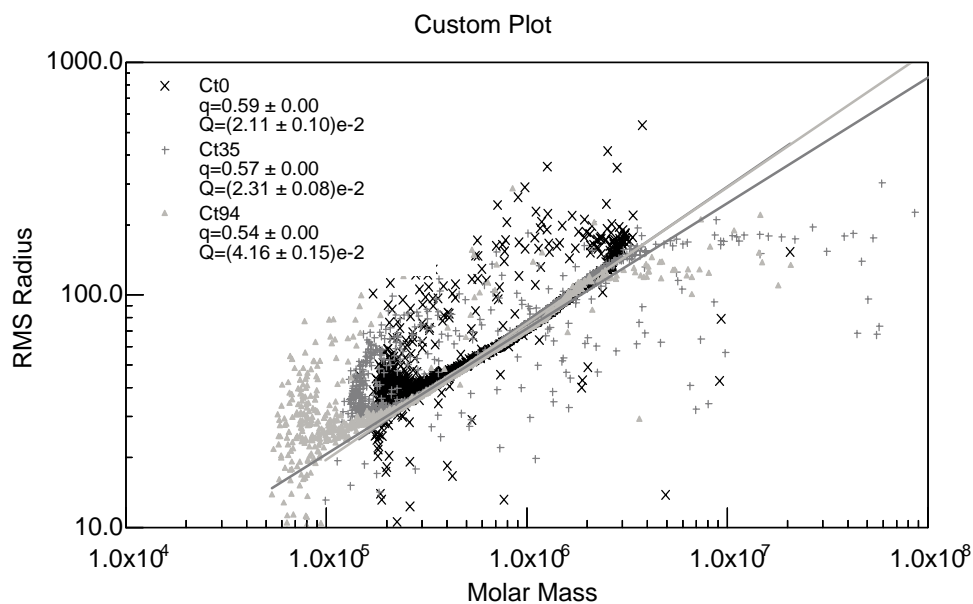


Figure 6.3-5. Overlaid average rms radii versus M_r (log-log scale) for Ct₀, Ct₃₅ and Ct₉₄.

Table 6.3-4 reports also the average values obtained for the root mean square radii (rms) average numbers r_n , r_w and r_z for aged and unaged Whatman No.1. The actual rms radius measured by the MALS, r_z , was of 80.3 nm, 71.6 nm and 56.3 nm for Ct₀, Ct₃₅ and Ct₉₄ respectively. These values correspond to a decrease in r_z of 11% between Ct₀ and Ct₃₅ and 30% between Ct₀ and Ct₉₄. A similar percent decrease in r_n and r_w of C with aging time was found. This is represented in Figure 6.3-6.

It must be noted that the decrease observed for M_r averages between Ct_0 and Ct_{35} (17%) and between Ct_0 and Ct_{94} (40%-45%) was slightly larger (Table 6.3-3). Such result was not unexpected and tended to confirm the findings on random coil conformation of cellulose in solution in LiCl/DMAc. As rms radii are a representation of the distribution of the mass within the molecule, only a fully extended conformation would yield equal changes in M_r averages and in rms radii.

Table 6.3-4. Average rms radii averages and values of q of the model papers aged and unaged: control (C) and sized samples (K2, K8, N2, N8 and Ar).

	AVG r_n (nm)	RSD % r_n	AVG r_w (nm)	RSD % r_w	AVG r_z (nm)	RSD % r_z	AVG q	RSD% q
Ct_0	45.2	5.1	62.4	1.3	80.3	2.1	0.59	4.6
Ct_{35}	40.4	2.7	55.3	2.2	71.6	6.0	0.57	5.0
Ct_{94}	30.5	4.7	43.1	1.3	56.3	2.6	0.54	7.3
$K2t_0$	45.6	1.1	63.5	0.3	82.7	1.8	0.60	2.6
$K2t_{35}$	38.7	1.7	55.5	1.8	74.9	5.8	0.57	5.4
$K2t_{94}$	30.6	4.9	43.4	2.1	57.0	4.2	0.50	5.0
$K8t_0$	-	-	-	-	-	-	-	-
$K8t_{35}$	43.5	5.9	57.9	2.8	72.8	3.5	0.55	8.6
$K8t_{94}$	35.5	N/A ¹	48.9	N/A	62.6	N/A	0.53	N/A
$N2t_0$	-	-	-	-	-	-	-	-
$N2t_{35}$	40.6	N/A	56.5	N/A	74.4	N/A	0.54	N/A
$N2t_{94}$	29.7	N/A	42.6	N/A	55.4	N/A	0.48	N/A
$N8t_0$	-	-	-	-	-	-	-	-
$N8t_{35}$	39.7	5.6	57.9	0.9	75.8	3.2	0.51	5.2
$N8t_{94}$	31.8	N/A	49.2	N/A	66.9	N/A	0.49	N/A
Art_0	36.0	3.6	55.7	2.2	80.3	3.6	0.62	6.1
Art_{35}	30.4	N/A	46.4	N/A	64.8	N/A	0.46	N/A
Art_{94}	25.1	2.6	38.6	3.7	55.3	9.6	0.44	N/A

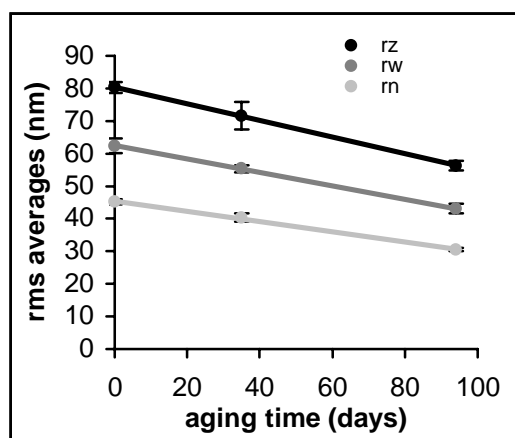


Figure 6.3-6. rms radii of Ct_0 , Ct_{35} and Ct_{94} as a function of aging time.

¹ N/A is reported when only two analyses were done

6.3.2.1.2 Kinetics of the degradation of pure cellulose paper

Degradation of cellulose from aging accelerated by the effects of heat and humidity is described in the literature as a process governed by random scissions of the polymer chains due to acid-catalysed hydrolysis [21,22,23]. Whitmore and Bogaard [24] have described acid hydrolysis as the main degradation pathway occurring during both the humid and dry-heat aging of cellulose.

The kinetic model for degradation of linear polymer molecules developed by Ekamstam in 1936 [25] based on first order kinetics (Appendix 6-3) is usually applied to explain the degradation of cellulose under a variety of different conditions. The equation of Ekamstam yields:

$$\frac{1}{M_{wt}} - \frac{1}{M_{wt0}} = k t$$

The slope k in the plot $(1/M_{wt} - 1/M_{wt0})$ as a function of time t is the rate constant of the reaction, *i.e.* the rate of glycosidic bond breakage. Although this model is unlikely to be fully applicable to the case of cellulose, it has been widely used to describe cellulose degradation. According to this model, the relationship between $(1/M_{wt} - 1/M_{wt0})$ and aging time t should be linear [26,27], and a constant k for glycosidic bond breaking can be calculated. However, deviation from linearity has been experimentally observed and characterised [28].

In the present work, the plot $(1/M_{wt} - 1/M_{wt0})$ (mol g^{-1}) versus aging time (days) (Figure 6.3-7) displayed a determination coefficient R^2 of 0.990, with a slope that was slightly steeper on the second half portion of the plot. This indicated a degradation process that was not purely random over the whole aging period. More data points would be required to ascertain this result as other variables such as for instance variables related to the SEC behaviour of cellulose related to column packing properties could play a role. However, the fact that polydispersity slightly increased after 94 days of aging tended to confirm this result (Table 6.3-1).

The average slope yielded a constant k of 1.17×10^{-8} ($\pm 11\%$) $\text{mol g}^{-1} \text{ days}^{-1}$. Multiplying k by the molar mass of an anhydroglucose unit (162 g mol^{-1}), the rate constant obtained for glycosidic bond breaking k' is 1.90×10^{-6} ($\pm 11\%$) days^{-1} . A constant calculated on each segment of the curve yields $k'_{10 \rightarrow 135} = 1.41 \times 10^{-6} \text{ days}^{-1}$ and $k'_{135 \rightarrow 194} = 2.14 \times 10^{-6} \text{ days}^{-1}$. This would indicate acceleration of the bond breaking on the second half of the aging period by about 1.5 times. However, this result must be cautiously interpreted, as the number of data points for such extrapolation is quite small.

The value of k' found was more than 10 times lower than k' for cotton linters aged at 90°C and 80 % rH as determined by Zou *et al.* [27]. This difference could be explained by the fact that the authors used a different cellulose source and more drastic aging conditions than those in the present study.

A slightly different way of processing the data can be achieved by following the kinetic model for chain scission as proposed by Hill *et al.* [29], which is derived from zero order considerations. This model (Appendix 6-3) defines the number of polymer chains per gram of sample N_C as:

$$N_C = N / M_n$$

Where N is the Avogadro number.

The slope of the plot of N_C as a function of aging time t (Figure 6.3-8) is the bond scission constant k'' . Our results yield $k'' = 1.58 \times 10^{11}$ chains $\text{g}^{-1} \text{s}^{-1}$, and a lower determination coefficient than calculated earlier, with $R^2 = 0.978$. For each segment of the plot, $k''_{t0 \rightarrow t35} = 9.77 \times 10^{10}$ chains $\text{g}^{-1} \text{s}^{-1}$ and $k''_{t35 \rightarrow t94} = 1.88 \times 10^{11}$ chains $\text{g}^{-1} \text{s}^{-1}$.

Both models tended to show that the number of chains cleaved was probably not constant over the whole aging period but increased upon prolonged aging time. Despite the limited number of data points, it has to be noted that our value of k'' was not far from the k'' of 1.5×10^{11} chains $\text{g}^{-1} \text{s}^{-1}$ determined by Hill *et al.*, which they found for Kraft pulp cellulose aged at 129°C over a period of 28 days, without oxygen and under vacuum (in order to prevent oxidation from air and hydrolysis by the water initially present).

Zou *et al.* [27] suggested the ratio DP_z/DP_w as a good guide to determine the homogeneity of the degradation process. They called this ratio the homogeneity index. They found a DP_z/DP_w ratio of 1.95 which remained constant over a seven-day period, then decreased to 1.70 by twenty days at 90°C and 80% rH for Whatman No.40 (100% cotton), while remaining at its initial value of 1.95 for cotton linters paper. From the latter result the authors concluded that for cotton, degradation proceeded homogeneously with random cleavage of the cellulose chains in the high- M_r and in the low- M_r .

Figure 6.3-9 shows both polydispersity indices M_z/M_w and M_w/M_n as a function of M_n . M_n was chosen as the abscissa in the polydispersity plots instead of aging time, as its changes were shown to closely reflect the rate of bond scission [29]. The polydispersity indices did not remain constant, but tended to drift up slightly with decreasing M_n , although not significantly. Initially around 1.51, M_z/M_w increased to 1.57 (*i.e.* +3.8%) upon prolonged aging, and M_w/M_n increased from 1.70 to 1.79 (*i.e.* +5%), which falls within the RSD% (Table 6.3-1).

We shall stress again that three data points are not enough to rely on for precise information, but short of a more comprehensive study, this result would indicate that Whatman No.1 paper displayed a rather homogeneous aging process: it seems that the cellulose chains underwent more or less random scissions. This is in contrast with the findings by Emsley *et al.* [28,30]. The authors found that polydispersity ratios of cotton linters drifted up during aging from 20% to 40% in heavily aged samples. They interpreted this by the occurrence of preferential scissions yielding small fragments, and proposed a model of a continuously changing degradation rate.

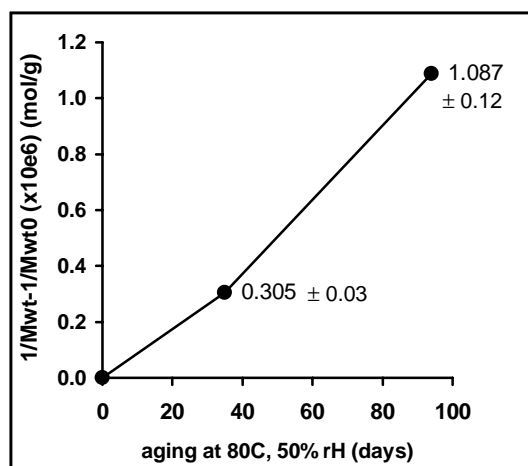


Figure 6.3-7. Plot yielding the glycosidic bond breaking constant k in $\text{mol g}^{-1} \text{days}^{-1}$.

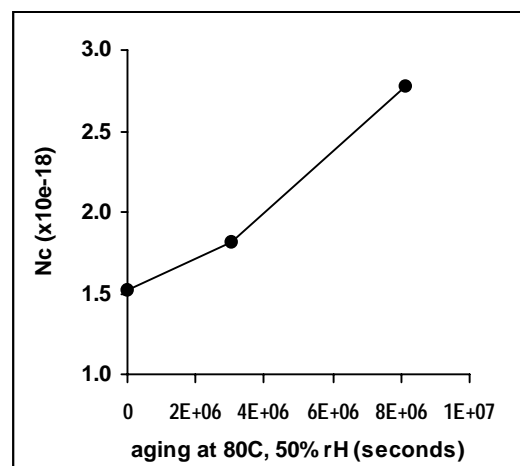


Figure 6.3-8. Plot yielding the glycosidic bond breaking constant k'' in chains $\text{g}^{-1} \text{s}^{-1}$.

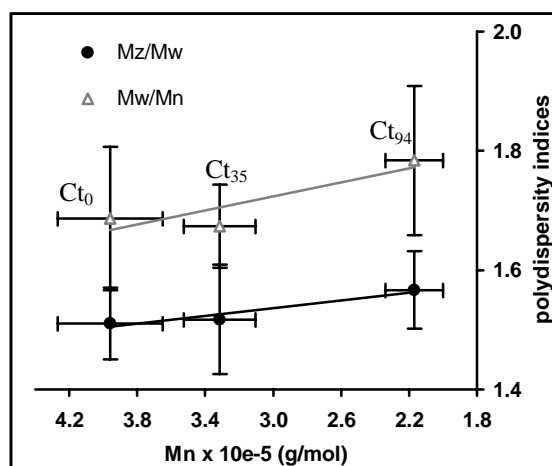


Figure 6.3-9. Change in the polydispersity indices of C as a function of M_n upon aging.

6.3.2.1.3 The aging of gelatine sized pure cellulose paper

Molar mass averages of sized and aged papers are reported in Table 6.3-1. M_n , M_w and M_z were slightly higher for K2t₀ than for Ct₀, by 2%, 2.7% and 4.2%, respectively, but these differences are negligible as they fall within the RSD%.

It was noted that gelatine precipitated out of solution above a certain concentration: little gelatine specks were visible on the sides of the dissolution vial for K8 and N8, while K2 and N2 remained clear and well dissolved. Although most of the gelatine was washed away during the swelling phase in water (activation), some protein residues could still be present. The impact that the presence of gelatine would have on the calculated M_r averages of cellulose is somewhat unpredictable but given the respective M_r average of both polymers (around 10^5 g mol^{-1} for gelatine, see Chapter 8), and the fact that any protein left would be residual (low concentration), the high- M_r fractions and the dn/dc of cellulose should not be affected.

In order to reproduce the washing process subsequent to the swelling phase during the first step of activation, a sample of K2t₀ was washed in warm water and analysed by Fourier Transform Infrared spectroscopy using an Attenuated Total Reflectance probe (Nicolet Avatar 360 FTIR) to check for a possible gelatine residue. The result was not totally conclusive probably due to the lack of sensitivity of the technique, but protein bands were not evidenced.

Figure 6.3-10, Figure 6.3-11, Figure 6.3-12, and Figure 6.3-13 show the overlaid differential molar mass graphs of papers aged and unaged sized with K and N gelatines.

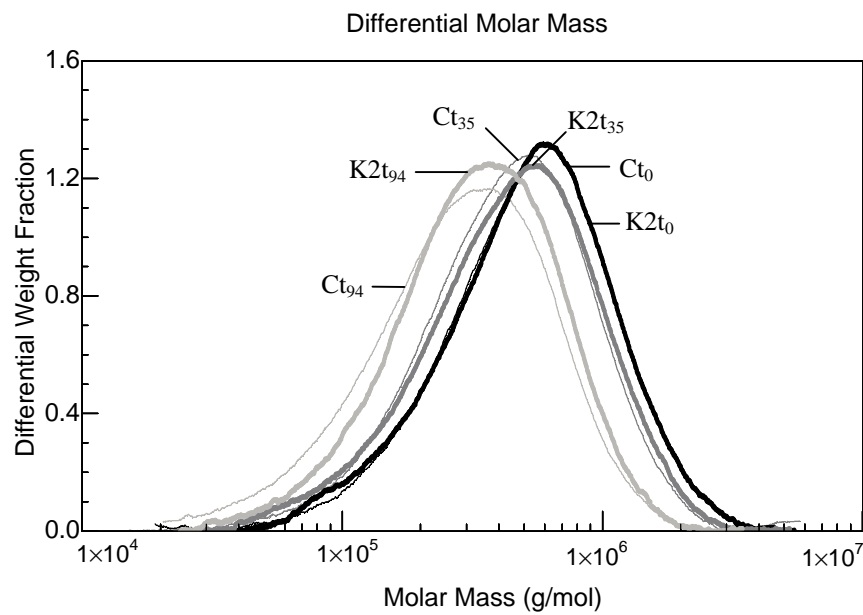


Figure 6.3-10. Overlaid differential molar mass graphs of K2 samples aged and unaged, compared to C samples aged and unaged.

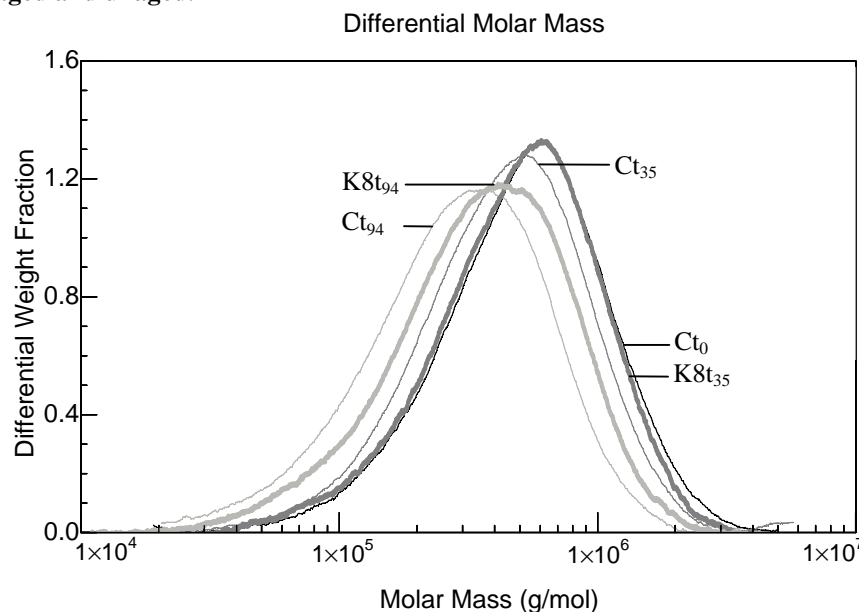


Figure 6.3-11. Overlaid differential molar mass graphs of K8 samples aged compared to C samples aged and unaged.

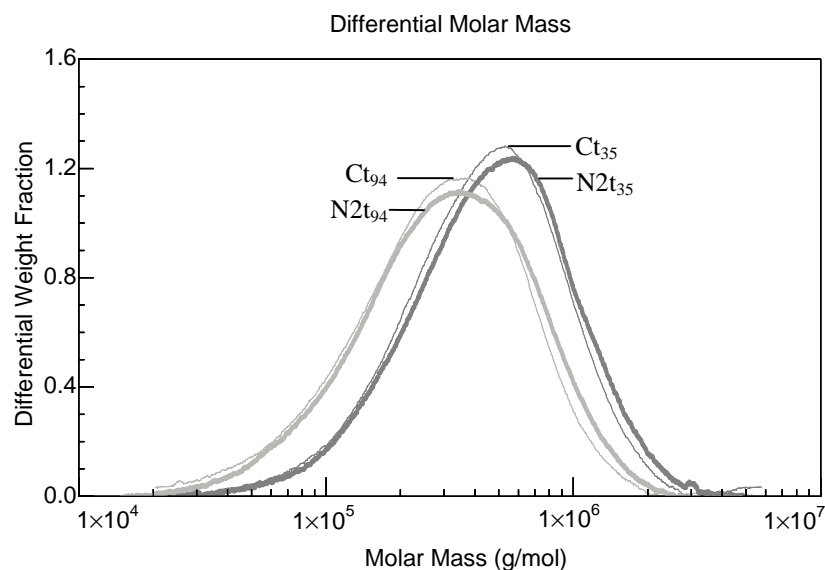


Figure 6.3-12. Overlaid differential molar mass graphs of N2 samples aged compared to C samples aged.

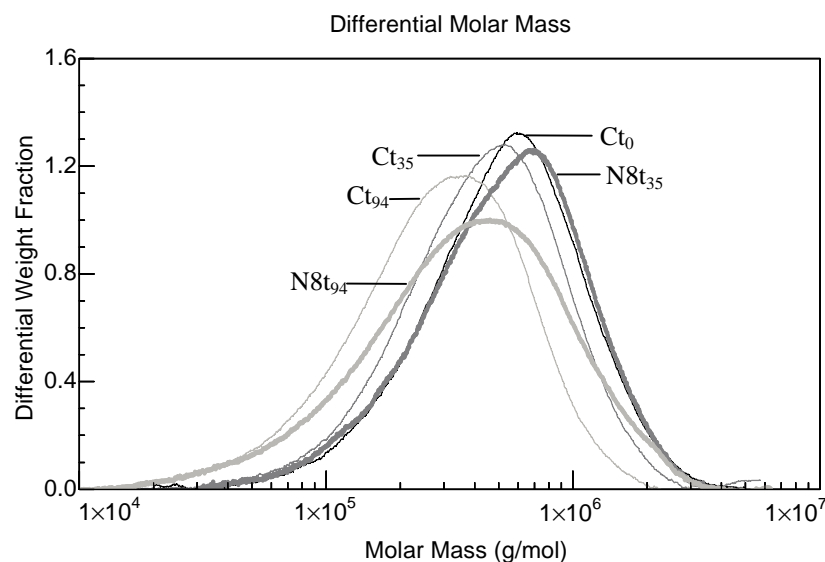


Figure 6.3-13. Overlaid differential molar mass graphs of N8 samples aged compared to C samples aged and unaged.

At first sight it was difficult to find a general trend in the M_r variations upon aging of the sized papers compared to the control papers. Overall the shape of the apex of the MMD profiles for the K, N and C papers were similar at each respective aging time. However, all the papers sized had to different extents a MMD shifted to higher- M_r compared to the unsized control papers. The papers containing 8% gelatine (K and N) seemed to have degraded less than the papers containing 2% gelatine (Table 6.3-3, Figure 6.3-14, Figure 6.3-15).

The changes upon aging in M_w indicated that in the initial stages of aging (from t_0 to t_{35}) all sized papers had a lower decay in M_w than the control papers (Figure 6.3-16) but that only for the papers containing 8% gelatine the decay remained lower in the long run (from t_{35} to t_{94}).

Polydispersity increased slightly upon aging and more markedly for N papers (PD of N8t₉₄ = 2.3) (Table 6.3-1).

For K2t₃₅ and K2t₉₄, albeit slightly higher, the M_r averages were not significantly different from those of Ct₃₅ and Ct₉₄ (Table 6.3-3, rows 3 and 4). For this reason it was decided not to analyse the samples containing 0.5% gelatine. The changes in M_r averages upon aging for K2 followed the same sequence as C, with $\Delta M_n\% > \Delta M_p\% > \Delta M_w\% > \Delta M_z\%$ (Table 6.3-3, rows 11 and 12) indicating enhanced production of low- M_r fractions.

The decrease in M_r averages for K8 upon aging was more peculiar: after 35 days, a reversed sequence was observed with a $\Delta M_z\%$ highest of all, while after 94 days, all $\Delta M_r\%$ were similar (Table 6.3-3, rows 13 and 14).

Overall, for a given aging time, the M_r averages of K8 were consistently higher than those of the control papers (Table 6.3-3, rows 5 and 6). This indicated that the impact of gelatine during aging was to reduce the rate of cleavage. However, at each given time, this difference was larger for M_n , followed by M_w and M_z . The effect was therefore not homogeneous for low- M_r and high- M_r cellulose molecules but the trend in the cleavage was opposite to that observed for the other sized samples. This unexpected effect could not be explained.

For both N2 and N8, the decrease in M_r averages upon aging was significantly lower than for the control papers (Table 6.3-3, rows 7 to 10). The difference was more pronounced in the high- M_r fractions, with a larger difference in M_z , followed by M_w and M_n (especially for N8). This indicated that the impact of the N gelatine in the paper was to decrease the cleavage rate in the highest- M_r fractions more efficiently. The changes in M_r averages upon aging for N2 and N8 followed the same sequence as for C and K2, which was $\Delta M_n\% > \Delta M_p\% > \Delta M_w\% > \Delta M_z\%$ (Table 6.3-3, rows 17 to 20), thereby also indicating enhanced production of low- M_r fractions.

The average root mean square radii averages r_n , r_w and r_z of the sized model papers are reported in Table 6.3-4 and represented in Figure 6.3-17. These values followed roughly the same trend with aging time as the average M_r .

The slope q in the log-log plot of rms radii versus M_r for sized papers is reported in Table 6.3-4. Increasing gelatine content (especially N gelatine) resulted in lower values of q (slightly below 0.5 for N2t₉₄ and N8t₉₄). These values indicated that the cellulose chains were in random coil conformation in solution but closer to theta conditions than the control paper (section 6.3.2.1.1), *i.e.* below optimal conditions. This is probably due to a slightly more compact conformation of the molecules. If any, the presence of residual gelatine could interact - although only weakly - with the cellulose coils by limiting solvent molecules to freely access the cellulose hydroxyl groups, by physical steric hindrance or by charge repulsion (gelatine being amphoteric, it is potentially ionisable in solution). Another possibility is that the measurement of M_r and/or rms radii are convoluted, (e.g. because of a slightly different dn/dc). Anyhow, it can be concluded that

gelatine did not stiffen the cellulose to rigid rod conformation in solution but on the contrary seemed to provoke a slight coil contraction resulting in a more compact conformation in solution.

A phenomenon of coil contraction was observed by Picton *et al.* [31] with cellulose derivatives where increasing hydrophobicity (achieved by alkyl chain grafting) resulted in poorer solvent strength, reflected by a lower second virial coefficient A_2 and smaller rms radius. A deviation from the Mark-Houwink-Sakurada relationship, with smaller values of intrinsic viscosity, showed also the contribution of hydrophobic interactions to the rms radius. According to the authors, it was, however, difficult to attribute the decrease in rms radius to the decrease in M_w alone or to a combination of a decrease in M_w and coil contraction.

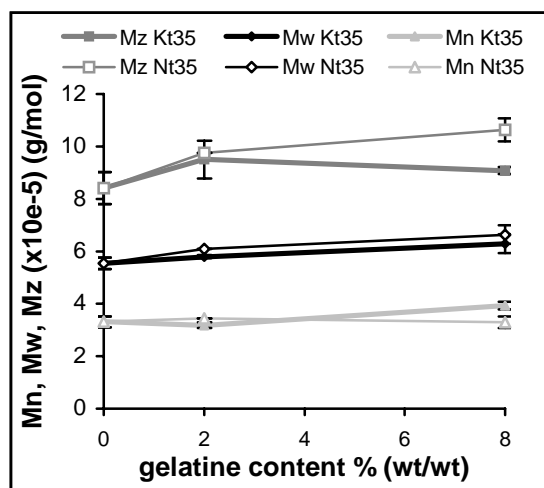


Figure 6.3-14. M_r averages as a function of gelatine content for K and N samples aged 35 days.

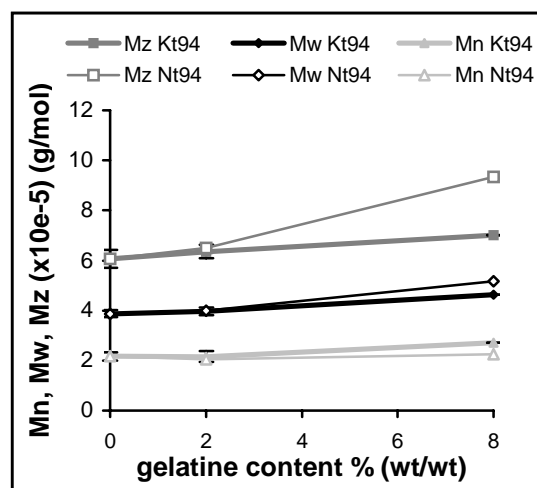


Figure 6.3-15. M_r averages as a function of gelatine content for K and N samples aged 94 days.

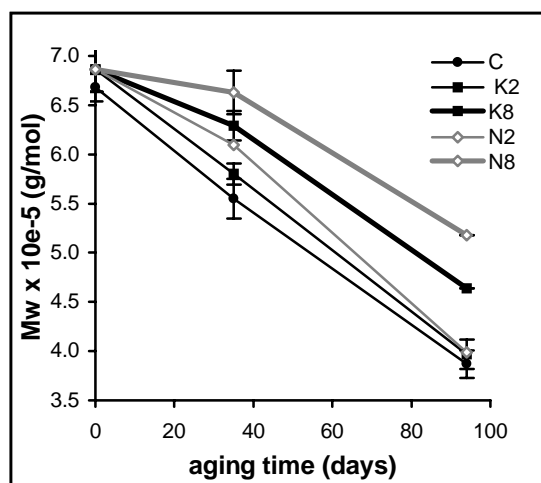


Figure 6.3-16. Changes in M_w with aging of C and sized samples (K2, K8, N2 and N8).

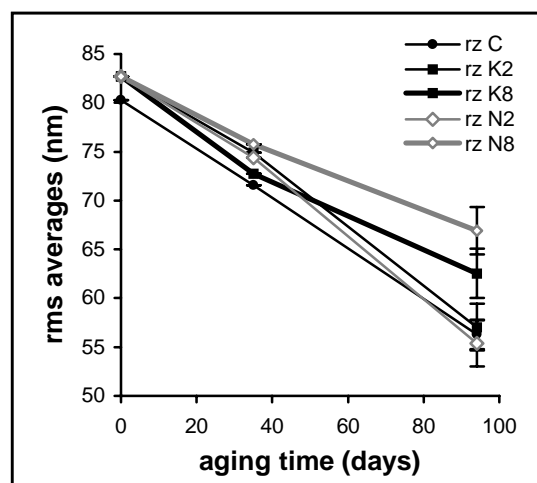


Figure 6.3-17. Change in rms radii averages with aging of C and sized samples (K2, K8, N2 and N8).

Figure 6.3-18 and Figure 6.3-19 show the polydispersity indices M_z/M_w and M_w/M_n as a function of M_n . Both indices tended to increase to different degrees with time (decreasing M_n), although most of these changes are in the limits of the RSD%. For N2 and N8 especially, the polydispersity indices increased slightly more than for the other samples, from 10% to 15%. It was noted here also that the case of K8 in the initial aging stage was in contrast to the other samples, with a decrease in polydispersity indices. This indicates that in papers sized with gelatine, as in control papers, the cleavage of the cellulose chains is mostly random, with a slight tendency of enhanced cleavage in the high- M_r fractions.

The plots $(1/M_{wt} - 1/M_{wt0})$ (mol g^{-1}) as a function of aging time (days) (Figure 6.3-20) evidence more clearly that all sized papers had a lower degradation rate upon aging than the unsized control papers. Only K2 samples had a similar degradation rate as the controls over the entire aging period. In all cases, as in the case of the unsized papers, the degradation rate was not constant from t_0 to t_{94} . The slope of each aging time-frame indicated that the degradation rate was essentially lowered from t_0 to t_{35} , and from then until t_{94} increased. For the papers with 8% gelatine, the degradation rate in the second aging period (t_{35} to t_{94}) was still well below that of the control papers while for the papers with 2% gelatine, the degradation rate increased rapidly to match that of the control papers around t_{94} .

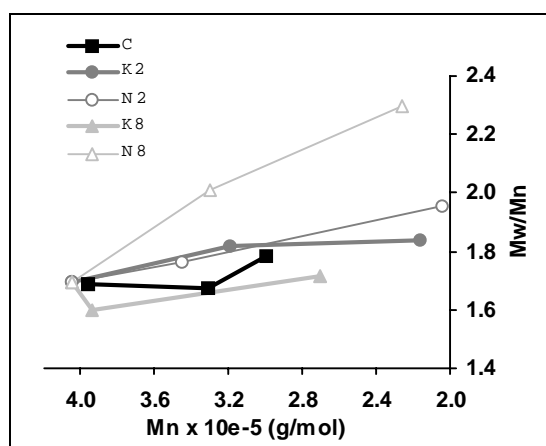


Figure 6.3-18. Polydispersity index M_w/M_n of C, K2, K8, N2 and N8 as a function of M_n .

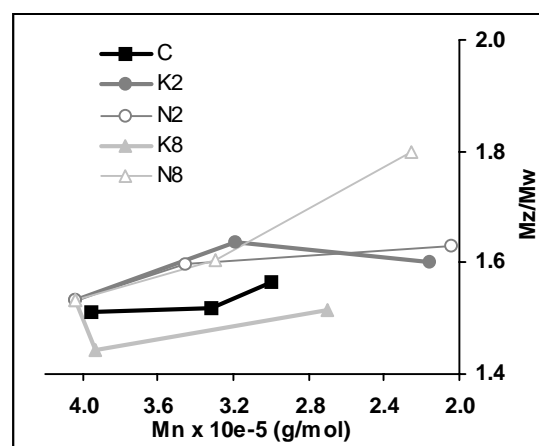


Figure 6.3-19. Polydispersity index M_z/M_w of C, K2, K8, N2 and N8 as a function of M_n .

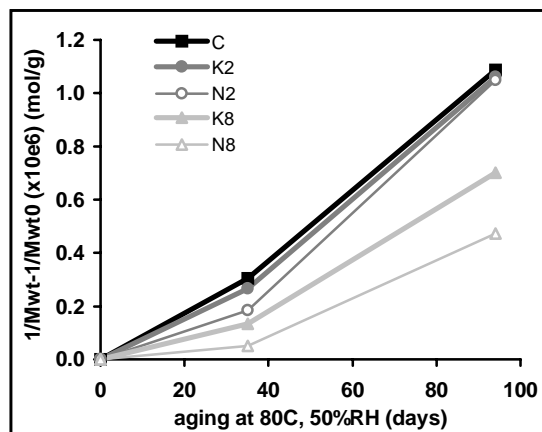


Figure 6.3-20. Plot yielding the glycosidic bond breaking constant k ($\text{mol g}^{-1} \text{days}^{-1}$) of the samples C, K2, K8, N2 and N8 (k is the slope of the plot).

This series of experiments showed that the two types of gelatine used had a similar effect on cellulose from the molecular point of view and that the impact of gelatine depended on its content in the paper. Up to 2%, although not clearly beneficial for cellulose, gelatine was certainly not detrimental. For higher gelatine contents the results showed a clear beneficial effect in lowering the degradation rate of the cellulose molecules.

6.3.2.1.4 *The aging of Arches paper*

The Arches (Ar) papers did not completely dissolve, as some fibres suspended in solution were visible even after 15 days in 8%LiCl/DMAc. The M_r averages of the Ar papers are reported in Table 6.3-1, and the rms radii averages in Table 6.3-4. The overlaid curves of differential molar mass (Figure 6.3-21) show the changes in the MMD profiles of Arches papers with aging. The PD of the unaged Ar paper ($1.97 \pm 6\%$) was slightly higher than that of the unaged Whatman No.1 ($1.70 \pm 7\%$), but was still in the typical range of a pure cellulose paper (Table 6.3-1).

The decrease in the various M_r averages upon aging follows the same sequence as for the Whatman No.1 sized papers with $\Delta M_n\% > \Delta M_w\% > \Delta M_z\%$ (Table 6.3-3), indicating an enhanced production of low- M_r fractions. However, $\Delta M_p\%$ was higher than $\Delta M_n\%$ while for Whatman paper, $\Delta M_p\%$ was between $\Delta M_n\%$ and $\Delta M_w\%$. This corresponded to an increase in PD of Ar from 1.97 at t_0 to 2.38 at t_{94} .

Unlike Whatman No.1, the MMD profiles of Ar were slightly asymmetric. The chromatogram of Art₀ presented a small shoulder near the apex on the low- M_r side, and the chromatogram of Art₉₄ a small shoulder near the apex on the high- M_r side (indicated by arrows in Figure 6.3-21). The chromatogram of Art₃₅ also had a small shoulder on the same side as Art₉₄ but the apex of the peak was quite flat as opposed to Art₀ and Art₉₄ peaks which both had a relatively sharp apex. The asymmetry of the peaks of Art₃₅ and Art₉₄ was also visible on the LS signals of the three Arches papers (as indicated by the arrows in Figure 6.3-22).

Such asymmetry in the MMD profiles of aged cellulose was also reported by Elmsley *et al.* [30] during dry-oven aging of pure cotton linters. The authors described a series of complex MMD profiles, from monomodal to bimodal in the different stages of aging. This particular feature of the MMD was more pronounced at the accelerated aging process caused by higher temperatures. At 120°C the MMD showed merely small shoulders while at 160°C, the MMD was clearly bimodal. The authors' interpretation was that degradation occurred preferentially at chain centres, such that an initially monomodal MMD became bimodal during aging, before returning to monomodal at the low- M_r . The MMD profiles in Figure 6.3-21 and Figure 6.3-22 tended to confirm this hypothesis. However, the aging conditions in the present study being much milder than those used by these authors, the asymmetry was not as pronounced. Additionally, it must be recall that

the present study does not claim to be a study on the kinetics of the degradation; it is therefore difficult to ascertain a conclusion using only three data points as aging times.

The values of r_z were 80.3 nm for Art₀ (same as for Ct₀), 64.8 nm for Art₃₅ and 55.3 nm for Art₉₄ (Table 6.3-4). These values corresponded for Art₃₅ and Art₉₄ to a decrease in r_z of 19% and 31% with respect to Art₀.

The plot of log rms radius versus V_e showed a regular linear decrease (Figure 6.3-23). Table 6.3-4 reports the values of the slope q and Figure 6.3-24 shows the log-log plot of rms radius versus M_r for the Ar samples. For Art₀, the slope was typical of a random coil polymer in a good solvent. However, for the aged Ar samples, as was observed for the sized Whatman No.1 papers, the value of q decreased below 0.5, which indicated conditions below theta of the polymer in solution.

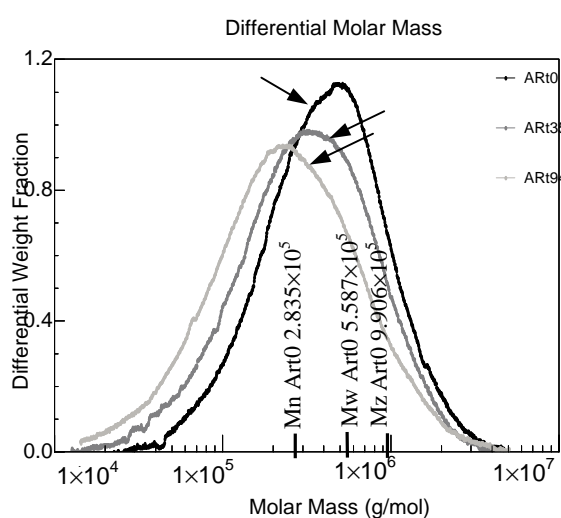


Figure 6.3-21. Overlaid differential molar mass graphs of aged and unaged Ar samples.

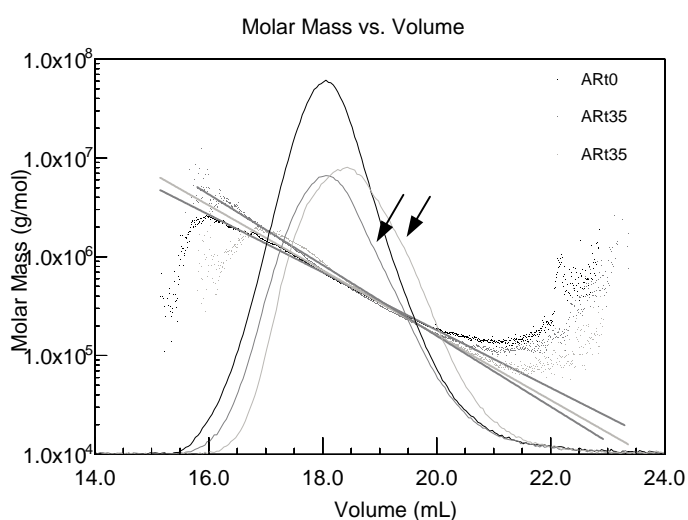


Figure 6.3-22. Overlaid LS signals of aged and unaged Ar samples.

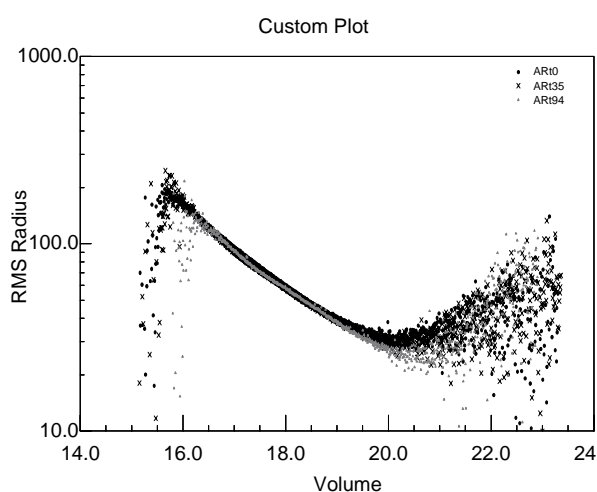


Figure 6.3-23. Overlaid rms radii as a function of V_e for aged and unaged Ar samples.

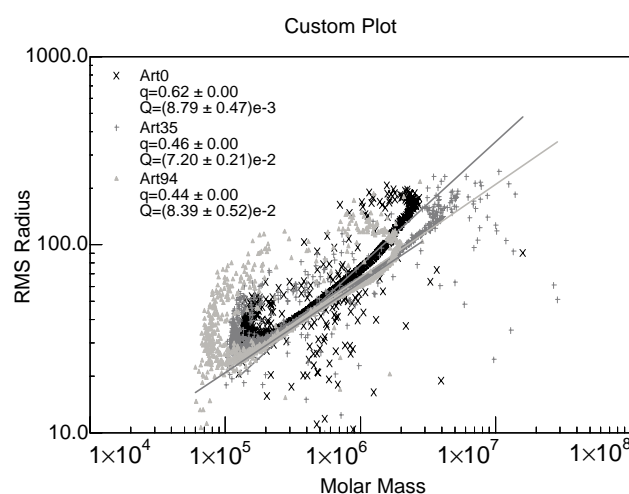


Figure 6.3-24. Overlaid average rms radii versus M_r (log-log scale) for Art₀, Art₃₅ and Art₉₄.

Figure 6.3-25 shows that the decay in M_w of Ar upon aging from t_0 to t_{35} was similar to that of unsized Whatman No.1 paper (same slope), and then decreased in the time interval from t_{35} to t_{94} . Figure 6.3-26 shows that the drop in r_z of Ar upon aging was quite similar to the drop in M_w . The polydispersity indices M_z/M_w and M_w/M_n are represented as a function of M_n in Figure 6.3-27. The increase in both polydispersity indices of Ar with aging time was more pronounced than in the case of the Whatman No.1 papers, and fell out of the RSD%, with M_z/M_w increasing by 14% and M_w/M_n by 17%. This would tend to indicate that the degradation of the Arches papers was not homogeneous over time, but that a cleavage of the longest molecules (high- M_r) seems to occur preferentially.

The results show that for Arches papers as for sized Whatman No.1 paper, the degradation rate was slowed by the presence of gelatine.

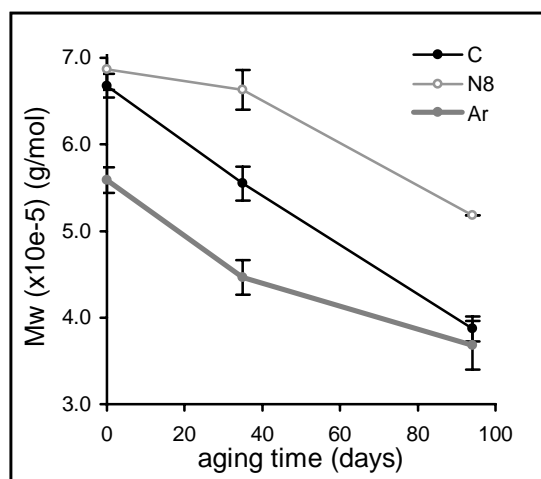


Figure 6.3-25. Change in M_w upon aging time for Ar samples compared to C and N8 samples.

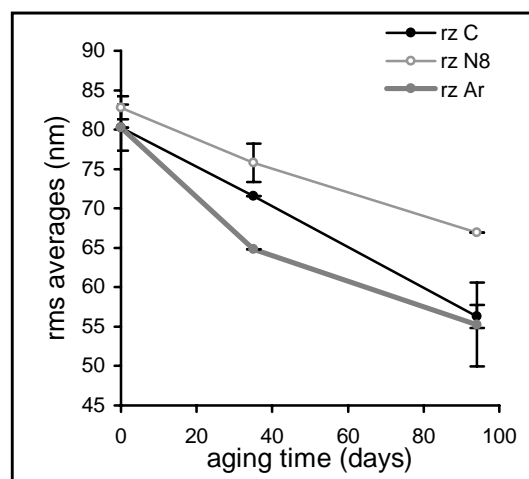


Figure 6.3-26. Change in rms radii upon aging time for Ar samples compared to C and N8 samples.

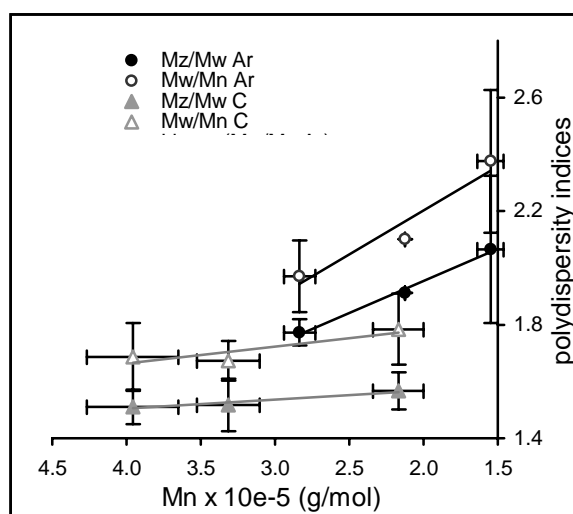


Figure 6.3-27. Polydispersity indices of Ar samples as a function of M_n compared to C samples (no error bars for Ar_{35} : the RSD could not be calculated as only two SEC runs were carried out).

6.3.2.2 SEC/MALS applied to the study of naturally aged historic papers

6.3.2.2.1 Seventeenth and eighteenth century papers

Table 6.3-5 summarises provenance, composition of the papers (fibre and pulp type, presence of gelatine and/or alum) and efficiency of dissolution in 8% LiCl/DMAc. The presence of gelatine was tested by the Biuret spot test method¹ [32] and the presence of aluminium was tested using the aluminon spot test² [33]. Analysis with scanning electron microscopy/energy dispersive X ray (SEM/EDX) (JEOL JSM 5410 LV SEM / Oxford EDS system) confirmed the presence of aluminium in NAT1, NAT2, NAT3, and its absence in NAT4. The fibre composition of the papers was determined by a microscopic fibre analysis using the staining method with Lofton-Merritt and Herzberg solutions [34].

The four historic papers were made of rag. NAT1, NAT3 and NAT4 were pure linen and NAT2 was a mix of cotton and linen. According to the results of the spot tests, only NAT3 seemed to contain no gelatine but yet contained aluminium (Table 6.3-5).

Table 6.3-6 reports the values of the M_r averages and Figure 6.3-28 shows the overlaid differential molar mass curves of NAT1, NAT2, NAT3 and NAT4.

Table 6.3-5. Specifications of the naturally aged papers and efficiency of the dissolution in 8% LiCl/DMAc.

sample	provenance	gelatine	alum	fibre and pulp type	fabrication	dissolution (days)	dissolution degree
NAT1	BvB ³	+	+	rag linen	handsheet	6	some undissolved
NAT2	BvB	+	+	rag cotton, linen	handsheet	4	total
NAT3	BvB	-	+	rag linen	handsheet	6	total
NAT4	BvB	+	-	rag linen	handsheet	13	some undissolved
SxU ⁴	NGA ⁵	Aqua-set	+	softwood	industrial	4	total and fast
SxS ⁴	NGA	Photo-Gelatin	+	softwood	industrial	4	total and fast

¹ The Biuret test is based on the violet colour yielded by the reaction of protein with copper sulfate and sodium hydroxide solutions. As a spot test it is applied directly to the material tested by wetting it with 2% copper sulfate solution, blotting off the excess liquid, and adding a 5% sodium hydroxide [32, p.103].

² Aluminon (aurintricarboxylic acid) test allows for the determination of Al³⁺ ions, as these form a red precipitate when reacting with aluminon. A drop of solution of aluminon prepared at 0.1% in water is applied to the sample, a red or pink colour indicates the presence of Al³⁺[33, p.35].

³ Museum Boijmans Van Beuningen, Rotterdam, The Netherlands.

⁴ In SxU and SxS, the x refers to the paper grammage (140, 160, 180, 220, and 320 g m⁻²).

⁵ National Gallery of Art, Washington DC, US.

Table 6.3-6. M_r averages and polydispersity indices of the naturally aged 17th and 18th century papers, and Strathmore papers.

	AVG $M_n \times 10^{-5}$ g mol ⁻¹	RSD % M_n	AVG $M_w \times 10^{-5}$ g mol ⁻¹	RSD % M_w	AVG $M_z \times 10^{-5}$ g mol ⁻¹	RSD % M_z	AVG $M_p \times 10^{-5}$ g mol ⁻¹	RSD % M_p	AVG PD (M_w/M_n)	RSD % PD	AVG M_z/M_w	RSD % M_z/M_w
NAT1	1.81	N/A ¹	3.80	N/A	6.61	N/A	2.84	N/A	2.1	N/A	1.74	N/A
NAT2	2.50	9.1	5.11	1.6	8.99	9.3	4.56	9.8	2.06	9.2	1.76	8.8
NAT3	1.11	7.6	2.60	5.5	4.86	13.9	2.20	6.2	2.34	3.7	1.87	9.8
NAT4	2.93	15.2	6.45	7.7	11.23	6.6	5.77	5.6	2.22	10.3	1.74	4.8
S160U	1.03	N/A	5.19	N/A	14.43	N/A	2.82	N/A	5.04	N/A	2.77	N/A
S160S	1.18	N/A	5.23	N/A	14.31	N/A	3.05	N/A	4.45	N/A	2.73	N/A
S320U	0.82	N/A	4.74	N/A	15.15	N/A	2.60	N/A	5.84	N/A	3.19	N/A
S320S	1.31	N/A	5.37	N/A	13.84	N/A	3.02	N/A	4.10	N/A	2.58	N/A

The cellulose in the four papers appeared to be in a different state of degradation. This was not unexpected as on the one hand the papers can have over 100 years age difference and on the other, there are multiple other causes for different degradation rate of papers, such as for instance fibrous and non-fibrous composition and conservation history. All things else being equal, it is logical to expect papers kept in good conservation conditions to be in better shape than those kept in inadequate conditions.

From Table 6.3-6 and Figure 6.3-28 it appears that the paper with lowest- M_r average was NAT3, which was also the only paper that tested negative for protein as well as positive for aluminium. The paper with highest M_r cellulose was NAT4, which was the only paper that tested positive for protein but negative for aluminium. Aluminium is present in alum, a source of acidity in the papers, which induces accrued degradation. Chapter 7 is dedicated to alum-containing papers and to the impact of gelatine/alum sizing in paper, and Chapter 8 studies the effect of the alum on the degradation of the gelatine. However, it must be noted that the aluminon test also gives positive results with kaolin (aluminium silicate), a mineral filler widely used in papermaking throughout history.

For all the papers, except for NAT2, the MMD profile tended to tail in the low- M_r end. The amount of tailing was not linked to lower M_r averages of the cellulose. For instance NAT4 was the paper that showed more tailing, with the formation of a small peak at low- M_r that produced an almost bimodal MMD, and was nevertheless the paper with the highest M_r of all the naturally aged papers (Table 6.3-6). Tailing can be due to the presence of hemicelluloses. Hemicelluloses are branched heteropolysaccharides of low- M_r (between 2×10^4 and 4×10^4 g mol⁻¹) which are present in wood and in most plants used in the fabrication of paper. Linen contains small quantities of hemicelluloses (2 to 6%). Cotton is the only fibre source plant that does not contain hemicelluloses. The sample exhibiting no tailing, NAT2, is most probably the paper with the lowest hemicelluloses content since it contains cotton fibres in addition to linen fibres.

¹ N/A: only two SEC runs were carried out, no standard deviation can be calculated.

The impact of this tailing in the low- M_r end is possibly more important on the value of M_n , and one possible consequence of this is the underestimation of the average M_n of the cellulose, as well as the overestimation of the polydispersity. Indeed NAT3 and NAT4, which were the two papers tailing the most, were also the papers with the largest PD (Table 6.3-6).

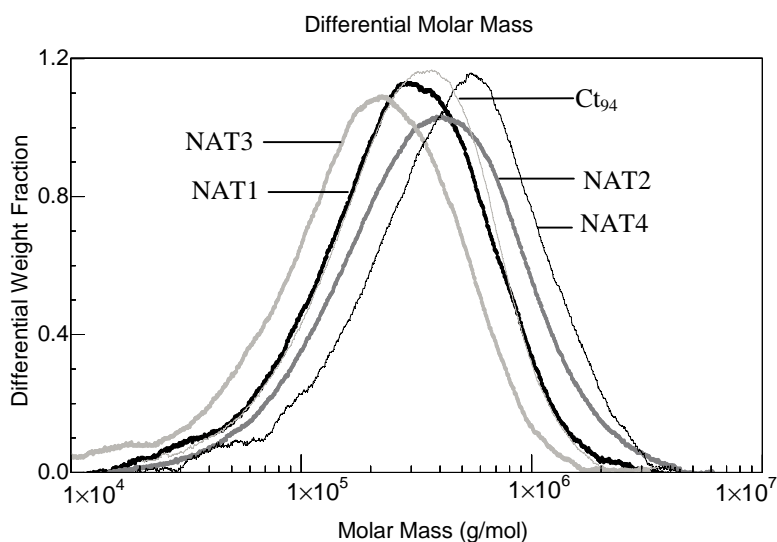


Figure 6.3-28. Overlaid differential molar mass graphs of 17th and 18th centuries papers and Ct₉₄.

Figure 6.3-29 shows the LS signals for NAT1, NAT3 and NAT4. The tailing at low- M_r (high V_e) is better seen (and quite pronounced) on these three chromatograms. The steep slope of the signal in the high- M_r end for NAT4 indicated the presence of very high- M_r molecules. For NAT3 especially, and to a lesser extent for NAT1, the MMD was almost bimodal (indicated by the arrow): the asymmetry of the signals is visible, with these small shoulders in the low- M_r region. This can be due either to the presence of hemicelluloses as stated above or to the fact that the naturally aged paper is in an intermediary stage of degradation, as was suggested in section 6.3.2.1.4 and supported by the theory of Elmsley *et al* [30].

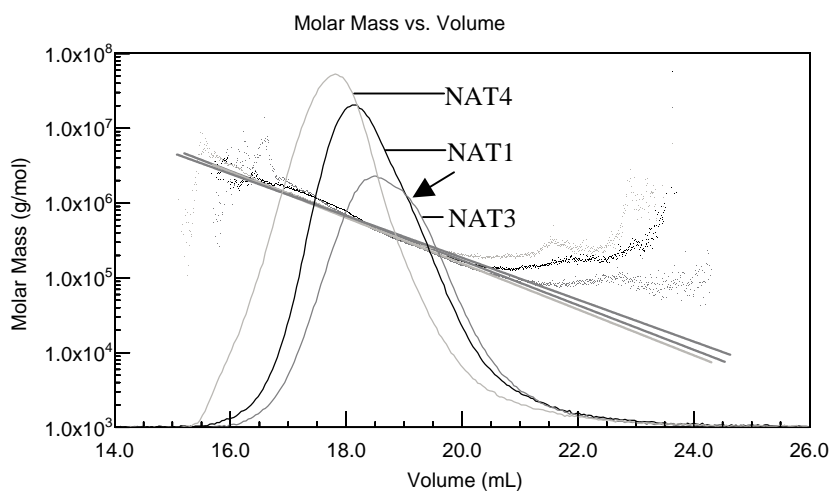


Figure 6.3-29. Overlaid 90° angle photodiode LS signals of NAT1, NAT3 and NAT4.

Figure 6.3-30 shows the log-log plot of rms radii versus M_r for the four naturally aged papers. The values of the slopes q and the average rms radii averages are reported in Table 6.3-7. As for the model papers, the cellulose of the naturally aged historic papers was found to be in random coil conformation in the solvent, with values of q ranging from 0.48 to 0.63. Here, q was also smaller for lower M_r cellulose. A parallel can be drawn with the observations made for the model papers, where q was smaller for samples aged longer, therefore those having lower M_r . This could support the explanation put forward in section 6.3.2.1.1 that the average number of hydroxyl groups per anhydroglucose unit on the cellulose chains falling below three, due to the formation of carboxyl and carbonyl groups along the cellulose chain, the solvent molecules and cellulose molecules are less complexed, which results in a lower solvation capacity.

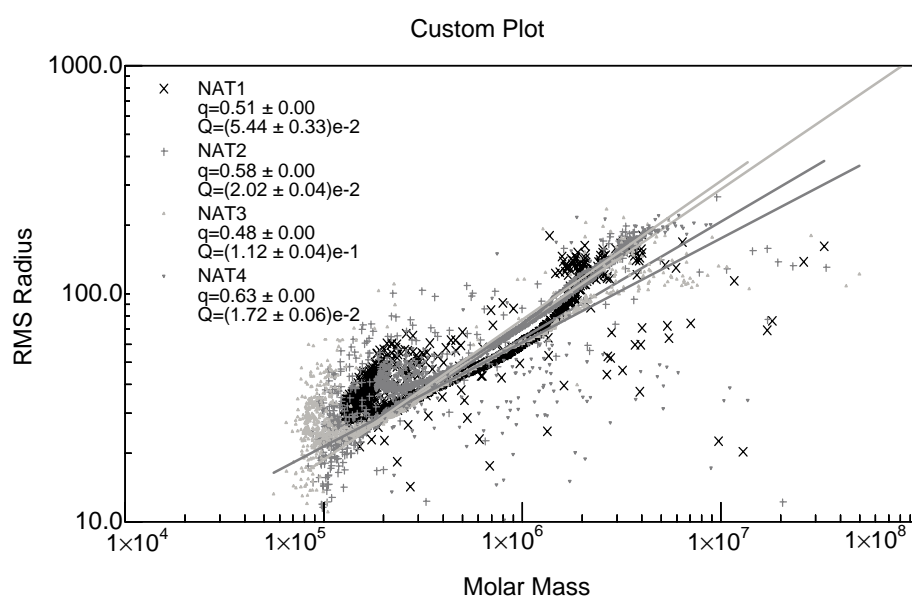


Figure 6.3-30. Overlaid average rms radii as a function of M_r for NAT1, NAT2, NAT3 and NAT4.

Table 6.3-7. Average rms radii averages and values of q of naturally aged 17th and 18th century's papers, and Strathmore papers.

	AVG r_n (nm)	RSD % r_n	AVG r_w (nm)	RSD % r_w	AVG r_z (nm)	RSD % r_z	AVG q
NAT1	26.4	N/A ¹	40.2	N/A	55.0	N/A	0.51
NAT2	32.3	3.9	51.0	2.5	73.0	6.6	0.58
NAT3	20.1	7.1	32.8	5.9	47.5	12.7	0.48
NAT4	37.2	9.4	61.5	5.8	87.7	4.8	0.63
S160U	17.2	N/A	47.2	N/A	88.6	N/A	0.69
S160S	18.0	N/A	46.5	N/A	86.8	N/A	0.72
S320U	15.3	N/A	43.4	N/A	84.7	N/A	0.59
S320S	19.5	N/A	47.7	N/A	85.5	N/A	0.67

¹ N/A: only two runs were done

Figure 6.3-31 shows the polydispersity indices M_z/M_w and M_w/M_n as a function of M_n for NAT1, NAT2, NAT3 and NAT4. The trend of M_w/M_n was not uniformly upward, probably due to the erroneous M_n as a consequence of tailing of the MMD as pointed out above. As for M_z/M_w , it appeared fairly constant for the three papers with higher M_r , *i.e.* in the higher portion of M_n (from 3×10^5 to 2×10^5 g mol⁻¹) but increased slightly for the paper with lowest M_n . However, this last data point could probably be disregarded, being that of NAT3, for which erroneous M_n was suspected. A constant value of M_z/M_w indicates a homogeneous group of degraded papers. This means that albeit degraded to different degrees, the mechanism of the degradation of cellulose of the four papers was most probably governed by the same mechanism.

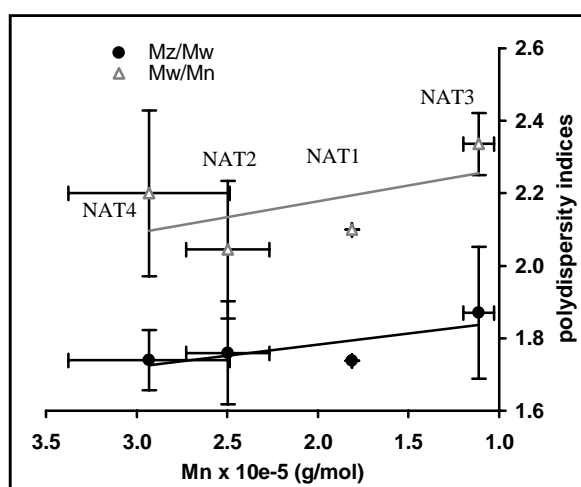


Figure 6.3-31. Polydispersity indices as a function of M_n of NAT1, NAT2, NAT3 and NAT4 (RSD% could not be calculated for NAT1, as only two SEC runs were carried out).

For these naturally aged papers a direct correlation between the values of the molar mass averages and the amount of gelatine present in the papers (section 8.3.3 of Chapter 8), is rather difficult to draw, since as seen above, the values of M_r averages can be subject to possible misestimating due the presence of the tailing in the low- M_r of the chromatograms. However, the overall tendency observed was that the samples from which the higher quantity of gelatine could be extracted (Chapter 8) were also those with higher M_r averages (NAT1, NAT2, NAT4), while the sample from which almost no gelatine was extracted (NAT3) corresponded to the sample with the lower M_r averages. Moreover, the sample with no aluminium (NAT4) appeared to be the one with the highest M_r averages.

6.3.2.2.2 Strathmore papers

The Strathmore papers dissolved in 8% LiCl/DMAc much faster than any of the pure cellulose model papers (Whatman No.1 and Arches) and any of the 17th - 18th century

papers, with a total clearing of the solutions occurring in little more than a couple of hours. Microscopic fibre analysis using the staining method with Lofton-Merritt and Herzberg solutions [34] showed that all the Strathmore papers were made of 100% bleached softwood chemical pulp (Table 6.3-5). This fast dissolution of softwood papers is consistent with observations in the literature [35].

Table 6.3-6 reports the values of the M_r averages and Figure 6.3-32 represents the overlaid differential molar mass graphs of the four papers analysed (S160U, S160S, S320U and S320S). Figure 6.3-33 shows the overlaid plots of rms radii versus V_e . The linearity of the plots indicated a normal elution with no column adsorption.

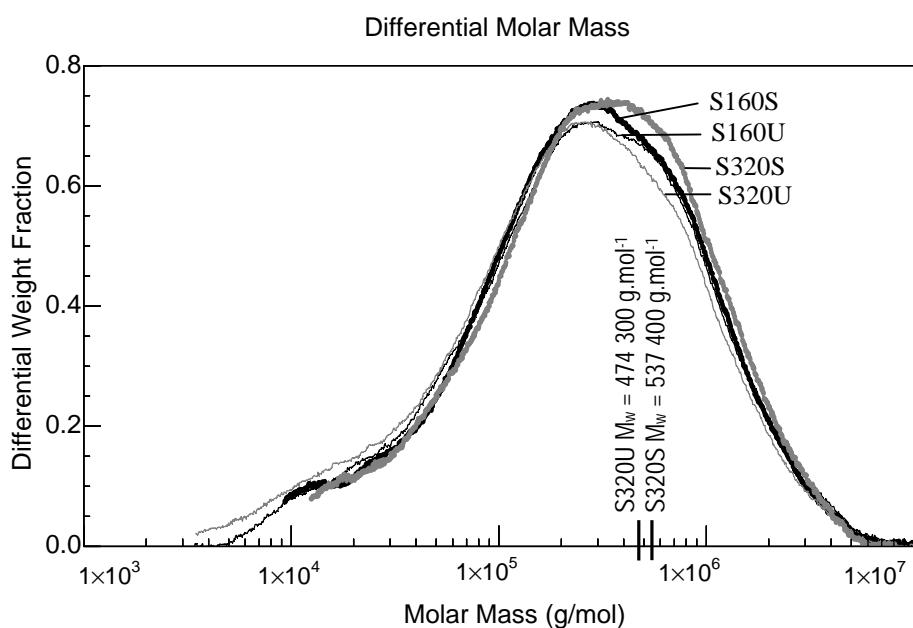


Figure 6.3-32. Overlaid differential molar mass graphs of S160U, S160S, S320U and S320S.

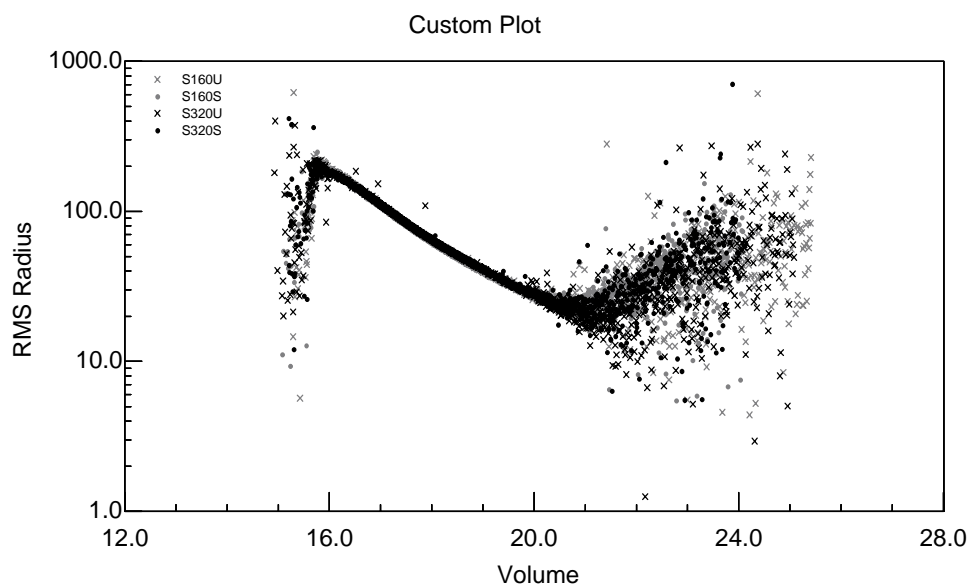


Figure 6.3-33. Overlaid average rms radii (log) as a function of V_e of S160U, S160S, S320U and S320S.

As expected for wood pulp paper, the MMD was much broader than for pure cellulose papers. The four Strathmore papers showed a quasi-bimodal MMD with the smaller peak in the low- M_r end, probably due to the hemicelluloses. Considering the date of fabrication, the process of the softwood pulp of the Strathmore papers was probably sulphite. Such pulps typically contain no lignin (if bleached), or traces amounts (if unbleached), and a maximum of 10 to 15% hemicelluloses, the remaining part being cellulose. The phloroglucinol spot test¹ [32] showed that the Strathmore papers were indeed totally exempt of lignins (the stain remained yellow). Here, more than in the case of the 17th-18th century papers, the composition had a significant impact on M_n . The MMD of softwood pulp is usually very broad because it contains low- M_r material but also cellulose molecules of very high- M_r . This resulted in larger polydispersities than for pure cellulose papers, with $PD > 4$ in all cases. Among all Strathmore papers, the highest M_z was found for S320U ($1.515 \times 10^6 \text{ g mol}^{-1}$).

It was also observed that the MMD was not symmetrical, with the presence of a small shoulder near the apex on the high- M_r side of the peak (Figure 6.3-32), similarly as that observed for the aged Arches papers. This small shoulder was more pronounced for S160 (U and S) than for S320 (U and S).

Table 6.3-7 reports the rms radii averages. The values of r_z were higher than for any of the papers previously tested: between 84.7 nm and 88.6 nm, which confirmed the presence of very high- M_r molecules. The LS signals for the four Strathmore papers (Figure 6.3-34) showed a much steeper slope in the high- M_r portion than in the case of the model papers. This again corroborates the presence of very high- M_r molecules, which approach the exclusion limit of the column set.

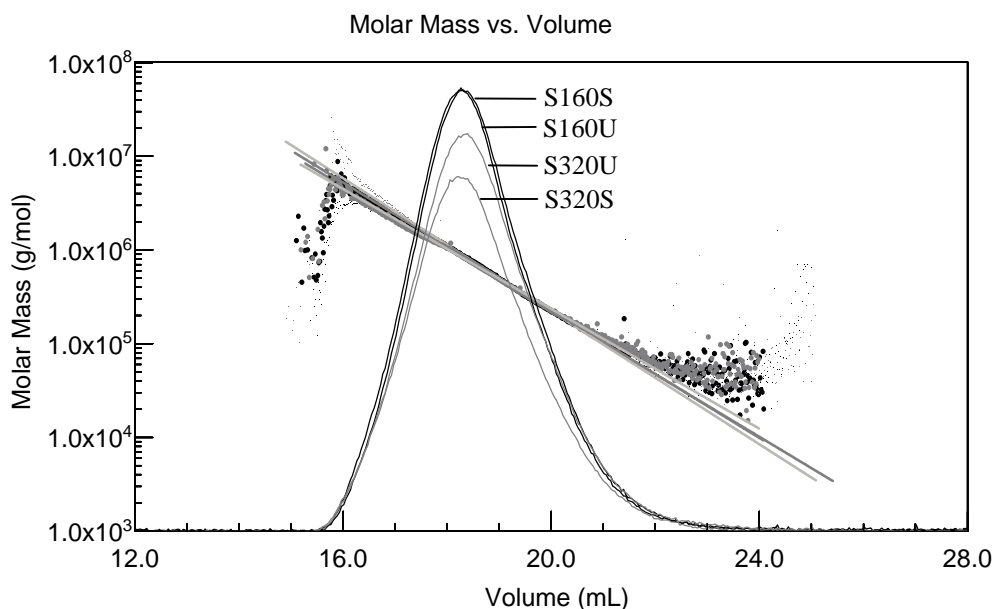


Figure 6.3-34. Overlaid 90° angle photodiode LS signals of S160U, S160S, S320U and S320S.

¹ Phloroglucinol (hydrochloric solution), prepared according to standard NFQ 03.001 (Prolabo) yields a bright red or magenta colour by reacting with groundwood and lignin-containing fibres. The depth of the colour is proportional to the amount of lignin present. A drop of the reagent is directly poured on the paper sample [32,p.72].

The M_w of the four papers is represented in Figure 6.3-35. The papers sized with gelatine showed slightly higher M_w than the unsized papers. Because the presence of the smaller peak in the low- M_r resulted in a significant error in the calculated M_r , the impact of gelatine was better assessed by comparing the MMD profiles than by comparing the M_r averages values. However, as this affects M_w less than M_n , the difference in M_w alone can still be indicative. Between S320 sized and unsized this difference in M_w was 12%, and only 2% between S160 sized and unsized. Considering the average precision of the method, this difference in the case of S320 is significant, while for S160, it falls within the RSD.

Unfortunately, no information could be obtained on the mode of sizing of the Strathmore papers. However, it is assumed to be surface sizing, *i.e.* sizing by immersion after the sheet formation (as for the model papers) rather than internal sizing, *i.e.* by adding size to the pulp before the sheet formation. These two types of sizing were used in papermaking factories at the time of fabrication of these papers but while the former was used for sizing with gelatine, the latter was most often applied to synthetic polymer sizing. Under the assumption of surface sizing with gelatine, the papers with higher grammage (S320) can absorb a greater quantity of gelatine and will therefore have higher gelatine content than the lower grammage papers (S160). Indeed, and as reported in the previous paragraph, S320S showed a MMD slightly more weighted in the high- M_r fractions than its unsized counterpart ($\Delta M_w = 12\%$), which for S160 was also observed but non-significantly ($\Delta M_w = 2\%$).

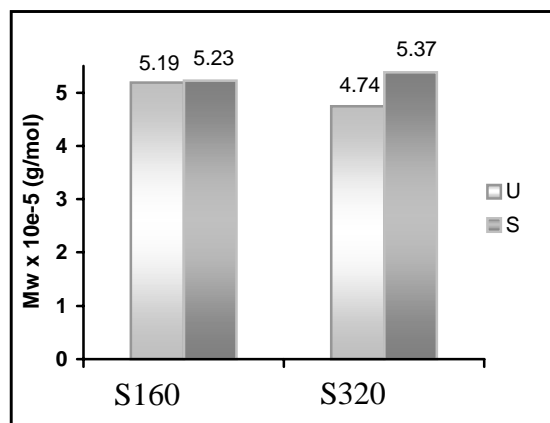


Figure 6.3-35. M_w of S160U, S160S, S320U and S320S.

Figure 6.3-36 shows overlaid log-log plots of rms radii versus M_r for the four Strathmore papers. The values of q were found between 0.58 and 0.74 (Table 6.3-7). This indicated that, as was observed for pure cotton and linen cellulose, chemical pulp cellulose also adopted a random coil conformation in solution in LiCl/DMAc. However values of 0.69 and 0.72 for the samples S160 (U and S) were quite high and indicated a slightly more

rigid conformation than typical random coil. This could be due to aggregation, either between cellulose molecules or between cellulose and the hemicelluloses.

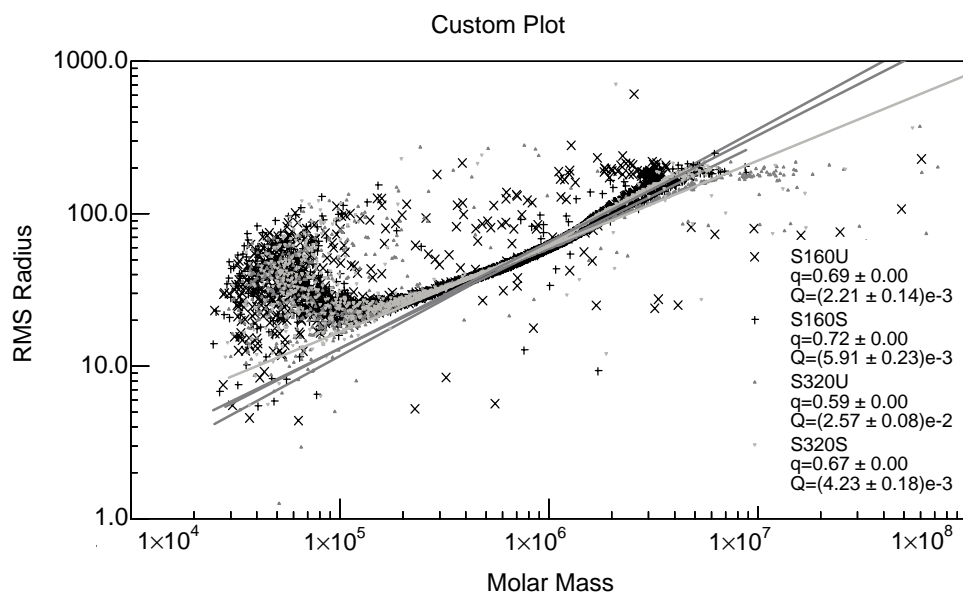


Figure 6.3-36. Overlaid average rms radii as a function of M_r of S160U, S160S, S320U and S320S.

Figure 6.3-37 shows the polydispersity indices M_z/M_w and M_w/M_n as a function of M_n between sized and unsized Strathmore papers. Both polydispersity indices increased remarkably with decreasing M_n . This tendency was more pronounced for S320. Only M_z/M_w for S160 was almost constant whether sized or unsized.

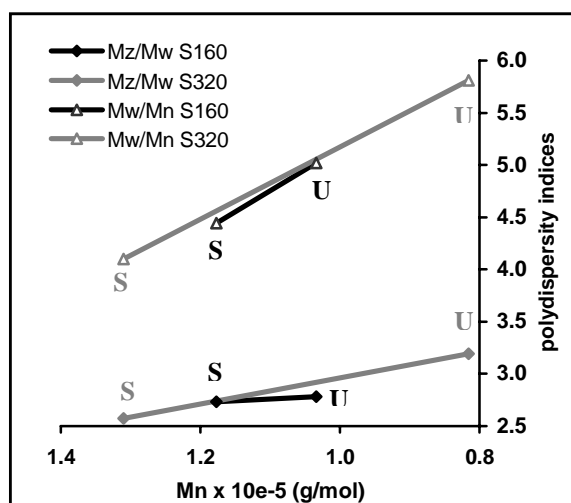


Figure 6.3-37. Polydispersity indices as a function of M_n of S160U, S160S, S320U and S320S.

With the above results, it seems reasonable to conclude from the analysis of the Strathmore papers that the effect of gelatine, as in the case of the model papers, was to

decrease the degradation rate of the cellulose upon aging. However, this has to be considered merely as a tendency, as 70 years of natural aging appears not to be enough to extrapolate with absolute certainty.

6.3.3 Conclusions on SEC/MALS

The results of SEC/MALS experiments showed that pure cellulose paper undergoes more or less random cleavage with accelerated aging. A slightly higher production of low- M_r molecules is noted, although this was just on the verge of being significant in most cases. Therefore, the aging process is rather homogeneous over the aging period, except for the Arches papers, in which the cellulose chains seem to undergo scissions preferentially in the longest chains.

The presence of gelatine was generally beneficial for cellulose facing hydrolytic attack upon aging. Not always in a significant manner, but in all cases, the M_r averages and rms radii of the sized model papers were higher than the M_r averages and rms radii of their unsized counterpart at comparable aging time. The protection seemed to be slightly more efficient in lowering the depolymerisation rate in the high- M_r molecules than in the low- M_r molecules, except for one model paper (K8), for which no reason could be found. If the above-mentioned effect was not always clearly evidenced for naturally aged papers, it was nevertheless totally ascertained that gelatine had no detrimental effect on the degradation of the cellulose upon aging.

When studying naturally aged papers the difficulty in evaluating the effects of gelatine is mostly due to their unknown conservation history, and to the fact that unsized references to compare these samples to are not available. In that respect the Strathmore papers were a precious source of information by providing sized and reference papers of the same age and type, and comparable conservation history. Despite the limited number of historic papers analysed, the results corroborated the findings from the model papers, although they should be interpreted cautiously.

SEC/MALS proved to be an extremely sensitive technique allowing for very precise information on M_r averages, MMD, rms radii averages and conformation of cellulose from diverse origin and from diversely prepared papers. The method of analysis of cellulose in LiCl/DMAc was found totally appropriate to this research, and could be applied to the study of model papers as well as naturally aged papers. No aggregation occurred in the solvent, except maybe in the case of the Strathmore papers S160. LiCl/DMAc was confirmed to be a good solvent for unaged cellulose, while in the case of aged cellulose solvation came closer to theta conditions probably due to the presence of oxidised groups along the molecule. Cellulose displayed a random coil conformation in solution. However upon aging, some of the model papers (N and Arches) seemed to adopt a more compact conformation in solution, which was attributed both to the presence of oxidised groups and to possible residual gelatine.

6.4 Colour monitoring of unsized and sized papers during aging

Gelatine sized papers are generally believed to yellow significantly upon aging. In order to investigate further this aspect of the aging behaviour, colour measurements were done on the model papers and naturally aged papers. The colour changes were evaluated in correlation with the other measurements and analyses, *i.e.* pH and especially SEC/MALS.

6.4.1 Experimental

Colour measurements were done in the trichromatic system CIE $L^*a^*b^*$ [2], and total chromatic differences (ΔE^*) between unsized/sized and unaged/aged papers were calculated. Additionally, indices such as Yellowness (E313-96), Whiteness (E 313-96), and R457 ISO brightness (reflectance at 457 nm), as well as the total hue difference (ΔH^*), were measured. The equations of CIE $L^*a^*b^*$ values and other measured indices as well as their significance with respect to visual appreciation can be found in Appendix 6-4.

A spectrophotometer UltraScan XE (Hunter Associates Laboratory, Inc.) was used (specifications in Appendix 6-4). The measurements were carried out in diffuse reflectance, the specular component included (RSIN) with illuminant D65, 10° standard observer, using the 25mm diameter measuring area, at five different locations of a sheet of paper as represented in Figure 6.4-1.

For the model papers, five different sheets of each sample type were measured. The values reported in the tables are the average of 25 measurements per sample type. For Strathmore papers only one sheet per sample type was available, therefore the reported values are averages of 5 measurements. The historic papers NAT1, NAT2, NAT3, and NAT4 could not be used because their size was too small for colour measurements.

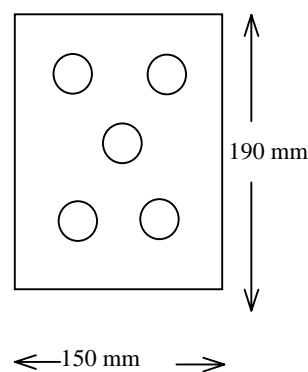


Figure 6.4-1. Locations of the colour measurements on a paper sheet.

6.4.2 Results and discussion

6.4.2.1 Pure cellulose paper

Table 6.4-1 reports the CIE $L^*a^*b^*$ values of the Whatman No.1 aged and unaged control papers. Figure 6.4-2 and Figure 6.4-3 show the changes in b^* and ΔE^* upon aging time. The amplitude of the change in these two parameters appeared closely related.

It was noted that the papers aged in the SE-600-3 chamber (Thermotron Industries) and those aged in the Versatenn chamber (Tenney Environmental) did not exhibit the same discolouration. The former yellowed more with larger relative standard deviation (RSD) on the values than the latter. The reason for this discrepancy could not be determined with certainty. Since the SEC/MALS experiments showed that control samples aged in the two chambers have same M_r averages and MMD profiles, this difference in discolouration is therefore not correlated to accrued hydrolysis of the cellulose. Oxidation in turn has been often pointed out as responsible for the yellowing of paper. It can therefore be speculated that this yellowing is rather due to oxidation. Low molecular weight carboxylic acids such as formic, acetic, lactic, malonic, malic, succinic and α -ketoglutaric acid have been identified as degradation products off-gassing from the papers during the aging [36,37,38,39,40]. These volatile organic compounds (VOCs) mostly arise from end-group oxidation, and their formation does not affect the molar mass of the polymer, but they can in turn catalyse further the oxidation of the cellulose. Different ventilation in the two chambers that would lead to a different dissipation rate of these VOCs could therefore be responsible for the different yellowing rate of the papers in the two aging chambers.

However, considering this fact and in order to accurately follow the changes in colour of the papers sized upon aging, the colorimetric parameters were only compared between samples aged in the same chamber, *i.e.* the SE-600-3 chamber for K and N papers, and the Versatenn chamber for papers containing alum (studied in Chapter 7).

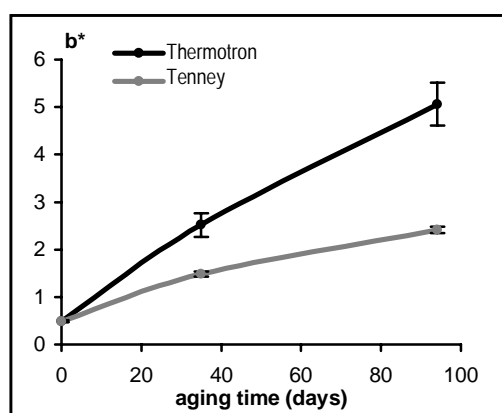


Figure 6.4-2. b^* as a function of aging time for C samples.

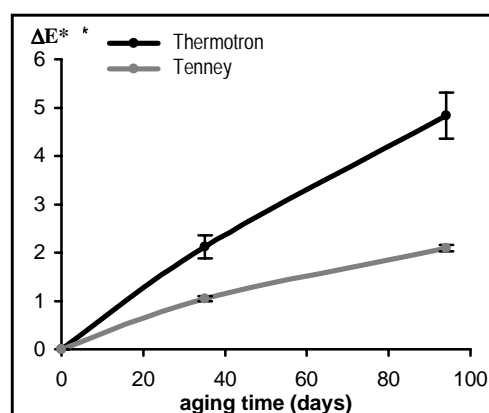


Figure 6.4-3. ΔE^* as a function of aging time for C samples.

Table 6.4-1. Trichromatic values, indices (brightness, yellowness and whiteness), total chromatic and total hue difference for the model papers upon aging: control samples, sized samples, and Arches papers.

	L*	a*	b*	ΔE^*1 (vs Ct _x)	ΔE^*2 (vs Xt ₀)	Brightness R457	YI E313-96	WI E313-96	ΔH^*3 (vs Ct _x)	ΔH^*4 (vs Xt ₀)
Ct₀	95.33 ± 0.06	-0.57 ± 0.005	0.49 ± 0.02	0.00	0.00	87.89 ± 0.14	0.51 ± 0.04	86.16 ± 0.17	0.00	0.00
Ct₃₅	94.75 ± 0.05	-0.77 ± 0.02	2.52 ± 0.25	2.12 ± 0.24	2.12 ± 0.24	84.03 ± 0.37	4.22 ± 0.46	75.54 ± 1.19	-0.78 ± 0.07	-0.78 ± 0.07
Ct₉₄	93.74 ± 0.16	-0.69 ± 0.02	5.06 ± 0.45	4.83 ± 0.48	4.83 ± 0.48	78.65 ± 0.90	9.08 ± 0.86	61.43 ± 2.48	-1.38 ± 0.09	-1.38 ± 0.09
K05t₀	95.21 ± 0.06	-0.58 ± 0.01	0.56 ± 0.03	0.15 ± 0.045	0.00	87.51 ± 0.13	0.62 ± 0.05	85.56 ± 0.14	-0.04 ± 0.02	
K05t₃₅	94.90 ± 0.03	-0.88 ± 0.02	2.41 ± 0.16	0.21 ± 0.09	1.90 ± 0.16	84.52 ± 0.18	3.92 ± 0.30	76.39 ± 0.70	0.14 ± 0.05	
K05t₉₄	94.05 ± 0.13	-0.87 ± 0.01	4.84 ± 0.32	0.42 ± 0.25	4.45 ± 0.34	79.63 ± 0.68	8.51 ± 0.60	63.19 ± 1.81	0.21 ± 0.32	
K2t₀	95.19 ± 0.06	-0.60 ± 0.01	0.65 ± 0.05	0.22 ± 0.02	0.00	87.36 ± 0.1	0.79 ± 0.09	85.10 ± 0.16	-0.09 ± 0.03	
K2t₃₅	94.93 ± 0.05	-0.98 ± 0.01	2.44 ± 0.08	0.29 ± 0.02	1.84 ± 0.07	84.60 ± 0.09	3.90 ± 0.15	76.35 ± 0.31	0.23 ± 0.02	
K2t₉₄	94.19 ± 0.05	-1.11 ± 0.02	4.70 ± 0.17	0.70 ± 0.08	4.20 ± 0.17	80.15 ± 0.23	8.07 ± 0.32	64.12 ± 0.79	0.48 ± 0.17	
K8t₀	94.85 ± 0.07	-0.72 ± 0.01	0.98 ± 0.04	0.70 ± 0.05	0.00	86.17 ± 0.17	1.32 ± 0.08	82.81 ± 0.23	-0.21 ± 0.02	
K8t₃₅	94.69 ± 0.04	-1.19 ± 0.02	2.71 ± 0.06	0.46 ± 0.04	1.81 ± 0.06	83.74 ± 0.13	4.27 ± 0.10	74.48 ± 0.31	0.32 ± 0.01	
K8t₉₄	94.35 ± 0.06	-1.33 ± 0.03	4.24 ± 0.11	1.20 ± 0.08	3.55 ± 0.12	81.15 ± 0.23	7.04 ± 0.20	66.64 ± 0.60	0.80 ± 0.11	
N05t₀	95.31 ± 0.06	-0.60 ± 0.01	0.58 ± 0.02	0.11 ± 0.03	0.00	87.71 ± 0.13	0.66 ± 0.04	85.68 ± 0.14	-0.05 ± 0.01	
N05t₃₅	94.92 ± 0.05	-1.07 ± 0.02	2.84 ± 0.10	0.47 ± 0.08	2.35 ± 0.08	84.05 ± 0.15	4.59 ± 0.19	74.46 ± 0.46	0.18 ± 0.03	
N05t₉₄	94.07 ± 0.08	-1.12 ± 0.03	5.67 ± 0.14	0.82 ± 0.010	5.27 ± 0.15	78.71 ± 0.30	9.86 ± 0.26	59.39 ± 0.79	0.32 ± 0.03	
N2t₀	95.31 ± 0.036	-0.62 ± 0.01	0.68 ± 0.033	0.20 ± 0.033	0.00	87.62 ± 0.10	0.83 ± 0.06	85.27 ± 0.19	-0.10 ± 0.02	
N2t₃₅	94.89 ± 0.052	-1.38 ± 0.03	3.72 ± 0.098	1.35 ± 0.099	3.55 ± 0.096	82.99 ± 0.09	5.99 ± 0.17	70.41 ± 0.37	0.19 ± 0.02	
N2t₉₄	93.93 ± 0.042	-1.45 ± 0.07	7.19 ± 0.276	2.27 ± 0.271	6.71 ± 0.28	76.67 ± 0.37	12.38 ± 0.47	52.03 ± 1.34	0.38 ± 0.05	
N8t₀	95.10 ± 0.057	-0.74 ± 0.02	1.11 ± 0.056	0.68 ± 0.062	0.00	86.60 ± 0.16	1.55 ± 0.10	82.81 ± 0.31	-0.26 ± 0.02	
N8t₃₅	94.81 ± 0.041	-1.89 ± 0.02	5.06 ± 0.133	2.77 ± 0.125	5.43 ± 0.011	81.25 ± 0.10	8.08 ± 0.23	64.05 ± 0.53	0.22 ± 0.03	
N8t₉₄	94.17 ± 0.045	-2.24 ± 0.05	8.93 ± 0.186	4.20 ± 0.174	8.02 ± 0.19	75.28 ± 0.29	14.86 ± 0.33	44.57 ± 0.94	0.75 ± 0.04	
Art₀	94.41 ± 0.03	-1.12 ± 0.01	6.08 ± 0.06		0.00	79.03 ± 0.12	10.59 ± 0.11	58.37 ± 0.31		0.00
Art₃₅	92.56 ± 0.07	-1.34 ± 0.08	13.69 ± 0.23		7.83 ± 0.20	66.36 ± 0.34	24.42 ± 0.39	17.31 ± 1.21		-0.8 ± 0.05
Art₉₄	90.48 ± 0.21	-0.28 ± 0.09	16.96 ± 0.27		11.60 ± 0.28	59.19 ± 0.60	30.91 ± 0.53	-2.86 ± 1.73		-1.69 ± 0.27

6.4.2.2 Gelatine sized pure cellulose paper

CIE L*a*b* values are reported in Table 6.4-1. Figure 6.4-4 and Figure 6.4-5 show the changes in b* for K and N samples respectively. The general tendency was an increase in b* with aging, which translates visually by an increased yellowing. However, for K samples, this increase was constant regardless of the gelatine content, whereas for N samples, b* increased also with increasing gelatine content. Figure 6.4-6 shows that this

¹ ΔE^* versus (vs) Ct_x is the total chromatic change between the sample and the control unsized at comparable aging time.

² ΔE^* vs Xt₀ is the total chromatic change of a given sample between time t₀ and times t₃₅ or t₉₄.

³ ΔH^* vs Ct_x is the total hue change between the sample and the control unsized at comparable aging time.

⁴ ΔH^* vs Xt₀ is the total hue change of a given sample between time t₀ and times t₃₅ or t₉₄.

significant increase in b^* upon aging was accompanied by a small decrease in a^* , which corresponds visually to a decrease in the red component.

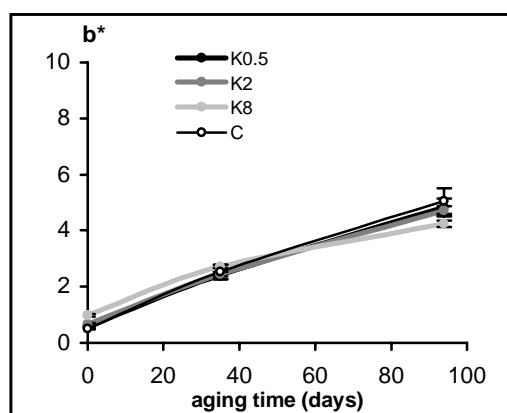


Figure 6.4-4. b^* as a function of aging time for K samples.

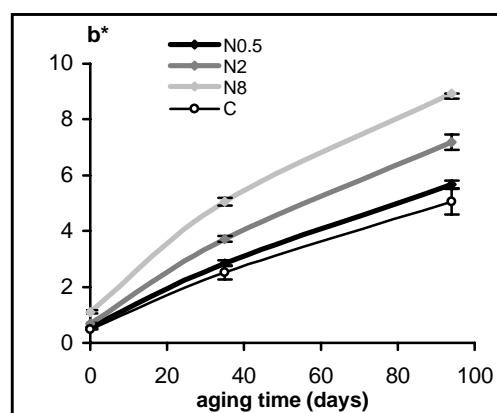


Figure 6.4-5. b^* as a function of aging time for N samples.

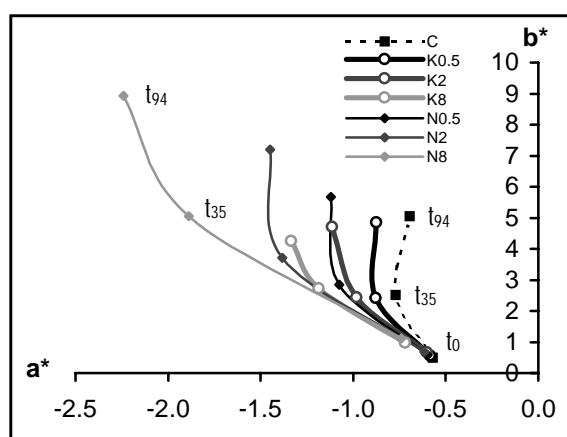


Figure 6.4-6. Changes in (a^*, b^*) for K, N and C samples, aged and unaged.

The changes in ΔE^* relative to the respective unaged in each sample category are shown in Figure 6.4-7. Here also, ΔE^* followed the same trend as b^* . N samples underwent a significantly larger colour change upon aging than both C samples and K samples (no matter the gelatine concentrations). ΔE^* relative to Nt_0 ranged from 5.27 for $N0.5t_{94}$ to 8.02 for $N8t_{94}$. For K samples, the values of ΔE^* relative to Kt_0 were smaller. Remarkably all ΔE^* values obtained for these samples were smaller than those of C, ranging from 3.55 for $K8t_{94}$ to 4.45 for $K0.5t_{94}$, when for C samples, ΔE^* of Ct_{94} relative to Ct_0 was 4.83. The threshold value for a distinct colour change to the naked eye depends to a certain extent on the observer, but a general agreement is that ΔE^* between 1.5 and 2 represents a just noticeable change.

It is also noteworthy that the rate of discolouration was higher from t_0 to t_{35} than from t_{35} to t_{94} , especially for the more discoloured samples N2 and N8. This is contrary to the degradation rate, as determined by the changes in M_r where an increase in the rate of degradation occurred on the second portion of the aging process.

As it is a relative value, ΔE^* depends on the reference a given sample is compared to. Figure 6.4-8 shows the changes in ΔE^* of the sized papers relative to C in each comparable aging category. These values of ΔE^* roughly followed the same trend as observed on Figure 6.4-7, with N samples exhibiting larger ΔE^* than K samples. Here, for both N and K samples, ΔE^* was proportional to the gelatine content. However, it has to be noted that these ΔE^* values were all relatively small, mostly below 1.5. Only N samples N2 t_{94} , N8 t_{35} , and N8 t_{94} had ΔE^* relative to C t_{94} that could be qualified as the expression of a readily noticeable colour change to the naked eye with ΔE^* of 2.27, 2.77 and 4.2 respectively.

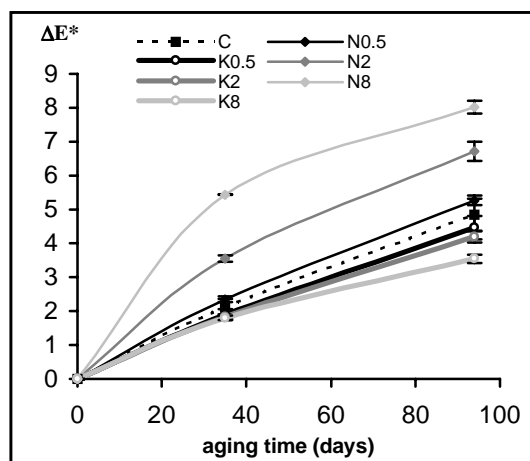


Figure 6.4-7. ΔE^* for K and N samples relative to the respective unaged sample in each category.

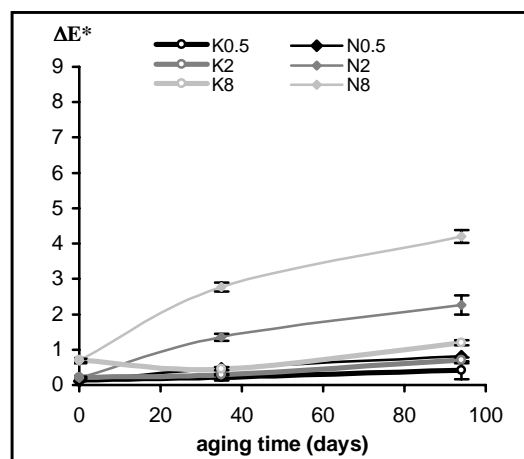


Figure 6.4-8. ΔE^* for K and N samples relative to C in each respective aging category.

The general information that colour measurements provided about gelatine sizing was that N gelatine resulted in considerably more discolouration of the papers than K gelatine. The reader is reminded that N is a pharmaceutical/food grade gelatine and contains more impurities than K, a photographic grade gelatine. Contaminants such as metallic residues or sugars could be responsible for this difference in aging behaviour. Trace metals will catalyse oxidation reactions, especially under the heat/humid conditions used in accelerated aging, and proteins in the presence of sugars can lead to Maillard reactions (see Appendix 3.1 and section 8.3.1.1.3 of Chapter 8).

For both N and K, the discolouration was relative to the amount of size in the paper, with a larger discolouration occurring for the papers with higher gelatine content with respect to C t_0 . Gelatine being naturally yellowish to light-brown, a slight yellow colouration of

the paper was expected to start with. However, in the case of K gelatine, the results showed that the yellowing rate that was strictly attributed to gelatine during aging was smaller than the overall paper yellowing rate. In other words, the contribution of K gelatine to the aging-induced discolouration of the papers was smaller than the contribution of other components in the paper and reaction parameters. In the case of Whatman No.1, no component other than cellulose is present. Therefore, the aging of cellulose was the main factor responsible for the discolouration of paper sized with K gelatine. N gelatine, as opposed to K, did significantly contribute to the aging-induced discolouration of the paper.

6.4.2.3 Arches papers

CIE $L^*a^*b^*$ values are reported in Table 6.4-1. Unaged Arches papers exhibited larger b^* values than most of the sized Whatman No.1 papers (both aged and unaged), and they yellowed even further upon aging, as shown in Figure 6.4-9. The changes in ΔE^* relative to the respective sample at t_0 were also more pronounced than for Whatman No.1 papers as shown in Figure 6.4-10. However, the same trend with an initial high rate of discolouration that tailed-off asymptotically was found.

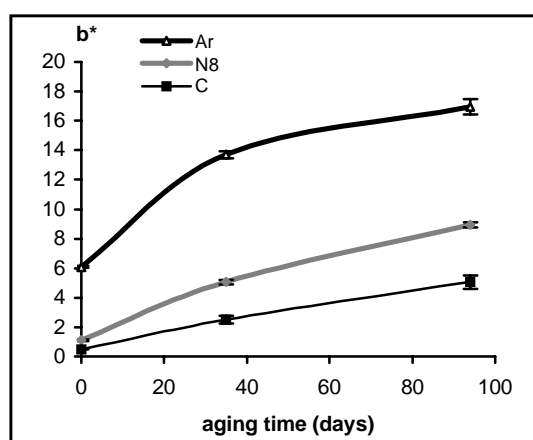


Figure 6.4-9. b^* as a function of aging time for Arches samples (compared to C and N8 samples).

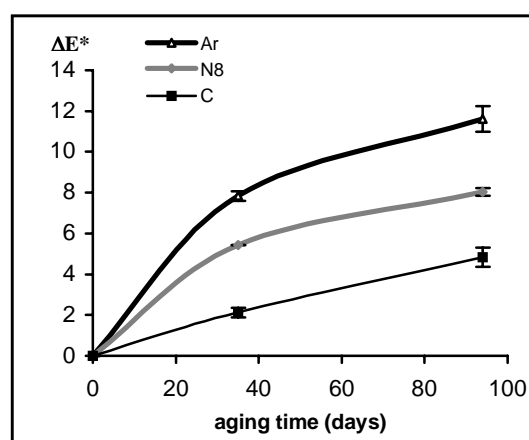


Figure 6.4-10. ΔE^* for Ar samples relative to the respective unaged sample (compared to C and N8 samples).

The reason for this high rate of yellowing of the Arches papers can be due to the paper composition, *i.e.* the nature of the fibre and the presence of additives that contribute to the yellowing. For instance, the presence aluminium sulphate (called papermakers alum) or aluminium potassium sulphate, could be responsible for increased discolouration upon aging, as alum is a source of acidity leading to degradation of the cellulose in papers. In historic papermaking, alum was added in the gelatine size. The reasons for it are detailed in the general introduction to this thesis, and the contribution of alum in the degradation

of papers is evaluated in Chapter 7. Aluminium salts are therefore quite common in modern and in historic papers, but alum is not the only source of aluminium. This element is also present in some mineral fillers such as aluminium silicate (kaolin), which is widely used as filler material.

An analysis of the Arches papers by scanning electron microscopy/energy dispersive X-ray spectroscopy (SEM/EDX) (JSM 5410 LV from JEOL, Oxford EDS) indeed evidenced the presence of aluminium.

6.4.2.4 Naturally aged Strathmore papers

CIE $L^*a^*b^*$ values for Strathmore papers are reported in Table 6.4-2. As illustrated in Figure 6.4-11, all papers sized showed larger b^* values than their unsized counterpart. Here also, ΔE^* followed the same trend: although being mostly below visual discriminating sensitivity ($\Delta E^* < 2$), all sized papers resulted in a slightly higher discolouration than their unsized counterpart (Figure 6.4-12). This corroborates our previous results of a significant contribution of the gelatine to the yellowing of the paper upon aging.

Table 6.4-2. Trichromatic values, indices (brightness, yellowness and whiteness), total chromatic and total hue difference for the Strathmore papers upon aging.

sample	L^*	a^*	b^*	ΔE^*	Brightness	YI	WI	ΔH^*
				S vs U	457	E313-96	E313-96	S vs U
S140U	92.31 ± 0.03	-1.16 ± 0.04	10.60 ± 0.08		69.53 ± 0.14	18.93 ± 0.18	31.95 ± 0.42	
S140S	91.78 ± 0.123	-1.11 ± 0.01	11.53 ± 0.185	1.07 ± 0.22	67.44 ± 0.45	20.68 ± 0.35	25.64 ± 0.32	-0.14 ± 0.03
S160U	92.16 ± 0.08	-1.14 ± 0.05	11.66 ± 0.14		68.06 ± 0.30	20.83 ± 0.29	26.59 ± 0.83	
S160S	91.86 ± 0.08	-1.07 ± 0.07	12.13 ± 0.163	0.56 ± 0.17	66.97 ± 0.30	21.75 ± 0.30	23.60 ± 0.90	-0.11 ± 0.07
S220U	92.06 ± 0.06	0.12 ± 0.05	12.23 ± 0.10		67.12 ± 0.22	22.83 ± 0.22	23.88 ± 0.59	
S220S	91.91 ± 0.08	0.26 ± 0.01	12.55 ± 0.12	0.38 ± 0.13	66.48 ± 0.28	23.52 ± 0.22	22.01 ± 0.74	-0.13 ± 0.01
S280U	90.47 ± 0.08	0.75 ± 0.06	14.51 ± 0.22		61.59 ± 0.34	27.61 ± 0.44	8.49 ± 0.99	
S280S	91.85 ± 0.03	0.33 ± 0.03	12.82 ± 0.06	2.22 ± 0.06	66.10 ± 0.11	24.06 ± 0.12	20.56 ± 0.33	0.36 ± 0.03
S320U	91.91 ± 0.09	0.39 ± 0.04	12.12 ± 0.10		66.93 ± 0.29	22.88 ± 0.22	24.02 ± 0.72	
S320S	91.89 ± 0.03	0.34 ± 0.03	12.80 ± 0.07	0.69 ± 0.07	66.20 ± 0.14	24.03 ± 0.15	20.76 ± 0.41	0.07 ± 0.03

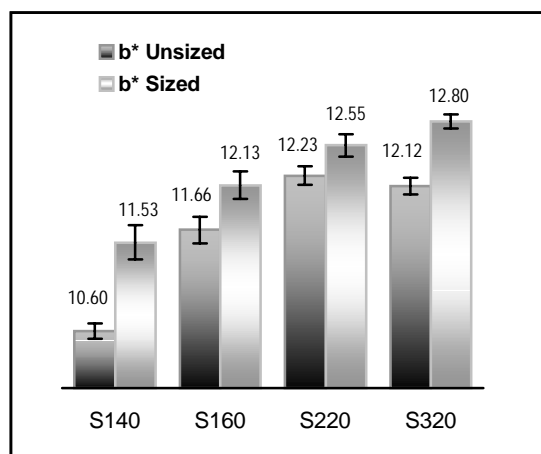


Figure 6.4-11. b^* of Strathmore papers.

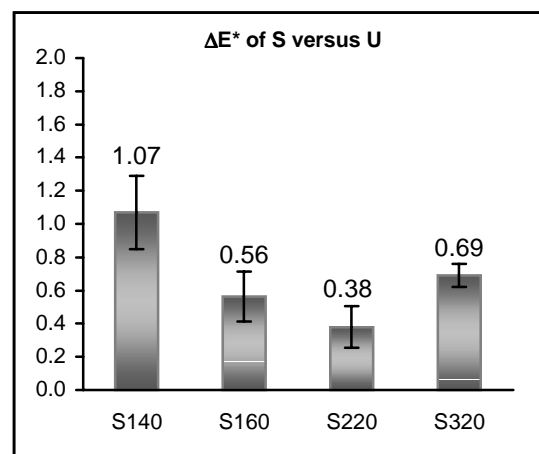


Figure 6.4-12. ΔE^* between sized and unsized Strathmore papers.

6.4.3 Conclusions on colour measurements

The results obtained for all the papers tested in the colour measurements confirmed that gelatine sized papers have generally an accrued tendency to yellow upon aging. The extent of the discolouration depends on the amount, type and purity of the gelatine in the paper. The initial yellowing caused by the gelatine in the model papers was due to the natural yellowish-brown colour of these particular gelatines. But while photographic gelatine from cattle bone (K) did not add significantly to the aging-induced discolouration, pharmaceutical/food grade gelatine from fish (N), of lower purity, played an important role in the discolouration upon aging. Arches papers displayed also significant yellowing upon aging, which could be due to the presence of aluminium salts. The results obtained with the model papers were confirmed with the naturally aged Strathmore papers.

6.5 pH of model papers

6.5.1 Experimental

The cold extract pH of the papers was measured according to the TAPPI standard method T 509 om-88 [3] to which modifications were made keeping the ratio of weight of paper to volume of water. The weight of paper was downsized to 0.5 g and the volume of water to 35 mL. The solution was purged with N_2 under low flow until a stable pH was attained, at which point bubbling was stopped to allow for a pH stabilisation, and the final reading was made. Measurements could be carried out on the model papers only, as even downsizing the sample as described above, there was not sufficient quantity of naturally aged papers.

6.5.2 Results and discussion

Table 6.5-1 reports the pH of the papers and the initial pH of the gelatine solutions used to size the papers. Each reported value is an average of three measurements. Figure 6.5-1 plots the change in pH for all the samples during aging.

Table 6.5-1. Cold extraction pH of model papers: C, K2, K8, N2, N8, and Ar, and pH of the gelatine solutions used to prepare the K and N samples.

sample	pHc.e. ¹	RSD	pHsol. ²	sample	pHc.e.	RSD	pHsol.
Ct₀	7.01	± 0.03		Art₀	6.36	± 0.03	
Ct₃₅	6.66	± 0.05		Art₃₅	6.19	± 0.02	
Ct₉₄	6.47	± 0.03		Art₉₄	5.73	± 0.02	
K0.5t₀	6.90	± 0.05	6.14	N0.5t₀	6.93	± 0.01	6.45
K0.5t₃₅	6.61	± 0.03		N0.5t₃₅	6.40	± 0.05	
K0.5t₉₄	6.11	± 0.04		N0.5t₉₄	5.58	± 0.00	
K2t₀	6.84	± 0.02	5.92	N2t₀	7.07	± 0.05	6.10
K2t₃₅	6.45	± 0.02		N2t₃₅	5.83	± 0.04	
K2t₉₄	5.84	± 0.02		N2t₉₄	5.10	± 0.00	
K8t₀	6.51	± 0.24	5.72	N8t₀	6.43	± 0.02	5.98
K8t₃₅	6.47	± 0.01		N8t₃₅	5.47	± 0.02	
K8t₉₄	6.08	± 0.02		N8t₉₄	4.83	± 0.01	

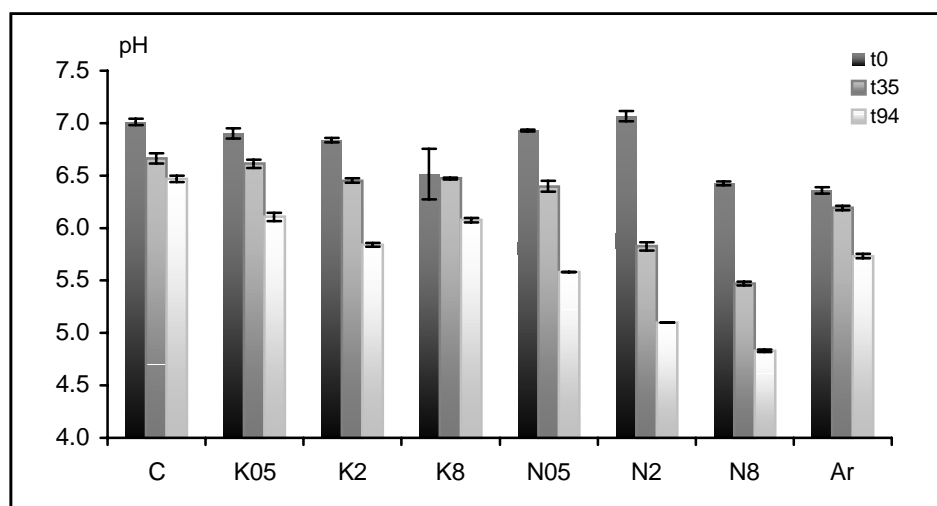


Figure 6.5-1. pH changes with aging time for the model papers: C, K2, K8, N2, N8, and Ar.

¹ pHc.e is the cold extract pH of the papers [3]

² pHsol. is the pH of the gelatine solutions used to size the papers.

The pH of the solutions used to size Whatman No.1 papers decreased with increasing gelatine concentration from 6.14 to 5.72 for K0.5 to K8 and from 6.45 to 5.98 for N0.5 to N8. The pH of the N gelatine solutions were all slightly less acidic than those of gelatine K for a given concentration.

The cold extract pH of all the papers at t_0 was higher than the pH of the corresponding size solutions, the pH of C_{t_0} being neutral.

The control paper C showed a decrease of about half a pH-unit with aging from 7.01 ± 0.03 to 6.47 ± 0.03 from t_0 to t_{94} with a steeper drop between t_0 and t_{35} than between t_{35} and t_{94} (Figure 6.5-1). Generally, higher gelatine content and longer aging time resulted in increased acidity. In the case of K8 only, the relative decrease in pH upon aging was smaller. All N samples exhibited steeper decrease in pH with time than K samples.

The decrease in pH upon aging of the Arches papers was quite limited, and contrary to the Whatman No.1 papers, it was smaller from t_0 to t_{35} than from t_{35} to t_{94} . This is probably due to the already lower initial pH of Art_0 (6.36 ± 0.03) compared to K and N samples at t_0 . It must be remembered that at t_0 , Arches papers and Whatman No.1 papers were not in a comparable “initial” state, as the former had “aged naturally” in the laboratory environment for 10 years, whereas Whatman No.1 was purchased for the purpose of this study and subsequently analysed without delay. Indeed, as demonstrated in Chapter 8, the gelatine extracted from Art_0 proved to be in fairly advanced degradation state compared to the unaged K and N gelatines, and this could account for its low initial pH.

The results of pH measurements showed that gelatine sized papers tended to be more acidic than unsized papers. This acidity was also related to the degradation state of the gelatine, to its content in the paper, and to its type and purity, as papers sized with N gelatine became more acidic upon aging than papers sized with K gelatine.

6.6 Investigation into correlations between M_r , pH and colour measurements

6.6.1 Background

How physical and chemical characteristics of polymers correlate to each other is a complex issue. The forces playing a role at the macroscopic level in the mechanical strength of a material such as paper translate at the molecular level in diverse and complex features. This is due to the nature of these varying forces on the one hand, and to the complexity of chemical composition of the material on the other.

Most commonly investigated relationships between chemical and physical characteristics of paper are molar mass of cellulose versus (1) tensile energy absorption index (TEA), (2) zero span index (Z), or (3) folding endurance (MIT) of paper, as each M_r average relates

to a specific physical characteristic. M_n relates to brittleness, M_w to tensile strength, and M_z to elongation and flexibility.

The precision in M_r is of course greatly related to the method used in the polymer characterisation. As stressed in Chapter 2, SEC is one of the most sensitive techniques in detecting early changes in M_r of cellulose. It has been shown that TEA and Z indices are not sensitive to these early changes, as initial decays are reported at already quite advanced chemical degradation states by determination with SEC [41,42,43].

The reasons for identifying such relationships are quite different whether from the point of view of industry or that of conservation research. While for industry the interest lies in a precise characterisation of a polymer for research and development or for quality control purposes, one of the main goals in conservation research is to assess the overall state of deterioration of the polymer with the aim of helping to predict the life expectancy of objects. Finding ways of increasing the longevity of cultural heritage artefacts and understanding the degradation pathways upon aging of materials is important in the design of conservation strategies. Other significant challenges include the development of appropriate techniques to easily assess both the state of conservation and of deterioration of objects by using simple, fast and non-destructive methods and, last but not least, the ability to transfer a user-friendly technology to the archivist, librarian and paper conservator. State assessment is indeed an important step in the evaluation of the conservation needs and the design of proper long-term preservation strategies when surveying a collection.

However, it is important to realise that there is no universal simple method that can reach these objectives, mainly because of the sheer variety in the materials that compose a collection, even when restricting the search to only one type of material such as paper.

Nevertheless, these parallels between macroscopic examination and molecular characterisation are necessary. Even if not universally applicable, they can inform on the state of conservation of specific classes of objects in the collections, like those particularly sensitive to certain types of deterioration factors. Conversely, other classes of objects can exhibit an unusual durability against the adversity of time, as is generally believed to be the case of historic gelatine sized papers, compared to that of modern papers.

Optical characteristics such as colour changes are non-destructive, easy to assess, and under certain conditions can be performed directly on historic artefacts. Measurements of the acidity of paper-based works and documents with aqueous extract pH, is also easily performed with an instrumentation that is affordable by most paper conservation workshops. The problem in this case is the sample size. However, recent microelectrode technology allows downsizing the sample to 1 mg of paper and below. Recent developments showed that it was possible to miniaturise the sampling to about 40 μg of paper and still obtain repeatable pH measurements [44].

Colour and pH measurements are currently often considered by the paper conservation community as important factors in assessing paper deterioration because both have usually been associated with changes in the strength of the material. This is the main reason why these measurements were performed in the frame of the present study. It seemed therefore interesting to compare the data obtained for M_r changes using SEC/MALS to the colour and pH data, in order to investigate any possible relationship in the particular case of gelatine sized papers.

6.6.2 Correlation between pH, colour measurements and M_r

The plot of M_w as a function of pH (Figure 6.6-1) shows that for all papers, the general trend associated with accrued acidity was that of a concomitant fall of M_w . Control papers showed a decay characterised by a steep slope, indicating that significant changes in M_w resulted in only small pH changes (about half unit).

For K and Ar papers, a small decrease in M_w resulted in slightly more pronounced pH decay, compared to C. For N papers this tendency was accentuated, with an initial significant decrease in pH upon aging while M_w remained almost stable, followed by a lesser decay rate that resembled the pH decay level of K papers.

As seen in section 6.3, gelatine has the ability to decrease the rate of depolymerisation of cellulose upon aging but from the results reported in section 6.5, the presence of gelatine is also accompanied by a drop in the pH of the paper. What Figure 6.6-1 shows is that these two phenomena are not consistently proportional for all sized samples.

It must be noted that the above observations are to be considered as a general trend. Precise correlations between changes in M_w consequent to acid-catalysed hydrolysis, and a buffering effect of gelatine would probably be best evaluated if instead of pH, the concentration of protons in the medium ($[H^+] = 10^{-pH}$) were plotted versus M_w . However, attempts to plot the data according to that theory did not yield additional information, as for a precise interpretation of the buffering capacity of gelatine more data points would be required for correct extrapolations.

Figure 6.6-2 and Figure 6.6-3 show plots of M_w as a function of b^* and ΔE^* . The curves are very similar to those in Figure 6.6-1. The same tendencies as observed for the changes in M_w relative to pH mirrored those of M_w relative to colour. A decay in M_w was concomitant to increasing values of ΔE^* and b^* for the respective groups of papers. Only Arches papers showed a larger increase in ΔE^* than the decrease in pH upon aging relative to M_w than any of the Whatman No.1 papers.

From these plots, the changes in pH and ΔE^* (or b^*) seemed to follow a similar trend. Figure 6.6-4 shows that indeed the decrease in pH was accompanied by a quasi-linear increment in ΔE^* for all sized papers at different rates. Except for C and Arches papers, all the data points of aged sized samples fall roughly on the same line.

Close examination of the data obtained for the control papers, led to the observation that while on the first aging portion (t_0 to t_{35}), the rate of discolouration and the decrease in pH were higher than on the second aging portion (t_{35} to t_{94}), the exact reverse phenomenon occurred with the decrease in M_w as shown in section 6.3.2.1.2. Such result could be explained if we consider that the two mechanisms of hydrolysis and oxidation occur concomitantly during the accelerated aging of the paper as proposed in section 6.4.2.1. End-group oxidation taking place firstly would result in the enhanced production of small acids and other volatile organic compounds (VOCs) that in turn would induce a larger pH decrease (soluble acids) and colour change, while also reinforcing the action of the acid-catalysed hydrolysis. Thus, the rate of depolymerisation would accelerate upon aging time, while the pH decrease and the colour change both would continue to occur but at a slightly slower pace. The present research could therefore provide supporting evidence for the theory of oxidation and hydrolysis reactions feeding each other as recently proposed by Shahani and Harrison [39].

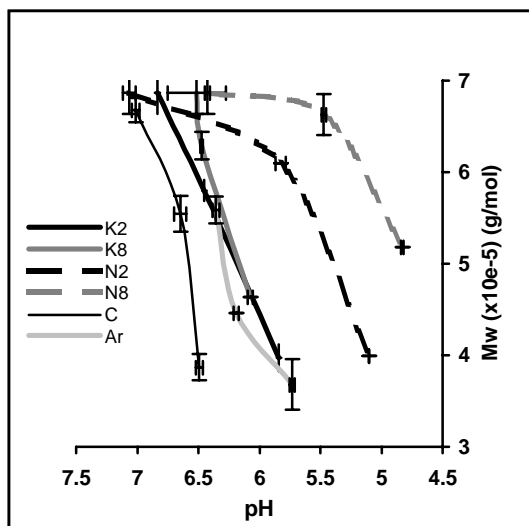


Figure 6.6-1. M_w as a function of pH.

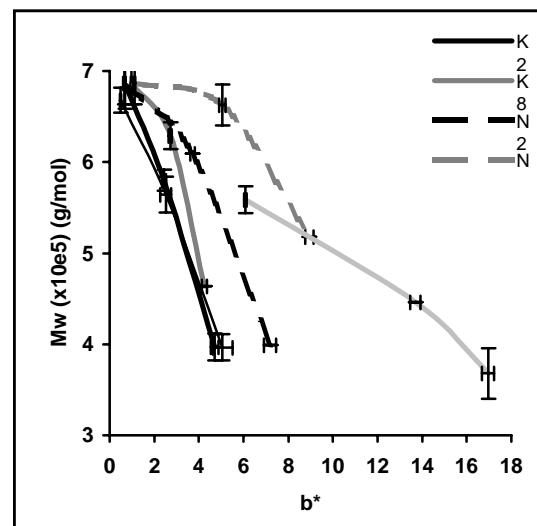


Figure 6.6-2. M_w as a function of b^* .

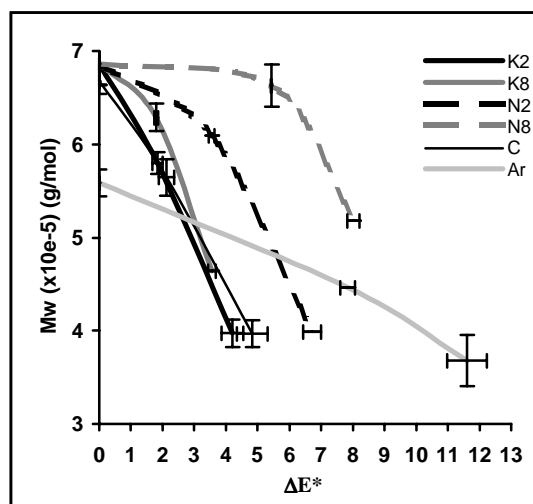


Figure 6.6-3. M_w as a function of ΔE^* .

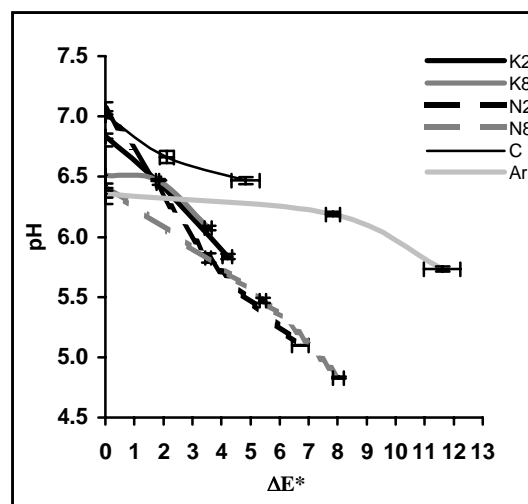


Figure 6.6-4. pH as a function of ΔE^* .

The results showed that pure cellulose sized papers, although having a higher M_r than their unsized counterpart under equal aging conditions yielded a lower pH and an accrued yellowing. These last two characteristics seemed to be closely related in the case of sized Whatman No.1 papers. In other words, the role of gelatine towards cellulose during aging, which is a protective one at the molecular level evidenced by the decrease in the rate of chain cleavage, also translates into a slightly higher acidity and accrued yellowing. This result disproves the common belief that accrued acidity and yellowing necessarily mean increased degradation, at least in the case of sized papers.

Therefore if easy tools are truly needed to assess paper deterioration, care must be taken in their choice, as the most common parameters currently used by conservation practitioners to assess paper degradation are not consistently representative indicators of the state of molecular degradation of the polymer.

6.7 Conclusion

This chapter showed that SEC/MALS was very well adapted to the study of both the differently prepared (sized) papers and the historic samples, as it yielded extremely precise determination of M_r and rms radii averages. The characterisation of MMD and the study of the conformation of cellulose in solution confirmed that LiCl/DMAc was a good solvent for paper of diverse origin and composition, as it could be applied to both model papers, containing or not containing gelatine, and to naturally aged papers.

The results from SEC/MALS experiments showed that the general impact of the gelatine in both model papers and historic papers was beneficial at the molecular level in decreasing the degradation rate. Pure cellulose sized papers had higher M_r than their unsized counterpart at any given aging time. The mechanism by which this protective effect of gelatine towards paper occurs was not investigated in the framework of the

present research. However, hypotheses can be exposed that rely both upon the physical and the chemical nature of gelatine. By covering the cellulose fibres, the protein can act as a physical barrier limiting the direct access of air and chemical reactants via the pores of the fibrillar structural units to the cellulose molecules. Gelatine in very close contact with the cellulose could have a chemical buffering effect, and this could happen at various structural levels of the fibres. The different water layers can produce different pH micro-environments at the fibre level. Of special interest is the molecular interfacial moisture layer closer to the cellulose (or hemicelluloses solid matrix). In this layer, the pH can be very acidic, due to the high ratio of protons liberated per volume of water. The amphoteric properties of gelatine could help in neutralising part of this core acidity. However, this would not be reflected by the pH measured in water extracts, due to the large amount of water used for the extraction and due to the physico-chemical equilibriums at the fibre surface.

Besides, as shown in Chapter 8, gelatine undergoes extensive hydrolysis during the heat/humidity aging of the paper. This leads to the likely possibility that the protein is more easily hydrolysed during aging than the cellulose molecules. Gelatine provides more bulky and amorphous areas more readily available to reactants than the more tightly packed cellulose fibres.

However, this work showed also that sized papers displayed lower pH and accrued yellowing, indicating that if gelatine had a protective role towards cellulose during aging reflected by a decreasing rate of chain cleavage, it nevertheless induced slightly higher discolouration and extractible acidity. The extent of these two parameters depended on the amount, type and purity of the gelatine, as well as on the presence of components other than cellulose in the paper. Photographic gelatine induced less discolouration and became less acidic than pharmaceutical/food grade gelatine. The results show that neither pH nor colour could be used as indicators of the depolymerisation, for which only M_r determination could be trusted to provide precise and accurate information.

Chemicals and materials

Lithium chloride (LiCl) and *N,N*-Dimethylacetamide (DMAc) were purchased from Acros Organics (Springfield, NJ, USA). Whatman No.1 filter paper was obtained from Fisher Scientific (Springfield, NJ, USA). Gelatine photographic type B was purchased from Kind and Knox Gelatine Inc. (Sioux City, IA, USA) and gelatine HMW type A was purchased from Norland Products Inc. (New Brunswick, N.J., USA).

Instruments

The climate chamber SE-600-3 was from Thermotron Industries (Holland, MI, USA), and Versatenn was from Tenney Environmental (Parsippany, NJ, USA). The spectrophotometer UltraScan XE was from Hunter Associates Laboratory, Inc. (Reston, VA, USA). Multiangle light scattering detector Dawn EOS and interferometric differential refractometre Optilab DSP were from Wyatt Technologies Corp. (Santa Barbara, CA, USA). Additional instrumentation relative to the separation and analysis by SEC/MALS/RI not cited in the present chapter are in the section Instruments of Chapter 4.

References

1. Henry, W., *Book and Paper Group Annual*, 5, The Book and Paper Group of the American Institute for Conservation of Historic and Artistic Works (1986) 108-119.
2. CIE 15.2-1986, *Colorimetry*, 2nd Ed., Commission Internationale de l'Éclairage (1986).
3. T 509 om-88, *TAPPI test methods*, Technical Association of the Pulp and paper Industry, TAPPI press, Atlanta (1988).
4. Diderot, J.J. *Encyclopédie ou Dictionnaire Raisonné de Sciences, des Arts et des Métiers, par une Société de Gens de Lettres* 11, A. Neufchastel, Samuel Faulche et Compagnie (1765).
5. De Lalande, J.J.J.F. *Art de faire le papier*, Académie Royale des Sciences (1761).
6. Barrett, T., Mosier, C., *J. Am. Inst. for Conservation*, 34 (1995) 173-186.
7. Schaeffer, T.T., *J. Am. Inst. for Conservation*, 34 (1995) 95-105.
8. Green, S.B. *Conference Papers Manchester 1992*, Institute of Paper Conservation, Fairbrass, S. Ed. (1992) 197-200.
9. Balston, T. *The Mill Ledger, James Whatman, Father and Son*, Balston, T. Ed, James Whatman, Father and Son, Methusen, London (1957) 59.
10. Norris, F.H. *Paper and Paper Making*, Ch.16, Oxford University Press (1952) 228.
11. Sanburn, W.H. *Personal Folder Notebook*, Waroronoro Paper Cie, Mass. (1909).
12. Barrett, T. *Paper Conservator*, 13 (1989) 7-27.
13. T 412 om-94, *TAPPI test methods*, Technical Association of the Pulp and paper Industry, TAPPI press, Atlanta, US (1994).
14. McCormick-Goodhart, M.H. *J. Imaging Sci. and Technol.*, 39, 2 (1995) 157-162.
15. Adelstein, P.Z.; Bigourdan, J.-L. and Reilly, J.M. *J. Am. Inst. Conserv.*, 36 (1997) 193-206.
16. Silva, A.A. and Laver, M.L. *Tappi J.*, 80, 6 (1997) 173-180.
17. Pincus, P. *Macromolecules*, 9 (1976) 386-388.
18. De Gennes, P.G. *Scaling Concepts in Polymer Physics*, Cornell University Press, Ithaca, New York (1979).
19. Laguna, M.T.R.; Medrano, R.; Plana, M.P. and Tarazona, M.P. *J Chromatogr. A.*, 919 (2001) 13-19.
20. Laguna, M.T.R. and Tarazona, M.P. *Polymer*, 42 (2001) 1751-1756.
21. Ott, E.; Spurlin, H.M. and Grafflin, M.W. *Cellulose and Cellulose Derivatives*, 2nd Ed., Wiley, New York (1971).
22. Fengel, D. and Wegener, G. *Wood: Chemistry Ultrastructure, Reactions*, Walter de Gruyter, Berlin (1984).
23. Nevell, T.P., *Cellulose Chemistry and its Applications*, Ch. 9, Nevell, T.P. and Zeronian, S.H. Eds, Wiley, New York (1985).
24. Whitmore, P.M. and Bogaard, J. *Restaurator*, 15 (1994) 26-45.
25. Ekamstam, A. *Ber. Dtsch. Chem. Ges. A.*, 69 (1936) 553-559.
26. Nevell, T.P., *Cellulose Chemistry and its Applications*, Ch. 9, editors Nevell T.P. and Zeronian S.H., Ellis Horwood Series Chemical Science (1985) 225.
27. Zou, X., Gurnagul, N., Uesaka, T. and Bouchard, J., *Polym. Deg. and Stab.*, 43 (1994) 393-402.
28. Emsley, A.M. and Heywood, R. *Cellulose*, 4 (1997) 1-5.
29. Hill, D.J.T.; Le, T.T.; Darveniza, M. and Saha, T. *Polym. Degrad. Stab.*, 48 (1995) 79-87.
30. Elmsley, A.M; Ali, M and Heywood, R.J. *Polymer*, 41 (2000) 8513-8521.
31. Picton, L.; Merle, L. and Muller G. *Int. J. Polymer & Characterization*, 2 (1996) 103-113.

-
32. Browning, B.L. *Analysis of Paper*, Marcel Dekker Inc., New York (1969).
33. Odegaard, N.; Carroll, S. and Zimmt, W.S. Material characterization tests for objects of art and archeology, Archetype Publications Ltd, London (2000).
34. Aitken, Y; Cadel, F. and Voillot, C., *Constituants fibreux des pâtes, papiers et cartons. Pratique de l'analyse*, EFPG et CTP, Ecole Française de Papèterie et des Industries Graphiques, Ed. 1. (1988).
35. Pionteck, H. and Berger, W. *Cellulose*, 3 (1996) 127-139.
36. Parks, E.J.; Guttman, C.M.; Jewett, K.L. and Brinckman, F.E. *NISTR 4456, Report prepared for the National Archives and Records Administration. U.S. Department of Commerce*, National Institute of Standards and Technology, Institute for Materials Science and Engineering, Polymers Division (1990).
37. Shahani, C.J.; Harrison, G.; Hengemihle, F.H.; Lee, S.B.; Sierra, M.L.; Song, P. and Weberg, N. *ISR Annual Report*, Preservation research and testing Division, Library of Congress, Washington, DC, (1998).
38. Dupont, A-L. and Tétreault, J. *Studies in Conservation*, 45 (2000) 201-210.
39. Shahani, C.J. and Harrison, G. IIC Congress: *Works of Art on Paper, Books, Documents and Photographs. Techniques and Conservation*, Daniels, V.; Donithorne, A. and Smith, P. (Eds), Int. Inst. for Conservation, London (2002) 189-192.
40. Dupont, A-L. and Vasseur, F., unpublished results.
41. Zou, X.; Gurnagul, T.; Uesaka, T. and Bouchard, J. *Polym. Degradation and Stability*, 43 (1994) 393-402.
42. Jerosch, H. *Evaluation de l'état de dégradation de la cellulose/holocellulose dans différents types de papiers par chromatographie d'exclusion stérique*, Thèse de Doctorat, Université Versailles-St. Quentin-En-Yvelines (2002).
43. Jerosch, H.; Lavédrine, B. and Cherton, J-C. IIC Congress: *Works of Art on Paper, Books, Documents and Photographs. Techniques and Conservation*, Daniels, V.; Donithorne, A. and Smith, P. (Eds), Int. Inst. for Conservation, London (2002) 108-113.
44. Saverwyns, S.; Sizaire, V. and Wouters, J. *Preprints ICOM-Committee for Conservation*, Rio de Janeiro (2002) 628-634.

Chapter 7. The influence of gelatine and alum in paper studied with SEC/MALS, pH and colour measurements

Abstract

The developed method of analysis of cellulose dissolved in lithium chloride/N,N-dimethylacetamide(LiCl/DMAc) by size-exclusion chromatography (SEC) using multiangle light scattering (MALS) and differential refractive index (DRI) detection is applied to the study of model papers sized with gelatine and alum (aluminium potassium sulphate hydrate). In this study, alum is found to considerably accelerate the rate of hydrolysis of the cellulose upon aging. Gelatine has in this case a marked protective role towards cellulose, as its alum-induced degradation is significantly hampered in the presence of gelatine. Moreover, the alum dramatically increases both the acidity and the discolouration of the papers upon aging. In that respect, compared to the results obtained by the determination of the molar mass (M_r) with SEC/MALS/DRI, neither the pH nor the colour measurements are found to be good indicators of the state of degradation of papers that contain gelatine and alum. However, for those papers containing only alum and prepared as reference in the evaluation of its impact, pH is found to correlate well with the changes in M_r . Both parameters display an asymptotical decrease versus the alum concentration, and a threshold value situated between 1 and 1.5 g L⁻¹ of alum is determined below which no changes in either pH or M_w (weight-average molar mass) can be detected. This limiting value of M_w was found to be 150,000 g mol⁻¹.

7.1 Introduction

Aluminium salts, known as alum, were added to gelatine almost immediately following the early use of gelatine as size in western paper mills in the fourteenth century. The presence of alum in fifteenth century papers was verified by Barrett [1]. Alum had a preserving role by retarding biodecomposition [2], it also had the property of fluidifying the size solution and helping bind the gelatine more tightly to the paper substrate. Alum is still commonly used in the paper industry as fluid retention agent during sheet formation, and for rosin sizing. In the photography industry alum is used as it acts as a gelatine hardener for silver-bromide photographs. The use of alum in papermaking throughout western history is detailed in the general introduction to this research.

Unfortunately, alum is a source of acid in the paper, by forming sulphur compounds with water. Many cellulose research studies have been dedicated to the determination and characterisation of the deleterious effects that alum has in paper when combined with rosin. Alum/rosin sizing in addition to the poor quality of the paper it was used with, *i.e.* groundwood mechanical pulp paper, are responsible for the limited stability of most of the papers produced from the mid-nineteenth to the mid-twentieth centuries. However, to our knowledge, the effect of alum used in conjunction with gelatine for sizing has never been studied.

The aim of this chapter is to investigate how the addition of alum in gelatine used for sizing, which was common practice in papermaking from 14th to 18th century and beyond, in the case of artists' papers, affects the behaviour of paper during aging. This was carried out by comparing the characteristics of gelatine/alum sized papers with alum-only containing papers and with gelatine-only sized papers (characterised in Chapter 6). The same methodology as in Chapter 6 was followed, namely, the molar mass (M_r) and the rms radii of cellulose were determined, and changes in molar mass distribution (MMD) were monitored using size-exclusion chromatography with on-line multi-angle light scattering and refractive index detection (SEC/MALS/DRI). Trichromatic values CIE $L^*a^*b^*$ and cold extraction pH were determined as well.

7.2 Description of the model papers studied

7.2.1 Preparation of the samples

Various amounts of alum in the form of the double salt aluminium potassium sulphate [$\text{AlK}(\text{SO}_4)_2 \cdot 12\text{H}_2\text{O}$] were added to solutions of gelatine type B Gelita Type 8039, Lot 1, from Kind and Knox, Inc. (specifications data sheet in Appendix 6-1). The gelatine was prepared with a concentration of 8.3 g L^{-1} in deionised water (milli-Q, Millipore). This concentration resulted in a gelatine uptake of 2% in the paper (dry wt/dry wt) (calculations are detailed in Appendix 6-2). According to historic traditional recipes, this was representative of medium gelatine content in paper [3]. Varying concentrations of alum were added to these solutions: 0.083 g L^{-1} , 0.83 g L^{-1} and 2.49 g L^{-1} , *i.e.* 1%, 10% and 30% (wt alum / wt gelatine). These alum contents in paper were chosen according to historical and modern sizing recipes, in order to cover the wide range of alum concentration used reported in the literature [4,5,6,7,8,9,10].

The model paper was Whatman No.1 filter paper, and was manually sized by immersing each sheet (150 mm x 190 mm) one at a time in the aqueous gelatine/alum solutions in a thermostated water bath kept at 40°C. The papers sized with these solutions were abbreviated KA1, KA10 and KA30. A second set of samples was prepared by immersing paper sheets in aqueous solutions of alum in the same concentrations as above, *i.e.* 0.083 g L^{-1} , 0.83 g L^{-1} and 2.49 g L^{-1} . The papers immersed in these solutions were abbreviated

A1, A10 and A30. After immersion in gelatine/alum or alum-only, the papers were air-dried in ambient conditions by hanging as shown in Figure 6.2-1 of Chapter 6.

7.2.2 Artificial aging

Artificial aging conditions of the papers were identical to those of the samples sized with gelatine only: 80°C and 50% relative humidity (rH). Paper sheets were suspended individually in a climate chamber Versatenn (Tenney Environmental) for thirty-five and ninety-four (t_{35} and t_{94}) days. The aging conditions were chosen in order to remain below the glass transition temperature T_g of gelatine [11,12] for the reasons mentioned in section 6.2.1.2 of Chapter 6. In each category, a set of papers was kept in the dark according to the TAPPI standard T 412 om-94 [13] conditions, at 23°C and 50% rH as a reference for unaged conditions.

7.3 Degradation of cellulose characterised by SEC/MALS

7.3.1 Experimental: sample preparation and chromatographic procedure in LiCl/DMAc

Defibrillation of the paper and sample preparation, solvent, activation procedure of cellulose, and dissolution method in LiCl/DMAc are reported in sections 3.2.1.2 and 3.2.4 of Chapter 3. The instrumentation, the SEC/MALS set-up and the method in LiCl/DMAc are reported in section 4.2.3 of Chapter 4.

7.3.2 Results and discussion

7.3.2.1 The impact of alum in the model papers

The presence of alum in the papers resulted in a tremendous increase in the degradation of cellulose upon aging. Figure 7.3-1 shows the significant shift of the MMD profiles towards low- M_r that occurred following 35 days of aging for all the papers immersed in alum solutions (A1 t_{35} , A10 t_{35} and A30 t_{35}). Even for the lowest alum content samples A1 t_{35} , M_r averages suffered a drastic decrease, with $M_n = 2.050 \times 10^5 \text{ g mol}^{-1}$, $M_w = 3.785 \times 10^5 \text{ g mol}^{-1}$ and $M_z = 5.985 \times 10^5 \text{ g mol}^{-1}$ (Table 7.3-1). This corresponds to 37%, 31% and 29% decreases respectively with respect to C t_{35} (Table 7.3-2, row 8).

The degradation was further accelerated for the high alum content papers: M_w was $1.744 \times 10^5 \text{ g mol}^{-1}$ for A10 t_{35} and $1.318 \times 10^5 \text{ g mol}^{-1}$ for A30 t_{35} , *i.e.* 68% and 76% decreases respectively compared to C t_{35} (Table 7.3-2, rows 9 and 10). Given the advanced degradation state of these papers following just 35 days of aging, and due to time

constraints, it was deemed unnecessary to carry out SEC/MALS analysis of those alum-only samples that had been aged for 94 days.

Table 7.3-1. M_r averages and polydispersity indices of model papers aged and unaged: KA, A and C samples.

	AVG $M_n \times 10^{-5}$ g mol ⁻¹	RSD % M_n	AVG $M_w \times 10^{-5}$ g mol ⁻¹	RSD % M_w	AVG $M_z \times 10^{-5}$ g mol ⁻¹	RSD % M_z	AVG $M_p \times 10^{-5}$ g mol ⁻¹	RSD % M_p	AVG PD (M_w/M_n)	RSD % PD	AVG M_z/M_w	RSD % M_z/M_w
Ct₀	3.96	7.8	6.68	2.0	10.09	4.5	6.24	5.5	1.70	7.1	1.51	4.0
Ct₃₅	3.24	4.6	5.45	2.7	8.42	10.7	5.23	5.7	1.69	5.3	1.52	6.0
Ct₉₄	2.07	7.6	3.81	3.5	6.06	5.6	3.48	6.2	1.85	7.0	1.57	4.2
KA1t₃₅	2.97	7.3	5.31	3.9	8.22	4.8	5.15	2.5	1.80	5.9	1.55	3.2
KA1t₉₄	1.93	5.9	3.49	2.0	5.62	3.9	2.85	12.6	1.82	8.1	1.61	4.1
KA10t₀	4.00	N/A ¹	6.91	N/A	10.85	N/A	6.22	N/A	1.72	N/A	1.57	N/A
KA10t₃₅	2.23	5.2	3.95	3.3	6.09	2.9	3.56	1.9	1.77	2.7	1.54	1.2
KA10t₉₄	1.34	9.3	2.48	3.7	4.19	15.0	2.04	8.0	1.86	10.0	1.69	12.3
KA30t₀	3.62	14.4	6.33	8.0	9.69	4.0	5.69	10.1	1.77	10.2	1.54	4.13
KA30t₃₅	0.95	N/A	1.74	N/A	3.50	N/A	1.44	N/A	1.84	N/A	1.99	N/A
A1t₀	3.68	N/A	6.88	N/A	11.06	N/A	6.44	N/A	1.87	N/A	1.61	N/A
A1t₃₅	2.05	N/A	3.79	N/A	5.99	N/A	3.30	N/A	1.85	N/A	1.58	N/A
A10t₀	3.97	N/A	6.50	N/A	9.57	N/A	6.18	N/A	1.64	N/A	1.47	N/A
A10t₃₅	0.89	N/A	1.74	N/A	2.87	N/A	1.46	N/A	1.95	N/A	1.64	N/A
A30t₀	3.78	N/A	6.29	N/A	9.24	N/A	6.13	N/A	1.67	N/A	1.47	N/A
A30t₃₅	0.75	N/A	1.32	N/A	2.15	N/A	1.08	N/A	1.75	N/A	1.63	N/A

Table 7.3-2. Percent differences in M_r averages between aged and unaged model papers: KA, A and C samples.

row	samples	ΔM_n %	ΔM_w %	ΔM_z %	ΔM_p %
1	Ct₀ – Ct₃₅	18	18	17	16
2	Ct₀ – Ct₉₄	48	43	40	44
3	Ct₃₅ – KA1t₃₅	8	3	2	2
4	Ct₉₄ – KA1t₉₄	7	8	7	18
5	Ct₃₅ – KA10t₃₅	31	27	28	32
6	Ct₉₄ – KA10t₉₄	35	35	31	41
7	Ct₃₅ – KA30t₃₅	71	68	58	72
8	Ct₃₅ – A1t₃₅	37	31	29	37
9	Ct₃₅ – A10t₃₅	72	68	66	72
10	Ct₃₅ – A30t₃₅	77	76	75	79

¹ N/A is reported when only two analyses were done

Figure 7.3-2 and Figure 7.3-3 show the signals of the light scattering (LS) detector (90° angle photodiode) and the differential refractometer (DRI) as a function of elution volume (V_e), respectively. The lines across the chromatograms represent the trend for the variation of molar mass with V_e . The actual values, represented by the scatter points, indicate a significant dispersion from the trend lines at the limiting values of M_r . Besides the separation range of the column set, this dispersion shows the limits of the detection for the very-high- and very-low- M_r molecules, as these are in very low concentration (small DRI signal). The DRI peaks are a close reflection of the MMD profiles on the differential molar mass graphs. The LS signals of A10t₃₅ and A30t₃₅ have considerably low intensity, which accounts for a significantly low M_r as the cellulose of these two samples was extremely degraded.

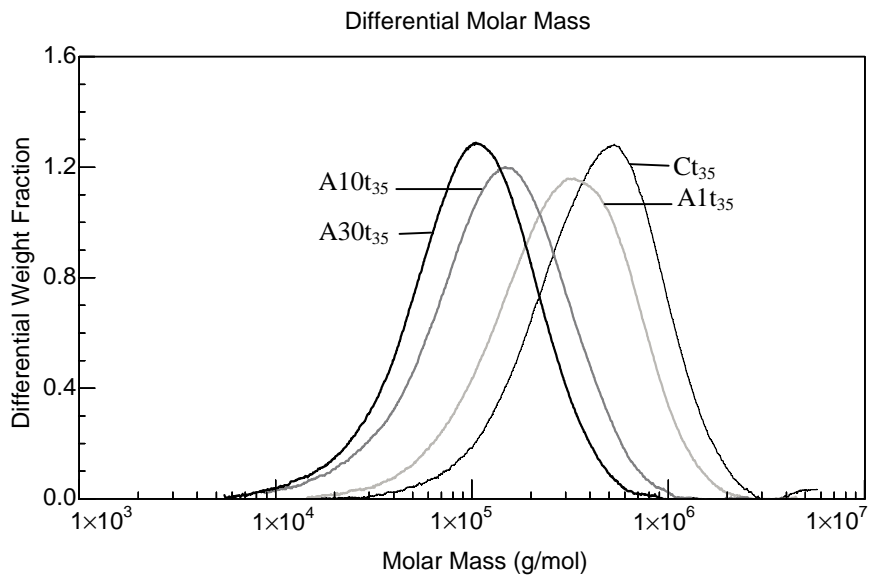


Figure 7.3-1. Overlaid differential molar mass graphs of A1t₃₅, A10t₃₅, A30t₃₅ and Ct₃₅.

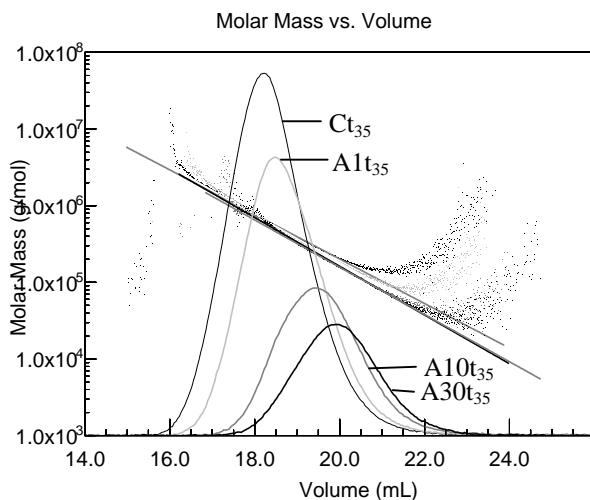


Figure 7.3-2. Overlaid 90° angle photodiode LS signals of A1t₃₅, A10t₃₅, A30t₃₅ and Ct₃₅.

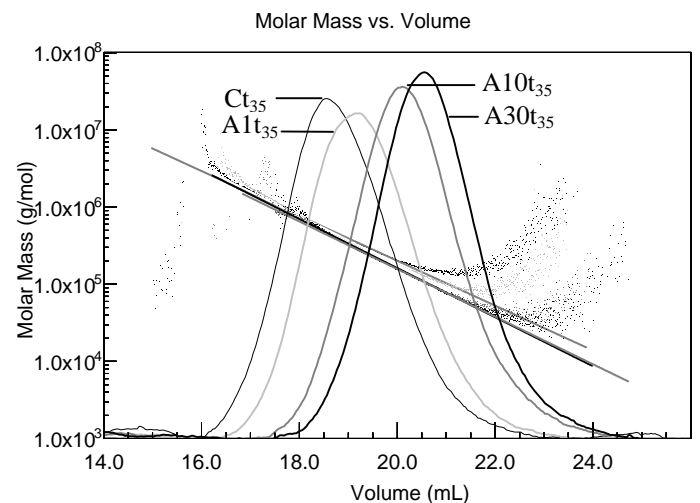


Figure 7.3-3. Overlaid DRI signals of A1t₃₅, A10t₃₅, A30t₃₅ and Ct₃₅.

The plot of rms radii versus V_e shows a regular linear decrease for all the alum containing papers aged for 35 days (Figure 7.3-4), which indicated a normal chromatographic elution with no adsorption.

Table 7.3-3 reports the average values obtained for the root mean square radii averages r_n , r_w and r_z of the papers containing alum, as well as the average values of the slopes q . The values of q are also indicated in Figure 7.3-5, which is the log-log plot of rms radii versus M_r . The values of q are determined between 0.5 and 0.6, and point to a random coil conformation of cellulose in solution. However, they were lower and closer to 0.5 when both aging and alum concentration increased, indicating the polymer was in those cases somewhat closer to theta conditions, *i.e.* below optimal conditions. The same observation was made for unsized aged papers and for gelatine sized papers (section 6.3.2. of Chapter 6), and was attributed to the increased presence of oxidised groups along the cellulose chains, thereby decreasing solvation properties.

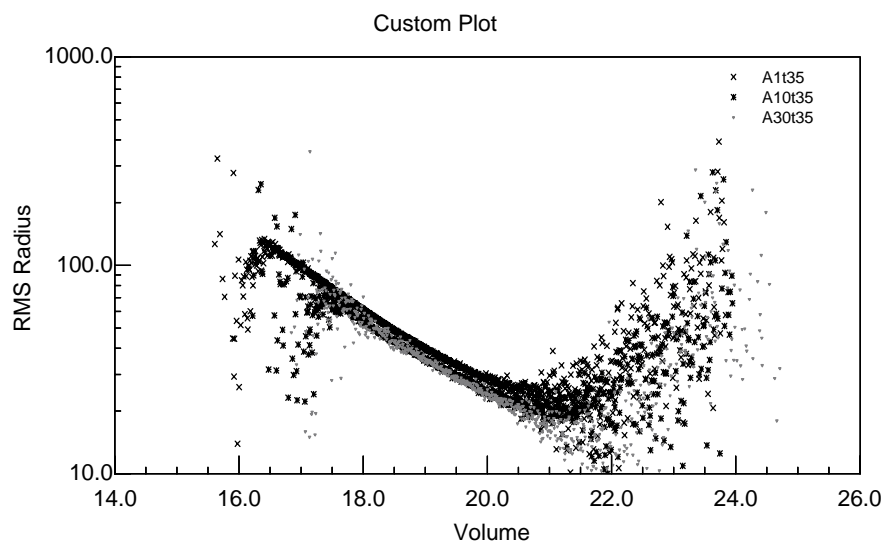


Figure 7.3-4. Overlaid rms radii as a function of V_e of A1t₃₅, A10t₃₅ and A30t₃₅.

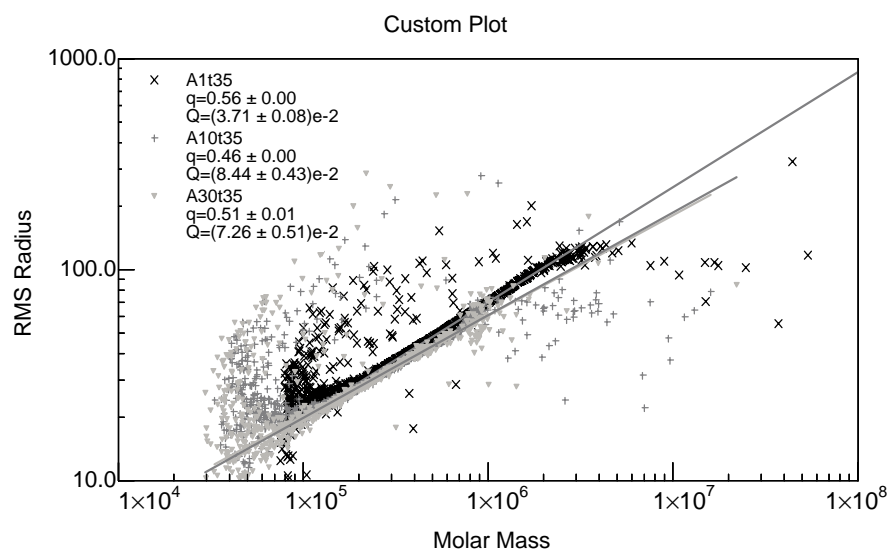


Figure 7.3-5. Overlaid average rms radii as a function of M_r (log-log scale) of A1t₃₅, A10t₃₅ and A30t₃₅.

Table 7.3-3. Average rms radii averages and values of q of model papers aged and unaged: KA, A and C samples.

	AVG r_n (nm)	RSD % r_n	AVG r_w (nm)	RSD % r_w	AVG r_z (nm)	RSD % r_z	AVG q	RSD % q
Ct₀	45.2	5.1	62.4	1.3	80.3	2.1	0.59	5.6
Ct₃₅	40.4	2.7	55.3	2.2	71.6	6.0	0.57	5.0
Ct₉₄	30.5	4.7	43.1	1.3	56.3	2.6	0.54	7.3
KA1t₃₅	37.4	3.5	53.1	0.7	68.9	1.4	0.56	2.8
KA1t₉₄	28.9	5.4	41.0	1.2	54	0.9	0.58	2.8
KA10t₀	43.3	N/A	62.7	N/A	82.2	N/A	0.58	N/A
KA10t₃₅	30.6	3.1	42.6	1.3	54.6	1.3	0.53	3.2
KA10t₉₄	23.0	2	32.0	2.3	42.2	8.3	0.46	7.8
KA30t₀	43.3	6.6	60.3	2.2	77.8	1.4	0.56	10.2
KA30t₃₅	19.5	N/A	25.9	N/A	35.4	N/A	0.40	N/A
A1t₀	43	N/A	62.7	N/A	83.4	N/A	0.58	N/A
A1t₃₅	29.5	N/A	42.1	N/A	55.0	N/A	0.56	N/A
A10t₀	45.1	N/A	61.5	N/A	78.4	N/A	0.57	N/A
A10t₃₅	19.0	N/A	26.4	N/A	33.8	N/A	0.46	N/A
A30t₀	42.2	N/A	57.7	N/A	73.0	N/A	0.54	N/A
A30t₃₅	17.1	N/A	22.5	N/A	28.6	N/A	0.51	N/A

The changes in M_w showed that all papers immersed in alum solutions exhibited significantly larger decrease in M_w upon aging than the control papers (Figure 7.3-6). The grey curve in Figure 7.3-7 illustrates that at time t_{35} this decrease in M_w as a function of the alum concentration was asymptotical, and reached a plateau for concentrations of alum above a value situated roughly between 1 and 1.5 g L⁻¹. This is a threshold value beyond which M_w does not decrease much further. The corresponding value of M_w was found in the range 1.4×10^5 to 1.6×10^5 g mol⁻¹, *i.e.* DP_w in the range 800-1000. This is a limiting value of M_w ; the depolymerisation has reached a point where it cannot proceed further at the same speed. The changes in the values of the z-average rms radii followed the same trend as those in M_w , as shown in Figure 7.3-8.

Figure 7.3-9 shows the polydispersity index M_z/M_w as a function of M_n . The tendency was for the index to increase to varying degrees with time, especially for A10 and A30, but only by about 10%, which is not significant enough to clearly indicate that in the papers immersed in alum the cellulose of high- M_r underwent cleavage at preferential sites upon aging. For A1 the polydispersity index remained unchanged, which was consistent with the behaviour of C on the first aging portion. However, it has to be noted that only two data point for samples containing alum can merely be indicative of a trend in the polydispersity.

Figure 7.3-10 clearly indicates the impact of the alum concentration on the degradation rate of cellulose. The plots of $(1/M_{wt} - 1/M_{wt0})$ as a function of aging time yield the rate of

glycosidic bond breakage of cellulose, which is the slope k (see section 6.3.2.1.2 of Chapter 6 and Appendix 6-3). Unfortunately, the data points for A1t₉₄, A10t₉₄ and A30t₉₄ are missing because as mentioned earlier, these three samples could not be analysed in SEC/MALS. However from the steep slopes obtained for A10 and A30, it can be extrapolated that the levelling-off degree of polymerisation (LODP) asymptote would likely be attained sometime between t₃₅ and t₉₄.

As was explained in Chapter 1, the values of LODP depend on the fibre source and are an indication of the size of the crystallites and fibrillar aggregations. The values of DP_w for A10t₃₅ and A30t₃₅ were respectively 1076 ($M_w = 0.892 \times 10^5 \text{ g mol}^{-1}$) and 813 ($M_w = 0.754 \times 10^5 \text{ g mol}^{-1}$) (Table 7.3-1). The values of LODP of cotton cellulose reported in the literature vary but are usually comprised between 150 and 400 [14]. The range 150-250 is usually accepted as the lower limit below which the paper loses all its mechanical strength [15]. However, it is worth mentioning that these values have usually been determined using viscosity measurements [14], which as was demonstrated in Chapter 5, have the inconvenience of considerably underestimating the DP. Additionally, as was hypothesised in Chapter 5 (p.101), the possibility that the values of M_w for cellulose in LiCl/DMAc are overestimated by the MALS detector due to the nature of the links between cellulose and solvent, namely hydrogen bonding between hydroxyl groups and the chloride anion of LiCl could not be ruled out. In this case the values of DP_w found experimentally in the present study would also be overestimated. Recently Jerosch [16] proposed a critical M_w value of 10^5 g mol^{-1} ($DP_w \approx 610$) as a limit below which the fibres in any type of paper tested, start losing their mechanical strength properties very quickly, as measured by the zero-span index Z. It has to be noted that the author used the dissolution method of cellulose in LiCl/DMAc, and therefore that critical M_w could also be slightly overestimated.

The polydispersity of the samples containing alum and the polydispersity of the control samples were not significantly different (Table 7.3-1). This is consistent with a degradation mainly governed by acid-catalysed hydrolysis reactions where random cleavage occurs.

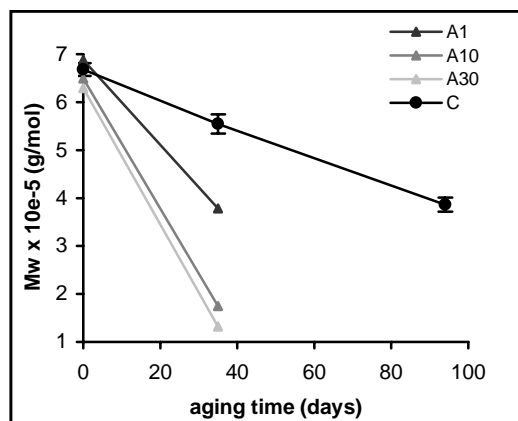


Figure 7.3-6. M_w as a function of aging time for A and C samples.

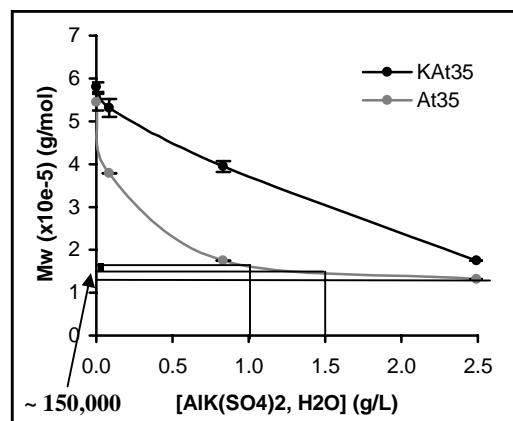


Figure 7.3-7. M_w as a function of concentration of alum for A and C samples.

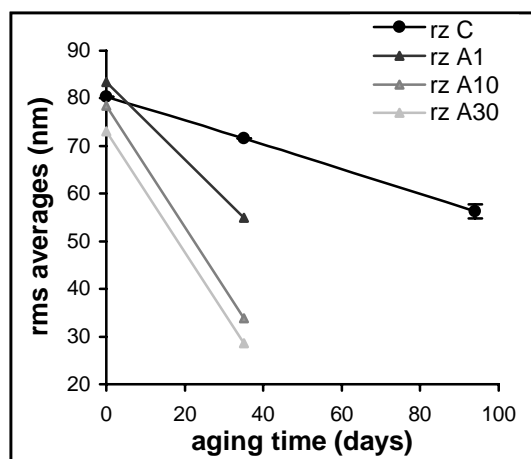


Figure 7.3-8. z-average rms radii as a function of aging time for A and C samples.

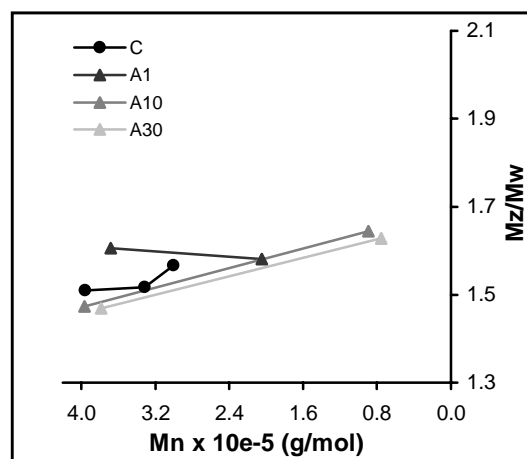


Figure 7.3-9. Polydispersity index M_z/M_w of A and C samples as a function of M_n .

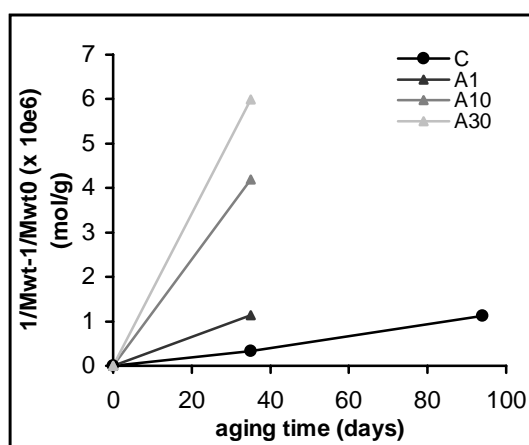


Figure 7.3-10. Plot yielding the glycosidic bond cleavage rate k' ($\text{mol g}^{-1} \text{days}^{-1}$) for A and C samples.

7.3.2.2 The impact of gelatine/alum in the model papers

The papers sized with gelatine and alum degraded more than the control papers. For KA10_{t35} and KA30_{t35}, M_w was $3.952 \times 10^5 \text{ g mol}^{-1}$ and $1.744 \times 10^5 \text{ g mol}^{-1}$ respectively (Table 7.3-1), which corresponds to a decrease of 27% and 68% with respect to the M_w of Ct₃₅ (Table 7.3-2, rows 5 and 7). At t_{94} , the same trend was observed; the percent decreases in M_w for KA1_{t94} and KA10_{t94} with respect to Ct₉₄ were 8% and 35% respectively (Table 7.3-2, rows 4 and 6).

Figure 7.3-11 shows the differential MMD profiles at t_{35} of the samples sized with gelatine/alum (KA1_{t35}, KA10_{t35} and KA30_{t35}) compared to the control samples (Ct₃₅). Figure 7.3-12 and Figure 7.3-13 are the signals of the LS (90° angle photodiode) and the DRI detectors as a function of V_e respectively. The LS signal of KA30_{t35} has about the same amplitude as the LS signal of A10_{t35}. These two samples had approximately the same M_w (Table 7.3-1).

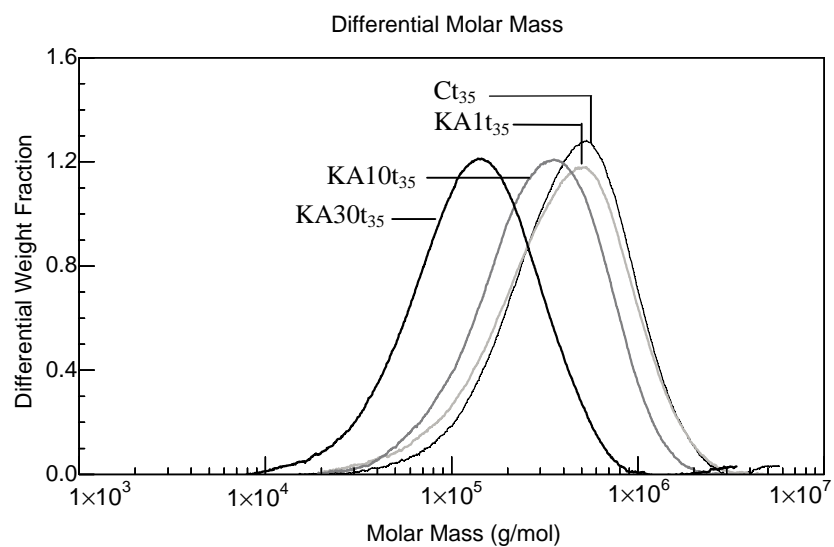


Figure 7.3-11. Overlaid differential molar mass graphs of $KA1t_{35}$, $KA10t_{35}$, $KA30t_{35}$ and Ct_{35} .

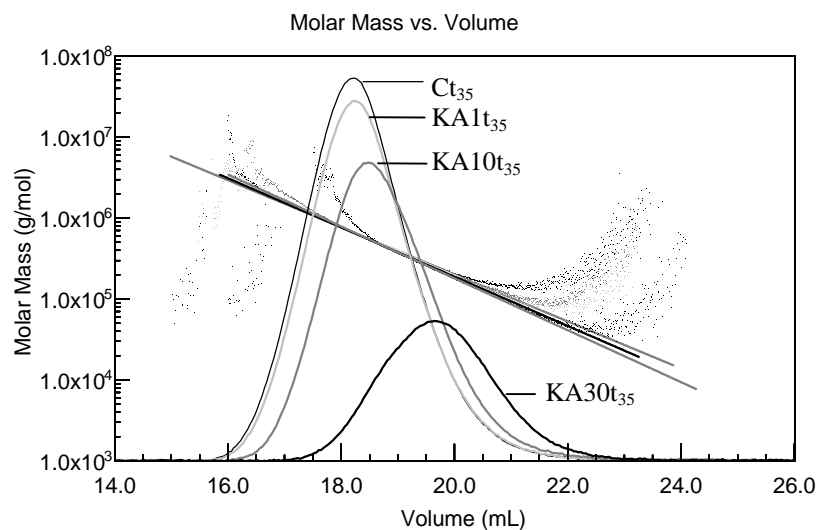


Figure 7.3-12. Overlaid 90° angle LS signals of $KA1t_{35}$, $KA10t_{35}$, $KA30t_{35}$ and Ct_{35} .

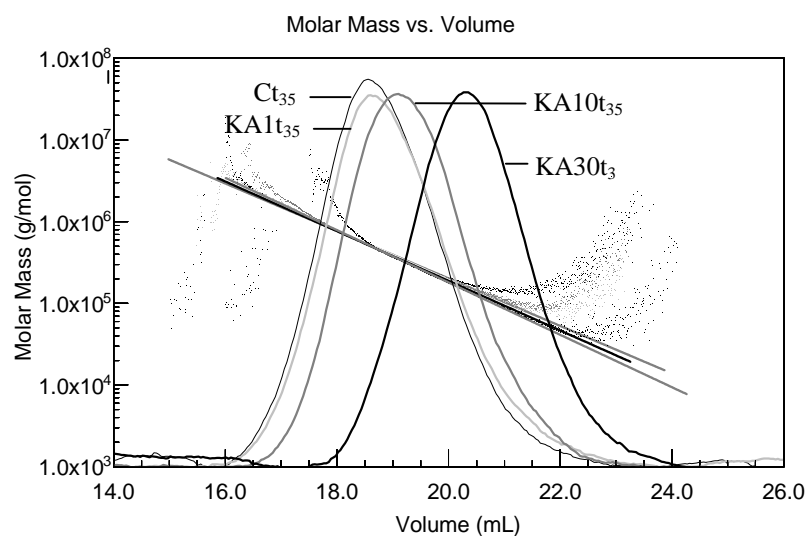


Figure 7.3-13. Overlaid DRI signals of $KA1t_{35}$, $KA10t_{35}$, $KA30t_{35}$ and Ct_{35} .

Table 7.3-3 reports the average values obtained for the root mean square radii averages r_n , r_w and r_z of the papers sized with gelatine/alum, as well as the average values of the slopes q in the log-log plot of rms radii versus M_r . The log-log plot of rms radius versus M_r shows the difference in slope q between the samples depending on the alum content (Figure 7.3-14). For KA1t₃₅ and KA10t₃₅ the slope corresponded to a random coil polymer, in optimal solvent conditions for the former, and in theta conditions for the latter. For KA30t₃₅ the value q was rather small, of 0.40, which corresponded to a more compact polymer conformation in solution.

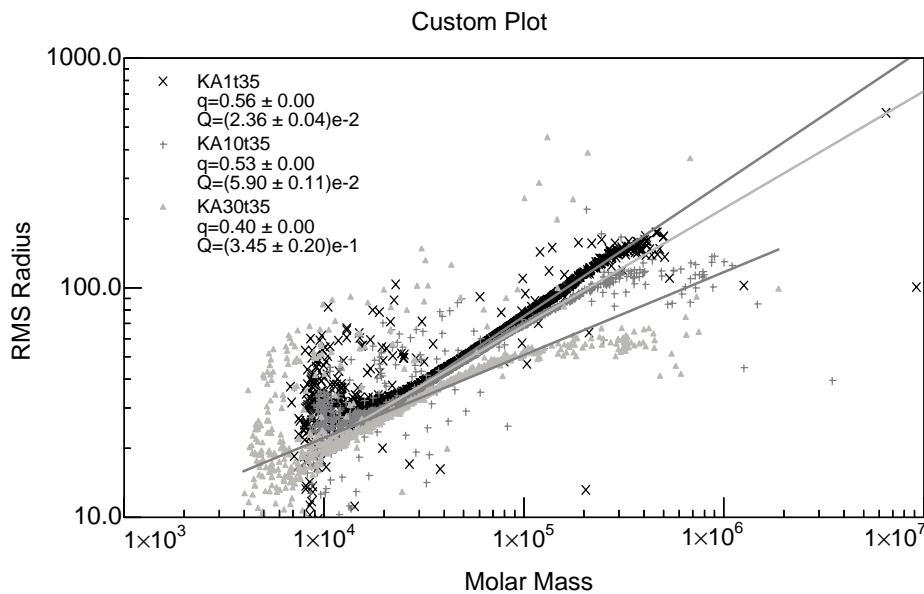


Figure 7.3-14. Overlaid average rms radii as a function of M_r (log-log scale) of KA1t₃₅, KA10t₃₅ and KA30t₃₅.

The black line in Figure 7.3-7 shows the changes in M_w at t_{35} versus alum concentration in the gelatine size for the gelatine/alum samples. As opposed to the alum-only samples, the slope for KA samples was approximately constant over the alum concentration range studied.

The plot of M_w versus aging time (Figure 7.3-15) indicates that all KA papers exhibited a larger decrease in M_w upon aging than the control papers. The values of M_w of the samples containing alum only are reported on the same graph for comparison. This graph shows that M_w of all samples containing alum was lower than M_w of C, over the whole aging period. However, here again it appears clearly that the samples containing gelatine/alum degraded less rapidly than those containing alum only.

Figure 7.3-16 shows the polydispersity index M_z/M_w as a function of M_n . The values for the samples containing alum only are reported on the same graph for comparison. The polydispersity index tended to increase to different degrees with aging time, although not significantly considering the RSD on the values (for those where the RSD could be

calculated). Therefore, in the papers containing gelatine/alum, as in control papers and in alum-only containing papers, the cellulose molecules most likely underwent random cleavage.

KA1 had the same initial degradation rate as the reference C from t_0 to t_{35} . This indicates that when gelatine was present in addition to alum, and contrary to the alum-only papers, the lowest alum concentration (0.083 g L^{-1}) had no incidence on the degradation of cellulose on the first aging portion (until t_{35}). However, in the second period of aging, from t_{35} to t_{94} , even such a low alum concentration (KA1) induced a degradation rate that was slightly higher than that of C (Figure 7.3-17).

For higher alum concentration in the size (KA10, KA30), the degradation of cellulose was considerably accelerated with respect to C and, as expected, a faster degradation occurred for the higher concentration KA30 than for KA10.

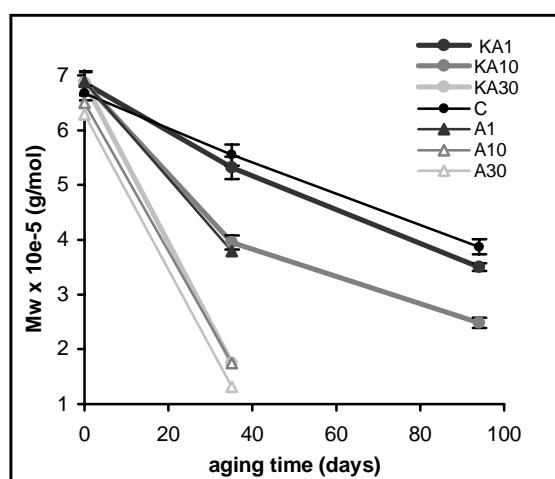


Figure 7.3-15. M_w as a function of aging time for KA samples (compared to A and C samples).

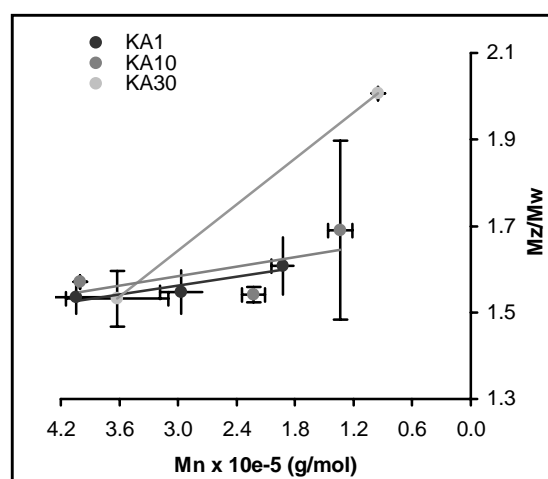


Figure 7.3-16. Polydispersity index M_z/M_w for KA and C samples as a function M_n (RSD could not be calculated for those data points when only two SEC runs were carried out).

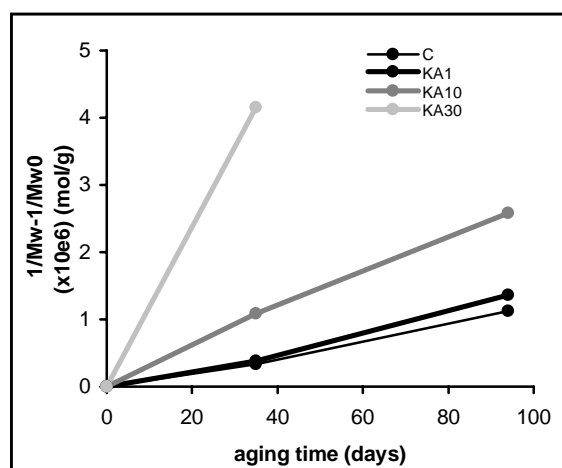


Figure 7.3-17. Plot yielding the glycosidic bond cleavage rate k ($\text{mol g}^{-1} \text{ days}^{-1}$) for KA and C samples.

7.3.3 Conclusions on SEC/MALS

These results showed that the papers sized with gelatine-alum exhibited a different artificial aging rate than those containing alum only. Comparing the results at t_{35} of gelatine-alum sized papers and alum-only papers, it appears that the presence of gelatine considerably slowed the degradation induced by the alum at all comparable concentrations. After 35 days of aging, M_w of KA10 and KA30 were, respectively, 56% and 24% higher than M_w of A10 and A30.

The role of gelatine in slowing the acid-catalysed hydrolysis of cellulose caused by alum was demonstrated in this series of experiments. This protective role was efficient over the whole range of concentration of alum in the size, although considerably more at the two lower concentrations used (0.083 g L^{-1} and 0.83 g L^{-1}) than at the highest concentration (2.49 g L^{-1}). However, it must be noted that this highest alum concentration was used for the purpose of the present research as an extreme case study, and that such a concentration in gelatine size was in fact seldom used in paper manufacturing. Very high alum concentrations reported in early twentieth century recipes, and used as bibliographic reference for this study correspond to a historical period of active research and experimentation in the field of sizing in the paper industry, and were most probably representative of experimental new sizing techniques than currently used practice.

7.4 Colour monitoring of the model papers containing gelatine and/or alum during aging

7.4.1 Experimental

Colour measurements were carried out in the trichromatic system CIE $L^*a^*b^*$, and total chromatic differences ΔE^* between reference and gelatine and/or alum containing papers as well as unaged/aged papers were measured. The yellowness index E313-96, whiteness index E 313-96, and R457 ISO brightness (reflectance at 457 nm), as well as the total hue difference ΔH^* were also measured. The equations of CIE $L^*a^*b^*$ values and additional measured indices as well as their significance for the appreciation to the naked eye can be found in Appendix 6-4.

A spectrophotometer UltraScan XE (Hunter Associates Laboratory, Inc) was used (specifications are in Appendix 6-4). The measurements were performed as described in section 6.4.2 of Chapter 6, with the illuminant D65, 10° observer, and with a 25 mm diameter measuring area, at five different locations of a sheet of paper as represented in Figure 6.5-1 of Chapter 6. Five different sheets were measured for each sample type. The tables report the average of 25 measurements per sample type.

7.4.1 Results and discussion

7.4.1.1 The impact of alum in the papers

As described in section 6.4.2.1 of Chapter 6, Whatman No.1 control papers showed a variable discolouration rate whether they were aged in the SE-600-3 (Thermotron Industries) or in the Versatenn (Tenney Environmental) climate chamber. Since all the papers containing alum were aged in the Versatenn chamber, the controls used for the calculation of ΔE^* and ΔH^* were taken from among those aged in that chamber.

Table 7.4-1 reports the CIE $L^*a^*b^*$ values and other colorimetric values of the samples A1, A10 and A30.

Table 7.4-1. Trichromatic values, indices (brightness, yellowness, whiteness), total chromatic and total hue differences for the model papers upon aging: control, alum and gelatine/alum samples.

	L^*	a^*	b^*	ΔE^{*1} (Vs Ct_x)	ΔE^{*2} (Vs Xt_0)	Brightness R457	YI E313-96	WI E313-96	ΔH^{*3} (Vs Ct_x)
Ct₀	95.33 ± 0.06	-0.57 ± 0.005	0.49 ± 0.02	0.00	0.00	87.89 ± 0.14	0.51 ± 0.04	86.16 ± 0.17	0.00
Ct₃₅	94.95 ± 0.04	-0.58 ± 0.01	1.48 ± 0.06	1.06 ± 0.06	1.06 ± 0.06	85.76 ± 0.11	2.39 ± 0.11	80.79 ± 0.27	-0.52 ± 0.02
Ct₉₄	94.49 ± 0.05	-0.52 ± 0.02	2.41 ± 0.07	2.76 ± 0.06	2.76 ± 0.06	83.51 ± 0.13	4.21 ± 0.14	75.41 ± 0.33	-0.86 ± 0.03
A1t₀	95.33 ± 0.06	-0.59 ± 0.01	0.49 ± 0.03	0.02 ± 0.06	0.00	87.88 ± 0.13	0.49 ± 0.06	86.16 ± 0.15	0.01 ± 0.02
A1t₃₅	94.86 ± 0.04	-0.59 ± 0.01	1.87 ± 0.05	0.39 ± 0.05	1.45 ± 0.05	85.06 ± 0.11	3.12 ± 0.09	78.80 ± 0.26	-0.12 ± 0.01
A1t₉₄	93.70 ± 0.11	-0.31 ± 0.04	4.00 ± 0.15	1.79 ± 0.18	3.88 ± 0.18	79.79 ± 0.39	7.41 ± 0.32	66.21 ± 0.91	-0.42 ± 0.05
A10t₀	95.34 ± 0.05	-0.60 ± 0.01	0.54 ± 0.02	0.06 ± 0.02	0.00	87.85 ± 0.08	0.57 ± 0.04	85.98 ± 0.05	-0.01 ± 0.02
A10t₃₅	94.28 ± 0.09	-0.46 ± 0.03	2.99 ± 0.14	1.66 ± 0.17	2.67 ± 0.16	82.32 ± 0.39	5.37 ± 0.29	72.26 ± 0.26	-0.48 ± 0.04
A10t₉₄	91.97 ± 0.26	0.27 ± 0.10	6.54 ± 0.30	4.90 ± 0.40	6.94 ± 0.39	73.01 ± 0.88	12.77 ± 0.66	50.15 ± 2.02	-1.02 ± 0.08
A30t₀	95.35 ± 0.05	-0.60 ± 0.01	0.53 ± 0.02	0.05 ± 0.02	0.00	87.89 ± 0.1	0.55 ± 0.04	86.04 ± 0.1	0.00 ± 0.02
A30t₃₅	93.58 ± 0.19	-0.33 ± 0.05	4.02 ± 0.27	2.97 ± 0.34	3.93 ± 0.33	79.47 ± 0.73	7.45 ± 0.56	65.82 ± 1.69	-0.73 ± 0.06
A30t₉₄	89.34 ± 0.44	1.21 ± 0.15	9.28 ± 0.33	8.76 ± 0.54	10.77 ± 0.30	64.61 ± 1.18	18.95 ± 0.80	30.65 ± 2.65	-1.64 ± 0.08
KA1t₀	95.19 ± 0.11	-0.61 ± 0.01	0.61 ± 0.02	0.11 ± 0.06	0.00	87.43 ± 0.24	0.70 ± 0.04	85.30 ± 0.23	-0.05 ± 0.02
KA1t₃₅	94.92 ± 0.05	-0.95 ± 0.01	2.55 ± 0.05	1.09 ± 0.04	1.98 ± 0.043	84.41 ± 0.09	4.14 ± 0.09	75.80 ± 0.18	-0.04 ± 0.01
KA1t₉₄	94.14 ± 0.08	-1.04 ± 0.04	5.03 ± 0.13	2.68 ± 0.13	4.56 ± 0.142	79.66 ± 0.30	8.75 ± 0.25	62.50 ± 0.76	-0.04 ± 0.03
KA10t₀	95.22 ± 0.06	-0.63 ± 0.01	0.65 ± 0.02	0.16 ± 0.03	0.00	87.44 ± 0.13	0.77 ± 0.04	85.17 ± 0.12	-0.07 ± 0.01
KA10t₃₅	94.76 ± 0.03	-0.98 ± 0.01	3.10 ± 0.07	1.62 ± 0.07	2.51 ± 0.072	83.39 ± 0.10	5.15 ± 0.14	72.92 ± 0.34	-0.15 ± 0.02
KA10t₉₄	93.28 ± 0.08	-0.79 ± 0.04	7.00 ± 0.13	4.58 ± 0.13	6.64 ± 0.148	75.42 ± 0.32	12.63 ± 0.27	51.26 ± 0.80	-0.42 ± 0.03
KA30t₀	95.25 ± 0.05	-0.63 ± 0.01	0.63 ± 0.02	0.14 ± 0.03	0.00	87.53 ± 0.11	0.72 ± 0.03	85.36 ± 0.12	-0.06 ± 0.01
KA30t₃₅	93.95 ± 0.05	-0.68 ± 0.03	4.35 ± 0.13	2.99 ± 0.12	3.95 ± 0.132	79.97 ± 0.22	7.77 ± 0.27	65.18 ± 0.66	-0.57 ± 0.04
KA30t₉₄	90.08 ± 0.19	0.73 ± 0.08	10.42 ± 0.26	7.98 ± 0.26	11.16 ± 0.31	64.94 ± 0.63	20.50 ± 0.55	27.11 ± 1.69	-1.44 ± 0.04

¹ ΔE^* Vs Ct_x is the total chromatic change between the sample and the unsized control at the respective aging times.

² ΔE^* Vs Xt_0 is the total chromatic change of a given sample between time t_0 and times t_{35} or t_{94} .

³ ΔH^* Vs Ct_x is the total hue change between the sample and the unsized control at the respective aging times.

Figure 7.4-1 and Figure 7.4-2 which represent the changes in the values of b^* and L^* show the tremendous increase in yellowing and decrease in lightness of the paper caused by alum upon aging. As expected, the intensity of the discolouration (measured by b^*) increased and the lightness (measured by L^*) decreased with increasing alum concentration.

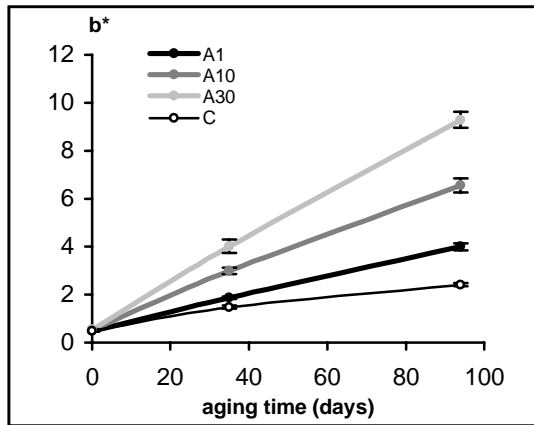


Figure 7.4-1. b^* as a function of aging time for A and C samples.

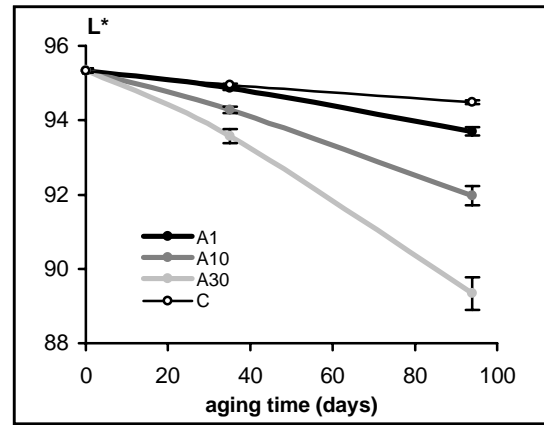


Figure 7.4-2. L^* as a function of aging time for A and C samples.

Figure 7.4-3 shows the plot of b^* as a function of a^* . As opposed to the papers sized with gelatine only (Figure 6.4-6, Chapter 6), the increase in the value of b^* was accompanied by a significant increase in a^* . This visually translates in both accrued yellow and red components, which yields a brownish colour. It is interesting to note that all the papers, regardless of aging time and alum concentration, and including the control with no alum, fell roughly on the same (a^* , b^*) curve. This result indicated that alum did accelerate the discolouration introduced by heat/humidity aging, and did not introduce a new discolouration mechanism. The course of the degradation reaction as indicated by the colour change, was homogeneous, and the rate of the discolouration was dependent on the alum concentration. This is consistent with the SEC/MALS results where the degradation by acid-catalysed hydrolysis was found to increase due to the presence of alum.

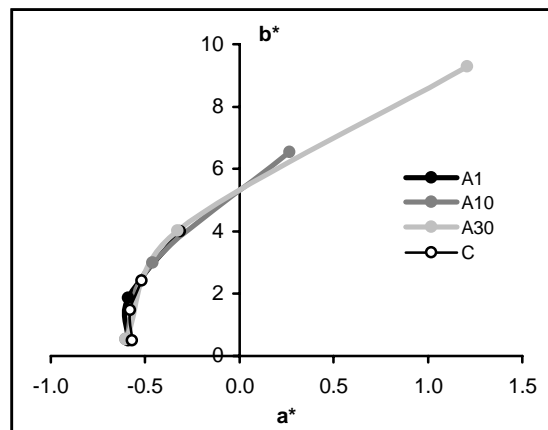


Figure 7.4-3. (a^* , b^*) plot for A and C samples.

The changes in ΔE^* upon aging relative to the respective unaged sample in each alum concentration category are shown in Figure 7.4-4. As observed in Chapter 6, ΔE^* followed mainly the same trend as b^* (Figure 7.4-1). Figure 7.4-5 shows the changes in ΔE^* of the sized papers relative to C, in the respective aging category (C_{t_0} , $C_{t_{35}}$ and $C_{t_{94}}$). These ΔE^* followed almost exactly the same trend as that observed in Figure 7.4-4. From these two figures it can be concluded that the presence of alum was the main factor responsible for the increase in ΔE^* with aging. In other words, the discolouration imputable to alum is the more significant discolouration factor during aging.

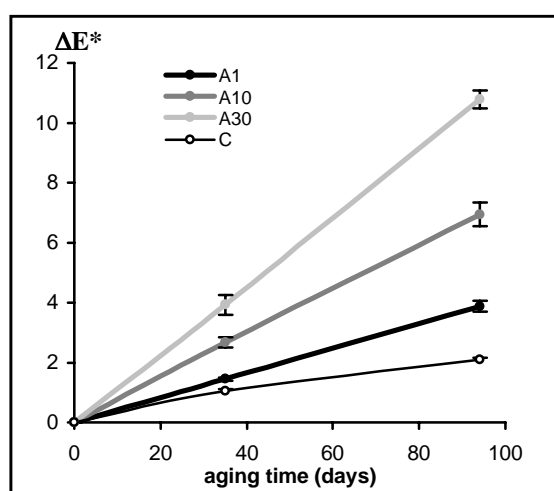


Figure 7.4-4. ΔE^* relative to the respective unaged sample in each category for A and C samples.

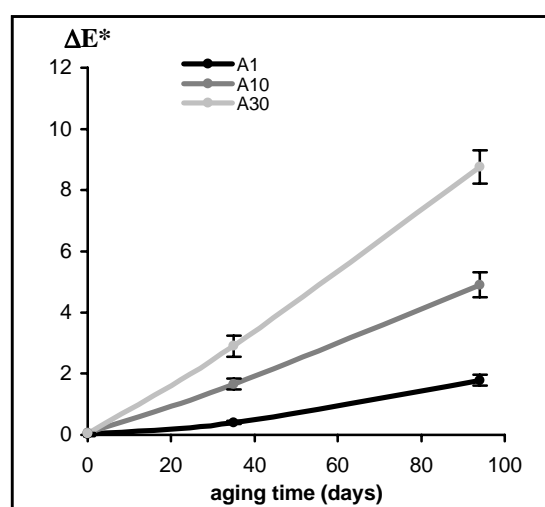


Figure 7.4-5. ΔE^* relative to C samples in each respective aging category for A samples.

7.4.1.2 The impact of gelatine/alum in the papers

Table 7.4-1 reports the CIE $L^*a^*b^*$ values of the samples KA1, KA10 and KA30. Figure 7.4-6 and Figure 7.4-7 represent the changes in the values of b^* and L^* upon aging time. These show that, in each respective aging category, the increase in yellowing (increase in b^*) of papers caused by gelatine/alum upon aging was more pronounced than for alum-only papers, but conversely the decrease in lightness was more pronounced for the latter (samples A1, A10 and A30 are represented in the same figures for comparison).

Therefore, the presence of gelatine added to the discolouration already induced by alum. Since the amount of gelatine is the same in the three types of samples (2% uptake), this indicated that as expected, the intensity of the discolouration increased with the alum concentration in the paper.

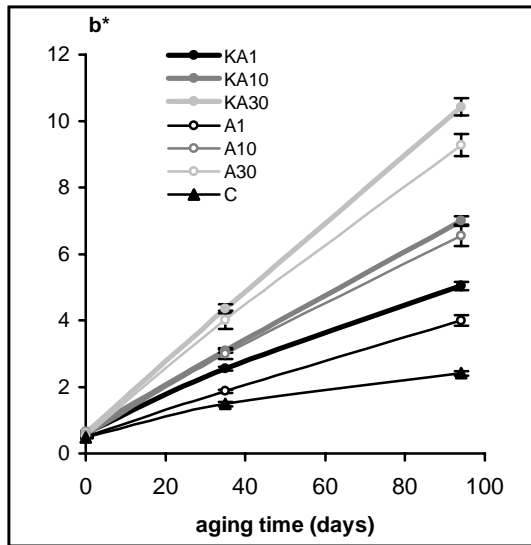


Figure 7.4-6. b^* as a function of aging time for KA, A and C samples.

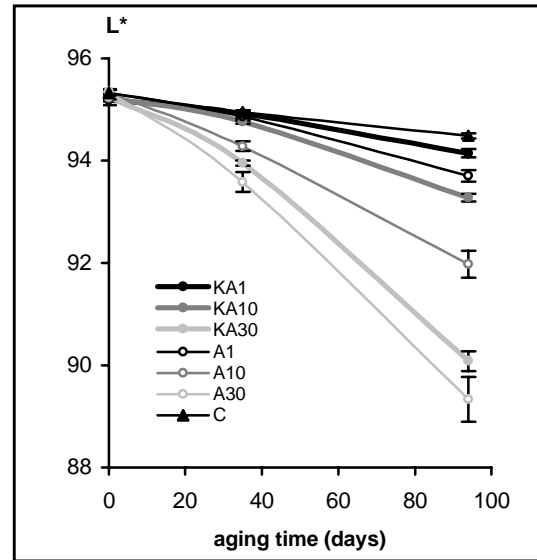


Figure 7.4-7. L^* as a function of aging time for KA, A and C samples.

Figure 7.4-8 shows that the colour changes upon aging for the samples containing gelatine/alum as showed in the plot of (a^* , b^*) spanned from the changes of the gelatine-only samples (Figure 6.4-6 of Chapter 6) to those of the alum-only samples (Figure 7.4-3). The colour changes brought by the increasing concentration of alum tended to override the colour changes induced by the gelatine.

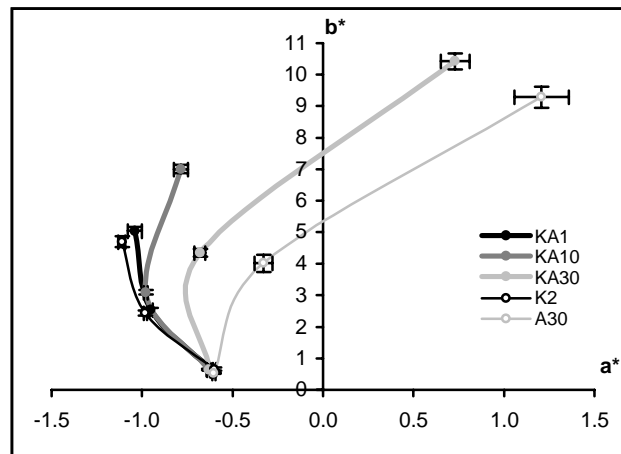


Figure 7.4-8. (a^* , b^*) plot of KA (compared with K2 and A30 samples).

The changes in ΔE^* upon aging relative to the respective unaged sample in each gelatine/alum concentration category (Figure 7.4-9) followed almost exactly the changes in ΔE^* of the alum-only samples (represented on the same plot for ease in the comparison).

Figure 7.4-10 shows the changes in ΔE^* of the sized papers relative to C in each aging category (C_{t_0} , $C_{t_{35}}$ and $C_{t_{94}}$). This figure, when compared to Figure 7.4-9, allows the

visualisation of the impact of gelatine on ΔE^* . It shows that the same rate of change upon aging occurred as in alum-only papers as compared to C, except for the lower alum concentration where the sample with gelatine/alum discoloured more significantly upon aging than the sample with alum only. This indicates that the impact of gelatine on the discolouration was not significant in compositions above 10% alum in the size, compared to the alum-induced discolouration.

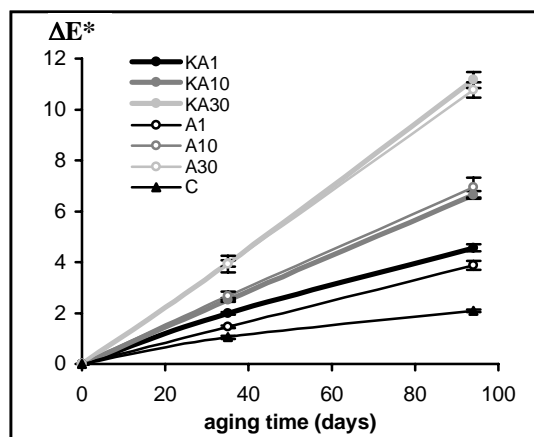


Figure 7.4-9. ΔE^* for KA, A and C relative to the respective sample unaged in each category.

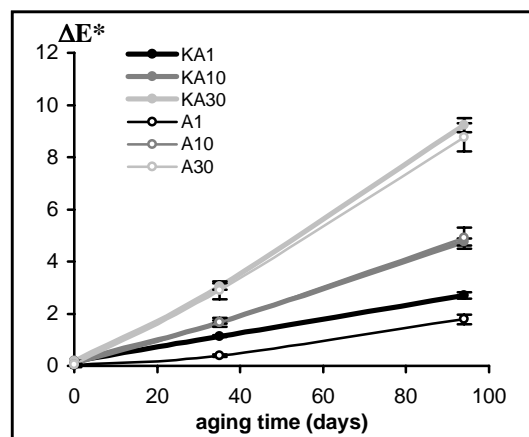


Figure 7.4-10. ΔE^* for KA and A relative to C samples in each respective aging category.

The influence of alum concentration on the rate of discolouration is represented in Figure 7.4-11. The long-term trend for both KA samples and A samples is an increase in ΔE^* with increasing both alum content in the papers and aging time. However, the initial changes differ in the low alum concentration range from 0 to about 0.8 g L^{-1} ($\approx 10\%$) in each aging category, as shows the zoom in Figure 7.4-12, with a faster discolouration occurring for KA samples than for A samples. This confirmed that the gelatine induced colour changes but that this discolouration was overridden by the colour change caused by the alum at all aging times when its content in paper was above 10%.

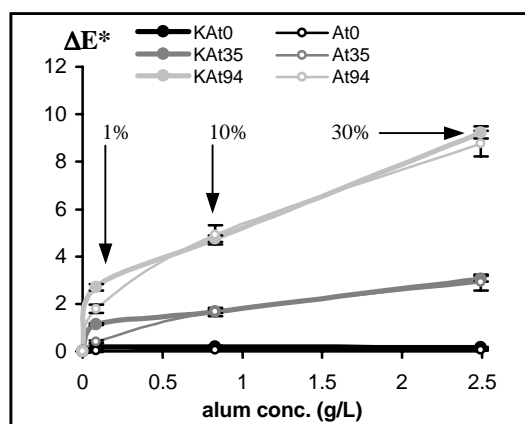


Figure 7.4-11. ΔE^* for KA and A relative to C samples in each respective aging category as a function of the alum concentration.

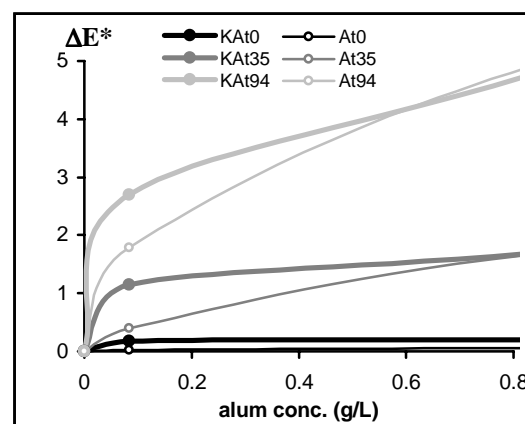


Figure 7.4-12. Zoom of Figure 7.4-11 in the low alum concentrations.

7.5 pH of alum papers and gelatine/alum papers

Table 7.5-1 reports the cold extraction pH of the papers as measured according to TAPPI standard method T 509 om-88 [17] to which some modifications were made (see section 6.5.1. of Chapter 6). Figure 7.5-1 shows that the decrease in pH as a function of time was due to both the aging time and the increasing alum concentration. However, Figure 7.5-2 shows that the major contribution to the decrease in pH was imputable to alum rather than aging.

For all the papers sized with gelatine/alum, pH values were lower than for the papers containing alum only (at respective equivalent alum concentration). This is opposite to the changes affecting M_r . This result corroborated the findings for gelatine-only containing papers, in that the pH was not a good indicator of the state of degradation of sized papers. This is reflected by the profile of the M_r curve as a function of alum concentration for samples KA_{t35}, that followed a quasi-linear decrease (Figure 7.3-6, black line), whereas the plots of pH versus alum concentration (Figure 7.5-2) exhibited a decrease that tailed off asymptotically at all aging times. In the case of papers containing alum only, the curves with a steep initial pH decrease at alum concentration below 1 g L^{-1} followed by a portion of the curve tending to a plateau between 1 to 1.5 g L^{-1} , and a flat portion beyond that, had roughly the same profile as the plots of M_r versus alum concentration for these samples at t_{35} (Figure 7.3-6, grey line). Thus, for the A samples, both pH and M_r decreased asymptotically with increasing alum concentration, the plateau being reached above a threshold value situated between 1 to 1.5 g L^{-1} . The limiting value of M_w was found of $1.5(\pm 0.1) \times 10^5 \text{ g mol}^{-1}$.

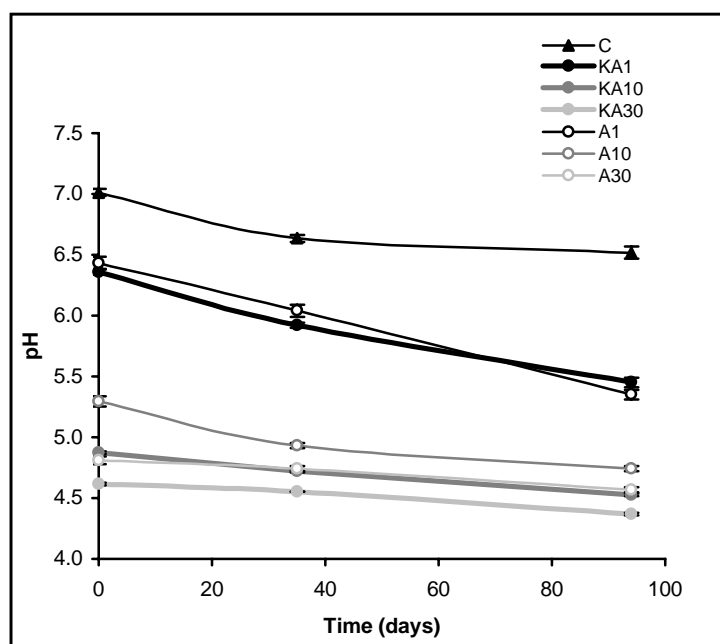


Figure 7.5-1. pH as a function of aging time for KA, A and C samples.

Table 7.5-1. Cold extraction pH of KA, A and C samples and pH of the gelatine/alum and alum solutions used to prepare these samples.

sample	pH c.e. ¹	RSD	pH sol. ²	sample	pH c.e.	RSD	pH sol.
Ct₀	7.01	0.03					
Ct₃₅	6.63	0.03					
Ct₉₄	6.52	0.05					
A1t₀	6.43	0.05	4.94	KA1t₀	6.36	0.02	5.67
A1t₃₅	6.04	0.05		KA1t₃₅	5.92	0.02	
A1t₉₄	5.35	0.04		KA1t₉₄	5.45	0.04	
A10t₀	5.29	0.04	4.17	KA10t₀	4.87	0.01	4.48
A10t₃₅	4.93	0.02		KA10t₃₅	4.72	0.01	
A10t₉₄	4.74	0.02		KA10t₉₄	4.53	0.01	
A30t₀	4.81	0.03	3.93	KA30t₀	4.62	0.01	4.09
A30t₃₅	4.74	0.02		KA30t₃₅	4.55	0.00	
A30t₉₄	4.57	0.02		KA30t₉₄	4.37	0.01	

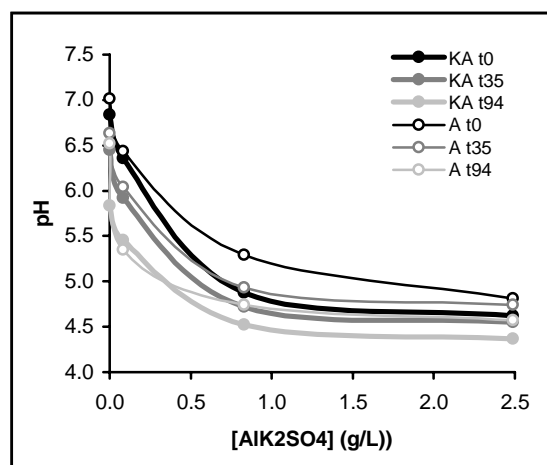


Figure 7.5-2. pH as a function of alum concentrations for KA and A samples.

7.6 Investigation into correlations between pH, colour measurements and M_r

7.4.1 Correlations based on the parameter time

The plot of M_w as a function of pH (Figure 7.6-1) shows that in each sample category, a large decrease in M_w was accompanied by a rather small pH decrease. The initial

¹ pH c.e is the cold extract pH of the papers.

² pH sol. is the pH of the gelatine solutions used to size the papers.

acidification of the samples due to high alum content was more significant than the subsequent acidification occurring during the aging, but conversely the depolymerisation during aging was quite dramatic. The samples containing 1% alum (KA1 and A1) showed higher pH and higher M_w than the samples containing 10% and 30% alum (KA10, A10, KA30 and A30) at the same aging times.

Figure 7.6-2 and Figure 7.6-3 are plots of M_w as a function of b^* and ΔE^* respectively. On both plots, KA and A displayed slightly different behaviour, each group followed a decay curve of M_w as a function of discolouration clearly delimited by that of the control samples. The samples with gelatine/alum displayed a higher discolouration than the alum-only samples but showed considerably smaller M_w decay. In each category, higher discolouration and lower M_w were correlated to higher alum concentration.

Figure 7.6-4 plots pH versus ΔE^* and shows the clear separation in two groups of samples KA and A as noted previously in discussing Figure 7.6-1. On one side the two samples containing 1% alum (KA1 and A1) displayed the steeper slopes: the decrease in pH was larger than the increase in ΔE^* when compared to the other samples. In the other group, the four samples containing 10% and 30% alum (KA10, A10, KA30 and A30) showed a relatively smaller pH decrease concomitantly with a larger increase in ΔE^* . From Figure 7.6-4 it can also be noted that the discolouration of KA and A samples varied in the same range with aging. This shows that the separation into two groups, which is visible in Figure 7.6-3 is in fact a separation driven by the difference in M_w .

These plots show that the presence of gelatine clearly influenced the aging behaviour in the papers containing alum by decreasing the depolymerisation rate but also by inducing slightly larger decrease in pH and increase in the discolouration rate.

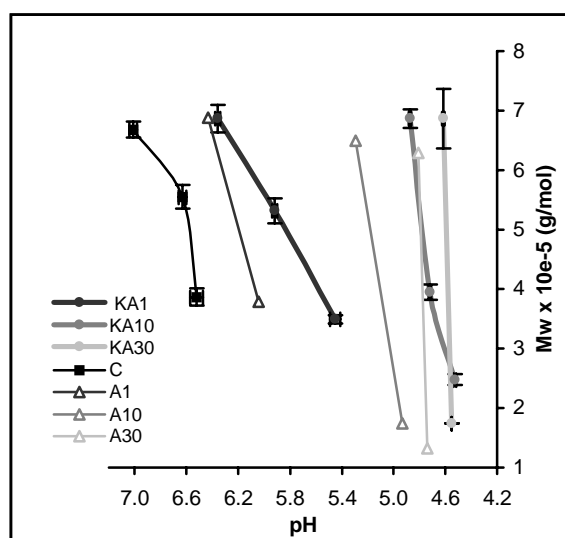


Figure 7.6-1. M_w as a function of pH of the samples upon aging.

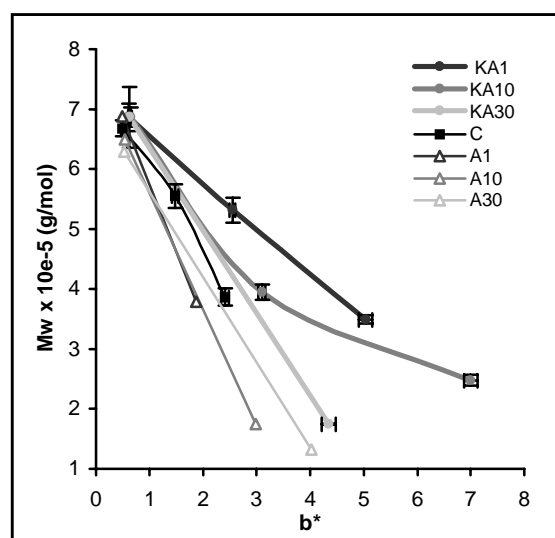


Figure 7.6-2. M_w as a function of b^* of the samples upon aging.

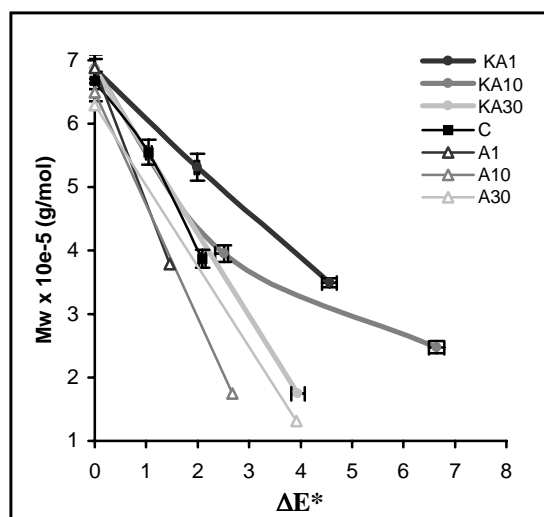


Figure 7.6-3. M_w as a function of ΔE^* of the samples upon aging.

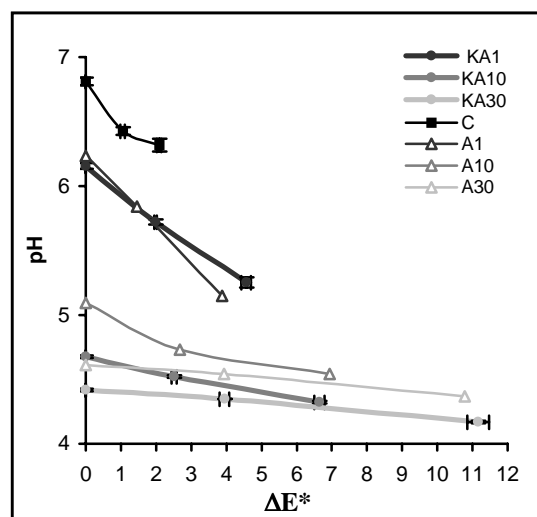


Figure 7.6-4. pH as a function of ΔE^* of the samples upon aging.

7.4.2 Correlations based on the parameter of the alum concentration

Investigating correlations based on alum concentration leads to Figure 7.6-5, Figure 7.6-6 and Figure 7.6-7 where the variations in pH, ΔE^* and M_r of the papers with gelatine/alum and alum-only are compared at fixed aging time (t_{35}).

Figure 7.6-5 shows that for the alum-only papers, both pH and M_r decreased in an approximately linear fashion with increasing alum concentration over the whole range. For papers with gelatine/alum, the decrease was linear up to 10% alum, with a shallower slope indicating a slower depolymerisation rate than for the A samples. This was followed by a steep decrease in M_r with almost no further pH decrease for the highest alum concentration (30%). The extrapolation from 0% to 30% alum resulted in a line parallel to the curve of A samples. This indicated that for gelatine/alum papers, in the range below 10% alum, the gelatine induced a decrease in the depolymerisation rate compared to the alum-only papers. Above 10%, the rate of degradation accelerated considerably and matched the degradation of the alum-only papers.

This confirms the previously reported results on the protective role of gelatine towards cellulose in acid-catalysed degradation reactions (Chapter 6). This behaviour of gelatine towards cellulose is more pronounced when alum is present in the paper than in gelatine-only papers, probably because, as alum is a factor in the acidification of paper, the acids produced react faster with gelatine than with cellulose.

The relationship between ΔE^* and M_r of KAt_{35} and At_{35} papers with increasing alum concentration (Figure 7.6-6) is in contrast to that between pH and M_r , as it was approximately linear for KAt_{35} but curved for At_{35} , for which above 10% alum, M_r only

slightly decreased while ΔE^* increased drastically. This illustrates well the fact that gelatine/alum papers discoloured more but were less chemically degraded (higher M_w) than alum-only papers.

Figure 7.6-7 shows that no direct correlation can be found between pH and ΔE^* . However, for both KAt₃₅ and At₃₅ papers, the curve shows a clear elbow, indicating that even though the pH did not lower much for concentrations of alum beyond 10%, ΔE^* initiated a drastic increase.

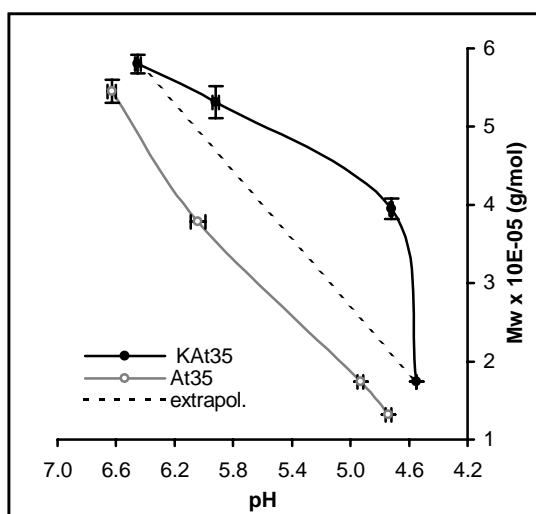


Figure 7.6-5. M_w as a function of pH, changes with alum concentration.

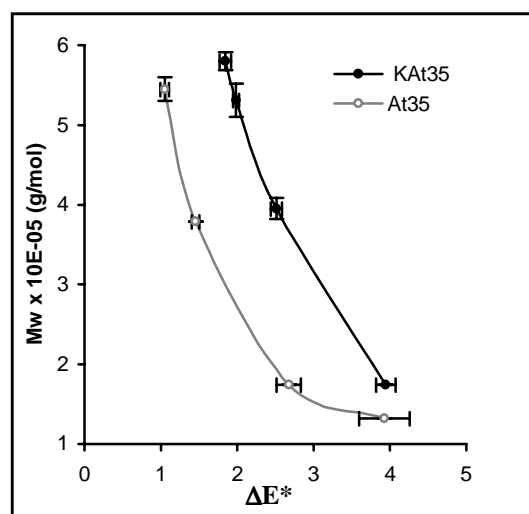


Figure 7.6-6. M_w as a function of ΔE^* , changes with alum concentration.

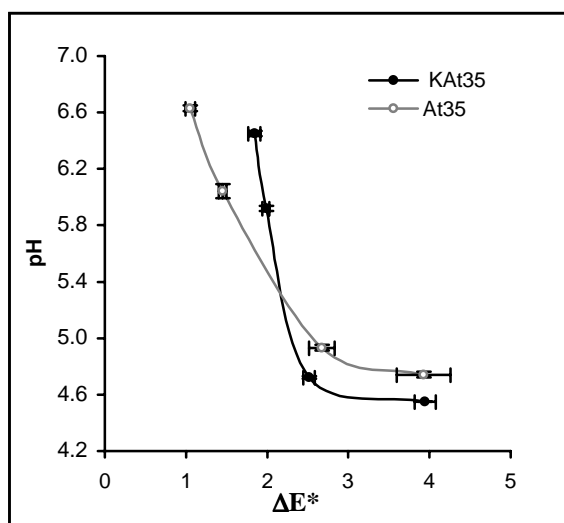


Figure 7.6-7. pH as a function of ΔE^* , changes with alum concentration.

7.7 Conclusion

SEC/MALS proved to be a very useful tool for the characterisation of the chemical state of the cellulose constituent of the diversely prepared papers, allowing the detection of minute as well as significant changes in the molar mass. The eventual residues of non-fibrous material such as alum and gelatine were not an obstacle for the dissolution of the paper in LiCl/DMAc and the analysis with the methodology developed for this study.

The presence of alum in the paper significantly accelerated the aging-induced degradation by acid-catalysed hydrolysis. The only sample found to be relatively unaffected by the presence of alum was the gelatine/alum sized sample with the lowest alum concentration of 0.083 g L^{-1} (1%), and only up to 35 days of aging. However, the acceleration of the degradation rate compared to the control papers was noted for this sample at longer aging times.

At all concentrations of alum in the size, the gelatine had a significant beneficial effect towards cellulose by slowing the degradation process catalysed by the alum. Although this work does not pretend to elucidate the mechanism by which this protective effect occurs, some hypotheses can be ventured and these are discussed hereafter.

The characterisation of the degradation of gelatine in the paper upon artificial aging as presented in Chapter 8, showed that at and above 10% alum in the gelatine/alum size, the aging induced hydrolysis of the protein was accelerated, while 1% alum did not have any impact on the rate of the protein degradation. These results, combined with those in the present chapter, show that even when the gelatine is degraded to a fair extent, its role in slowing the acid hydrolysis of cellulose catalysed by alum is still very efficient. This effect is thought to be due to the preferential degradation of the protein molecules over the hydrolysis of cellulose.

The role of alum as a gelatine hardener is well known, especially in photography. Aluminium salts react with the ionised carboxyl groups of gelatine. However, too high an alum concentration probably results in an excess of free alum, which in turn could catalyse the hydrolysis of both the gelatine and the cellulose, and thus accelerate the aging induced degradation. Nevertheless, alum is more likely to react with gelatine because of the higher number of different functional groups in the protein and its less compact spatial conformation, that makes it more readily accessible to reactants than the tightly packed cellulose molecules.

Compared to the results obtained from the determination of the M_r with SEC/MALS/DRI, neither the pH nor the colour parameters b^* , L^* and ΔE^* were found good indicators of the state of degradation of papers that contain both gelatine and alum. The trend in the discolouration of gelatine/alum papers was similar to that in alum-only papers, and was proportional to both alum content and aging time. As for the pH, its lower values were associated with a higher M_r in the case of gelatine/alum compared to the alum-only

papers. The threshold concentrations of 1 to 1.5 g L⁻¹ could be found delimiting a range beyond which a plateau was reached asymptotically for both pH and M_r . This threshold was also applicable to the discolouration rate, as above this value colour changes were significantly larger. This plateau corresponded to a value of M_w of $1.5(\pm 0.1) \times 10^5$ g mol⁻¹, which was determined as a limiting value of M_w , where the depolymerisation reached a point where it cannot proceed further at the same speed.

On the practical side, this work could have implications in paper conservation treatments such as washing and resizing. The washing of paper documents sized with gelatine/alum in warm water often results in a dissolution of the size and a decrease in the amount of size left in the paper. This is accentuated if the gelatine is in a highly hydrolysed state since in this case part of the protein becomes more soluble. Although we lack information on how much gelatine and alum would dissolve while washing a historic paper document - mainly because the life history and state of degradation of each document are usually unknown, resizing a washed gelatine/alum sized paper with gelatine is worth considering, especially in the case of high alum content sizes [18]. However, it must be kept in mind that this study was limited to gelatine, and the potential benefits of other polymers, such as cellulose ethers, which are also currently used by paper conservators for resizing purposes, could not be investigated in the time frame of the present research.

Chemicals and materials

Lithium chloride (LiCl), aluminium potassium sulphate hydrate ($[AlK(SO_4)_2 \cdot 12H_2O]$) and *N,N*-Dimethylacetamide (DMAc) were purchased from Acros Organics (Springfield, NJ, USA). Whatman No.1 filter paper was obtained from Fisher Scientific (Springfield, NJ, USA). Gelatine photographic type B was purchased from Kind and Knox Gelatine Inc. (Sioux City, IA, USA) and gelatine HMW type A was purchased from Norland Products Inc. (New Brunswick, NJ, USA).

Instruments

The climate chamber SE-600-3 was from Thermotron Industries (Holland, MI, USA) and the Versatenn chamber was from Tenney Environmental (Parsippany, NJ, USA). The spectrophotometer UltraScan XE was from Hunter Associates Laboratory, Inc. (Reston, VA, USA).

Multiangle light scattering detector Dawn EOS and interferometric differential refractometre Optilab DSP were from Wyatt Technologies Corp. (Santa Barbara, CA, USA). Additional instrumentation relative to the separation and analysis by SEC/MALS/RI not cited in the present chapter are in the section Instruments of Chapter 4.

References

1. Barrett, T. *Paper Conservator*, 13 (1989) 32-38.
2. Brückle, I. *Conference Papers Manchester 1992*, The Institute of Paper Conservation, Fairbrass, S. Ed. (1992) 201-206.
3. Barrett, T., Mosier, C., *J. Am. Inst. for Conservation*, 34 (1995) 173-186.
4. Diderot, J.J. *Encyclopédie ou Dictionnaire Raisonné de Sciences, des Arts et des Métiers, par une Société de Gens de Lettres* 11, A. Neufchastel, Samuel Faulche et Compagnie (1765).
5. De Lalande, J.J.J.F. *Art de faire le papier*, Académie Royale des Sciences (1761).
6. Green, S.B. *Conference Papers Manchester 1992*, Institute of Paper Conservation, Fairbrass, S. Ed. (1992) 197-200.
7. Balston, T. *The Mill Ledger, James Whatman, Father and Son*, Balston, T. Ed, James Whatman, Father and Son, Methusen, London (1957) 59.
8. Norris, F.H. *Paper and Paper Making, CH.16*, Oxford University Press (1952) 228.
9. Sanburn, W.H. *Personal Folder Notebook*, Waroronoro Paper Cie, Mass. (1909).
10. Barrett, T. *Paper Conservator*, 13 (1989) 7-27.
11. McCormick-Goodhart, M.H. *J. Im. Sci. and Techn.*, 39, 2 (1995) 157-162.
12. Adelstein, P.Z.; Bigourdan, J.-L. and Reilly, J.M. *J. Am. Inst. for Conservation*, 36 (1997) 193-206.
- 13 T 412 om-94, *TAPPI test methods*, Technical Association of the Pulp and paper Industry, TAPPI press, Atlanta, US (1994).
14. Nevell, T.P. and Zeronian, S.H. *Cellulose Chemistry and its Applications*, Ch. 9, Wiley, New York (1985).
15. Schroff, D. and Stannett, A.W. *IEE Proc. C. G.B.* 132, 6 (1985), 312-319.
16. Jerosch, H. *Evaluation de l'état de dégradation de la cellulose/holocellulose dans différents types de papiers par chromatographie d'exclusion stérique*, Thèse de Doctorat, Université Versailles-St. Quentin-En-Yvelines (2002) 113-126.
17. T 509 om-88, *TAPPI test methods*, Technical Association of the Pulp and paper Industry, TAPPI press, Atlanta (1988).
18. Dupont, A-L., *J. of Chromatogr. A*, 950 (2002) 113-124.

Chapter 8. Study of the degradation of gelatine in paper upon aging using aqueous size-exclusion chromatography

Abstract

We studied the aging behaviour of gelatine used to size paper. Degradation of the protein was characterised and the impact of paper components, such as cellulose, and aluminium potassium sulphate was evaluated. Whatman No. 1 filter papers sized with two types of gelatines (A from fish skin and B from cattle bones) were prepared as model samples. Commercially sized modern papers (Arches) were also included in order to compare laboratory samples with real artist papers. Both types of papers were artificially aged at 80°C, 50% relative humidity for 35 and 94 days. Historic papers were included in this research in order to compare artificially aged with naturally aged gelatine. The aqueous extracts from the papers were characterised by aqueous size-exclusion chromatography (SEC) using four PL-Aquagel-OH columns and UV photodiode array detection at 220, 254 and 280 nm. Results showed that gelatine undergoes hydrolysis upon aging, type A gelatine showing a faster degradation rate than type B. The result was an increase in the lower-molar mass fractions under $50,000 \text{ g mol}^{-1}$, and especially in a characteristic fraction with a peak molecular mass (M_p) of $14,000 \text{ g mol}^{-1}$. A significant decrease in the extraction yields of α -, β - and γ -chains occurred after aging. This was attributed to crosslinking, leading to the formation of less-soluble polypeptides with very high molar mass ($> 800,000 \text{ g mol}^{-1}$). Less than 10% alum had no impact on the degradation rate; higher alum contents accelerated hydrolysis reactions.

8.1 Introduction

Since the beginning of papermaking in western Europe, gelatine was used to size papers in order to improve the buffer effect and feathering of the inks. The size was prepared by boiling animal hides, skins and bones in water. For the finest quality papers, sturgeon gelatine could be used [1]. Initially, papermakers added aluminium salts (alum) in order to decrease paper permeability. Additionally, alum also retarded biodeterioration and decreased the viscosity of the size [2,3]. The use of alum persisted and rosin/alum was used to size mechanical wood pulp papers well into the twentieth century. Nowadays, papers are still sized with alum/rosin (current quality paper) or with synthetic sizes such

as alkyl ketene dimer (AKD) and alkenyl succinic anhydride (ASA) (alkaline paper), which were developed for the paper industry in 1953 and 1974, respectively [4], but gelatine/alum sizing continues to be used for artist quality papers.

Collagens are the most abundant and ubiquitous proteins on earth. Most collagens are fibrillar proteins. Three left-handed α -chains form a collagen molecule, two α_1 and one α_2 are intertwined to form a right-handed triple helix called γ -chain [5,6,7,8]. α_1 and α_2 contain about 1000 amino acids each. They have a molar mass (M_r) of 95,000 g mol⁻¹ and differ slightly in the composition of the telopeptides (C and N terminal), α_2 being richer in basic amino acids.

Collagen is structured in highly ordered regions (crystalline) alternating with less ordered regions (amorphous). The high proportion of amino acid triplets (glycine - X - Y) in the α -chains, where X is most often proline (Pro) and Y is most often hydroxyproline (Hyp), is responsible for the compact crystalline structure. Hyp is found exclusively in collagen. Gly (glycine), Pro and Hyp represent more than 50% of the amino acid content, Gly alone accounts for more than 30%. The amorphous regions are present mostly in the telopeptides. They form globular ends and are rich in polar amino acids with bulky side-chains, such as arginine (Arg), lysine (Lys), aspartic acid (Asp) and glutamic acid (Glu). Differences in length, charge distribution and structure of the telopeptides lead to different possible assemblies forming the quaternary structure of the protein. The latter is responsible for the different physiological functions of collagens [5,8,9].

Gelatine is produced by partial hydrolysis of collagen either in alkaline or in acid medium, both treatments resulting in a partly denatured protein. Gelatine from bovine origin is alkali produced (type B) and acid-treated gelatine (type A) is from porcine or fish origin. Depending on the origin of the protein there are some differences in the physical properties and in the amino acid content [10]. Treatment results in the individualisation of a high proportion of the α -chains. Multimers of α -chains linked together, such as β -chains (α -chain dimers) and non-hydrolysed or partially renatured triple helices are also present in gelatine, albeit in smaller amounts. Low-molar mass peptides (500-4000 g mol⁻¹) and polypeptides of approximately 30,000 g mol⁻¹ arising from the degradation of the α -chains are formed [10,11,12].

Scientific research on gelatine is mainly driven towards photographic, food and pharmaceutical applications. This research provides valuable information on gelatine as a biomaterial, and on its chemical and physical properties. However, research in paper conservation has its own particular problems. A prime concern for ensuring the conservation of our cultural heritage is understanding the degradation pathways of the materials used to produce paper-based artefacts of artistic and historical value. Hydrolysis and oxidation occur during the aging process of cellulose and result in a progressive weakening of the physical strength of the paper over time. Counteracting these reactions and limiting their occurrence is crucial for improving the stability and longevity of paper artefacts. The task is far from simple, the numerous components of paper other than

cellulose, whether of organic origin, e.g. starch and gelatine, or mineral and synthetic origin, e.g. optical brighteners, fillers and synthetic sizes, are numerous parameters contributing to the complexity of the chemistry taking place during natural aging. In particular, the role of the size in the aging process of paper has largely been ignored.

The work presented here shows how gelatine degrades in paper upon aging at 80°C, 50% relative humidity (rH) and how the presence of aluminium potassium sulphate influences the aging behaviour. This study is part of broader research into the relationships between gelatine, alum and cellulose (chapters 6 and 7). We analysed Whatman No. 1 filter papers sized with different combinations and concentrations of gelatine and gelatine/alum. Naturally aged historic papers as well as modern watercolour quality papers (Arches) were also included in the study. They were all, except for the historic papers, artificially aged at 80°C and 50% rH for 35 and 94 days. Aqueous extracts from the papers were characterised by size-exclusion chromatography (SEC) on a set of four PL-Aquagel-OH columns (Polymer Labs.) using UV photodiode array detection (DAD).

8.2 Experimental

8.2.1 Samples description

Modern and historical seventeenth and eighteenth centuries gelatine sized papers were selected for this study. The modern papers included Whatman No. 1 filter paper, made of pure cellulose, and Arches (cold pressed), a 100% cotton paper from Canson¹. Arches paper was sized to saturation by the manufacturer with type B gelatine. Whatman No. 1 paper was manually sized in our laboratory with gelatine type A and type B. We chose a photographic grade type B gelatine by Kind and Knox produced from alkali-treated cattle bones (further referred to as "K") and a pharmaceutical/food grade type A gelatine by Norland produced from acid-treated fish skin (further referred to as "N"). The specifications data sheets are in Appendix 6-1. The sizing was done by immersing the sheets of Whatman No. 1 (150 mm × 190 mm) one by one in aqueous solutions of gelatine kept at 40 °C in a thermostated water bath (see Figure 6.2-1 in Chapter 6).

In order to achieve dry mass uptakes of gelatine in the papers of approximately 0.5, 2 and 8% (dry gelatine mass/dry paper mass), the concentrations of the aqueous gelatine solutions needed were 2.3, 8.3 and 32.3 g L⁻¹ for K and 2.1, 8.9 and 36.1 g L⁻¹ for N (calculations are detailed in Appendix 6-2). These gelatine uptakes were representative of light, mid and heavy sizing [13]. The water used was Milli-Q 18.2 MΩ cm (RiOs Elix, Millipore). The gelatine was equilibrated at 50% rH and 23 °C prior to use [14].

A set of papers was sized in solutions of K gelatine at 8.3 g L⁻¹ (2% uptake) containing various amounts of aluminium potassium sulphate [AlK(SO₄)₂·12H₂O]. Three concentrations of aluminium salts were used: 0.083, 0.83 and 2.49 g L⁻¹, *i.e.* 1%, 10% and

¹ Canson is now Arjo-Wiggins

30% of alum (mass of alum/mass of gelatine). These were chosen in order to cover the range of alum concentrations used in historical and modern sizing practices [1,15,16,17,18,19].

8.2.2 Artificial aging

In each series, one set of papers was kept in the dark at 23°C, 50% rH, and two sets were aged for 35 and 94 days at 80°C, 50% rH individually (hanging sheets) in a heat/humidity aging chamber. The papers without alum were aged in a SE-600-3 Thermotron chamber (Thermotron Industries) and the papers containing alum were aged in a Versatenn chamber (Tenney Environmental). Under these aging conditions, gelatine remained below its glass transition temperature [20,21].

A few grams of K granules and N flakes were aged in glass beakers for 35 days at 80°C, 50% rH in the Versatenn chamber.

8.2.3 Conditions

8.2.3.1 Method and instrumentation

All analyses were carried out on a Hewlett-Packard liquid chromatograph HP 1090 equipped with a built-in thermostated column compartment. UV detection was performed using a photodiode array detector (HP series L Diode Array Detector). A set of four columns PL-Aquagel-OH (Polymer Labs.) 300 mm × 7.5 mm and 8 µm particle diameter, 50-40-40-30, preceded by a guard column (Polymer Labs.) were connected in series. The molar mass operating range of the columns was 50,000-1,000,000 g mol⁻¹ for column 50, 10,000-200,000 g mol⁻¹ for columns 40, and 100-30,000 g mol⁻¹ for column 30. The packing is made of a rigid macroporous material with a highly hydrophilic polyhydroxylated surface. The mobile phase was 18 g L⁻¹ sodium dodecyl sulphate (SDS) in Milli-Q water and was filtered through 0.45 µm filters AH (Millipore) prior to use. SEC runs lasted 73 min at a flow-rate of 0.5 mL min⁻¹ (±10 µL min⁻¹) and sample injection volume was 20 µL. Gelatine concentration in the samples ranged from 1 to 5 µg µL⁻¹. The temperature of the column compartment was set to 50±0.5°C. UV detection was carried out at 220, 254 and 280 nm.

220 nm is commonly used for the detection and quantitation of peptides, the amide bond absorption range being 210-225 nm. In addition, absorptions at 254 and 280 nm were used because they are selective for tyrosine (Tyr) and phenylalanine (Phe). These two aromatic amino acids are located mainly in the telopeptidic (amorphous) regions and represent together only about 1.5% of the total amino acid content in bovine gelatine and about 2% in fish gelatine.

8.2.3.2 The mobile phase

The use of sodium dodecyl sulphate in SEC is widespread. SDS is an anionic surfactant, complexing with the polypeptides allowing them to unfold into a rod-shaped conformation. This minimizes the error in M_r determination due to differences in the hydrodynamic volume between the sodium polystyrene sulfonate standards (PSS) and gelatine, and among the gelatine polypeptides themselves. Additionally, the negative charges on SDS help reduce the problem of ionic interactions between the solutes in the mobile phase and the stationary phase. However, it should be noted that the cold water extract pH [22] of all the gelatine sized papers were above 5.07, the isoelectric point (pI) of gelatine (Table 6.5-1, Chapter 6) with the exception of aged papers containing 10 and 30% alum, which were slightly below a pH of 5 (Table 7.5-1, Chapter 7). Under the experimental conditions, gelatine in water extracted from the papers was mostly negatively charged.

Both pH and ionic strength are known to influence the elution volume of polypeptides [23]. The choice of the mobile phase was made after comparing 1.8% SDS in water with 1.8% SDS in 50 mM phosphate buffer pH 6.63, in order to evaluate if better resolution in the chromatograms of gelatine could be obtained with a buffer of higher ionic strength and stable pH. The buffer was prepared with 4.5 g $[\text{NaH}_2\text{PO}_4 \cdot \text{H}_2\text{O}]$ and 4.64 g $[\text{Na}_2\text{HPO}_4 \cdot 7\text{H}_2\text{O}]$ in 1 L of an aqueous solution with 1.8% SDS. Several gelatine samples were extracted in the mobile phase from papers without and with alum (10%), aged 35 and 94 days and unaged.

8.2.3.3 Sample preparation

The papers were equilibrated for several days in a temperature and humidity controlled room at 23°C, 50% rH [14]. They were cut into 3-4 mm² pieces. 0.5 g was weighed in a test tube and 2 mL of mobile phase was added. After 45 min incubation at room temperature, the supernatant was withdrawn and heated to 50 °C for 15 min in a thermostated water bath. The samples were filtered through poly(vinylidene difluoride) (PVDF) filters, 0.45 µm pore, 4 mm diameter (Alltech), before injection.

Gelatine solutions were also prepared by dissolving 2.5 mg of K granules and 2.8 mg of N flakes in 1 mL mobile phase for 1 h at 50°C (water bath), preceded by overnight soaking.

8.2.4 Calibration

A total exclusion volume (V_e) of 17 mL was determined by injecting a sodium polystyrene sulfonate (PSS) standard with a weight-average molar mass (M_w) of 1,188,400 g mol⁻¹. A total permeation volume (V_0) of 35 mL was determined by injecting

L-alanine (89.1 g mol^{-1}). The calibration curve for M_w determination was constructed using 11 PSS standards dissolved in mobile phase at concentrations of 0.2 to $0.3 \mu\text{g } \mu\text{L}^{-1}$. M_w values of PSS are $1,188,400 - 801,100 - 505,100 - 262,600 - 127,000 - 57,500 - 34,700 - 16,600 - 8000 - 4950 -$ and 1640 g mol^{-1} . The calibration curve is shown in Figure 8-1. The resulting polynomial equation for M_w as a function of retention time (t_R) using a cubic fit match (Equation 8-1) was used for all the M_r determinations:

Equation 8-1:

$$\log M_w = -6.41006 \times 10^{-4} t_R^3 + 8.64594 \times 10^{-2} t_R^2 - 4.00442 t_R + 68.51491$$

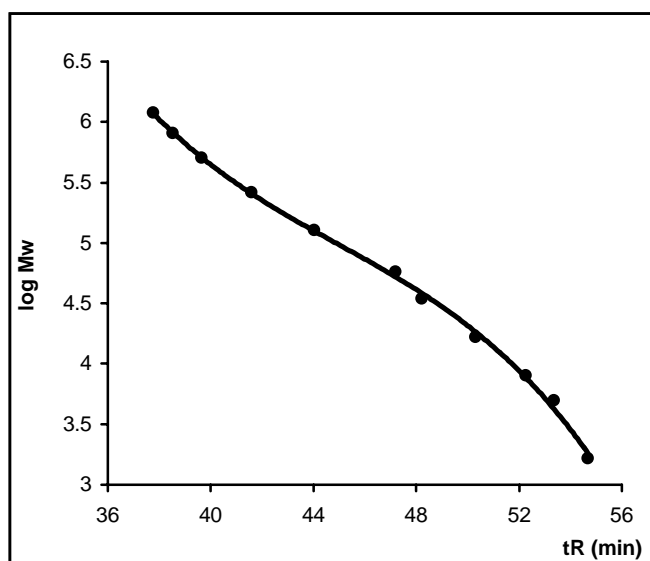


Figure 8-1. Weight-average molar mass calibration with PSS narrow standards; $\log M_w$ as a function of retention time t_R (min).

Among the polymer standards tested, PSS were chosen for calibration because they provided the best M_r estimation for SDS-gelatine complexes. They are soluble in water and absorb significantly at 220 nm . PSS were prepared in mobile phase for consistency with the preparation of the samples, but it is likely that SDS does not complex with PSS, both molecules being charged negatively. This assumption was corroborated by our experience showing that, whether dissolved in mobile phase or in water, PSS eluted with exactly the same retention volumes. On the other hand, M_r determination of the eluted gelatine fractions using a calibration curve constructed with SDS-globular protein complexes (electrophoresis molecular mass standards from Pharmacia) resulted in significantly underestimated values. This is due to the difference in protein families and confirms that SDS-protein complexes derived from globular proteins cannot be used as M_r standards for SDS-collagen derivatives.

8.2.5 Method validation (220 nm): precision, linearity and limit of detection

Calibration curves for quantitation of gelatine were constructed for K and N. The data were also used for assessing the precision and linearity of the method and the detection limit, and to estimate the extraction yields of gelatine from unaged paper (section 8.3.2.1.1).

Table 8-1 shows the relative standard deviations (RSD) in retention time (t_R), peak area, height and width obtained with eight injections performed on four different days of a mix of two polystyrene sulfonate standards of 8000 g mol⁻¹ (0.285 µg µL⁻¹) and 262,600 g mol⁻¹ (0.28 µg µL⁻¹). The method showed good repeatability in t_R (RSD ≤ 0.5%). Peak area, height and width have slightly higher RSD values, which is probably mostly due to the positioning of the baseline. However, it is not unusual to obtain such RSD values with aqueous SEC methods, which are extremely dependent on the precision of the instrument and on minute fluctuations in the run parameters, usually due to the precision of the delivery system. The precision of the HP 1090 solvent delivery system was ±2%. Ideal SEC conditions require a precision of 0.1% in flow-rate.

Table 8-1. Relative standard deviations in retention time (t_R), peak area, peak width and peak height on eight injections of a mix of PSS 8000 g mol⁻¹ and PSS 262,000 g mol⁻¹

	RSD (%)			
	t_R (min)	Area (mAU min)	Height (mAU)	Width (min)
PSS 8000	0.41	2.36	2.92	2.37
PSS 262,000	0.38	3.53	3.13	4.52

The linearity of the method was assessed with solutions of gelatine (unaged) of known concentrations: a stock solution of K at 20.71 µg µL⁻¹ and six dilutions (1/2, 1/8, 1/16, 1/64, 1/128, 1/256), and a stock solution of N at 40.25 µg µL⁻¹ and six dilutions (1/4, 1/8, 1/16, 1/32, 1/128, 1/256). The areas subtending the entire chromatograms were integrated and plotted versus concentration.

For K, we obtained:

$$\text{Area} = 12864 c + 475 \quad \text{Equation 8-2}$$

And for N,

$$\text{Area} = 11764 c + 210 \quad \text{Equation 8-3}$$

Where the area is in mAU min and c is the concentration of gelatine in µg µL⁻¹. These equations were used for quantitation measurements. Correlation coefficients were 0.9999 for K and 0.9998 for N.

In order to determine the limit of detection (LOD), signal-to-noise ratios (S/N') for the smallest peak (C) in the chromatograms at a peak molar mass (M_p) of $14,000 \text{ g mol}^{-1}$ (Figure 8-2) were calculated with the solution stock/256 (*i.e.* $8.5 \cdot 10^{-4} \mu\text{g } \mu\text{L}^{-1}$ of K and $1.6 \cdot 10^{-3} \mu\text{g } \mu\text{L}^{-1}$ of N). S/N' values obtained were 30 for K and 6 for N. The concentrations of gelatine in all the injected samples were at least 10^3 times higher.

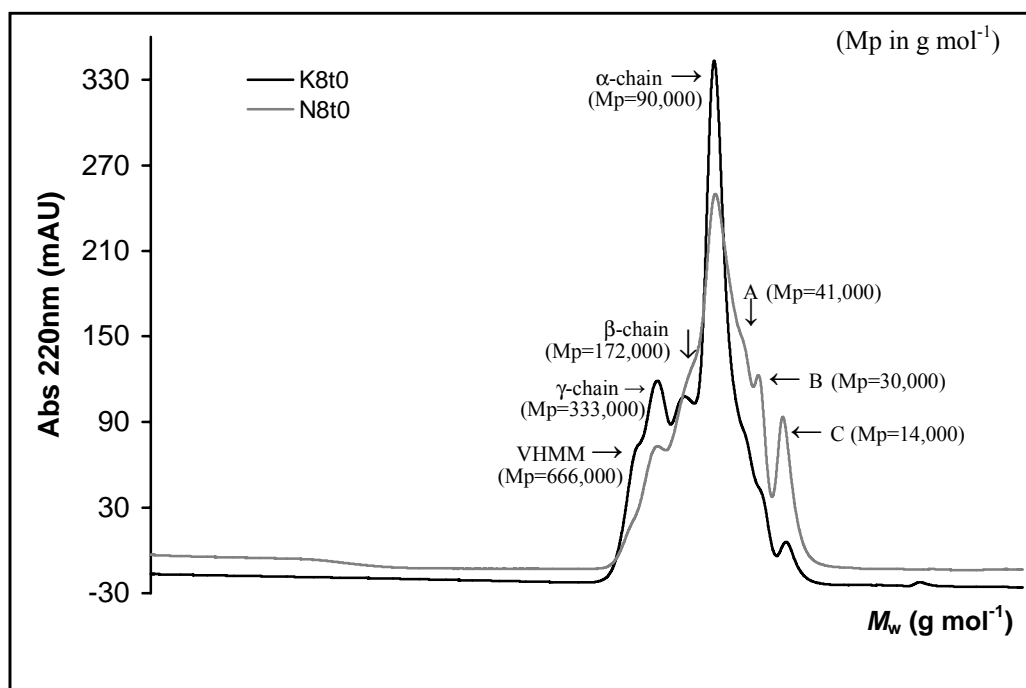


Figure 8-2. Overlaid chromatograms of K gelatine and N gelatine extracted from 8% uptake unaged Whatman No. 1 paper (respectively K8t₀ and N8t₀).

8.3 Results and discussion

8.3.1 The choice of the mobile phase

Compared to the MMD profiles obtained with 1.8% SDS in water as mobile phase (Figure 8-2), with 1.8% SDS in 50 mM phosphate buffer pH 6.63 the elution volume of the gelatine fractions increased. The hydrodynamic volume of gelatine in phosphate buffer was smaller than in the unbuffered, low ionic strength mobile phase. The molar mass distribution (MMD) profiles for unaged gelatine were similar to the MMD profiles in 1.8% SDS in water, only shifted slightly towards lower M_r . For the aged gelatine from papers with and without alum, the MMD profiles were markedly shifted to lower M_r and the resolution of peaks A, B and C was less than with 1.8% SDS in water. The corresponding SEC chromatograms can be found in Appendix 8-1. Consequently, it was decided to run SEC with 1.8% SDS in water for sample preparation and mobile phase.

8.3.2 SEC of gelatine extracted from Whatman No. 1 papers

8.3.2.1 Papers without alum

8.3.2.1.1 Extraction yields of gelatine from unaged and aged papers

Both the aged 35 days and unaged K granules dissolved completely in the mobile phase. We evaluated whether cross-comparisons for quantitation were possible between unaged and aged gelatine based on the respective UV absorption. The recovered mass of gelatine for aged K granules was back-calculated by integrating the area subtending the entire chromatogram using Equation 8-2. The calculated mass matched the actual known injected mass. This result confirmed that the equation established for quantitation of unaged gelatine Equation 8-2 could also be used for the quantitation of aged gelatine.

Using Equation 8-2 and Equation 8-3, the extraction yields of gelatine from unaged Whatman No. 1 paper were found to range from 72 to 86% for K and from 43 to 47% for N. The theoretical concentrations were calculated based upon the dry mass uptakes, and the calculated injected masses were estimated by integrating the entire chromatogram area. For the aged Whatman No. 1, the extraction yields of gelatine were significantly lower, between 13 and 24% for K and between 23 and 33% for N.

8.3.2.1.2 M_r determination and MMD profiles of gelatine from unaged papers

Figure 8-2 shows MMD profiles of K and N extracted from unaged papers with 8% gelatine uptake. The major peak had M_p value of 90,000 g mol⁻¹. This fraction was attributed to the α -chains. The high- M_r portion of the chromatograms showed a shoulder of M_p 666,000 g mol⁻¹ and two small peaks of M_p 333,000 and 172,000 g mol⁻¹ for K - respectively two shoulders and a peak for N. The latter two were attributed respectively to β -chains and γ -chains non-degraded or reformed upon cooling of the gelatine after production [5]. The very-high- M_r polypeptides ($M_w = 666,000$ g mol⁻¹) were multimers of α -chains probably formed by aggregation or cross-linkage of α -, β - and γ -chains, and are not present in native collagen [5]. These stable aggregates seem to be a particular feature of gelatine, and they were still present in the chromatogram of samples of K diluted down to $8 \cdot 10^{-2}$ $\mu\text{g } \mu\text{L}^{-1}$ (stock/256).

The low- M_r regions showed two shoulders with M_p values of 41,000 and 30,000 g mol⁻¹ (peaks A and B) and a small peak of M_p 14,000 g mol⁻¹ (peak C) for K - respectively a shoulder (A) and two peaks (B and C) for N. These low- M_r fractions resulted from the degradation of collagen during the production of gelatine [10]. Overall, it was observed

that the MMD profile of N was slightly more weighted in the low- M_r regions than the MMD profile of K. This observation corroborated results found in the literature [10].

The chromatograms of gelatine extracted from unaged papers with 2% and 0.5% uptake, and the chromatograms of unaged K granules and N flakes were similar to those shown in Figure 8-2. The sizing process did not change the MMD of the gelatine to any detectable level regardless of the concentration of gelatine in solution.

8.3.2.1.3 M_r determination and MMD profiles of gelatine from aged papers

Three MMD profiles of gelatine extracted from papers with 8% gelatine uptake unaged, aged 35 days and aged 94 days are shown in Figure 8-3 (K) and Figure 8-4 (N). There was a significant decrease in high- M_r fractions in the extract upon aging. In the 35-day aged paper extracts, the γ -chain fraction was absent while the β -chain fraction was barely present and reduced to a small tailing. The α -chain fraction was considerably reduced as well. After 94 days, the β -chain tail disappeared and the α -chain fraction was further reduced. The decrease in high- M_r fractions was likely due to a decrease in the solubility of this polypeptidic portion as observed previously (section 8.3.2.1.1). This could arise from cross-linking of the high- M_r fractions of the gelatine during aging or from a binding of the polypeptides to the cellulose molecules through links other than hydrogen bonds. Fourier transform infrared spectroscopy using an attenuated total reflectance probe (Nicolet Avatar 360 FTIR) was performed on the papers after extraction in order to verify whether residual gelatine was left, but the result proved inconclusive as no protein bands were clearly evidenced probably due to the lack of sensitivity of the technique.

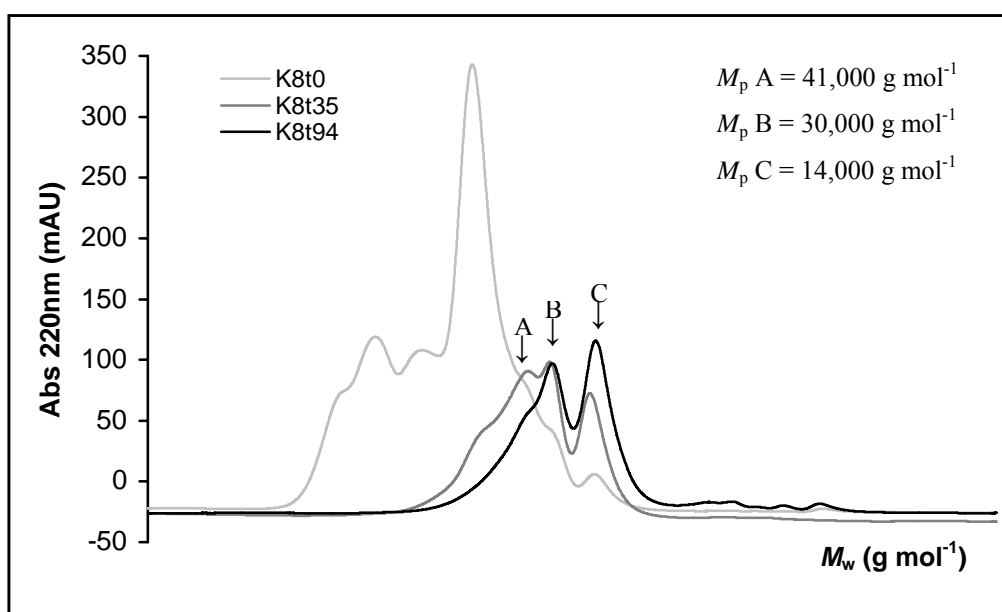


Figure 8-3. Overlaid chromatograms of K gelatine extracted from 8% uptake Whatman No. 1 paper unaged (K8t₀), aged 35 days (K8t₃₅) and aged 94 days (K8t₉₄) at 80 °C, 50% rH.

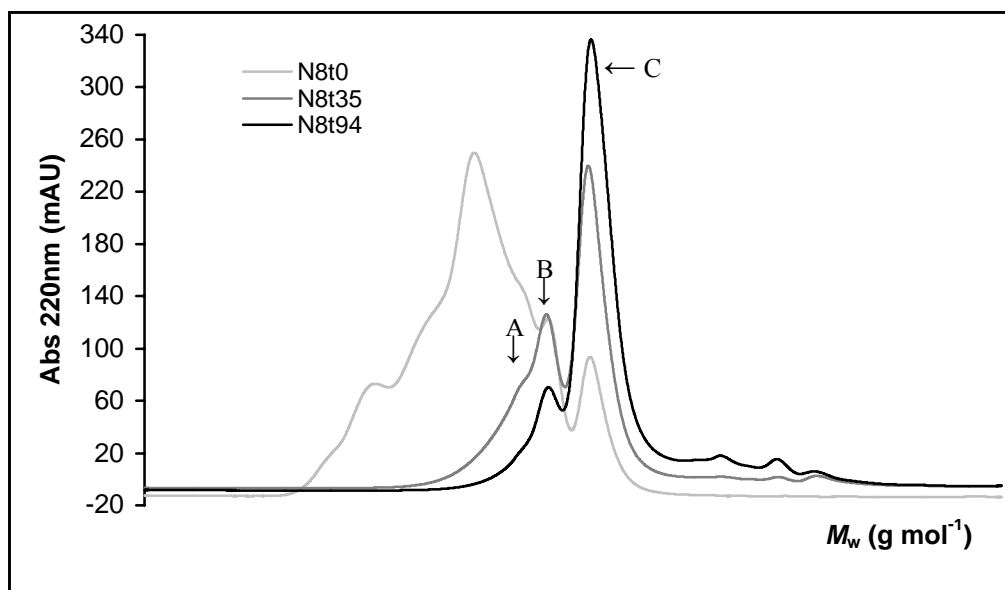


Figure 8-4. Overlaid chromatograms of N gelatine from 8% uptake Whatman No. 1 paper unaged (N8t₀), aged 35 days (N8t₃₅) and aged 94 days (N8t₉₄).

The main peaks in the chromatograms of the extracts of aged papers were the three low- M_r fractions corresponding to peaks A, B and C (Figure 8-3 and Figure 8-4). Upon aging, peak C increased considerably while peak B decreased and peak A progressively disappeared. Hydrolysis of high- M_r γ -, β - and α -chains seemed to occur at preferential weak points, leading to this substantial increase in specific low- M_r fractions. This result confirmed the findings of a study on the degradation of photographic gelatine induced by pollution. Exposure to a mixture of SO_2 (27 mg m^{-3}) and NO_2 (38 mg m^{-3}) for 18 and 30 days resulted in fewer high- M_r fractions, while a characteristic low- M_r fraction below $20,000 \text{ g mol}^{-1}$ was shown to increase [24].

Peak C, the main characteristic fraction formed in both 35- and 94-day aged samples, could be an indicator of gelatine degradation upon aging. A plot of peak C height versus aging time showed a non-linear but steady increase (Figure 8-5). A kinetic study would be necessary to gain more insight.

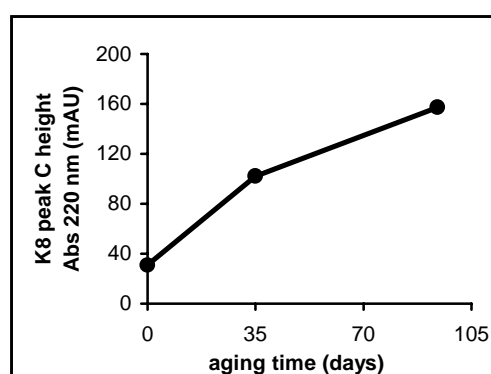


Figure 8-5. Peak C height in mAU, detection at 220 nm (K gelatine extracted from 8% uptake Whatman No. 1 paper) as a function of aging time in days (values averaged from two different samples).

A hypothesis for preferential hydrolysis points leading to specific low- M_r fractions can be proposed. It is known that amino acids in peptides are unequally sensitive to partial hydrolysis [25]. For instance, in a dipeptide the positively charged ammonium group close to the amide bond tends to repel acidic protons. The amide bond of a dipeptide is thereby more stable than an analogous bond in a polypeptide. On the opposite end, aspartyl residues are very susceptible to hydrolysis in dilute acid, because the negatively charged carboxyl groups of aspartic acid attract hydrogen ions, which decreases the stability of the neighbouring peptide bonds. Other effects, such as steric hindrance, are involved in the relatively better resistance to acid hydrolysis of peptides with valine and leucine as amino-terminal residues. In this case, the isopropyl and isobutyl side chains of valine and leucine hinder the approach of the acidic proton. These effects are more complex and less known for polypeptides. In the case of the degradation of gelatine upon heat/humid aging, partial-hydrolysis specificity is quite likely to be involved and responsible for the specific low- M_r fragments formed.

Figure 8-6 shows three MMD profiles: unaged K granules, K granules aged 35 days and K extracted from 2% uptake papers aged 35 days. A new peak with M_p 830,000 g mol⁻¹ appeared for the aged K granules. There were also fewer γ -, β - and α -chains, but higher proportions of low- M_r fractions (A, B and C) in the aged K granules as compared with unaged K granules. Hence, the aging of K granules resulted in two distinct outcomes taking place concomitantly. On the one hand, there was a substantial increase in the low- M_r fractions, especially in the peak C fraction. On the other hand, very-high- M_r polypeptides ($M_p > 800,000$ g mol⁻¹) were formed. The latter most likely arose from crosslinking or aggregation of some of the β - and γ -chains [26]. This presence of crosslinked networks in high- M_r gelatines as a structural feature retained from the native collagen structure has been observed by other authors [27].

The presence of crosslinked fractions was consistent with the low-mass recovery and with the observation made throughout this study of the absence of high- M_r fractions in the gelatine extracts from aged papers. Crosslinking arising from a progressive dehydration of the bound water of gelatine seemed to occur in sized paper upon aging and resulted in a solubility decrease.

However, we observed in the case of K granules that, after aging, the crosslinked fraction was still soluble in the mobile phase. One hypothesis to explain why, when gelatine was aged in paper, the crosslinked fraction became insoluble, involves the role of sugars and aldehydic compounds and their favouring of protein crosslinking. Numerous sugars and oxidised sugars have been identified as degradation products of cellulose upon aging [28,29] and recent research showed that they decrease the solubility of gelatine by promoting crosslinking of the protein [30]. The proposed mechanism is via an Amadori rearrangement [31] where the aldehyde group of a reducing sugar can react with a free amino group of gelatine, resulting in the formation of an amino glycoside, which can further react with another gelatine amino group, thereby giving rise to the crosslinked structure. Because of their dialdehydic nature, sugars oxidised with periodic acid, for

instance, were shown to be more efficient and lead to a more complete interaction with gelatine polypeptides [30]. Bonding between the gelatine and the cellulose molecules was probably also involved to some extent, since oxidised radicals on the cellulose can form without cleavage from the polysaccharidic chain. Polysaccharide-protein interactions are complex. Earlier work showed that hydrogen bonds between non-substituted hydroxyl groups of methylcellulose and carboxyl groups of gelatine form when both components are mixed in certain proportions [32].

Figure 8-7 shows MMD profiles of N flakes unaged and aged 35 days. As calculated with Equation 8-3, only an estimated 26% of the latter dissolved in the mobile phase. The very-high- M_r fraction ($M_p > 800,000 \text{ g mol}^{-1}$) was only a small shoulder in both chromatograms. This result suggested that, in the 35-day aged N flakes, only a small part of the very-high- M_r fraction was soluble. Here also, N showed a faster degradation rate than K.

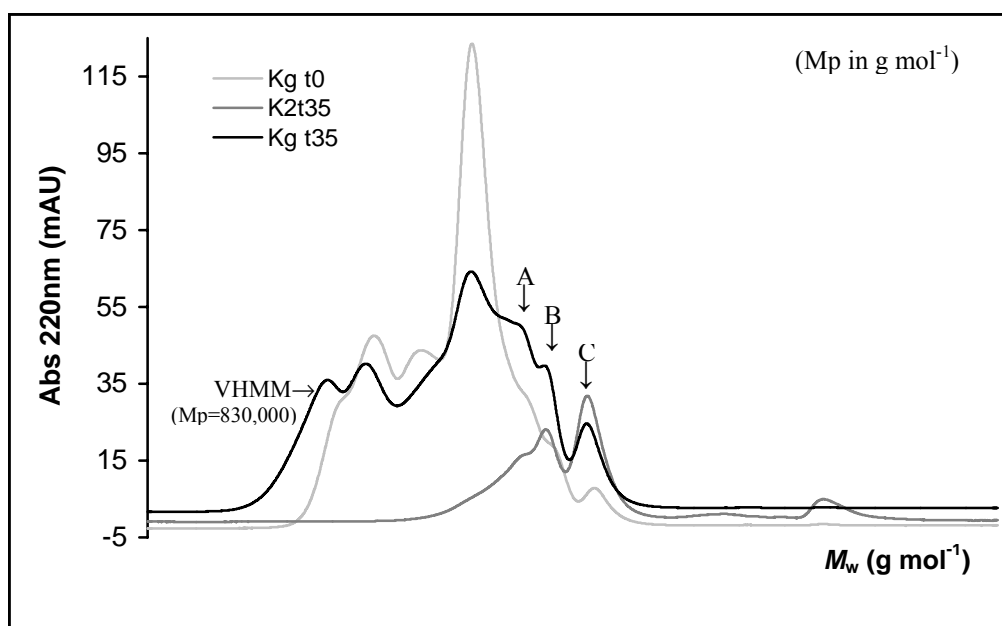


Figure 8-6. Overlaid chromatograms of K gelatine granules unaged ($2.59 \mu\text{g } \mu\text{L}^{-1}$) ($\text{Kg } t_0$), K gelatine granules aged 35 days ($2.5 \mu\text{g } \mu\text{L}^{-1}$) ($\text{Kg } t_{35}$) and K gelatine extracted from 2% uptake Whatman No. 1 papers aged 35 days (estimated $4.7 \mu\text{g } \mu\text{L}^{-1}$) ($\text{K2}t_{35}$).

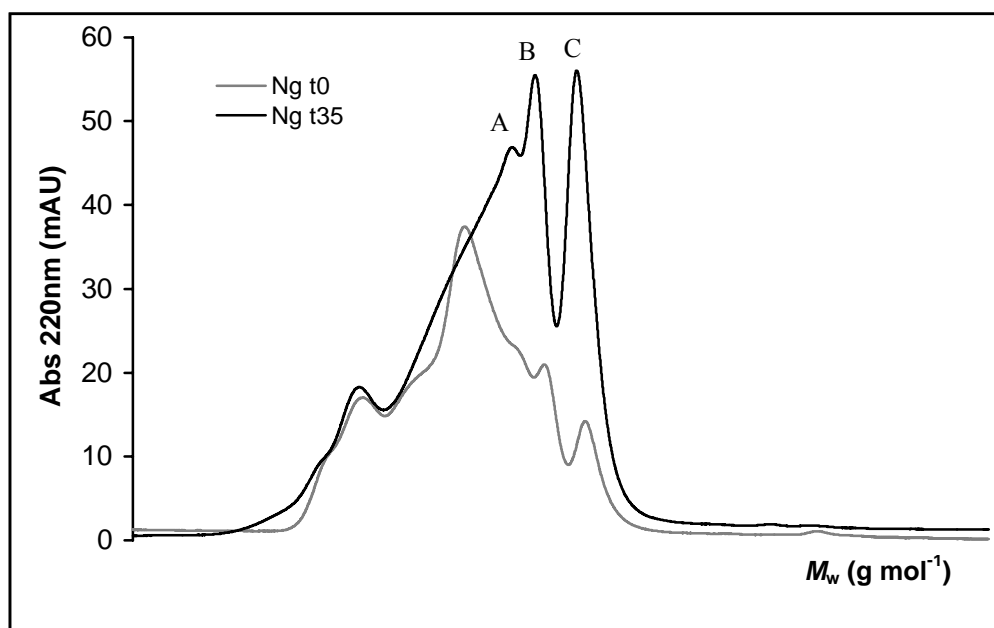


Figure 8-7. Overlaid chromatograms of N gelatine granules unaged ($1.25 \mu\text{g } \mu\text{L}^{-1}$) (Ng t_0) and N gelatine flakes aged 35 days (estimated $2.1 \mu\text{g } \mu\text{L}^{-1}$) (Ng t_{35}).

8.3.2.2 Papers with alum

The MMD profiles of the gelatine from papers containing 1 and 10% alum (mass alum/mass gelatine) were similar to those with no alum for each respective aging time. The hydrolysis of gelatine due to aging was not accelerated by the presence of alum in quantities of up to 10%. However, 30% alum in the size resulted in a more extensive hydrolysis of the gelatine to smaller peptides upon aging. After 35 days aging, the MMD profile was similar to that of 94-day aged samples containing no alum. After 94 days, profiles showed a significantly decreased peak B and an increased peak C (Figure 8-8).

It was also observed that the extraction yields of gelatine from unaged papers decreased with the increase in alum content, especially in the high- M_r fractions α -, β - and γ -chains, as shown in Figure 8-9. The role of alum as a hardener of gelatine is well known, especially in photography. Aluminium salts react with the ionised carboxyl groups of gelatine [12,33,34]. It can be hypothesized that the mechanism by which alum formed bridges between gelatine and cellulose is most likely similar to the mechanism described in the literature by which alum forms bridges between rosin and cellulose in rosin/alum sizing (Figure 8-10) [35]. Results showed that while the areas subtending the chromatograms of the gelatine extracted from the aged papers without alum and the aged papers with 1% alum were similar, the areas subtending the chromatograms of gelatine from aged papers with 10 and 30% alum increased proportionally to the increase in alum content. In the aged papers, the height of the low- M_r peaks increased with the alum content.

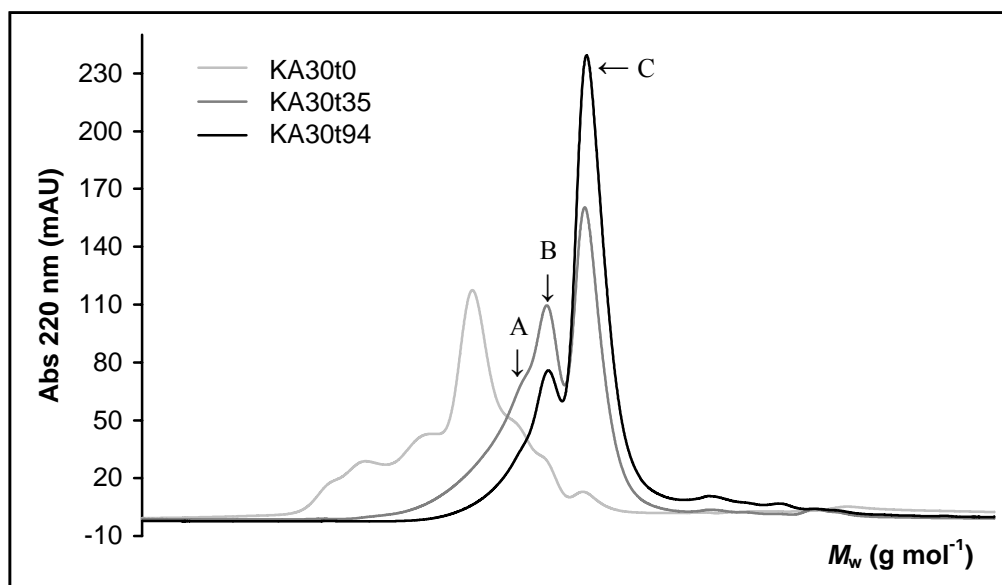


Figure 8-8. Overlaid chromatograms of gelatine extracted from Whatman No. 1 papers sized with K 2% uptake and 30% alum unaged (KA30t₀), aged 35 days (KA30t₃₅) and aged 94 days (KA30t₉₄).

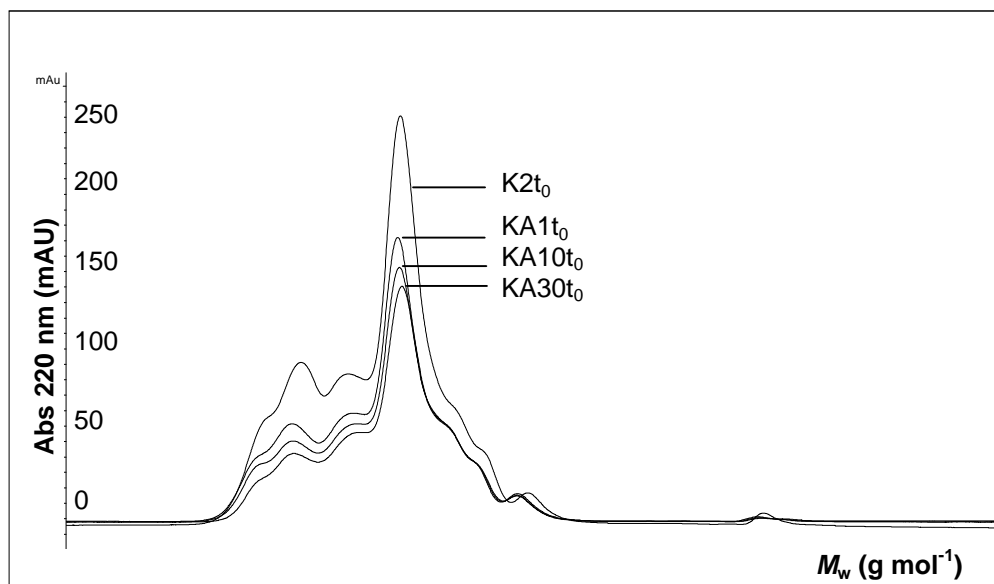


Figure 8-9. Overlaid chromatograms of gelatine extracted from unaged Whatman No. 1 papers sized with K 2% uptake with no alum, 1% alum, 10% alum or 30% alum (K2t₀, KA1t₀, KA10t₀ and KA30t₀ respectively).

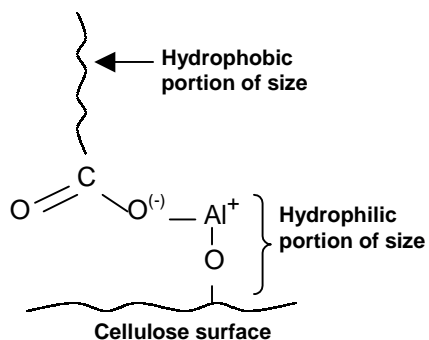


Figure 8-10. Model of aluminium bridge between cellulose surface and a size [35].

Upon aging, 10 to 30% alum accelerated the hydrolysis of gelatine, producing a higher proportion of easily extractable low- M_r fractions. Thirty percent alum additionally resulted in a more extensive hydrolysis of the protein to smaller peptides.

8.3.3 SEC of gelatine extracted from Arches papers

Figure 8-11 shows chromatograms of gelatine extracted from unaged and aged Arches papers. The high- M_r fraction was absent in the chromatogram of the unaged Arches paper. The further shift towards low- M_r fractions upon aging occurred earlier than for the Whatman No. 1 papers. Gelatine extracted from unaged Arches paper was poor in high- M_r molecules, as γ -, β - and α -chain fractions were small shoulders, and the MMD profile was similar to the profile of gelatine from the 8% K uptake Whatman No. 1 papers aged 35 days. The Arches papers were kept in the laboratory for 10 years before analysis. Despite the fact that the commercial sizing procedure and the grade of the gelatine used by the manufacturer could not be documented, the result suggested that, under natural aging conditions, the two phenomena observed, namely hydrolysis and crosslinking started fairly early in time. Analysis of the Arches papers with scanning electron microscopy/energy dispersive X-ray (SEM/EDX) (JEOL JSM 5410 LV SEM/Oxford EDS system) showed the presence of aluminium. The presence of alum in the Arches papers could explain the high degradation rate of the gelatine. However, aluminium is also present in some mineral fillers such as aluminium silicate (kaolin), which is a widely used filler material.

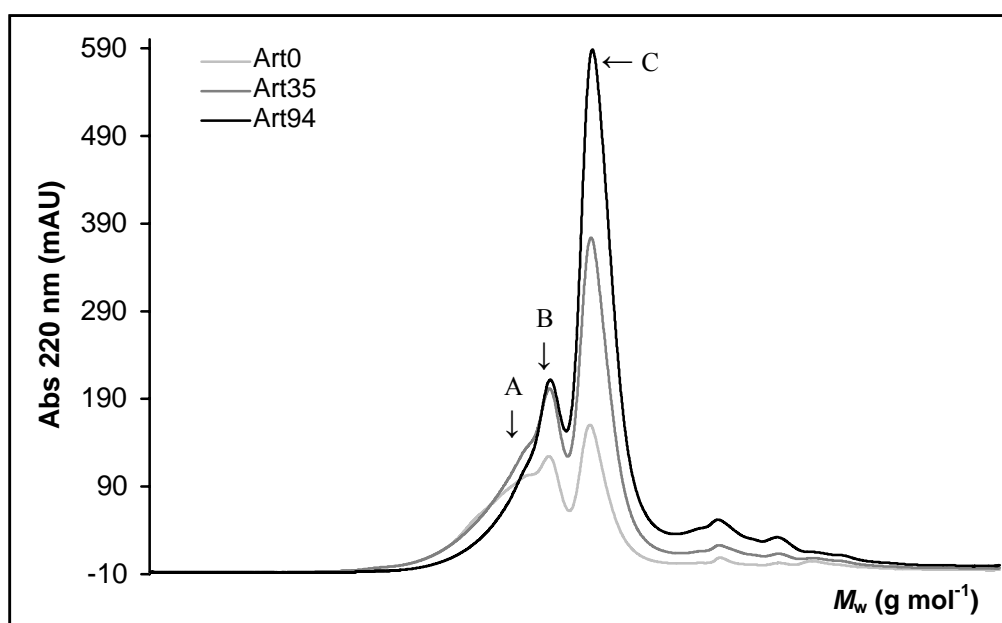


Figure 8-11. Overlaid chromatograms of gelatine extracted from Arches (Canson) papers unaged (Art_0), aged 35 days (Art_{35}) and aged 94 days (Art_{94}).

8.3.4 SEC of gelatine extracted from naturally aged papers

Figure 8-12 shows the chromatograms of five different naturally aged historic papers from the seventeenth and eighteenth centuries, sized with gelatine: NAT1, NAT2, NAT3 and NAT4, the samples analysed by SEC/MALS described in section 6.3.2.2.1 of Chapter 6, and an additional sample NAT5. The gelatine MMD profiles were skewed towards the low- M_r region, showing peaks B and C characteristic of highly degraded gelatine. The closest match for the MMD profiles were the profiles of gelatine extracted from papers sized with K aged 94 days, but peak A (shoulder) was even smaller.

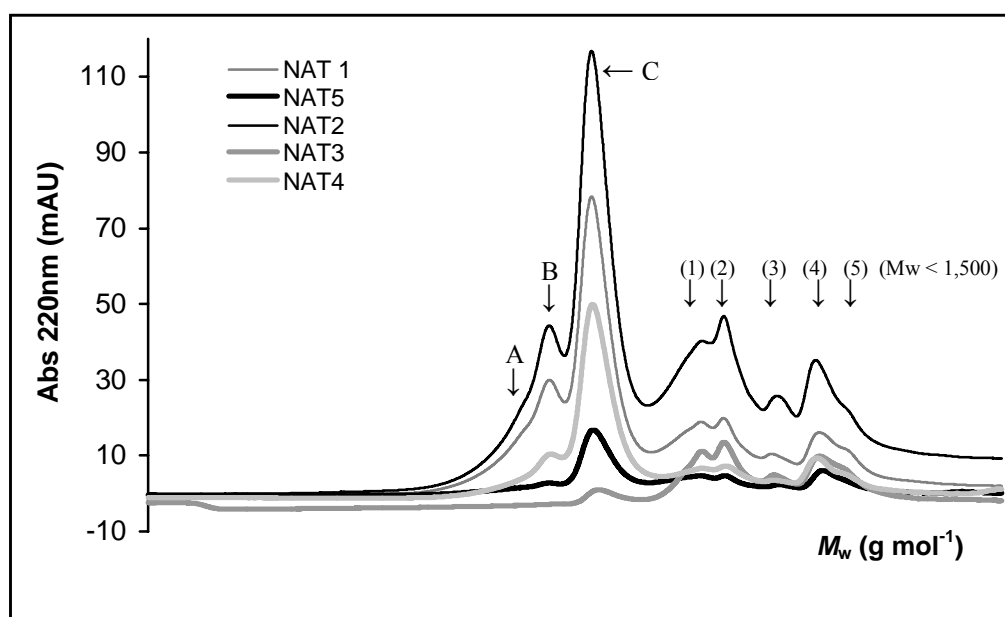


Figure 8-12. Overlaid chromatograms of gelatine extracted from five different naturally aged papers (17th and 18th centuries) NAT1, NAT2, NAT3, NAT4 and NAT5.

Across the very-low- M_r end in the chromatograms of all naturally aged papers, a series of five small peaks were found spreading from t_R 56 to 62 min ($M_p < 1500$ g mol⁻¹). The very last of these small peaks (5) (Figure 8-12) was most likely a ghost peak since it was also present in the chromatograms of unaged gelatine granules and in the chromatograms of extracts of control Whatman No. 1 unaged unsized (not shown). The three small peaks (1, 2 and 4) were found elsewhere exclusively in the chromatograms of the extracts of aged Whatman No. 1 papers (sized and unsized) and Arches papers. No correlation could be found between the area of these peaks and the amount of gelatine and/or alum in the papers. These three small peaks were attributed to soluble UV-absorbing degradation products from cellulose and in that respect could be indicative of extensive degradation of the paper [28]. The very small peak (3) seemed to be present only in the chromatograms of aged, sized papers and Arches papers and probably arose from the aging of gelatine.

8.3.5 Absorption at 254 and 280 nm

Detection at 254 and 280 nm provided useful additional information. Absorption at either wavelength was very low (2 to 10 mAU) since Tyr and Phe are present in minute quantities in gelatine, but the general MMD profiles at 254 and 280 nm of unaged and aged gelatines resembled the profiles at 220 nm (Figure 8-13). It was interesting to note that, for the major peaks ($M_w \geq 14,000 \text{ g mol}^{-1}$), the A_{220}/A_{254} ratios were single digit numbers, while for the very-low- M_r peaks (1 to 4), the A_{220}/A_{254} ratios exceeded a value of 10 or even 100. This seemed to indicate that Tyr and Phe were quite evenly distributed among the polypeptide fractions before and after aging, but that they were more numerous in the fractions of $M_w < 1500 \text{ g mol}^{-1}$ arising from aging. The amorphous regions of gelatine, the telopeptides, which contain a higher proportion of these amino acids, undergo, upon aging, extensive cleavage to form small peptides. The exposure of gelatine to atmospheric pollutants showed similar degradation behaviour, where amino acids from the telopeptides were found to elute in the total-permeation peak [24]. However, as suggested earlier, chemical species other than amino acids could also be involved in the UV absorption at 254 and 280 nm of the very-low- M_r fractions most likely, UV-absorbing species from the degradation of cellulose [28,36].

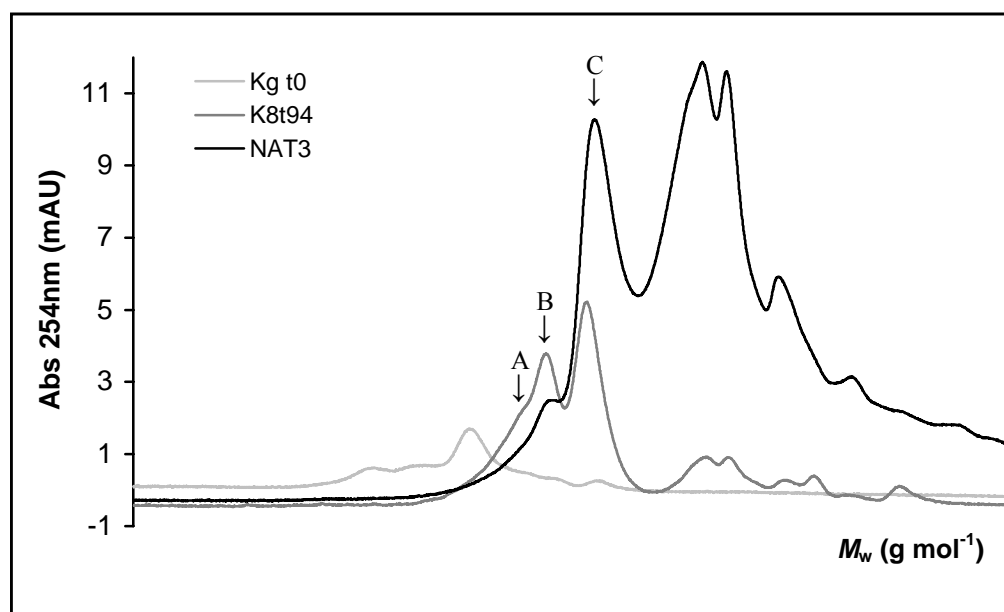


Figure 8-13. Overlaid chromatograms of K granules unaged ($2.59 \mu\text{g } \mu\text{L}^{-1}$) ($\text{Kg } t_0$), K gelatine extracted from 8% uptake Whatman No. 1 paper aged 94 days ($\text{K8}t_{94}$) and gelatine extracted from naturally aged paper 3 (NAT3). Detection at 254 nm.

8.4 Conclusions

Upon heat/humid aging gelatine in paper underwent significant degradation. The α -chains were shown to break at weak points, producing specific low- M_r fractions. The peptide

bonds were cleaved and native γ -, β - and α -chains were progressively lost, concomitantly giving rise to two main low- M_r fractions. A fraction with M_p 14,000 g mol⁻¹ (peak C) was the most characteristic fraction to increase significantly upon aging. Peak C could potentially be used as a marker for monitoring gelatine degradation. Peak C was also present in very small quantities in unaged gelatine, forming the so-called "non-gel" portion [9,10], *i.e.* small fragments produced by cleavage of the α -chains during the production of gelatine. A hypothesis for preferential hydrolysis points involving the different sensitivities of the amino acids in peptides to partial hydrolysis was proposed. The characterisation of the terminal amino acids of the peptides in the low- M_r fractions using hyphenated mass spectrometry techniques would help clarify this phenomenon and possibly determine the most labile amide bonds in gelatine.

Another remarkable observation in this study was the formation upon accelerated aging of a very-high- M_r fraction of $M_p > 800,000$ g mol⁻¹, *i.e.* well above the M_r of native collagen γ -chains, which appeared at the same time as hydrolysis proceeded in other areas of the protein to yield low- M_r fractions. This very-high- M_r fraction, which cannot be extracted from the sized papers aged, most likely arose from a crosslinking between the γ -, β - and α -chains. The crosslinking was a consequence of the heat/humid aging treatment and could be further enhanced by the presence of sugars and oxidised sugars produced by the degradation of cellulose.

Chemicals

Sodium dodecyl sulphate, disodium hydrogenphosphate heptahydrate and sodium dihydrogenphosphate monohydrate were purchased from Acros Organics (Springfield, NJ, USA). L-Alanine was from the amino acid standard kit 22 from Pierce (Rockford, IL, USA). Sodium polystyrene sulfonate (PSS) standards (M_r range 1600–120,000 g mol⁻¹) were from Scientific Polymer Products (Ontario, NY, USA). Gelatines used were Gelita Photographic Gelatin Type 8039, Lot 1 from Kind and Knox Gelatin (Sioux City, IA, USA) and "High Molecular Weight Gelatin" batch No. 7345 from Norland Products (New Brunswick, NJ, USA). Electrophoresis "Low Molecular Weight Calibration Kit" (Phosphorylase *b*, albumin, ovalbumin, carbonic anhydrase, trypsin inhibitor and α -lactalbumin) and "High Molecular Weight Calibration Kit" (thyroglobulin, ferritin, catalase, lactate dehydrogenase and albumin) were purchased from Pharmacia (Peapack, NJ, USA). The set of PL-Aquagel-OH columns (one 50, two 40, one 30), and the guard column were from Polymer Laboratories Inc. (Amherst, MA 01002, USA).

Instruments

The liquid chromatograph HP 1090 equipped with a built-in thermostated column compartment, the photodiode array detector (series L Diode Array Detector), and the data acquisition and reduction software Chemstation for LC were from Hewlett-Packard, now Agilent Technologies (Palo Alto, CA, USA).

References

1. Diderot, J.J. *Encyclopédie ou Dictionnaire Raisonné de Sciences, des Arts et des Métiers, par une Société de Gens de Lettres* 11, A. Neufchastel, Samuel Faulche et Compagnie (1765).
2. Brückle, I. *Abbey Newsl.* 17, 4 (1993) 53-57.
3. Brückle, I. *Conference Papers Manchester 1992*, Institute of Paper Conservation, Fairbrass, S. Ed., Leigh Lodge (1992) 201-206.
4. Roberts, J.C. *Paper Chemistry*, Ch. 9, Roberts, J.C. Ed., 2nd Ed., Blackie, Glasgow (1996) 140-160.
5. Traub, W. and Piez, K.A. *Advances in Protein Chemistry* 25, Anfisen Jr, C.B.; Edsall, J.T. and Richards, F.M. Eds., Academic Press, New York (1971) 243-341.
6. Rich, A. and Crick, F.H.C. *J. Mol. Biol.*, 3 (1961) 483.
7. Ramachandran, G.N. *Treatise on Collagen* 1, Ramachandran, G.N. Ed., Academic Press, New York (1967) 103.
8. Bella, J.; Eaton, M.; Brodsky, B. and Berman, H.M. *Science*, 266 (1994) 266-275.
9. MacGregor, E.A. and Greenwood, C.T. *Polymers in Nature*, MacGregor, E.A. and Greenwood, C.T. Eds, Wiley, Chichester (1980) 142-147.
10. Rose, P.I., *The Theory of the Photographic Process*, Ch. 2, 4th Ed., Rose, P.I. Ed., McMillan, New York (1977) 51-67.
11. Harding, J.J. *Advances in Protein Chemistry*, 20, Anfisen Jr., C.B.; Edsall, J.T.; Richards F.M. and Anson M.L. Eds, Academic Press, New York (1965), 109-181.
12. Croome, R.J. and Clegg, F.G. *Photographic Gelatin*, Croome, R.J. and Clegg, F.G. Eds, Focal Press, London (1965) 49-51.
13. Barrett, T. and Mosier, C. *J. Am. Inst. Conserv.*, 34 (1995) 173-186.
14. T 412 om-94, TAPPI Test Methods, Technical Association of the Pulp and Paper Industry, Atlanta (1994).
15. De Lalande, J.J.J.F. *L'art de Faire le Papier*, Académie Royale des Sciences (1761).
16. Green S., *Conference Papers Manchester 1992*, Institute of Paper Conservation, Fairbrass, S. Ed., Leigh Lodge (1992) 197-200.
17. Balston, T. *The Mill Ledger, James Whatman, Father and Son*, Balston, T. Ed, James Whatman, Father and Son, Methusen, London (1957) 59.
18. Norris, F.H. *Paper and Paper Making*, Ch.16, Norris, F.H. Ed., Oxford University Press, Oxford (1952) 228.
19. Sanburn, W.H. *personal folder notebook*, Waroronoro Paper, MA (1909).
20. McCormick-Goodhart, M.H. *J. Imaging Sci. and Technol.* 39, 2 (1995) 157-162.
21. Adelstein, P.Z.; Bigourdan, J.-L. and Reilly, J.M. *J. Am. Inst. Conserv.*, 36 (1997) 193-206.
22. T 509 om-88, TAPPI Test Methods, Technical Association of the Pulp and Paper Industry, Atlanta (1988).
23. Shinagawa, S.; Kameyama, K. and Takagi, T. *Biochim. Biophys. Acta*, 1161 (1993), 79-84.
24. Nguyen, T.-P. *Etude des effets de la pollution atmosphérique sur la dégradation de la gélatine photographique*, Thèse Doctorale, Université de Rouen, U.F.R de Sciences (1998).

-
25. Hill, R. *Advances in Protein Chemistry*, 20, Anfisen Jr., C.B.; Edsall, J.T.; Richards, F.M. and Anson, M.L. Eds, Academic Press, New York (1965), 39-52.
 26. Bailey, A.J.; Robins, S.P. and Balian, G. *Nature*, 251 (1974) 105-109.
 27. Veis, A. and Cohen, J. *Nature*, 186 (1960) 720-721.
 28. Dupont, A.-L. *Restaurator*, 17 (1996) 145-164.
 29. Erhardt, D.; Mecklenburg, M. and Tumosa, C. *ICOM-CC Preprints II, 11th Triennial Meeting, Edinburgh* (1996) 903-910.
 30. Cortesi, R.; Nastruzzi, C. and Davis, S.S. *Biomaterials*, 19 (1998) 1641-1649.
 31. Hodge, J.E. *J. Agric. Food Chem.*, 1 (1953) 928-940.
 32. Nishinari, K.; Hofmann, K.E.; Kohyama, K.; Moritaka, H.; Nishinari, N. and Watase, M. *Biorheology*, 30 (1993) 243-252.
 33. Burness, D.M. and Pouradier, J. *The Theory of the Photographic Process*, 4th Ed., Burness, D.M. and Pouradier, J. Eds, Mcmillan, New York (1977) 77-87.
 34. Brown, E.M.; Dudley, R.L. and Elsetinow, A.R. *J. Am. Leather Chem. Assoc.*, 92 (1997) 225-233.
 35. Gess, J.M. *Paper Chemistry*, 2nd Ed., Ch. 8, Roberts, J.C. Ed., Blackie, Glasgow (1996) 128-130.
 36. Eusman, E. *Conservation Research*, National Gallery of Art, Washington, DC (1995) 11-27.

General conclusion

While several factors involved in the stability and durability of paper have been investigated in the past, the issue of sizing was largely ignored. The present research, dedicated to investigating the role of gelatine in the longevity of paper, helped comprehend the complexity of these factors and shed some light on the neglected, yet important aspect of sizing with gelatine in historical papermaking. The analytical tools used to characterise both the cellulose and the gelatine proved very well adapted to the study of the differently prepared model papers and the historic naturally aged samples. The method developed to dissolve the cellulose and the selected associated solvent were found appropriate for papers of diverse origin and composition, and were clearly the most suitable among those tested. This was demonstrated in the precision of the results and in the stability of the solutions of cellulose, as the solubilised polymer did not degrade with time.

The findings show that gelatine plays a significant role in the conservation of papers, which is more or less pronounced depending on whether the size contains alum. Gelatine is shown to be beneficial by slowing the degradation rate of the cellulose upon aging. Although this role is not always clearly demonstrated in the case of papers with low gelatine content, it is substantial in those papers with high gelatine uptake, and those that contain alum in all the ranges of concentrations studied. This effect is thought to be due to the preferential hydrolysis of the protein molecules over those of cellulose.

From the perspective of paper conservation and particularly its practical side, the outcomes of this study inevitably bring up new questions concerning conservation treatments, and more specifically on the issue of sizing and resizing paper artefacts after a wet treatment such as washing or deacidifying. Despite the lack of information on how much gelatine and alum would dissolve in each particular case of an aged document, mainly because the life history and state of degradation of each one are usually unknown or uncharacterised, it is undeniable that part of the gelatine of a sized paper remains soluble in water. This is accentuated when the gelatine is in a highly hydrolysed state, as part of the protein becomes more soluble. As this is the case with very degraded papers, and as the latter are often those artefacts that benefit the most from a washing treatment, would it then be advisable to resize them with gelatine following the washing?

It can be a difficult task to provide general advice relative to conservation practice, mostly because each artefact is unique, if not in its composition, then certainly in its conservation history. If the assessment of the conservation state and the decision whether or not to resize an object are of concern to the paper conservator, the findings of the

present research can help in the choice of the resizing material, as they provide detailed information on the effects of gelatine sizing.

However, such choices cannot be straightforward. For instance, whereas gelatine considerably helps in reducing the hydrolysis rate of cellulose, it does so at the expense of a slightly larger discolouration rate. This study shows in particular that the macroscopic properties usually associated with a greater deterioration state of the paper, such as yellowing and acidity for instance, do not necessarily relate directly to the molecular state of the polymer.

However, things must always be considered in their context. It must be kept in mind that this study was limited to gelatine, and that the potential benefits from using other polymers, such as cellulose ethers, which are also currently used for resizing, could not be investigated in the time-frame of the present research. The aim of this research was to contribute to the knowledge of the materials historically used in papermaking, and of their behaviour in time. However, in order to extrapolate with certainty the results obtained from the laboratory samples to real artefacts, more research must be carried out, in particular in the area of accelerated aging. As a general observation, despite extensive research, the usefulness of artificial aging methods in modelling natural aging is still an open question. The issue is probably never to be resolved completely, as too many parameters and phenomena that cannot be reproduced artificially are involved and contribute to natural aging. This issue summarises much of the difficulty that conservation science faces when transferring the knowledge and applying the research to conservation practice.

Appendix 3-1. Maillard reactions

Maillard reactions are non-enzymatic autocatalytic browning reactions between reducing sugars and amino acids. Thus, they can occur with proteins or peptides and carbohydrates. They have three basic phases, which are represented in Figure A3-1. 1.

The initial phase is the condensation of an amino acid with the reducing group of a sugar, which loses a molecule of water, to form a N-substituted aldosylamine. This compound is unstable and undergoes Amadori rearrangement to form 1-amino-1-deoxy-2-ketoses, known as ketosamines.

In the second phase, the ketosamines can react in three ways. These are dehydration, fission, and polymerisation reactions. Dehydration leads to the formation of reductones and dehydro reductones. In short chain hydrolytic fission, compounds such as hydroxyacetyl, hydroxyacetone, glycolaldehyde or pyruvaldehyde are formed. These can undergo Strecker degradation by reacting with amino acids to form aldehydes, and condensation to form aldols. The third path is the Schiff base/furfural path. It involves a loss of three water molecules followed by reaction with amino acids and water yielding furfural (from pentoses) and hydroxymethyl furfural (from hexoses).

In the third phase, the compounds react further with amino acids to form insoluble brown pigments called melanines.

Maillard reactions are promoted by high pH, temperature and high amount of moisture. The products of Maillard reactions depend on the type of sugar and amino acid that reacted in the first place and their concentration.

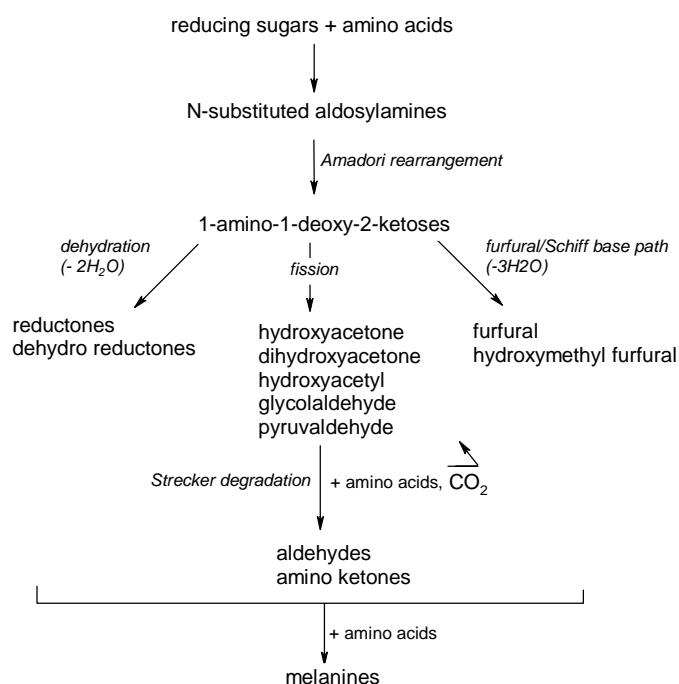


Figure A3-1. 1. Scheme of Maillard reactions between amino acids and reducing sugars.

Appendix 5-1. Viscometry method for the analysis of dilute solutions of cellulose in Cadoxen

A5-1.1 Experimental¹

A5-1.1.1 The dissolution method

A5-1.1.1.1 Cadoxen solvent preparation

Cadoxen is an aqueous solution of cadmium tri-ethylenediamine dihydroxide $[\text{Cd}(\text{En})_3](\text{OH})_2$ ($\text{En} = \text{H}_2\text{N}(\text{CH}_2)_2\text{NH}_2$).

Cadoxen was prepared according to the procedure described by Donetzhuber [1]. Ethylenediamine was purified by re-distillation, and the fraction of boiling point (b.p.) 116-117° was collected. A solution of about 6.5 M was made by mixing 466.5 mL of this purified ethylenediamine with 1080 mL of water in a 2L-erlenmeyer flask. The solution was kept overnight at 4°C.

The flask was then placed in an ice-sodium chloride bath and chilled to a temperature between -8°C and -16°C under constant stirring. 135 g of cadmium oxide was then added slowly over a period of 3 hours. The mixture was stirred for one additional hour and placed at 4°C for 24 to 48 hours to allow the settling of the excess precipitate of cadmium hydroxide.

The clear solution was separated from the precipitate by centrifugation at 3000 rpm for 20 minutes. An aqueous solution of sodium hydroxide (2.26 M) made by dissolving 21 g of NaOH in 232.5 mL of water was mixed with 90.3 mL of purified ethylenediamine. This solution was cooled to 4°C and mixed with the cold cadmium oxide/ethylenediamine prepared previously to make up the Cadoxen stock solution. The Cadoxen stock was left overnight at room temperature before use.

A solution of Cadoxen 50% was prepared by diluting the Cadoxen stock in water in a 1:1 ratio to be used as the viscosity effluent. The water used for all solutions was milli-Q 18.2 MΩ cm (RiOs Elx, Millipore).

A5-1.1.1.2 Sample pre-treatment

The paper was immersed in a solution of sodium borohydride 0.5 M in ethanol with a 1/0.1 (wt/v) ratio for 16 hours. NaBH₄ reduces the carbonyl residues present on the

¹ The experiments detailed here were carried out at the Canadian Conservation Institute (CCI), Ottawa, Canada.

cellulose chain to hydroxyl groups. This reduction is a preventive treatment in order to decrease the solvent-induced degradation during dissolution [2].

The solution was decanted and the paper thoroughly rinsed several times in water until the pH of the rinse water was neutral. The paper was air dried for at least three days at room temperature and its moisture content was determined according to the standard TAPPI T 412 om-94 [3].

A5-1.1.1.3 Dissolution

The procedure was done following the method by Doty and Spurlin [4] later modified by Burgess [5]. Paper is cut in pieces 2 mm × 2 mm, weighted, and placed in a 20 mL Erlenmeyer flask. Twenty millilitres of Cadoxen stock solution was added.

The amount of paper needed in order to fall in the kinetic viscosity range specified by the viscometer supplier is usually between 60 and 300 mg, depending on the molar mass of cellulose (state of degradation) and on the presence of other fibrous and non-fibrous compounds in the paper.

The suspension of paper in Cadoxen was left dissolving under magnetic stirring for 90 minutes at room temperature. Then 20 mL of water was added to obtain the sample stock solution. This solution was centrifuged for 15 minutes at 3000 rpm, and the supernatant used for the dilutions. With pure cellulose Whatman No.1 paper, dissolution is complete, and no residue is observed.

A5-1.1.1.4 Sample solutions

Three solutions of cellulose at different concentration are required for the viscometry measurement in order to extrapolate the value of the intrinsic viscosity ($[\eta]$). Two more solutions in addition to the stock solution are prepared by diluting the sample stock solution with Cadoxen 50% in 1:1 and 2:1 ratios.

A5-1.1.2 Viscosity measurements

Seven millilitres of the solution to be analysed was poured into the capillary viscometer Routine 100 (Cannon-Fenske) (Figure A5-1 1) from the tubular branch end (1) using a pro-pipette. The viscometer was placed in a water bath at $30 \pm 0.1^\circ\text{C}$ to equilibrate for a few minutes. The liquid was then suctioned up with a suction bulb in (2) to slightly above (A) mark. The efflux time of the liquid, which is the time taken for the solution to flow from (A) to (B) was then measured.

The measurement began with the solvent Cadoxen 50%, followed by the solutions of cellulose, starting with the more diluted. For each solution the measurement was repeated

until three consecutive efflux times agreed within 0.1 seconds maximum difference. The viscometer was then drained, rinsed twice with 3.5 mL of the cellulose solution to be analysed, and drained again well before charging with the 7 mL aliquot of the next solution. Three viscosity repeat measurements were carried out for each sample, and the efflux time values averaged. After one series of dilutions, the viscometer was well rinsed with Cadoxen 50% before rinsing with the next cellulose solution.

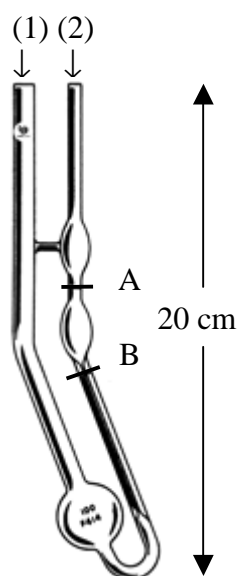


Figure A5-1 1. capillary glass viscometer Routine 100 (Cannon-Fenske).

A5-1.2 Calculation of the intrinsic viscosity and DP_v

The viscosity of a polymer solution depends not only on the size and shape of the molecular chains but also on its concentration, as well as on the temperature, pressure and solvent.

The viscosity average molar mass (M_v) of cellulose is calculated by measuring the intrinsic viscosity of cellulose in dilute solutions, typically of the order of 1% by mass [6]. From M_v the value of the viscosity-average degree of polymerisation (DP_v), which is the ratio of M_v of cellulose by the molecular mass of an anhydroglucose unit (162 g mol^{-1}) is calculated.

$$DP_v = \frac{M_v}{162}$$

For cellulose, M_v is obtained from the Mark-Houwink-Sakurada (MHS) equation:

$$[\eta] = K' M_v^a$$

Where K' and a are constants for a given polymer-solvent system, temperature and molar mass range. For cellulose in Cadoxen at 30°C , the equation is [1]:

$$[\eta] = 3.85 \times 10^{-4} M_v^{0.76}$$

Converting M_v to DP_v , the equation becomes:

$$[\eta] = 1.84 \times 10^{-2} DP_v^{0.76}$$

$$\text{Then, } DP_v = \left(\frac{[\eta]}{1.84 \times 10^{-2}} \right)^{1.316}$$

In order to obtain the value of $[\eta]$, the specific viscosity (η_{sp}) of each diluted solution of cellulose has to be calculated. In practice the viscosity is not measured directly. Instead, as explained in section A5-1.1.2, the time of flow for the polymer solutions and pure solvent in a capillary viscometer, the so-called efflux time is measured. We have:

$$\eta_{sp} = \frac{t_{cell} - t_{solv}}{t_{solv}}$$

t_{cell} is the average efflux time of the solution of cellulose (seconds).

t_{solv} is the average efflux time of the Cadoxen 50% (seconds).

The reduced viscosity (η_{spc}) in $dL\ g^{-1}$ for each dilution is calculated by:

$$\eta_{spc} = \frac{\eta_{sp}}{c}$$

Where c is the concentration of cellulose in solution ($g\ dL^{-1}$) calculated using the dry mass of the paper (m_{dry}), which is defined by:

$$m_{dry} = m \left(1 - \frac{MC}{100} \right)$$

Where m_{dry} is the dry mass of paper (g),

m is the mass of sample weighted (g),

MC is the moisture content (%).

The concentration of the stock sample solution is then:

$$c_{stock} = 2.5 \times m_{dry}$$

The concentration of each diluted solution is then calculated, and the curve $\eta_{spc} = f(c)$ is plotted. We have:

$$[\eta] = \lim_{c \rightarrow 0} \eta_{spc}$$

Thus, the value of the intrinsic viscosity $[\eta]$ is given by the intercept of the linear regression curve $\eta_{spc} = f(c)$. The correlation coefficient R is determined. In the present measurements, a value of $[\eta]$ was accepted only when R^2 exceeded 0.998. The viscosity measurement for the sample was otherwise repeated.

Chemicals and materials

Sodium chloride (NaCl), ethanol and sodium hydroxide were obtained from Fisher Scientific (Springfield, NJ, USA). Sodium borohydride (NaBH₄) and ethylenediamine (En) were purchased from Sigma-Aldrich Corp. (St. Louis, MO, USA).

Instruments

The capillary glass viscometer Routine 100 was obtained from Cannon-Fenske, now Cannon Instrument Cie (State College, PA, USA).

References

1. Donetzhuber, A. *Svensk Papperstidning årg*, 63, 14 (1960) 447-448.
2. Burgess, H.D. *Preprints of Ninth Triennial Meeting of the Committee for Conservation II*, ICOM, Dresden, Germany (1990) 447-452.
3. T 412 om-94, *TAPPI test methods*, Technical Association of the Pulp and paper Industry, TAPPI press, Atlanta, US (1994).
4. Doty, P.M. and Spurlin, H.M. *High Polymers*, 5, III, Interscience, New York (1955) 1133-1188.
5. Burgess, H.D. Master Degree Thesis, Queen's University, Kingston, ON, Canada (1979) 58-61.
6. Nicholson, J.W. *The Chemistry of Polymers*, 2nd Ed., The Royal Society of Chemistry, Cambridge, UK (1994) 104-106.

Appendix 5-2. Size-exclusion chromatography (SEC) method for the analysis of cellulose tricarbanilate (CTC) in tetrahydrofuran

The preparation of the cellulose tricarbanilate (CTC) and the SEC/LALS/UV experiments detailed in this Appendix were carried out at Ecole Française de Papèterie et des Industries graphiques (EFGP/INPG), Grenoble, France, according to the procedure described by Lauriol *et al.* [1,2].

A5-2.1 Preparation of the cellulose tricarbanilate

A5-2.1.1 Theory

CTC is formed from the reaction of cellulose with phenylisocyanate (PIC). The chemical formula of CTC is illustrated in Figure A5-2. 1.

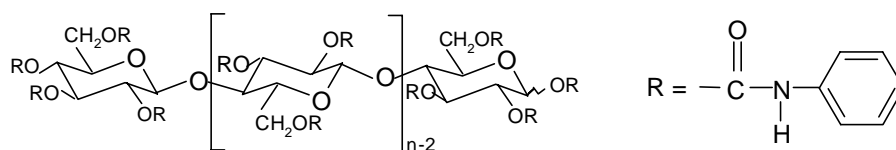
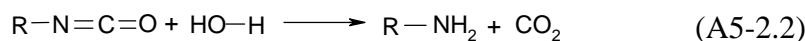
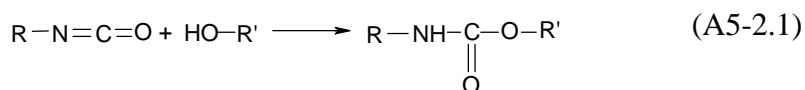
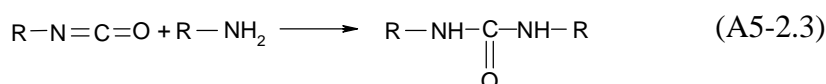


Figure A5-2. 1. Formula of cellulose tricarbanilate.

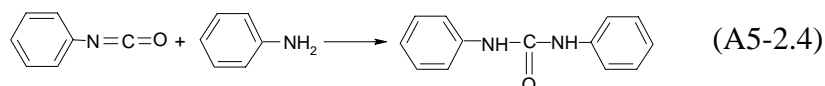
The general reaction of chemical compounds containing alcohol groups with an isocyanate is given by (A5-2.1). The rate of the reaction decreases in the order primary < secondary < tertiary alcohol.

Isocyanates react with water - at a reaction rate similar to that of a secondary alcohol - to produce carbon dioxide (A5-2.2) and an amine compound, which in turn reacts with isocyanate to yield a di-substituted urea molecule (A5-2.3).





With PIC (A5-2.3) yields diphenyl urea according to (A5-2.4).



A5-2.1.2 Experimental

A5-2.1.2.1 Activation

About 2 g of paper was defibrillated in a hammer mill (Poitemill/Forplex), from which 0.2 g were taken and placed in flat bottom reactors with two glass layers allowing water circulation in between. The reactors were capped with a three-necked ground glass cover. A water reflux refrigerant was connected to one of the apertures and the two other apertures were closed. The two reactors were connected in series in order to prepare two sets of CTC at the same time, and were thermostated at $70 \pm 1^\circ\text{C}$. Thirty millilitres of dimethylsulfoxide (DMSO) were added to the paper.

The paper was left activating in refluxing DMSO for 5 to 6 hours under slow magnetic stirring. DMSO has the ability to swell cellulose, which eases the accessibility of cellulose in the derivatisation phase. DMSO is particularly appropriate for the nucleophilic reaction that takes place with PIC in the next step since it is an aprotic solvent (one that does not contain any reactive protons).

A5-2.1.2.2 Derivatisation reaction

Ten millilitres of PIC were added in the reactor one drop at a time, using a glass pipette. This excess of PIC (8 times the stoichiometry) was required to compensate for the amount that reacted with the moisture in the cellulose substrate (which leads to the formation of di-substituted urea). Five millilitres of DMSO were then poured on the internal sides of the reactor in order to rinse eventual residues of PIC.

The reaction took place at $70 \pm 1^\circ\text{C}$ during 48 hours. This relatively long reaction time was expected to compensate for the solvent polarity, the low temperature and the absence of catalyst.

In the first hours of the reaction, the viscosity increased and the solution turned somewhat yellow. After 24 hours, except for some specks in suspension, the solution was clear.

The degree of substitution (DS) of the carbanilated cellulose is usually determined by measuring the nitrogen content using the Kjeldhal method. Lauriol [1] showed that given

the precision of the method, carbanilates could be considered as tri-substituted when DS \geq 2.8. Under the same reaction conditions as those used in the present experiment, Lauriol obtained a DS of 2.8 for cotton linters. The CTC prepared as described here were therefore considered as fully substituted.

A5-2.1.2.3 Stop reaction

The excess PIC had to be fully eliminated to enable a correct integration of the chromatographic signal. For this purpose, 20 mL of acetone were slowly added in each reactor under strong magnetic stirring. Acetone reacts with the excess PIC.

A5-2.1.2.4 Recovery and cleaning

Ten millilitres of the CTC solution were then sampled with a glass pipette and slowly poured one drop at a time under vigorous stirring in 150 mL of ethanol previously filtered (fluoropore filter 0.5 μ m, Millipore). A white precipitate with a fibrous aspect instantly formed, which was the solid tricarbanilated cellulose.

As CTC precipitate formed, it was removed with tweezers and placed in a beaker containing 50 mL of clean ethanol to complete the thorough washing. This cleaning stage is necessary in order to fully eliminate the DMSO, the products formed by the reaction of PIC with acetone and the diphenyl urea, as precipitation tends to trap diphenyl urea inside the CTC network. When the precipitation solution became too cloudy, ethanol was refreshed, and care was taken not to lose any of the CTC. Refreshing of the solution is essential, as ethanol is solvent of low molar mass compounds. The operation was repeated with another 10 mL of the CTC solution for a final 20 mL.

The precipitated CTC was left in the washing ethanol for about 15 minutes, after which it was deposited on an aluminium foil and dried in the oven at 40°C for 24 hours.

A5-2.2 SEC method

A5-2.2.1 Dissolution of the CTC

About 20 to 30 mg of CTC was weighed ($\pm 10^{-5}$ g) in a 20 mL volumetric flask. After having been filtered through 0.5- μ m pore fluoropore filter (Millipore), ten millilitres of tetrahydrofuran (THF) (Pro Analyti, Merck) were added and the flask was capped airtight. The CTC sample was totally dissolved in 16 hours, and the volume was completed to 20 mL with THF.

Prior to injection onto the SEC columns, the sample was filtered through a 0.2- μm Anotop filter, 10 mm diameter (Whatman) in a 1 mL vial filled to the top and tightly capped in order to avoid evaporation.

A5-2.2.2 SEC method of CTC in THF

A5-2.2.2.1 Instrumentation and setup

The SEC set-up is illustrated in Figure A5-2. 2. It consisted of a Spectra System P-1500 pump from TSP (Thermo Separation Products), 7125 injector model (Rheodyne) and Spectra System UV 2000 detector (Spectra Physics). The UV detector was connected on-line with the low angle light scattering (LALS) detector KMX-6 (Chromatix).

The interdetector delay volume was minimised as much as possible. The latter was determined to be 0.167 mL by collecting the signals of the two detectors after injecting a sample without the columns set.

The refractive index increment dn/dc of CTC in THF is needed for M_w calculations. It was measured in THF at 20°C with a Brice Phoenix differential refractometer at 632.8 nm by Lauriol *et al.* [1,2] as $0.169 \pm 0.002 \text{ mL}\cdot\text{g}^{-1}$. The data acquisition and reduction was carried out using the software code CARB developed at EFPG [1].

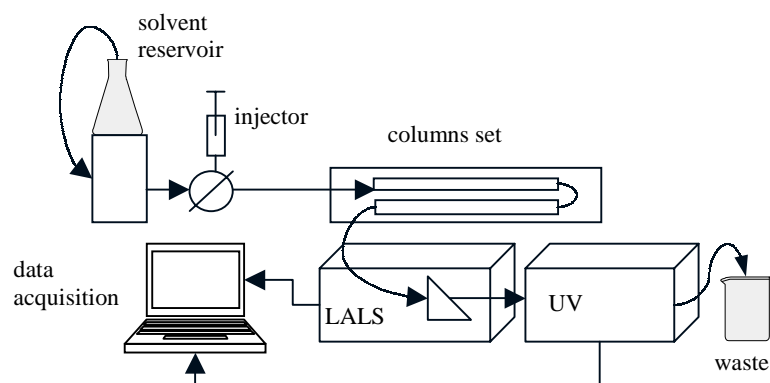


Figure A5-2. 2. Schematic representation of the SEC/LALS/UV line.

A5-2.2.2.2 KMX-6 characteristics and LALS theory

The KMX-6 has a 2 mW helium-neon laser source operating at 633 nm, which emits vertically polarised light. The scattering angles form an annulus and are 6-7 degrees forward (3-4 real degrees).

A photomultiplier with adjustable gain measures the intensity of scattered light G_θ and transmitted light G_0 . The gain was adjusted in order to yield a full-scale signal for G_θ . As the scattered intensity is nine orders of magnitude smaller than the incident intensity, a

series of calibrated attenuators placed between the transmitted signal and the detector cell allow the measurement of G_0 in the same sensitivity range as G_θ . The scattered light was reduced with the field stop 0.2 mm. The attenuators used for the measurement of G_0 (No. 1, 3 and 4) were expected to provide a transmittance of 1.22×10^{-8} ; this is the theoretical attenuation factor (D). The experimental determination yielded $D = 1.419 \times 10^{-8}$.

The attenuation factor is a parameter of the Rayleigh ratio, which forms the basis of the light scattering equation for the determination of M_w , and is calculated in LALS by the following equation (details in section 4.1.2.2 of Chapter 4):

$$R_\theta = \left(\frac{G_\theta}{G_0} \right) \left(\frac{D}{\sigma' l'} \right) \quad \text{Equation A5-2. 1}$$

Where σ' is the solid angle of detected scattered light and l' is the length of the scattered volume, called the equivalent path. Therefore, $\sigma' l'$ is a constant of the instrument that depends on the cell geometry, the measurement angle, the refractive index of the solvent and the beam area reduction according to the field stop used. It is measured by independent measurement during the calibration of the LS instrument.

The quartz lenses of the optical system were carefully cleaned with MEK prior to the SEC runs in order to eliminate any dust, which would induce stray light and decrease the signal-to-noise ratio. The 6328 Å narrow band interference filter was wiped with a piece of Teflon filter. The interference filter is placed before the detection cell and absorbs most of the Raman and fluorescence radiation from the sample. The detection cell is made of high quality fused silica and its volume is 15 µL. The actual scattering volume is smaller.

In SEC mode, *i.e.* at very low concentrations, the transmitted light is independent of the concentration. Therefore at a given photomultiplier gain, the following equation holds:

$$G_\theta \text{ solution} = G_\theta \text{ solvent}$$

The signal recorded by the LALS is ΔG_θ , which allows the calculation of the excess Rayleigh ratio as follows:

$$\Delta R_\theta = \left(\frac{\Delta G_\theta}{G_0} \right) \left(\frac{D}{\sigma' l'} \right) \quad \text{Equation A5-2. 2}$$

Where $\Delta R_\theta = R_\theta \text{ solution} - R_\theta \text{ solvent}$ and $\Delta G_\theta = G_\theta \text{ solution} - G_\theta \text{ solvent}$

The relationship that allows calculating M_w from ΔR_θ is:

$$\frac{K^* c}{\Delta R_\theta} = \frac{1}{M_w} + A_2 c \quad \text{Equation A5-2. 3 (see section 4.1.2.2.2 of Chapter 4)}$$

Where A_2 is the second virial coefficient (mL mol g^{-2}), a thermodynamic parameter, which characterises solvent-solute interaction, and K^* is an optical parameter defined in section 4.1.2.2.1 of Chapter 4:

$$K^* = 4\pi^2 \left(\frac{dn}{dc} \right)^2 n_0^2 N^{-1} \lambda_0^{-4}$$

Where n_0 is the refractive index of the solvent

N is Avogadro's number

λ_0 is the wavelength of the incident light in the vacuum

The values of A_2 for a wide range of cellulose tricarbonylates in THF measured with the Chromatix KMX-6 equipped with the 150 μL cell were found to vary from 5.5×10^{-4} to $2.7 \times 10^{-4} \text{ mL mol g}^{-2}$, and appeared to be unrelated to the values of M_w [1]. For example, for M_w around $3 \times 10^5 \text{ g mol}^{-1}$, using A_2 values ranging from 2×10^{-4} to $7 \times 10^{-4} \text{ mL mol g}^{-2}$ the error incurred on the value of M_w was less than 2%.

In SEC mode, since the working concentrations are very low, A_2 can safely be omitted if the following relation holds:

$$2A_2 c M_w \ll 1$$

In this experiment the concentration of the samples injected was about $1.5 \times 10^{-4} \text{ g mL}^{-1}$ and the M_w about $4 \times 10^5 \text{ g mol}^{-1}$ (see Chapter 5), thus the term $(2A_2 c M_w)$ was of 0.07 in the worst case, and could therefore be safely omitted.

A5-2.2.2.3 Calculation of M_r averages and concentration

The concentration detector connected online with the light scattering detector measures the concentration of the solute in each slice of the chromatogram, for which the polymer is considered monodisperse. DRI detectors use the dn/dc value to enable the calculation of the concentration of the polymer from the DRI signal (see section 4.1.2.2.2 of Chapter 4). In the DRI signal the height h_i is the i^{th} value measured and is related to concentration c_i of the eluted fraction by the relation:

$$h_i = n_i \times M_i$$

Where n_i is the number of molecules of molar mass M_i .

Therefore, the equations for M_n , M_w and M_z as expressed in section 2.1 of Chapter 2 become:

$$M_n = \frac{\sum_i h_i}{\sum_i h_i M_i^{-1}} \quad M_w = \frac{\sum_i h_i M_i}{\sum_i h_i} \quad M_z = \frac{\sum_i h_i M_i^2}{\sum_i h_i M_i} \quad M_{z+1} = \frac{\sum_i h_i M_i^3}{\sum_i h_i M_i^2}$$

M_v can be calculated derived from SEC data if the MHS exponent a is known:

$$M_v = \left[\frac{\sum_i h_i M_i^a}{\sum_i h_i} \right]^{1/a}$$

A5-2.2.2.4 Separation

The separation was carried out on a set of 2 columns Ultrastyrigel P/N 10681 (Waters) 7.8 mm I.D. \times 300 mm with poly (styrene-divinyl benzene) (PSDVB) packing and linear separation in the range 2×10^3 to 4×10^6 g mol⁻¹. Flow rate was set to 1 mL min⁻¹. The injection loop volume was 100 μ L, with an effective measured volume of 109 μ L. Runs were carried out at ambient temperature and lasted 30 minutes. The mobile phase was THF (Merck), filtered through 0.5 μ m Teflon filters (Fluoropore, Millipore) and was degassed under vacuum prior to its use.

Chemicals and materials

Dimethylsulfoxide (DMSO), phenylisocyanate (PIC), acetone and ethanol were purchased from Fluka (Saint-Quentin Fallavier, France). Tetrahydrofuran (THF) was obtained from Merck (Darmstadt, Germany). Anotop filters (0.2 μ m pore size, 10 mm diameter) were from Whatman plc (Maidstone, UK) and Fluoropore filters (FG 0.22 μ m and 0.5 μ m pore size) were from Millipore (Guyancourt, France). Poly (styrene-divinyl benzene) (PSDVB) columns Ultrastyrigel P/N 10681 (7.8 mm I.D. \times 300 mm) were from Waters (Milford, MA, USA).

Instruments

The UV detector 2000 was from Spectra Physics (Darmstadt, Germany) and the low angle light scattering (LALS) detector KMX-6 was from Chromatix (Neckargemünd, Germany). The pump Spectra System P-1500 was from Thermo Separation Products, now Thermoquest Thermo Finnigan (San Jose, CA, USA), and the injector 7125 from Rheodyne L.P. (Cotati, CA, USA).

References

1. Lauriol, J-M. *Contribution à l'étude de Celluloses Dégradées par la Détermination de leurs Distributions de Masses Moléculaires*, Thèse de Docteur-Ingénieur, Institut National Polytechnique de Grenoble (1983).
2. Lauriol, J-M.; Froment, P.; Pla, F. and Robert, A. *Holzforschung*, 41, 2 (1987) 109-113.

Appendix 6-1. Specification data sheets of the gelatines used in this study

The certificate of analysis of the gelatine provided by Dr John M. Dolphin, Manager, Research and Development at Kind and Knox Gelatine Inc. is reproduced below.

**CERTIFICATE OF ANALYSIS
OF GELITA PHOTOGRAPHIC GELATINE
KIND AND KNOX GELATINE, INC.**

Identification : Gelita Type 8039, Lot 1
Date : December 21, 1998
Reserved Weight : 1 Kg sample
Prepared for : Anne Dupont
National Gallery of Art

TESTS	Gelita T8039 Lot 1
Bloom, g, 6 ² / ₃ %	249
Viscosity, mPa s, 6 ² / ₃ %, 60°C	4.86
Transmittance, %, 6 ² / ₃ %, 450 nm	85.3
Transmittance, %, 6 ² / ₃ %, 620 nm	96.4
pH, 6 ² / ₃ %	5.68
Isoionic pH (pI), 1½%	5.07
Ash, %	0.54
Calcium, ppm	2933
Iron, ppm	2.08
Copper, ppm	0.08
Mercury, ppm	<0.5
Labile sulfur (Abribat), ppm	0.8
Reducing substances, ppm	11.48
Chloride, ppm	11
Plate count	<10

The certificate of analysis of the gelatine provided by Richard Norland, Norland Products Inc. is reproduced below.

CERTIFICATE OF ANALYSIS
OF NORLAND HMW FISH GELATIN, DRIED
(HIGH MOLECULAR WEIGHT)
NORLAND PRODUCTS, INC.

	normal specifications	batch No. 7345 HMWD
Appearance	granulate	OK
Color	pale yellow	OK
Odor	none	OK
Identity	corresponds	OK
pH of 10% solution	4.0 - 7.0	5.7
Viscosity of 10% solution @ 30°C	20 -35 cs	26.0 cs
Loss on drying	max. 13.5%	12.4%
Total ash	max 2.0%	< 2.0%
Heavy metals	< 20 ppm	0.8 ppm
Arsenic	< 1 ppm	0.2 ppm
Chromium	< 10 ppm	0.8 ppm
Hydrogen peroxides	< 100 ppm	0 ppm
Sulfur dioxide	< 50 ppm	NA ¹
Aerobic bacteria count	max. 1000/g	40/g
Yeast and mold count	max. 100/g	< 50/g
Enterobacteria	negative in 1 g	PASS
E. coli	negative in 25 g	PASS
Salmonella	negative in 25 g	PASS

¹ N/A: not applicable. Sulfites were not used in the manufacture of this gelatin.

Appendix 6-2. Calculations of the uptake of gelatine in the papers

A6-2.1 Moisture content of Whatman No.1 unsized and sized with gelatine

Whatman No.1 paper was equilibrated in an environmental chamber at 23°C, 50% relative humidity (rH) according to TAPPI standard 412-om-94 [1]. The papers were sized with either Kind & Knox gelatine (K) or Norland gelatine (N) (see technical data sheets in Appendix 6-1). Four solutions at 2, 20, 50 and 100 g L⁻¹ were prepared with K and N. This consisted in dissolving solid-state gelatine (granules in the case of K and flakes in the case of N) in deionised water (milli-Q, 18.2 MΩ cm⁻¹) at 40-45°C.

The sizing was carried out by immersing four samples of Whatman No.1 (9.5 cm²) in 20 mL of each solution, in excess volume in order not to deplete the solution. The paper samples were called K2, K20, K50, K100, N2, N20, N50 and N100 according to gelatine type and concentration.

After sizing, the samples were air dried flat on a plastic mesh screen at room temperature, and placed in the environmental chamber for equilibration of their moisture content at 50% rH, 23°C for 120 hours. The weight of the thirty-two sized samples ($\pm 10^{-4}$ g) was then recorded. Monitoring of the weight of the samples showed that they had equilibrated after 48 hours except for N100 samples. The latter needed 120 hours for equilibration, as their moisture content (MC) still decreased by 0.06% (= 0.36 mg) from 48 to 120 hours.

The sized samples were cut in pieces of 5 mm², and the papers with same gelatine type and concentration were mixed together for better sampling. The edges were trimmed off (0.8 to 1 cm) before cutting, as these tend to accumulate larger amounts of gelatine.

MC measurements were carried out according to TAPPI standard 412-om-94 [1], with a slight modification due to the specificity of the samples. Instead of 1 g, approximately 0.5 ($\pm 10^{-4}$) g of paper was weighed. Since the weight monitoring after 1, 2, and 3 hours showed that 2 hours were required to completely drive the moisture off all the samples, oven drying at 105°C was prolonged for 2 hours.

Three measurements of moisture content were performed for each sample, as well as for the reference unsized Whatman No. 1 paper (U), and were averaged. The averages are reported in Table A6-2. 1.

Table A6-2. 1. Average moisture content of sized papers

gelatine	c (g.L ⁻¹)	MC %	RSD
K	100	8.43	0.039
	50	7.31	0.040
	20	6.49	0.048
	2	6.19	0.005
N	100	6.52	0.017
	50	5.73	0.044
	20	5.78	0.076
	2	6.12	0.039
U	0	5.16	0.013

A6-2.2 Relationship between gelatine concentration in solution and gelatine uptake in the paper

Once the exact weight before and after sizing of the thirty-two samples equilibrated at 23°C, 50% rH is known, the quantity of absorbed gelatine by the paper in each solution at a given concentration c was calculated.

The wet weights for each group of samples before and after sizing were averaged, yielding average values for wet weight unsized (WWU) and wet weight sized (WWS). Using the values of MC of unsized and MC of sized Whatman No.1 samples, the dry weights prior to, and following sizing were calculated by retrieving the weight of moisture in each sample. The dry weights were then averaged in each sample category yielding the dry weight unsized (DWU) and the dry weight sized (DWS). The difference (DWS – DWU) yields the uptake of gelatine, *i.e.* the dry weight of gelatine (DWG), and the gelatine content, *i.e.* the percentage of gelatine in dry state in the samples (DG%). Table A6-2. 2 reports the values of dry and wet weight for the sized and unsized samples.

Table A6-2. 2. Dry and wet weights (g) of sized and unsized Whatman No.1 samples and concentration (g L⁻¹) of gelatine solutions.

	c	WWU	WWS	MC % S	W H ₂ O	DWS	MC% U	W H ₂ O	DWU	DWG	DG%
K	100	0.78825	1.0899	8.43	0.091879	0.998021	5.16	0.040674	0.747576	0.2504451	25.09
	50	0.800625	0.934125	7.31	0.068285	0.86584	5.16	0.041312	0.759313	0.1065277	12.30
	20	0.7961	0.846875	6.49	0.054962	0.791913	5.16	0.041079	0.755021	0.0368916	4.66
	2	0.8105	0.8247	6.19	0.051049	0.773651	5.16	0.041822	0.768678	0.0049729	0.64
N	100	0.796725	1.04325	6.52	0.06802	0.97523	5.16	0.041111	0.755614	0.2196161	22.52
	50	0.788775	0.889325	5.73	0.050958	0.838367	5.16	0.040701	0.748074	0.0902925	10.77
	20	0.784825	0.82565	5.78	0.047723	0.777927	5.16	0.040497	0.744328	0.0335994	4.32
	2	0.7953	0.81075	6.12	0.049618	0.761132	5.16	0.041037	0.754263	0.0068696	0.90

Figure A6-2. 1 plots the curves of gelatine content obtained with the above calculations (in %) as a function of the concentration of gelatine in solution. For both K and N, the plots yielded straight lines with determination coefficients of 0.999. The resulting equations were:

$$\% \text{ K uptake} = 0.25 c - 0.08 \quad (R^2 = 0.9996) \quad \text{Equation A-6.2. 1}$$

$$\% \text{ N uptake} = 0.22 c + 0.04 \quad (R^2 = 0.9988) \quad \text{Equation A-6.2. 2}$$

From Equation A6-2.1 and Equation A6-2.2, in order to obtain gelatine contents of 0.5%, 2% and 8% (dry) for the final sized samples to be used throughout this study, the gelatine solutions needed to be of 2.3, 8.3 and 32.3 g L⁻¹ for K respectively, and of 2.1, 8.9 and 36.1 g L⁻¹ for N.

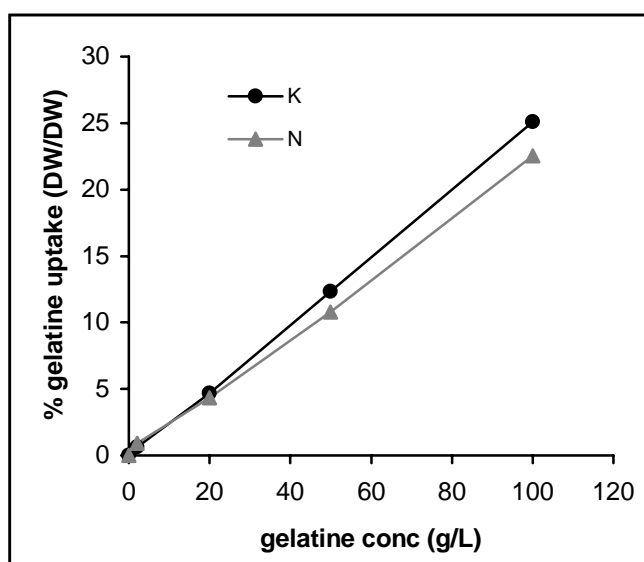


Figure A6-2. 1. Dry gelatine uptake in the paper as a function of gelatine concentration in solution.

A6-2.3 Moisture content of gelatine

The moisture content of the K and N gelatines that had been conditioned at 23°C and 50% rH for 100 hours was measured following the procedure described above for the MC of paper, but varying the quantity of gelatine and drying period. One gram of granules (K) or flakes (N) was placed in the oven at 105°C for 65 hours. This period of time was chosen after a monitoring that showed that at least 55 hours were necessary to completely drive the moisture out of the gelatine. Five measurements were carried out for each gelatine type, and the average MC values were 12.09±0.02% for K and 12.13±0.02% for N.

The MC of the gelatine samples that were kept in the laboratory environment (no climate control) yielded the same values (five measurements each) with MC of $12.10 \pm 0.007\%$ for K and $12.18 \pm 0.01\%$ for N.

References

1 T 412 om-94, *TAPPI test methods*, Technical Association of the Pulp and paper Industry, TAPPI press, Atlanta, US (1994).

Appendix 6-3. Kinetic models for cellulose chain scission

A6-3.1 Model proposed by Ekamstam

The model for the degradation of linear polymers as proposed by Ekamstam [1] is based on first order reaction kinetic.

If a polymer degrades following the reaction:



The first order equation for the degradation is:

$$\frac{dA}{dt} = k [A]$$

From which:

$$[A] = [A_0] e^{-kt}$$

Where k is the reaction rate constant, $[A]$ is the concentration of reactant chains at time t and $[A_0]$ is the initial concentration of reactant chains.

In the case of a linear polymer such as cellulose, which undergoes random degradation, $[A]$ can be replaced by the total number of glycosidic unbroken bonds remaining at time t , l_t .

At time zero:

$$l_0 = N_0 - M_0$$

With $DP_0 = \frac{N_0}{M_0}$, the equation becomes:

$$l_0 = N_0 \left(1 - \frac{1}{DP_0} \right)$$

Where l_0 is the initial total number of glycosidic unbroken bonds, M_0 is the initial number of molecules, N_0 the initial number of monomers in the polymer, and DP_0 is the initial degree of polymerisation.

At time t ,

$$l_t = N_0 - M_t$$

With $DP_t = \frac{N_0}{M_t}$, the equation becomes:

$$l_t = N_0 \left(1 - \frac{1}{DP_t} \right)$$

Where l_t is the total number of glycosidic unbroken bonds at time t , M_t is the number of molecules at time t , and DP_t is the degree of polymerisation at time t .

In first order kinetics, the rate is proportional to the remaining unbroken bonds:

$$-dl / dt = k l_t$$

Thus,

$$l_t = l_0 e^{-kt}$$

Therefore,

$$\ln \left(1 - \frac{1}{DP_t} \right) - \ln \left(1 - \frac{1}{DP_0} \right) = -kt$$

Considering DP_t and DP_0 large enough, this simplifies to:

$$\frac{1}{DP_t} - \frac{1}{DP_0} \approx kt$$

DP is directly proportional to the weight average molar mass M_w with:

$$M_w = DP \times 162$$

Where 162 (g mol^{-1}) is the molecular mass of the monomer, the anhydroglucose unit (AGU).

Therefore:

$$\frac{1}{M_{wt}} - \frac{1}{M_{w0}} = k' t$$

Thus a plot of $(1/M_{wt} - 1/M_w)$ as a function of time t yields k' , the rate of glycosidic bond breakage.

This approach is only applicable under the following assumptions:

- The polymer chain is linear and the molar mass is very high,
- The products of the scission are themselves high molar mass molecules,
- The end-peeling reactions are minor in the process,
- No loss of monomer units occurs during the scission.

A6-3.2 Model proposed by Hill *et al.*

Hill *et al.* [2] showed that the same kinetic model as proposed by Ekamstam can be derived from zero order reactions. They remarked that previous studies of kinetics of cellulose were based upon viscosity measurements - usually in copper ethylene diamine (CED) – and therefore yielded the viscosity average molar mass (M_v). However, in order to obtain the rate of glycosidic bond scission of cellulose, the number average molar mass (M_n) was required, and the problem is that usually for cellulose M_v is closer to M_w than to M_n (see section 2.1 of Chapter 2).

If chain scission occurs without significant depolymerisation, then the number of bonds (l) between anhydroglucose groups for 1 g of polymer is given by:

$$l = \frac{N}{M_G} - N_C$$

Where N is the Avogadro number, M_G is the molar mass of the AGU and N_C is the number of polymer chains per gram of sample.

According to a zero order reaction model, the rate of bond scission is constant. Thus,

$$\frac{-dl}{dt} = k$$

and, $l_t = l_{t_0} - kt$

Where l_t and l_{t_0} are the number of bonds present at time t and time zero t_0 respectively and k is the rate constant expressed in terms of bond scissions per gram of cellulose per second.

Therefore,

$$(N_C)_t = (N_C)_0 + kt$$

The number of chains present per gram of polymer is:

$$N_C = N/M_n$$

Therefore,

$$\left(\frac{N}{M_n} \right)_t = \left(\frac{N}{M_n} \right)_{t_0} + kt$$

With $DP_n = \frac{M_n}{M_G}$ or $M_n = M_G DP_n$

Then,

$$\left(\frac{N}{M_G DP_n} \right)_t = \left(\frac{N}{M_G DP_n} \right)_{t_0} + kt$$

Or,

$$\left(\frac{l}{DP_n}\right)_t = \left(\frac{l}{DP_n}\right)_{t_0} + k't$$

Where k' is given by:

$$k' = k \cdot \frac{M_G}{N}$$

References

1. Ekamstam, A. *Ber. Dtsch. Chem. Ges. A.* 69 (1936) 553-559.
2. Hill, D.J.T.; Le, T.T.; Darveniza, M. and Saha, T. *Polym. Degrad. Stab.* 48 (1995) 79-87.

Appendix 6-4. Colour measurements

A6-4.1 Instrumentation

The UltraScan XE (Hunter Associates Laboratory, Inc.) is a diffuse/8° spectrophotometer that can be used in both transmittance and reflectance mode. The geometry permits a diffuse illumination, with 8° viewing using a 6 inches integrating sphere coated with Spectraflex®. Illumination is provided by a xenon flash lamp, double beam optics, and the detection is carried out with a 40 element diode array, which provides 10 nm wavelength intervals measurements with a wavelength accuracy of 0.75 nm.

The colour measurements in all the experiments reported were done in diffuse reflectance with the specular component included (RSIN) with the illuminant D65, 10° standard observer, using the 25mm diameter measuring area.

A6-4.2 CIE L*a*b* trichromatic system

The L*a*b* colour-space system emerged in 1976 following a recommendation by the Commission Internationale de l'Eclairage (CIE) [1].

A colour space is a method that allows expressing the colour of an object or of a light source in a numerical manner. The L*a*b* colour-space system was designed in order to represent colour differences much as the human eye would see them, and more uniformly than the CIE tristimulus XYZ scale that prevailed earlier. The CIE L*a*b* diagram is sometimes called the “Psychometric Colour Diagram” (Figure A6-4. 1).

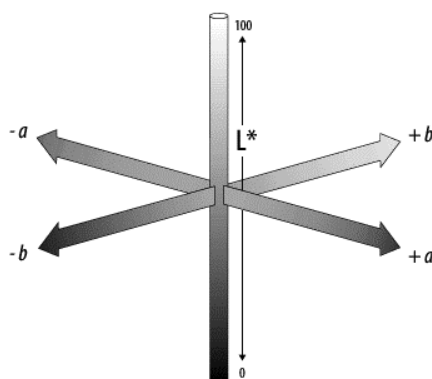


Figure A6-4. 1. L*a*b* colour-space system.

L* is the psychometric lightness and is represented on the central vertical axis from 0 (black) to 100 (white). On the colour axes (a*, b*) the values run from positive to

negative. The a^* axis covers from red ($+a^*$) to green ($-a^*$). The b^* axis ranges from yellow ($+b^*$) to blue ($-b^*$). On both axes, zero is neutral gray.

For the 10° standard observer and illuminant D65, the values of L^* , a^* and b^* are calculated with the following relationships:

$$L^* = 116 \left(\sqrt[3]{\frac{Y}{Y_n}} - 16 \right)$$

$$a^* = 500 \left(\sqrt[3]{\frac{X}{X_n}} - \sqrt[3]{\frac{Y}{Y_n}} \right)$$

$$b^* = 200 \left(\sqrt[3]{\frac{Y}{Y_n}} - \sqrt[3]{\frac{Z}{Z_n}} \right)$$

Where X , Y and Z are the CIE tristimulus values of the sample, and X_n , Y_n , Z_n the tristimulus values of the standard illuminant.

The Total Difference ΔE^* is defined by the following equation:

$$\Delta E^* = \sqrt{(\Delta L^*)^2 + (\Delta a^*)^2 + (\Delta b^*)^2}$$

Where,

$$\Delta L^* = L^*_{\text{sample}} - L^*_{\text{standard}}$$

$$\Delta a^* = a^*_{\text{sample}} - a^*_{\text{standard}}$$

$$\Delta b^* = b^*_{\text{sample}} - b^*_{\text{standard}}$$

A6-4.3 CIE L^*C^*h scale

CIE L^*C^*h is a polar representation of the CIE $L^*a^*b^*$ rectangular coordinate scale. It uses CIE $L^*a^*b^*$ to calculate the metric chroma (C^*) and hue angle (h) for the 10° standard observer and illuminant D65 as follows:

$$C^* = \sqrt{a^{*2} + b^{*2}}$$

$$h = \arctan \frac{b^*}{a^*}$$

ΔC^* is the chromaticity difference in the (a^* , b^*) plane and is defined as:

$$\Delta C^* = C^*_{\text{sample}} - C^*_{\text{standard}}$$

ΔH^* is the Hue Difference (CIE 1976), *i.e.* the difference between the hue angle of the standard and the hue angle of the sample in a polar coordinate system and is defined as:

$$\Delta H^* = \sqrt{(\Delta E^*)^2 - (\Delta L^*)^2 - (\Delta C^*)^2}$$

if $h_{\text{sample}} > h_{\text{standard}}$ then $\Delta H^* > 0$, and

if $h_{\text{sample}} < h_{\text{standard}}$ then $\Delta H^* < 0$

A6-4.4 Other colorimetric parameters measured

A6-4.4.1 ISO brightness R457

The ISO brightness R457 is the diffuse reflectance factor at 457nm. The brightness is the amount of light reflected by the sample expressed as a percentage. It is measured over the range of 400 to 510 nm in accordance to TAPPI standard T 452 [2].

A6-4.4.2 YI E313-96 and WI E313-96 (ASTM)

YI E313-96 and WI E313-96 are the yellowness and whiteness indices as measured according to the ASTM method E313-96 respectively [3].

Yellowness, whose definition is given in the equation below, is associated visually to general product degradation by light, chemical exposure and processing.

$$YI E313-96 = \frac{(C_x \cdot X - C_z \cdot Z)}{Y}$$

Where C_x and C_z are coefficients that depend on the illuminant and the observer. For the illuminant D65 and 10° observer, $C_x = 1.3013$ and $C_z = 1.1498$

Whiteness is associated with a region or volume in colour space in which objects are recognised as white. Degree of whiteness is measured by the degree of departure of the object from a perfect white. The whiteness index as defined by CIE is the same as defined by ASTM method E313-96 and is:

$$WI CIE = WI E313-96 = Y + 800(x_n - x) + 1700(y_n - y)$$

Where x and y are the chromaticity coordinates of the specimen with:

$$x = \frac{X}{(X+Y+Z)} \text{ and } y = \frac{Y}{(X+Y+Z)} ;$$

and x_n, y_n are the chromaticity coordinates for the CIE standard illuminant and source used.

With illuminant D65 and 10° observer, $x_n = 0.3138$ and $y_n = 0.3310$

References

1. CIE, *Colorimetry*, 2nd Ed. CIE publication 15.2, Commission Internationale de l'Eclairage, Vienna (1986).
2. T 452, *TAPPI test methods*, Technical Association of the Pulp and paper Industry, TAPPI press, Atlanta, US (1994).
3. ASTM Standard Method E313-96, ASTM Int. West Conshohocken, PA.

Appendix 8-1. Influence of the pH and the ionic strength of the mobile phase on the MMD profiles of gelatine aged and unaged

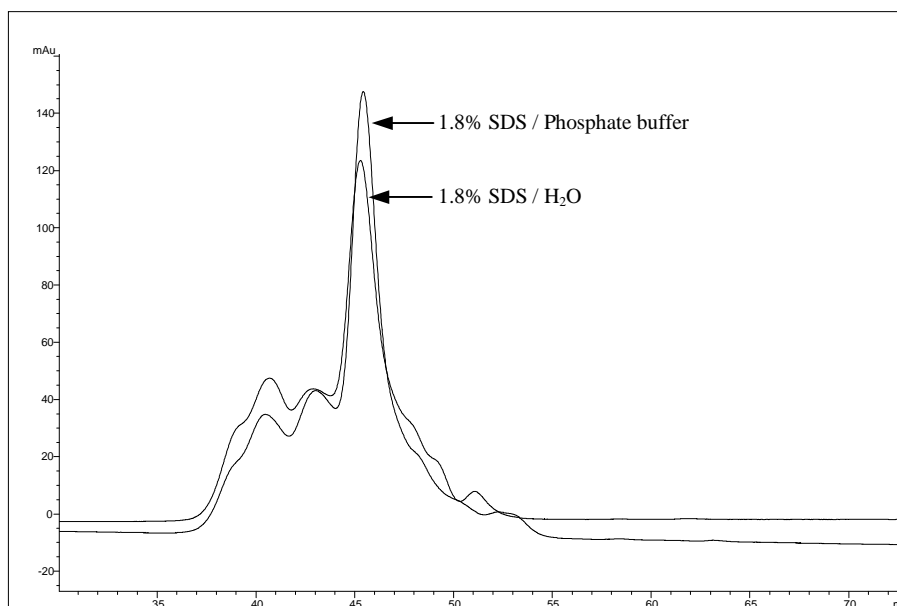


Figure 8-1. 1. SEC chromatograms of K gelatine granules dissolved and ran in two different mobile phases: 1.8% SDS / H₂O versus 1.8% SDS / Phosphate buffer 50 mM, pH 6.63.

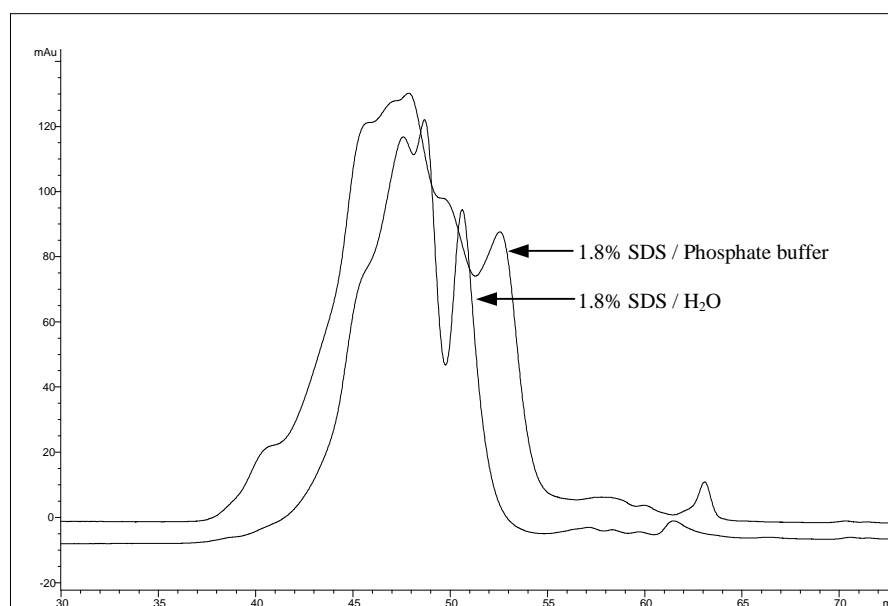


Figure 8-1. 2. SEC chromatograms of gelatine extracted from 8% uptake Whatman No. 1 paper aged 35 days (K8t₃₅) dissolved and ran in two different mobile phases: 1.8% SDS / H₂O versus 1.8% SDS / Phosphate buffer 50 mM, pH 6.63.

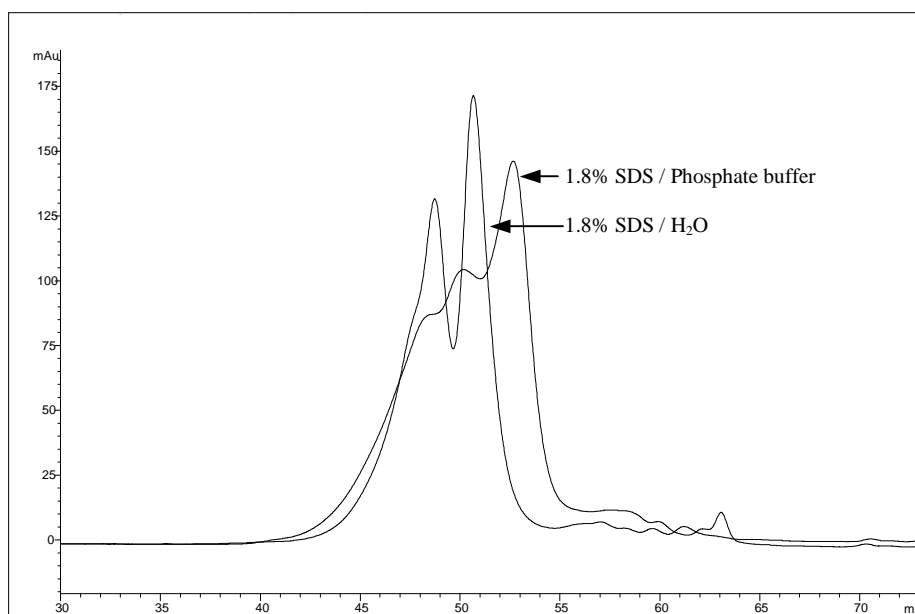


Figure 8-1. 3. SEC chromatograms of gelatine extracted from 8% uptake Whatman No. 1 paper aged 94 days (K8t₉₄) dissolved and ran in two different mobile phases: 1.8% SDS / H₂O versus 1.8% SDS / Phosphate buffer 50 mM, pH 6.63.

Summary

The issue of permanence and durability of paper is one of the major concerns in cellulose research and paper conservation. From the perspective of conservation research, the understanding of the long-lasting properties of paper begins with the investigation of the characteristics of papers in good physical condition that have best survived the passage of time. In European papermaking history, this is the case with early papers, which for the most part, present far better state of conservation than papers of more recent origins. Several facets that could explain the longevity and stability of paper have been investigated in the past, but one that has been largely neglected to date is the process of sizing. Papers dating from the fourteenth to the eighteenth centuries, in addition to having been fabricated from good quality fibres which partly explains their durability, have also in common that they were sized almost systematically with gelatine. The present study is dedicated to the investigation of the role of gelatine in pure cellulose paper. The research is approached mainly from the angle of polymer chemistry. The impact of gelatine sizing upon aging on the molecules of cellulose, and the changes incurred by varying the sizing material are studied. The analytical technique selected is size-exclusion chromatography (SEC), which is employed in the characterisation of both cellulose and the gelatine, and in the investigation of their degradation upon aging. Model papers were fabricated for this purpose, but the study also includes the characterisation of naturally aged papers.

A methodology was developed for dissolving paper in lithium chloride/*N,N*-dimethylacetamide (LiCl/DMAc), a solvent that was chosen for its non-degrading quality and its compatibility with the SEC columns packing. In order to better comprehend the solvation mechanism, the structure of cellulose and the characteristics of the molecule that condition its accessibility to reactants are presented in the first chapter. In the second chapter, the techniques available to date for the analysis and the characterisation of cellulose are evaluated, and the solvents most currently associated with these methods are reviewed. In order to understand the choices made in the present study, the advantages of SEC for polymer characterisation and those of LiCl/DMAc as a solvent for cellulose are detailed.

The procedure developed for the dissolution of cellulose involves as a first step the activation by solvent exchange, with a water/methanol/DMAc sequence, followed in a second step by dissolution in 8% LiCl/DMAc at 4°C. The experiments carried out in order to perfect this method are presented in Chapter 3. A study of the stability of the cellulose solutions in the actual experimental conditions showed that no degradation occurred during the solvation process and confirmed the non-aggressiveness of LiCl/DMAc.

As detection is a crucial aspect of SEC, the detection modes that are available and the type of information each one provides are reviewed in Chapter 4. The principles and the advantages of the detection using multiangle laser light scattering (MALS) coupled with differential refractive index (DRI) are outlined. A section is especially dedicated to the detectors set-up, and to the determination of the parameters required for the characterisation of the molar mass distribution (MMD) of the polymer, the calculation of the molar mass (M_r) averages, and the root mean square (rms) radii averages. Among these parameters is the refractive index increment (dn/dc) of cellulose in 0.5% LiCl/DMAc. The precision and reproducibility of SEC/MALS/DRI for the analysis of cellulose are evaluated in order to validate the method. MALS also allowed for the characterisation of the polymer in solution. The conformation of cellulose in LiCl/DMAc was determined to be random coil, and a study of the solvent efficiency showed that LiCl/DMAc was a good solvent in the chosen conditions.

The SEC/MALS/DRI method for what is referred as ‘directly dissolved cellulose’ or DDC in LiCl/DMAc is compared in Chapter 5 to two other methods currently used for cellulose analysis. These are viscometry in cadmium triethylene diamine dihydroxide or Cadoxen, and SEC using low-angle light scattering (LALS) and ultra-violet detection of cellulose derivatised to tricarbonylates or CTC. The values of the M_r averages of cellulose obtained with these different methods and the discrepancies on these values are discussed on the basis of the precision of each methodology and the action of the solvents on the polymer. As DDC yielded the highest M_r averages values and viscometry the lowest, several hypotheses are presented in order to account for these differences. Each method is also discussed on the basis of its suitability to characterise the aging-induced degradation of the paper.

In Chapter 6, SEC/MALS/DRI is applied to the study of cellulose from model papers and naturally aged papers. Firstly, the degradation of pure cellulose papers upon heat and humidity aging is characterised. Hydrolytic scissions seem to occur more or less randomly on the cellulose chains. The role of the gelatine sizing in the aging-induced degradation of the papers is evaluated, whether these are laboratory sized, commercially sized or historic samples. Although not always in a significant manner, the presence of gelatine is generally shown to be beneficial to the papers, as evidenced by the lower rate of aging-induced depolymerisation of the cellulose, especially in the high molar mass molecules. However upon aging, the gelatine induced some discolouration of the papers as well as a decrease in their pH, which varied with the type of gelatine, its purity and its concentration in the papers. It was found that the purest grade gelatine, *i.e.* the photographic gelatine type B, made from cattle bones, induced less yellowing and less acidification of the paper than the food/pharmaceutical grade gelatine type A, made from fish, and of lowest quality.

In Chapter 7, the method of analysis developed is applied to the study of model papers sized with both gelatine and alum (aluminium potassium sulphate hydrate). In this study, alum is found to considerably accelerate the rate of hydrolysis of cellulose upon aging.

Gelatine shows a marked protective role towards cellulose, as the alum-induced degradation of the paper is significantly hampered in the presence of gelatine. Additionally, the alum dramatically increases both the acidity and the discolouration of the papers upon aging. In that respect, compared to the results obtained from the determination of the M_r with SEC/MALS/DRI, neither the pH nor the colour measurements are found to be good indicators of the state of degradation of papers that contain both gelatine and alum. However, for those papers containing only alum and prepared as reference in the evaluation of its impact, pH is found to correlate well with the changes in M_r . Both parameters display an asymptotical decrease with the alum concentration, and a threshold value situated between 1 and 1.5 g L⁻¹ of alum is determined beyond which no changes in either pH or M_w (weight-average molar mass) can be detected. This limiting value of M_w was found to be 150,000 g mol⁻¹.

Finally, the degradation of gelatine in the model papers is characterised in Chapter 8. In this study, a SEC method using UV detection with a photodiode array is developed in order to evaluate the impact of the paper components, such as cellulose and alum on the degradation of the protein upon aging. The application of this method shows that gelatine undergoes hydrolysis and that a characteristic low- M_r fraction forms. The type A gelatine exhibits a faster degradation rate than the type B. The aging leads to a decrease in the extraction yields of gelatine from the paper, with the formation of very high- M_r polypeptides, which is attributed to crosslinking. The presence of alum below 1 g L⁻¹ is found to have no impact on the degradation while above that concentration the hydrolysis rate of gelatine is increased.



Samenvatting

De duurzaamheid van papier is een van de belangrijkste thema's in celluloseonderzoek en papierrestauratie en -conservering. Kennis van lange-termijn eigenschappen van papier, vanuit het gezichtspunt van conservering, begint met onderzoek naar de eigenschappen van papier in goede conditie, papier dat de tand des tijds goed heeft doorstaan. In de geschiedenis van het papiermaken in Europa is dit het geval met ouder papier, dat voor het merendeel in een aanzienlijk betere toestand van conservering verkeert dan papier dat later is vervaardigd. Een aantal aspecten die de duurzaamheid en stabiliteit van papier kunnen verklaren zijn in het verleden onderzocht, maar een facet dat tot nu toe grotendeels is verwaarloosd is het lijningsproces. Papier daterend uit de veertiende tot en met de achttiende eeuw heeft gemeen, afgezien van het feit dat het gemaakt is met vezels van goede kwaliteit, hetgeen de duurzaamheid ervan ten dele verklaart, dat het vrijwel zonder uitzondering is gelijk met gelatine. Het onderzoek beschreven in dit proefschrift is gewijd aan de rol die gelatine speelt in papier dat zuivere cellulose bevat. Het onderzoek is in hoofdzaak benaderd vanuit de invalshoek van polymeerchemie. De invloed tijdens veroudering van gelatinelijming op de cellulosemoleculen en de veranderingen tengevolge van variatie van lijningsmaterialen is onderzocht. De analytische methode die voor deze studie is gekozen is size exclusie chromatografie (SEC), en is gebruikt voor de karakterisering van de eigenschappen van zowel cellulose als gelatine, en voor het onderzoek naar de degradatie van beide materialen bij veroudering. Voor dit doeleinde werd modelpapier gemaakt, maar daarnaast is ook natuurlijk verouderd papier onderzocht.

Een methodologie werd ontwikkeld voor het oplossen van papier in lithiumchloride/*N,N*-dimethylacetamide (LiCl/DMAc), een oplosmiddel dat werd gekozen omdat het geen degradatie van cellulose veroorzaakt en omdat het verenigbaar is met de SEC kolompakking. Voor een beter begrip van het solvatatie-mechanisme worden in hoofdstuk 1 de structuur van cellulose en de aspecten van de molecuulstructuur die de toegankelijkheid voor reagentia beïnvloeden, beschreven. In hoofdstuk 2 worden de op dit moment beschikbare technieken voor de analyse en de karakterisering van cellulose geëvalueerd en er wordt een overzicht gegeven van de voornaamste oplosmiddelen die bij deze methoden worden gebruikt. Ter ondersteuning van de keuzes die in dit onderzoek zijn gemaakt worden de voordelen van SEC als een analysemethode voor polymeren en van LiCl/DMAc als oplosmiddel voor cellulose in detail beschreven.

De procedure ontwikkeld voor het oplossen van cellulose bestaat uit een eerste activeringsstap, waarbij achtereenvolgens een reeks van water/methanol/DMAc mengsels van verschillende samenstelling wordt toegevoegd, gevolgd door een tweede stap

bestaande uit oplossen in 8% LiCl/DMAc bij 4°C. De experimenten uitgevoerd om deze methode te perfectioneren worden beschreven in hoofdstuk 3. Onderzoek naar de stabiliteit van celluloseoplossingen onder de gebruikte experimentele condities hebben aangetoond dat er geen degradatie optreedt tijdens het oplosproces en hebben bevestigd dat LiCl/DMAc een niet-agressief oplosmiddel is.

Aangezien detectie een cruciaal aspect van SEC is, wordt een overzicht van de detectiemethoden die beschikbaar zijn en de aard van de informatie die elke methode verschaft gepresenteerd in hoofdstuk 4. Het principe en de voordelen van detectie met multi-angle laser light scattering (MALS) gekoppeld aan differentiële refractie index (DRI) detectie worden beschreven. Een speciale sectie is gewijd aan de set-up van de detectoren en aan de parameters nodig voor de bepaling van de moleculaire massaverdeling (MMD) van het polymeer, en de berekening van de gemiddelde moleculaire massa (M_r) en de root mean square (RMS) gemiddelde straal. Eén van de parameters is de brekingsindexverhoging (dn/dc) van cellulose in 0.5% LiCl/DMAc. De precisie en reproduceerbaarheid van SEC/MALS/DRI voor de analyse van cellulose werden geëvalueerd ter validatie van de methode. MALS maakte ook de karakterisering van het polymeer in oplossing mogelijk. De conformatie van cellulose in LiCl/DMAc werd bepaald als een random coil en een studie van de effectiviteit van het oplosmiddel toonde aan dat LiCl/DMAc een goed oplosmiddel is onder de gekozen condities.

De SEC/MALS/DRI methode voor wat wordt aangeduid als ‘direct opgeloste cellulose’ (DDC) in LiCl/DMAc wordt in hoofdstuk 5 vergeleken met twee andere gangbare methoden voor de analyse van cellulose. Deze methoden zijn viscometrie in cadmiumtriethyleendiaminedihydroxide of Cadoxen, en SEC met low-angle light scattering (LALS) en ultravioletdetectie van het tricarbanaal derivaat van cellulose (CTC). De gemiddelde waarden van M_r voor cellulose verkregen met deze verschillende methoden en de tegenstrijdigheden tussen deze waarden worden besproken op basis van de precisie van elke methode en de effecten van de oplosmiddelen op het polymeer. Aangezien DDC de hoogste gemiddelde waarden van M_r leverden en viscometrie de laagste, worden diverse hypothesen aangevoerd ter verklaring van deze verschillen. Elke methode wordt ook besproken op basis van geschiktheid voor de karakterisering van degradatie tengevolge van veroudering in papier.

In hoofdstuk 6 wordt de ontwikkelde SEC/MALS/DRI methode toegepast op de studie van cellulose in model papiermonsters en natuurlijk verouderd papier. Ten eerste wordt de degradatie van puur cellulosehoudend papier bij veroudering onder verhoogde temperatuur en vochtigheid gekarakteriseerd. Hydrolytische splitsing blijkt plaats te vinden op min of meer willekeurige locaties in de celluloseketen. De rol van gelatinelijming in de degradatie tengevolge van veroudering in papier wordt geëvalueerd in zowel papiermonsters die zijn gelijmd in het laboratorium als in commercieel gelijmde en historische papiermonsters. Hoewel niet altijd significant, wordt aangetoond dat de aanwezigheid van gelatine in het algemeen een gunstige invloed heeft op de papiermonsters, zoals blijkt uit de lagere depolymerisatiesnelheid bij veroudering van

cellulose, vooral in moleculen met hogere molecuulmassa. De gelatine veroorzaakt echter enige verkleuring bij veroudering van de papiermonsters, als ook een afname van de pH, hetgeen varieerde met de soort, de zuiverheid en de concentratie van de gelatine in de papiermonsters. De meest zuivere vorm van gelatine, fotografische gelatine, type B, gemaakt van rundveebeenderen, veroorzaakte minder vergeling en minder verzuring van het papier dan de voedings-/farmaceutische kwaliteit gelatine, type A, gemaakt uit vis en van de laagste kwaliteit.

In hoofdstuk 7 wordt de ontwikkelde analysemethode toegepast op de studie van modelpapier gelijmd met zowel gelatine als aluin (aluminiumkaliumsulfathydraat). In deze studie blijkt dat aluin de hydrolysesnelheid van cellulose bij veroudering aanzienlijk verhoogt. Gelatine blijkt een aanmerkelijk beschermende rol te hebben ten aanzien van cellulose. De door de aluin veroorzaakte degradatie van papier wordt aanzienlijk verminderd in aanwezigheid van gelatine. De aanwezigheid van aluin leidt bij veroudering tot een aanzienlijke verhoging van de zuurgraad en tot een sterke verkleuring. In vergelijking met de resultaten verkregen door bepaling van M_r met behulp van SEC/MALS/DRI blijken pH- noch kleurmetingen goede indicatoren voor de degradatietoestand van papier dat zowel gelatine als aluin bevat. Echter, in papier dat alleen aluin bevat en dat werd gemaakt als referentie in de evaluatie van de invloed hiervan, correleerde de pH goed met veranderingen in M_r . Beide parameters vertonen een asymptotische afname met de aluinconcentratie en een drempelwaarde tussen 1 en 1.5 g L⁻¹ werd bepaald waaronder geen veranderingen kunnen worden gedetecteerd in zowel pH als M_r .

Ten slotte wordt de degradatie van gelatine in de model papiermonsters gekarakteriseerd in hoofdstuk 8. In deze laatste studie wordt een SEC methode met UV-detectie d.m.v. een fotodiode-array ontwikkeld voor de evaluatie van de invloed van papiercomponenten, zoals cellulose en aluin, op de degradatie van het proteïne bij veroudering. De toepassing van deze methode laat zien dat gelatine hydrolyse ondergaat en dat een karakteristiek lage- M_r fractie wordt gevormd. Het 'type A' gelatine vertoont een hogere degradatiesnelheid dan het 'type B'. Veroudering leidt tot een afname van de extractieopbrengst van gelatine uit papier, wat wordt gewijd aan crosslinking, gepaard gaande aan de vorming van hoge- M_r polypeptiden. De aanwezigheid van aluin onder 1 g L⁻¹ blijkt geen invloed op de degradatie te hebben terwijl de hydrolysesnelheid van gelatine toeneemt boven deze concentratie.

List of publications relevant to the thesis

Dupont, A-L.

Study of the degradation of gelatin in paper upon aging using aqueous size-exclusion chromatography.

J. Chromatogr. A, 950 (2002) 113-124 (Chapter 8).

Dupont, A-L.

The role of gelatine/alum sizing in the degradation of paper: a study by size-exclusion chromatography in lithium chloride/*N,N*-dimethylacetamide using multiangle light scattering detection.

IIC Congress: Works of Art on Paper, Books, Documents and Photographs. Techniques and Conservation, Daniels, V.; Donithorne, A. and Smith, P. (Eds), Int. Inst. for Conservation, London (2002) 59-64 (Chapter 7).

Dupont, A-L.

Gelatine/alum sizing of paper and its impact on the degradation of cellulose; a study using size-exclusion chromatography with multiangle light scattering detection.

Actes du Congrès Art et Chimie: Les Polymères, Paris, France, Octobre 15-16 2002, CNRS Ed., in press (2003) (Chapter 7).

Dupont, A-L.

Size-exclusion chromatography with multiangle light scattering detection, a method for the characterisation of cellulose in lithium chloride/*N,N*-dimethylacetamide.

International Symposium on the Separation and Characterization of Natural and Synthetic Macromolecules, Amsterdam, The Netherlands, February 5-7 (2003), poster presentation (Chapter 4).

Dupont, A-L.; Mortha, G.

Comparative evaluation of size-exclusion chromatography and viscometry for the characterisation of cellulose.

Manuscript in preparation (Chapter 5).

Dupont, A-L., Harrison, G.

Determination of the dn/dc of cellulose in lithium chloride/*N,N*-dimethylacetamide.

Manuscript in preparation (Chapter 4).

Acknowledgements

This research was carried out during the Charles E. Culpeper Advanced Training Fellowship in Conservation Science at the National Gallery of Art, Washington, DC.

I am extremely grateful to Prof. Dr. René de la Rie, head of the scientific research department of the conservation division at the National Gallery of Art, and my Ph.D. supervisor, for his trust in giving me the opportunity to carry out this research, and for his support and encouragement throughout the project. Many of my colleagues of the scientific research department were helpful in many ways during my stay in Washington, not least, being my friends.

I have been fortunate to carry out part of this research at the Library of Congress, Washington, DC, and I wish to express my gratitude to Dr. Chandru Shahani, head of the preservation research and testing division at the Library of Congress, for welcoming me in his laboratory, thus providing technical and instrumental support without which much of this work would not have been possible; as well as to the colleagues at the preservation research and testing division. In particular, I am greatly indebted to Dr. Gabrielle Harrison, for sharing her experience and knowledge in analytical chemistry, and for the precious practical help and advice she generously dispensed all along. Her interest and enthusiasm for this research and the constructive discussions we had on paper conservation research issues, as well as her proofreading of this thesis were highly appreciated.

I am extremely grateful to have been able to spend some time researching at the Canadian conservation institute (CCI), Ottawa, ON, and at Ecole Française de Papèterie et des Industries Graphiques (EFPG), Grenoble. I must thank Dr. David Grattan, head of the conservation processes and materials research division at CCI, where the viscometry work was carried out. I very warmly thank Dr. Gérard Mortha, laboratoire de génie des procédés papetiers, chimie des procédés, for his entire availability during my stay at EFPG. I owe much to his help and insight in light scattering and paper technology, and to his thorough reviewing of this thesis.

I also wish to express my profound gratitude to Prof. Dr. Peter Schoenmakers, Polymer-Analysis Group, Department of Chemical Engineering, University of Amsterdam, for his critical and constructive in-depth reviewing of this work.

Among others who deserve special acknowledgements are Season Tse, CCI, for her continuous and stimulating encouragements during most of my training in conservation research over the years, and for her input in the brainstorming that led to the concretisation of this project; Dr. David Erhardt, Smithsonian Center for Materials

Research and Education, Suitland, MA, and Dr. Paul Whitmore, Center on the Materials of the Artist and Conservator, Carnegie Mellon University, Pittsburgh, PA, for the useful discussions during the phase of elaboration of the research project.

Many of my colleagues and friends at Centre de Recherches sur la Conservation des Documents Graphiques have been supportive during the writing of this thesis. I am particularly grateful to Dr. Bertrand Lavédrine, head of CRCDCG, for supporting this work and reviewing some of the material included in Chapter 7; Dr. Heike Jerosch for the stimulating and rewarding discussions on cellulose degradation and size-exclusion chromatography; and Julien Barthez for his help in the elemental analysis and his cheering presence in our laboratory.

I owe thanks to Dr. Michelle Chen and Dr. Thomas Scherrer, Wyatt Technologies, Santa Barbara, CA, for their help in critical moments, such as the installation of the SEC/MALS/DRI, and their input in helping understand and solve a few problems relative to the instrumentation, and interpretation of some of the results. Thanks are also due to Timothy Barrett, Director of the Center for the Book, University of Iowa, who was among the first researchers in the paper conservation field to look into the role of gelatine in paper, and whose articles were good starting points to this research.

Finally, I am profoundly thankful to Valérie, my sister, for carefully proofreading all the chapters and painstakingly editing my sometimes rather personal interpretation of the English grammar, but above all for being her own self. Special word of thanks also to my family, and to Jean Tétréault for his support and encouragement during the period this work was carried out.